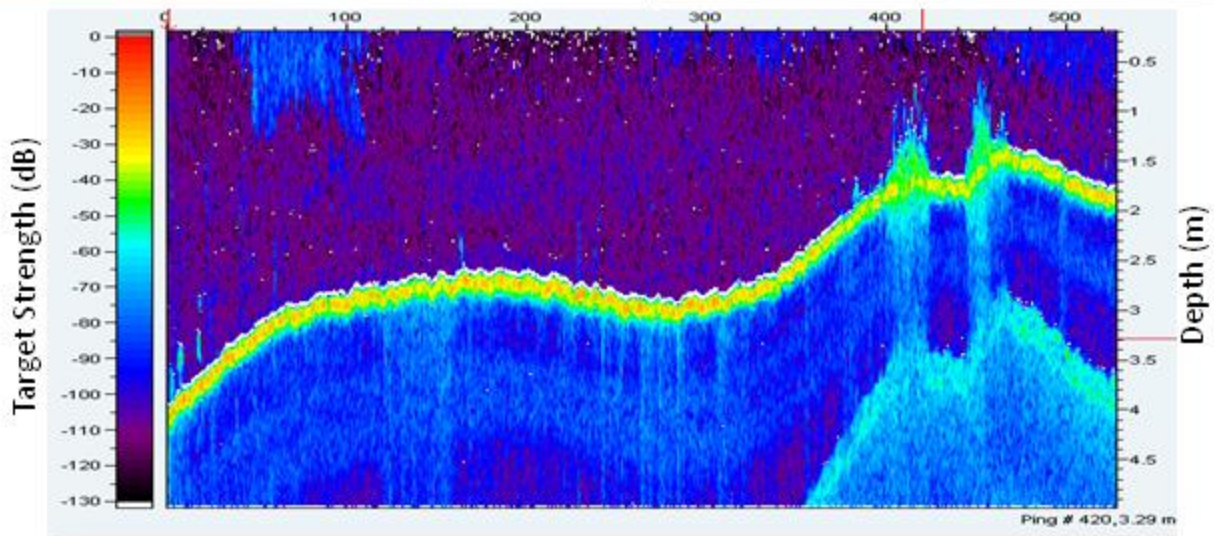
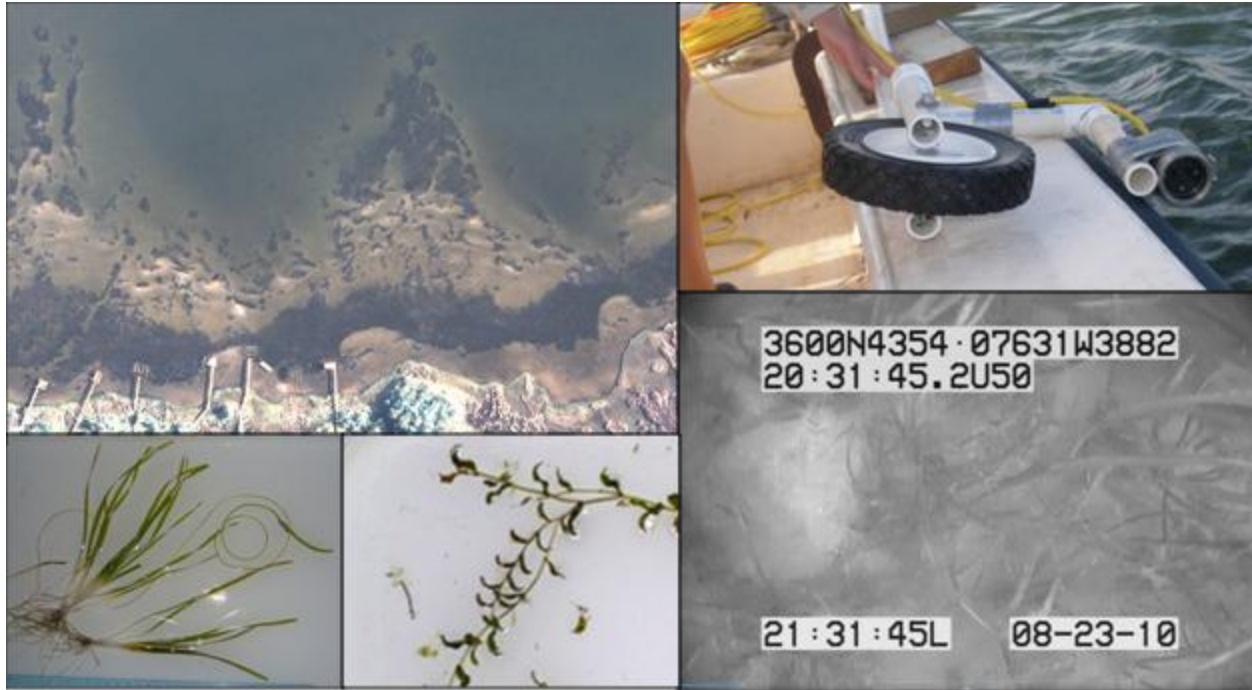


DEVELOPMENT OF SUBMERGED AQUATIC VEGETATION MONITORING PROTOCOLS IN NORTH CAROLINA



DEVELOPMENT OF SUBMERGED AQUATIC VEGETATION MONITORING PROTOCOLS IN NORTH CAROLINA

By:

W. Judson Kenworthy^{1,2}
Christine A. Buckel²
Dean E. Carpenter³
David B. Eggleston⁴
Don Field²
Cecilia S. Krahforst⁵
Joseph J. Luczkovich⁶
Gayle R. Plaia⁴

¹109 Holly Lane, Beaufort NC

²National Oceanic and Atmospheric Administration, NOS, NCCOS, Center for Coastal Fisheries and Habitat Research, Beaufort, NC

³Albemarle Pamlico National Estuary Program, Raleigh, NC

⁴Center for Marine Sciences and Technology, Dept. Marine, Earth & Atmospheric Sciences, North Carolina State University, Raleigh, NC

⁵Coastal Resources Management Doctoral Program, East Carolina University, Greenville, NC

⁶Department of Biology and Institute for Coastal Science and Policy, East Carolina University, Greenville, NC

Original CRFL project title:

Development of a Performance-Based Submerged Aquatic Vegetation Monitoring and Outreach Program for North Carolina

Applicants: Dean E. Carpenter, Joseph J. Luczkovich, W. Judson Kenworthy, David B. Eggleston and Gayle R. Plaia

Project Dates:

May 1, 2009 to September 21, 2012

Cover photos from top left clockwise: Aerial image near the NC Pine Knoll Shores Aquarium on Bogue Banks, North Carolina, showing dense and patchy SAV areas; underwater camera on wheeled mount; GPS, date, and time stamped underwater SAV video; screen grab of SONAR data classifying SAV in NC; sample of *Vallisneria americana*; and center sample of *Potamogeton perfoliatus*.

Table of Contents

List of Figures	vii
List of Tables	xiii
EXECUTIVE SUMMARY	1
INTRODUCTION AND OBJECTIVES	4
Review of SAV Monitoring Programs	11
Global Programs.....	12
Site-Specific Programs.....	13
Objectives.....	19
METHODS	19
Study Sites.....	19
Intensive Assessment Sites.....	20
Newport River.....	21
Jarrett Bay.....	21
Sandy Point.....	22
Blounts Bay	22
Rapid Assessment Sites.....	22
Boat-Based Monitoring Techniques.....	24
Underwater Videography.....	24
Video Classification Training.....	26
SONAR Monitoring Method	28
Diver Surveys	31
Remote Sensing Monitoring Method	31
Sampling Design.....	32
Intensive Assessment Sites.....	32
Rapid Assessment Sites.....	34
Time and Costs Estimates of Monitoring Methods	36
Data Analysis	36
Fraction of SAV	36
Accuracy Assessment.....	37
Surface Interpolation Analyses.....	37
Power Analyses for Detecting Change in SAV Abundance.....	40
Simulated Video Transects	40
Simulated SONAR Transects	43
RESULTS	44
Boat-Based Monitoring Techniques.....	44
Underwater Videography.....	44

Intensive Assessment Sites.....	44
Video Classification Training and Observer Calibration	54
SONAR	60
Intensive Assessment Sites.....	60
Diver Surveys	72
Rapid Assessment Sites.....	73
Fraction of SAV	73
Accuracy Assessment.....	74
Power Analyses for Detecting Change in SAV Abundance.....	74
Simulated Video Transects	74
Simulated SONAR Transects	76
Remote Sensing Results	78
Accuracy Assessment of Remote Sensing.....	80
Time Requirements for Monitoring Techniques	81
SONAR and Underwater Videography	81
Diver Surveys	81
Remote Sensing	82
DISCUSSION.....	83
Strengths & Limitations of Underwater Videography.....	83
Strengths & Limitations of SONAR	85
Strengths & Limitations of Diver Surveys	89
Strengths & Limitations of Kriging and Cokriging SONAR Data.....	92
Strengths & Limitations of Remote Sensing Surveys.....	93
Monitoring Tool Comparisons.....	94
Monitoring Protocol Recommendations.....	97
General Monitoring Strategy.....	97
Geographical Stratification	99
Phased Sampling Program.....	100
Mechanism for Establishing Priorities.....	100
Sentinel Sites.....	101
Definition of Sentinel Sites.....	102
Sentinel Site Selection in North Carolina	103
Sampling Strategy and Design.....	107
Sampling Metrics	108
Proof-of-Concept for Developing a Combined SONAR and Underwater Video Survey Method for SAV in the Albemarle - Pamlico Estuarine System.....	110
Sentinel Site Approach Using Intensive Site NPR (June 2009) as an Example.....	110
Suggested Project Design for SAV Acoustic Reconnaissance Surveys for Low-Salinity Areas in the Albemarle – Pamlico Estuarine System	116
Conclusions.....	117

Annual Budget Expenditures	119
Budget Deviations.....	119
REFERENCES	121
APPENDICES	130
Appendix 1. Preparing video files for classification	131
Appendix 2. Converting decimal degree to degree decimal minutes.....	133
Appendix 3. EcoSAV2 Algorithm	136
Appendix 4. Specifications for remote image acquisition for SAV classification in NC	138
Appendix 5. Selecting systematic random transects with GIS	139
Appendix 6. Selecting random quadrat locations.....	141
Appendix 7. Creating a Cokriging Surface Map from SONAR Reports.....	142
Creating a Cokriging Surface of the SAV Bed.....	142
Creating a Kriging Surface of Depth.....	144
Appendix 8. Depth Kriging and SAV Cokriging Models from the SONAR Acoustic Reports	145
Newport River.....	145
Jarrett Bay.....	148
Blounts Bay	149
Sandy Point.....	151

List of Figures

Figure 1. Submerged Aquatic Vegetation (SAV) salinity zones in North Carolina. Salinity zones were delineated based on principal SAV species present as noted in CHPP (Street et al. 2005, Deaton et al. 2010). Water body and landmark abbreviations: AS, Albemarle Sound; PS, Pamlico Sound; CH, Cape Hatteras; OI, Ocracoke Inlet; CL, Cape Lookout; CF, Cape Fear. 5

Figure 2. Map of submerged aquatic vegetation (SAV) in North Carolina. Dense SAV (>70% cover) is noted in red, patchy SAV is identified in yellow. This map was published in 2011 by the Albemarle-Pamlico National Estuary Program (APNEP). Water body abbreviations: Bogue Sound = BS, Bogue Sound; BkS = Back Sound. 6

Figure 3. Three seagrass distribution archetypes common to high-salinity environments of NC. These are images taken from: A. Shoreline fringing bed with continuous and patchy SAV cover in Bogue Sound, B. Patchy bed in Core Sound, C. Continuous bed in Core Sound interspersed with unvegetated blowouts 7

Figure 4. SAV species found in the high salinity environments of coastal North Carolina. Photos by P. Prado. 7

Figure 5. Abundance throughout the year of three seagrass species commonly found in high-salinity environments of North Carolina..... 8

Figure 6. SAV species found in the low salinity environments of coastal North Carolina. 9

Figure 7. Intensively studied sites in 2009 and 2010 at Sandy Point (SPS), Blounts Bay (BLB), Jarrett Bay (JBS), and Newport River (NPR), and their average environmental conditions.20

Figure 8. Study areas for rapid assessment study sites (low-salinity areas) using shore-parallel SONAR surveys paired with systematic drop camera points. 23

Figure 9. Underwater SAV video collection methods. (A) Schematic of vessel-mounted underwater video camera; (B) photograph of the underwater camera (Sartek®) and wheel mount; (C) screen capture of underwater video with position, date, and time stamp from the vessel-mounted GPS and electronics. Camera is in down-facing orientation at a fixed height above the bottom (13 cm) and frame size of 0.04 m². 25

Figure 10. Diagram of underwater video and geographic data collection methods. Merging video from a high resolution underwater camera (Sartek®) with high precision differential global positioning system (DGPS, Trimble®) while in the field produced geo-rectified underwater video that was classified in the laboratory. 26

Figure 11. SONAR system (BioSonics DTX echosounder with single-beam 420-kHz transducer, and Panasonic Toughbook laptop computer for data acquisition). BioSonics ECOSAV2 software was used to post-process each data file acquired by the DTX. All pings are classified by the ECOSAV2 algorithm as positive or negative for SAV and each acoustic report of 10 pings is summarized by latitude and longitude as % SAV cover (number of SAV-positive pings/10 possible pings x 100) in the ECOSAV2 output. The upper diagram (from BioSonics, Inc.) shows how the SONAR system is used from a moving vessel with two hypothetical acoustic reports shown (yellow pings are SAV positive, brown pings are SAV negative). Each ping in the diagram is shown as a circle, with 10 acoustic pings per report cycle, and all reports are geo-referenced at the mid-ping location using differential GPS. In this example, 40% SAV and 70% SAV was measured for the two acoustic reports. The bottom panel is an echogram showing what appears to the operator on screen of the

laptop as the vessel has passed over a SAV bed (green acoustic targets above the bottom between pings 400 and 500). Depth (m) was collected at each ping as well, so a continuous display of bottom depth and SAV coverage was obtained along transects, and these variables (date, time, latitude, longitude, % SAV cover depth, and plant height in cm above bottom) are reported by ECOSAV2 in an output file 29

Figure 12. Left: The echogram from Visual Acquisition software of the SAV at NPR acquired by the BioSonics DTX system in June 2009. The SAV plants are visible as a green region extending above the bottom beginning at approximately ping 400. The ultra-quiet zone (white zone) just above the bottom is an indication that the bottom is not covered with SAV at pings prior to that. Right: The single-ping echo envelope of the same site at ping number 770 (SAV-positive arrow shown in echogram). The echo envelope shows a bottom echo at 1.1 m depth and a plant echo extending from the bottom to echo to the depth of 0.9 m (canopy height). From this difference (canopy depth to bottom depth), a SAV plant height can be computed. EcoSAV2 algorithm parameters are indicated on this overlay..... 30

Figure 13. A visual depiction of a systematic sampling of a potential SAV study site, using a grayscale image of seagrass distribution in NC. The placement of the first transect is selected randomly anywhere to the left of the dashed line; thereafter, transects (solid lines) are equally spaced across the baseline of the survey area. 33

Figure 14. Photos of the SONAR (Biosonics DTX transducers on tow body, BioFin) and tow body being deployed at NR..... 35

Figure 15. Three seagrass distribution archetypes, common to high-salinity areas of NC, used in power analyses. In each case, an aerial photograph was taken from Bogue or Back Sound, NC, digitized such that individual pixels represented approximately 0.333 m x 0.333 m, the area typically in each video frame along boat-based transects. Gray represents cells occupied by SAV (presence), while white represents absence of SAV. 41

Figure 16. Fraction of SAV cover by transect at NPR in 2009, as classified by underwater video methods. Grand mean fraction SAV cover (\pm SE) by transect direction (E-W and N-S) are also provided. 45

Figure 17. Classified underwater video transects at NPR overlain on an aerial photograph of the site. Each point represents a classified video frame; SAV presence is colored green and absence is beige. SAV extent, based on aerial imagery from the 2006-2008 statewide SAV mapping, is delineated by yellow polygons. Dark areas in lower portion of the image are emergent marsh. 46

Figure 18. Fraction of SAV cover by transect at JBS and mean (\pm SE) for all transects in 2010 classified by underwater video..... 47

Figure 19. Classified underwater video from JBS in 2010. Each point represents a classified video frame; SAV presence is colored green and absence is beige. SAV extent, based on aerial imagery from the 2006-08 state-wide SAV mapping, is delineated by green (dense SAV) and yellow (patchy SAV) polygons..... 48

Figure 20. Fraction of SAV cover by transect and mean (\pm SE) for all random transects, excluding drops, at SPS in 2010, as classified by underwater video. 50

Figure 21. Classified underwater video from SPS in 2010. Each point represents a classified video frame; SAV presence is colored green and absence is beige. SAV extent, based on aerial imagery from the 2006-2008 state-wide SAV mapping, is delineated by green (dense) and yellow (patchy) polygons. 51

Figure 22. Fraction of SAV cover by transect and mean (\pm SE) for all random transects, excluding cross, at BLB in 2010 classified by underwater video.....	52
Figure 23. Classified underwater video from BLB in 2010. Each point represents a classified video frame; SAV presence is colored green and absence is beige. SAV extent, based on aerial imagery from the 2006-2008 state-wide SAV mapping, is delineated by polygons. .	53
Figure 24. Fraction of SAV for all observers (five novice [NOV] and three expert [EXP]) and all tracks. For repeated tracks, initial classifications are plotted (n per track ranged from 180 – 197).	55
Figure 25. Mean fraction SAV as classified by expert (n = 3) and novice (n = 5) classifiers from underwater video.....	55
Figure 26. Fraction SAV for replicate tracks by observer, five novice (NOV) and three experts (EXP).	58
Figure 27. Fraction SAV as quantified by observers (five NOV and three EXP) by replicates for three repeated tracks.	59
Figure 28. The fraction of SAV ($F_{sav} \pm 1 S.E.$) derived from SONAR at the four intensive sites in the SAV growing season in 2010. The growing season was defined as May through September and divided into samples taken early (May-June) and late (Aug – Sep) in the growing season.....	60
Figure 29. Transects driven at NPR in June 2009 by the SONAR (yellow dots) and underwater video (black dots) methods.	62
Figure 30. Two examples of the nearest neighbor accuracy analysis at the SONAR comparison points: A) NPR June 2009 and B) SPS August 2010. The circles represent points of agreement that no SAV is present (brown), SAV is present (green), or points of disagreement about the presence of SAV (yellow) between the underwater video and SONAR.	64
Figure 31. The SAV surface, rated as either SAV present or absent, using three cokriging models at NPR in June 2009: 1) the Ideal Cover model, which uses SAV cover (%) estimated from the acoustic reports produced in EcoSAV2; 2) the Ideal Binary model that uses a lag distance of 12 m and the 25 nearest neighbors; and 3) the Local Binary model, which uses a lag distance of 10 m and 6 nearest neighbors. The Ideal Binary and Local Binary cokriging models are very similar to one another, providing the greatest estimated area of SAV coverage. The Ideal Cover has the lowest area of SAV cover. All three models agree that a large bed of SAV is located in the lower right (SE corner) of the site. Ideal cover model does not show a bed in the upper right (NW corner) of NPR.	66
Figure 32. The bootstrapping accuracy values (relative to video classification) for 100 randomly selected comparison points, replicated 100 times for the three cokriging models used to estimate the presence of SAV at NPR in June 2009. The Ideal Binary model used depth (m) and presence-absence data on SAV determined from SONAR and ECOSAV2, with a lag distance of 12 m and 25 nearest neighbors to predict the surface. The Ideal Cover model used depth (m) and SAV cover (%) from ECOSAV2 acoustic reports to predict the surface, with a lag distance of 13 m and 35 nearest neighbors. The Local Binary SAV model used a “local” smoothing of the depth and SAV presence-absence data, with lag distance of 10 m and 6 nearest neighbors to predict the surface. The cross-validation results of the first and third models were optimized. The line within the box indicates the median, the upper and lower hinges includes the 25 th and 75 th percentiles, and * represent outlier values 1.5 times the inter-quartile range from the upper and lower quartiles	67

Figure 33. The prediction surface of depth using a kriging analysis obtained from classified SONAR reports at the four intensively-studied sites. Each image is from the 2009-2010 study period at: A) NPR (June 2009), B) JBS (June 2010), C) BLB (August 2010), and D) SPS (June 2010).....	68
Figure 34. The prediction surface showing the presence or absence of SAV using a cokriging analysis of depth and SAV (0, 1) obtained from classified SONAR reports at the four intensively-studied sites. Each image shows the peak prediction during the 2009-2010 study period at: A) NPR (June 2009), B) JBS (June 2010), C) BLB (August 2010), and D) SPS (June 2010).....	70
Figure 35. Relative area of SAV (R_{sav}) at JBS 2010 (black square), NPR 2009 (blue triangle), NPR 2010 (blue square), BLB 2010 (red circle), and SPS 2010 (pink circle) using the cokriging surface created from the SAV presence/absence data from SONAR reports.....	71
Figure 36. Accuracy of SONAR at the Rapid Assessment Sites and over all seven sites in the 2011 sample event.....	74
Figure 37. Predicted power to detect 10% declines (top panels), 20% declines (middle panels), and 40% declines (bottom panels) in SAV as a function of number of transects. Left panels give results for contiguous habitat, center panels give results for patchy habitat, and right panels give results for the blowout study area. Black circles represent results from simple random sampling (SRS), red triangles give results for systematic sampling where the naïve SRS variance estimator is employed (SYS_1), and blue x's give results for systematic sampling using the approach of Fewster (2011) to get variance estimates (SYS_2). Also shown are the realized proportion of simulations that resulted in type I errors (α).....	75
Figure 38. Power to detect 10%, 20%, and 40% change in SAV simulated over a surface obtained from the Ideal Binary cokriging model at each of the intensive sites using three power simulation models: 1) SRS (black circles), 2) SYS_1 (red triangles) and 3) SYS_2 (blue x's). In each case, the SYS_2 (Fewster 2011) model has the greatest power to detect changes with a small number of transects. With all simulations, fewer transects are required to detect a 40% change in SAV than 20% or 10% change.....	77
Figure 39. Dense (dark green) and patchy (light green) SAV distribution in NC mapped as part of the 2007-2008 coast-wide effort.....	78
Figure 40. Aerial images (represented as dots) collected during the 2007/08 coast-wide SAV mapping effort. Photos in regions of high (green) and low (blue) salinity are indicated. ...	79
Figure 41. Coefficient of variation (CV) in estimates of predicted SAV density as a function of the number of transects and sampling design/analysis type. Left panels give results for contiguous habitat, center panels give results for patchy habitat, and right panels give results for the blowout study area. Black circles represent results from simple random sampling (SRS), red triangles give results for systematic sampling where the naïve SRS variance estimator is employed (SYS_1), and blue x's give results for systematic sampling using the approach of Fewster (2011) to get variance estimates (SYS_2).	91
Figure 42. North Carolina estuary and river systems highlighting areas that can (green) and cannot (brown) reliably detect SAV using aerial surveys. Water body abbreviations: AS, Albemarle Sound; PS, Pamlico Sound; CH, Cape Hatteras; OI, Ocracoke Inlet; CL, Cape Lookout; CF, Cape Fear.....	94
Figure 43. Proposed geographical stratification of North Carolina estuaries and river systems. SAV monitoring would be phased in across five zones and implemented in a rotational sampling scheme over time.....	98

Figure 44. SAV prediction surface from cokriging at NPR.....	112
Figure 45. Standard error (SE) associated with the SAV prediction surface at intensive site NPR using geospatial cokriging of SONAR data.....	112
Figure 46. One hundred random underwater video validation points were used to assess the accuracy of the SAV prediction surface at intensive site NPR using cokriging. Underwater video points were stratified by total area of each standard error (SE) classification: low (n = 38), medium (n = 55), and high (n = 7).	113
Figure 47. The accuracy within each standard error (SE) stratum from cokriging surfaces of SONAR obtained at intensive site NPR in 2009 when compared against different number of video drop camera points. For each level of video camera sampling effort, a re-sampling estimate of 100 bootstrapped samples was used to derive the mean accuracy.....	115
Figure 48. The data collected at the NPR SAV bed (Jun. 2009 and May - Sep. 2010). The SONAR transects are represented by circles with both SAV-positive (purple) and SAV-negative (white) acoustic reports. The cokriging surface results show the interpolation of the acoustic report data as SAV-positive (green) polygons and SAV-negative (cream) polygons. Diver survey quadrat locations are indicated in squares. Quadrats without SAV are black, quadrats with SAV have proportionally increasing orange squares.....	146
Figure 49. The depth data collected using SONAR acoustic reports at the NPR SAV bed (Jun. 2009 and May - Sep. 2010). A depth polygon is represented as a gradation of color from shallow (red) to deep (blue). The data collection in May 2010 was interrupted during the survey, thus making the bathymetry inaccurate for that month. On that day, a 2-m tidal range occurred, and the eastern side data was collected at high tide and the western size collected at low tide.	147
Figure 50. The data collected at the JBS SAV bed (Jun. - Sep. 2010). The SONAR transects are represented by circles with both SAV-positive (purple) and SAV-negative (white) acoustic reports. The cokriging surface results show the interpolation of the acoustic report data as SAV-positive (green) polygons and SAV-negative (cream) polygons. Diver survey quadrat locations are indicated in squares. Quadrats without SAV are black, quadrats with SAV have proportionally increasing orange squares.....	148
Figure 51. The depth data collected using SONAR acoustic reports at the JBS SAV bed (Jun. - Sep. 2010). A depth polygon is represented as a gradation of color from shallow (red) to deep (blue).	149
Figure 52. The data collected at the BLB SAV bed (May - Sep. 2010). The SONAR transects are represented by circles with both SAV-positive (purple) and SAV-negative (white) acoustic reports. The cokriging surface results show the interpolation of the acoustic report data as SAV-positive (green) polygons and SAV-negative (cream) polygons. Diver survey quadrat locations are indicated in squares. Quadrats without SAV are black, quadrats with SAV have proportionally increasing orange squares.....	150
Figure 53. The depth data collected using SONAR acoustic reports at the BLB SAV bed (May - Sep. 2010). A depth polygon is represented as a gradation of color from shallow (red) to deep (blue).	151
Figure 54. The data collected at the SPS SAV bed (Jun. - Sep. 2010). The SONAR transects are represented by circles with both SAV-positive (purple) and SAV-negative (white) acoustic reports. The cokriging surface results show the interpolation of the acoustic report data as SAV-positive (green) polygons and SAV-negative (cream) polygons. Diver survey quadrat locations are indicated in squares. Quadrats without SAV are black, quadrats with SAV	

have proportionally increasing orange squares. The study site was extended in Aug. and Sep. 2010 to identify the edge of the SAV bed at this site. 152

Figure 55. The depth data collected using SONAR acoustic reports at the SPS SAV bed (Jun. - Sep. 2010). A depth polygon is represented as a gradation of color from shallow (red) to deep (blue). The study site was extended in Aug. and Sep. 2010 to identify the edge of the SAV bed at this site..... 153

List of Tables

Table 1. General characteristics of representative large scale SAV monitoring programs. Shown are three international programs and six from the United States. Characteristics include the approximate area of the water body where the monitoring occurs (km²), longevity of the monitoring program, and sampling frequency. Also shown are the different sampling designs and approaches used in each program indicated by either yes or no. NA = not applicable. ND = not determined. * In the Indian River Lagoon fixed transects are sampled every six months and aerial remote sensing is planned for every two years. # Performance-based monitoring program. 14

Table 2. Summary of study site types, site names and abbreviations, and salinity levels. 21

Table 3. Description of SAV habitat attributes for selected video tracks used in the observer calibration exercise, including total number of image classifications (total classifications). Segments denoted by asterisk were classified three times by each observer. Fraction of SAV (F_{sav}) was calculated as mean of all observers and all replicates for each track. 27

Table 4. Months in 2009 and 2010 where SONAR (S), video (V), and quadrat (Q) surveys were conducted at each intensively surveyed site. 33

Table 5. Sampling effort and Fraction of SAV from NPR using classified underwater video transects and quadrats (1 m²). 45

Table 6. Model II ANOVA effects table. 54

Table 7. Fraction of SAV by observer for all test tracks. Only the initial classifications of repeated tracks (denoted by *), were used in this comparison. 56

Table 8. Fraction of SAV by observer for all replicate video tracks including the absolute maximum difference of the fraction of SAV for an individual track replicate (max diff) and mean of absolute differences of the fraction of SAV. 57

Table 9. Repeated measures ANOVA of the F_{sav} data derived from SONAR method by factors Site and within-Site by Season in 2010. 61

Table 10. Hypothesis tests (repeated measures ANOVA F_{df} , and P-values) of no change in fraction of SAV (F_{sav}) between the early and late growing season in 2010 within each of the intensive sites. 61

Table 11. The mean fraction of SAV ($F_{sav} \pm S.E$) at the four intensive sites for each month sampled (May – September) derived from SONAR data in 2010. 61

Table 12. Accuracy of the SONAR at the four intensive sites and over all sites (2009/2010) at a nearest neighbor distance of 3 m and a depth ≥ 0.7 m. 63

Table 13. The total area and SAV-present area determined from a cokriging analysis of SAV presence/absence and depth (m) obtained at each site and date by SONAR surveys. The relative area of SAV (RA_{sav}) represents the proportion of the area covered by SAV by year, month, and site. The Ave. SE is the average standard error of the cokriging model, which is a combination of both measurement error and the variation around an interpolated point (see Appendix 8). In August and September 2010, the SPS site was extended offshore by 150 m (SPS Extend) to capture the deep edge of the bed. *Individual cokriging models were not produced for the extended regions. Instead, the extended models were clipped to the 90,000 m² study region. 69

Table 14. The best fit line for F_{sav} by month (2010) for the four intensively surveyed sites with divers. 73

Table 15. Survey date (2011), number of acoustic reports obtained along each transect, mean depth sampled, F_{sav} , maximum and median SAV patch lengths, and maximum and median unvegetated patch lengths at rapid assessment sites.	73
Table 16. Time requirements (hours) per transect and site for underwater video, SONAR, and quadrat data collection and analysis. This quadrat data cost-calculation is to check the accuracy of the cokriging surface predicted by the SONAR.	82
Table 17. One-time costs associated with evaluated SAV monitoring tools.	83
Table 18. Mean and standard deviation (SD) of F_{sav} by transect and method at each intensive site and over all four sites. Relative change detection levels between 10 and 40% were calculated for each method and used in the power analysis.	95
Table 19. The parameters used in the SAV (binary), depth (m) cokriging models produced for each site for each survey period (month, year). The parameters selected were model type, anisotropy, lag size (in m), and number of nearest neighbors. All other parameters were kept at the default levels.	154
Table 20. The results of the SAV (binary), depth (m) cokriging models produced for each site for each survey period (month, year). The parameters were optimized to obtain a model that has a mean = 0, root-mean-square = 0, average standard error = 0, mean standardized = 0, and root-mean-square standardized = 1.	154
Table 21. The parameters used in the depth kriging models produced for each site for each survey period (month, year). The parameters selected were model type, anisotropy, lag size (in m), and number of nearest neighbors. All other parameters were kept at the default levels.	155
Table 22. The results of the depth kriging models produced for each site for each survey period (month, year). The parameters were optimized to obtain a model that has a mean = 0, root-mean-square = 0, average standard error = 0, mean standardized = 0, and root-mean-square standardized = 1.	155

EXECUTIVE SUMMARY

In North Carolina (NC) coastal waters, submerged aquatic vegetation (SAV) consists of a diverse group of vascular plants that live in subtidal and intertidal waters in both high-and low-salinity environments. SAV is widely recognized for many important ecological functions, such as critical habitat for recreationally important species of fish, shellfish and invertebrates, and for providing a wide range of ecological and economic services to human populations. The importance of protecting and restoring these functions in NC are acknowledged within high-profile strategic plans such as the Coastal Habitat Protection Plan (CHPP) and the Albemarle-Pamlico National Estuary Program's Comprehensive Conservation Management Plan (CCMP).

Despite the need for regular SAV assessments to support adaptive management of a vital resource covering over 56,000 hectares (138,000 acres), where losses are not easily reversed and restoration is expensive and uncertain, there are no long-term SAV monitoring programs established in NC that can provide reliable quantitative data on its status and trends. Furthermore, the extensive size of the NC coastal ecosystem along with its multi-dimensional bio-physical complexity and the uncertainties of remote sensing have made it very difficult to implement a comprehensive coast-wide SAV monitoring program. In response to this deficiency, this report summarizes the results of a two-year project funded by the NC Coastal Recreational Fishing License (CRFL) Program to investigate the development of SAV monitoring protocols and recommendations for implementation of such a program.

Taking into consideration the large size, multi-dimensional complexity and prior experience in the NC estuarine system, we evaluated approaches to monitoring that incorporate multiple methods and scales. Based on a review of the methods used in other programs, we examined the potential application of two non-destructive boat-based methods in combination with aerial remote sensing. Hence, the specific project objectives were to: 1) determine the feasibility of developing monitoring protocols with a performance measure capable of detecting at least a 10% inter-annual change in SAV abundance, 2) evaluate a point-intercept visual census technique using a low-light underwater video camera deployed from a small vessel, 3) evaluate a boat-based hydroacoustic technique using the BioSonics 420 kHz single beam SONAR system with EcoSAV2 software deployed from a small vessel, 4) evaluate the capabilities of remote sensing SAV using aerial imagery, and 5) develop recommendations for implementing a state-wide monitoring program incorporating the best available methods.

Two types of study sites were established to evaluate underwater video and SONAR methods. "Intensive assessment" sites measuring approximately 0.09 km² involved more intensive data collection at a site and comprehensive testing of underwater video and SONAR techniques. More intensive data collection was necessary to test the feasibility of developing a

monitoring program capable of detecting subtle intra- and inter-annual change in SAV abundance. The primary objective of “rapid assessment” sites, running along a 10-km transect at the 1 m depth contour, was to explore a new technique to rapidly survey and map areas of low salinity by identifying SAV presence/absence. This method targeted only low-salinity areas because SAV classification based on aerial imagery in this environment has been unreliable and thus SAV distribution and abundance is largely undefined. Four intensive study sites were selected for the evaluation of our boat-based methods and protocols, two were in high-salinity environments (Newport River and Jarrett Bay) and two were in low-salinity environments (Blounts Bay and Sandy Point). Nine rapid assessment study sites were selected that represent SAV beds in low-salinity environments.

SAV beds were photo-interpreted (digitized) into two classes (continuous and sparse beds) with minimum mapping units of 0.03 ha, based on aerial imagery for coastal NC that was collected over a two-year period prior to this investigation yet specifically acquired to detect SAV.

Based on the need for a solution to a very challenging sampling problem with limited financial and infrastructure resources, our evaluation of the three monitoring tools suggested the use of a combination of methods in a phased approach organized by geographical stratification and implemented in a rotational sampling scheme. Based on SAV community composition and distinctive physical attributes, we propose that the NC coastal ecosystem be stratified into two large zones: high salinity and low salinity, then each stratified further by basin-scale areas. However, differences in watershed and estuarine characteristics among the strata, as well as potential differences in SAV communities and stressors, warrant more detailed consideration of these further subdivisions. Stratification based on measureable and meaningful characteristics has another important benefit by reducing the size of the monitoring area. Reducing the size of the monitoring areas to smaller and more discrete manageable units will facilitate prioritization of actions, program development, and implementation of monitoring plans.

We recommend that sampling be conducted in phases beginning with the immediate planning and implementation of a remote sensing acquisition of SAV coverage in the barrier island shelf and lagoon stratum. Concurrent with the remote sensing effort, we recommend initiating a second phase of the program whereby sentinel sites are established in a designated high-priority stratum in the low-salinity zone. Once the sentinel sites are selected in the high priority stratum, a boat-based pilot monitoring project should be initiated using the best available monitoring methods.

In concert with these initial phases of aerial and sentinel site monitoring, we propose two activities to help refine the monitoring protocol. Through a proof-of-concept scenario, we recommend development of the combined SONAR and underwater video camera method and,

where necessary, snorkel and diver quadrat surveys. We also suggest a design for SAV acoustic reconnaissance surveys for low salinity areas, thereby gaining knowledge about the extent of SAV that is hidden from aerial surveys.

INTRODUCTION AND OBJECTIVES

In North Carolina (NC) coastal waters, submerged aquatic vegetation (SAV) consists of a diverse group of vascular plants that live in subtidal and intertidal waters in both high-and low-salinity environments (Thayer et al. 1984, Ferguson and Wood 1994, Mallin et al. 2000, Deaton et al. 2010). SAV are recognized worldwide for many important ecological functions such as critical habitat for recreationally important species of fish, shellfish, invertebrates and wildlife, and providing a wide range of economic services to human populations conservatively estimated to be valued at \$12K per acre (Larkum et al. 2006). These functions are acknowledged in the NC Coastal Habitat Protection Plan (CHPP; Street et al. 2005, Deaton et al. 2010), prompting scientists, managers and the public to elevate their interest in closely monitoring the status and trends of SAV resources (Orth et al. 2006a). A recent assessment of monitoring programs worldwide revealed a global decline in seagrass abundance (Waycott et al. 2009). This assessment should be a concern for resource managers in NC, since there is evidence of marine SAV (seagrass) declines in other locations nearby in the mid-Atlantic region of the United States (US) and farther north in New England (Waycott et al. 2009, Orth et al. 2010; Costello and Kenworthy 2011). If SAV is changing (declining or increasing) in NC it is indeterminable at this time. There are no long-term SAV monitoring programs established in NC that can provide reliable quantitative data on the status and trends of the resource.

A further concern should be the recognition that SAV losses are not easily reversed and restoration is expensive and uncertain (Fonseca et al. 1998; Kenworthy et al. 2006). The development of a comprehensive long-term monitoring plan which assesses the status and trends of SAV resources and the stressors affecting them can be a valuable approach to minimizing and avoiding catastrophic losses or the need for restoration. Since SAV is a responsive bio-indicator of environmental change (Dennison et al. 1993, Biber et al. 2004), monitoring this resource can be used as a practical tool for early detection of environmental disturbance and anthropogenic impacts to coastal ecosystems in general.

In NC, SAV occurs in the second largest estuarine ecosystem in the continental United States. The greater proportion of this system, known historically as the Albemarle Pamlico Estuarine System (APES), is made up of a series of shallow sounds and inland waters that physically resemble large coastal lagoons with both high and low salinity regions (Figure 1). The largest inter-connected system ranges from Currituck Sound, near the border of NC and Virginia (VA), south to Bogue Sound and the White Oak River in Carteret County including Albemarle, Pamlico, Core, Back, and Bogue Sounds. Extending further south from the White Oak River, the inland waters down to Cape Fear consist of much narrower and smaller estuaries, lagoons, and regularly flooded tidal creeks inter-mixed with salt marshes. Nearly all of these

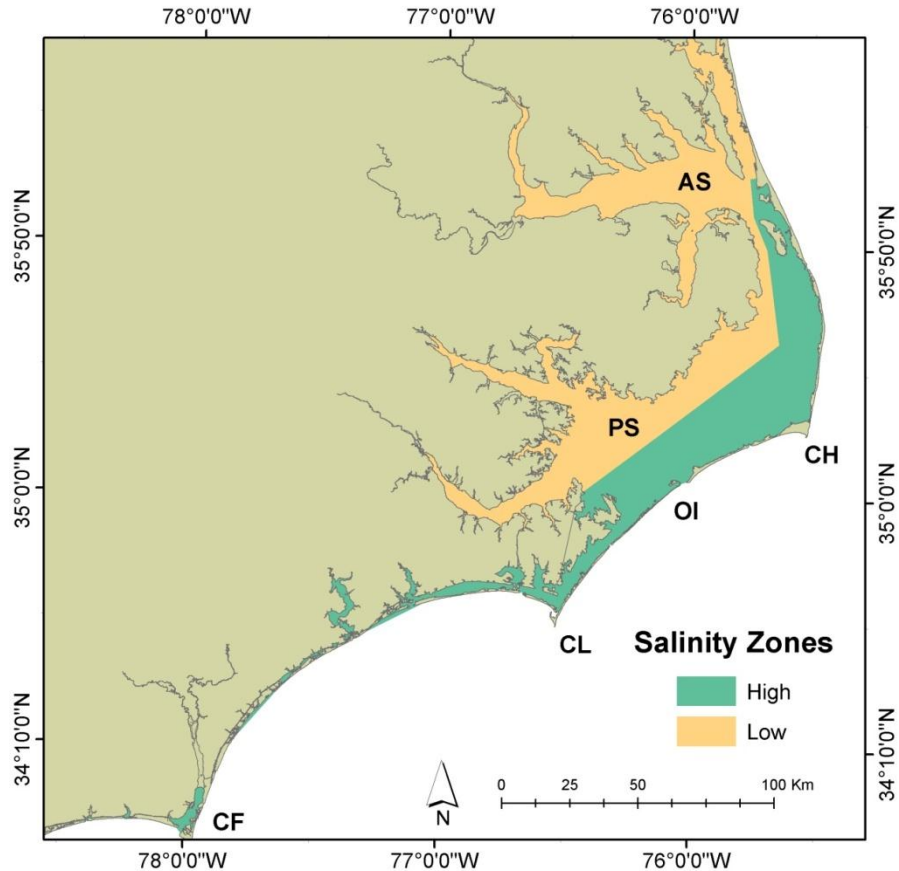


Figure 1. Submerged Aquatic Vegetation (SAV) salinity zones in North Carolina. Salinity zones were delineated based on principal SAV species present as noted in CHPP (Street et al. 2005, Deaton et al. 2010). Water body and landmark abbreviations: AS, Albemarle Sound; PS, Pamlico Sound; CH, Cape Hatteras; OI, Ocracoke Inlet; CL, Cape Lookout; CF, Cape Fear.

estuarine ecosystems are bordered on their eastern margins by barrier islands which protect the inland waters and SAV from the direct physical forces of the Atlantic and enable the development of shallow shelves and sounds leeward of the islands. Numerous inlets that pass through the barrier islands maintain regular tidal communication between the open Atlantic and the inland waters. This regular tidal exchange flushes the barrier shelves and sounds, diminishes water residence times, and maintains suitable water quality for SAV and other benthic primary producers to thrive in shallow water (< 2-3 m; Thayer et al. 1984, Wells and Kim 1989, Mallin et al. 2000, Street et al. 2005, Deaton et al. 2010). Largely for these reasons, the most extensive and well-documented SAV communities occur on the shallow shelves leeward of the barrier islands in the eastern margins of Pamlico, Core, Back, and Bogue Sounds (Figure 2, Carraway and Priddy, 1983, Ferguson and Wood 1994, Street et al. 2005, Deaton et al. 2010). The spatial distribution of SAV in these habitats is not always continuous. Distribution ranges from large meadows with nearly complete cover, to meadows with different degrees of patchiness and density (Figure 3). In this high-salinity zone, SAV communities are dominated by two marine

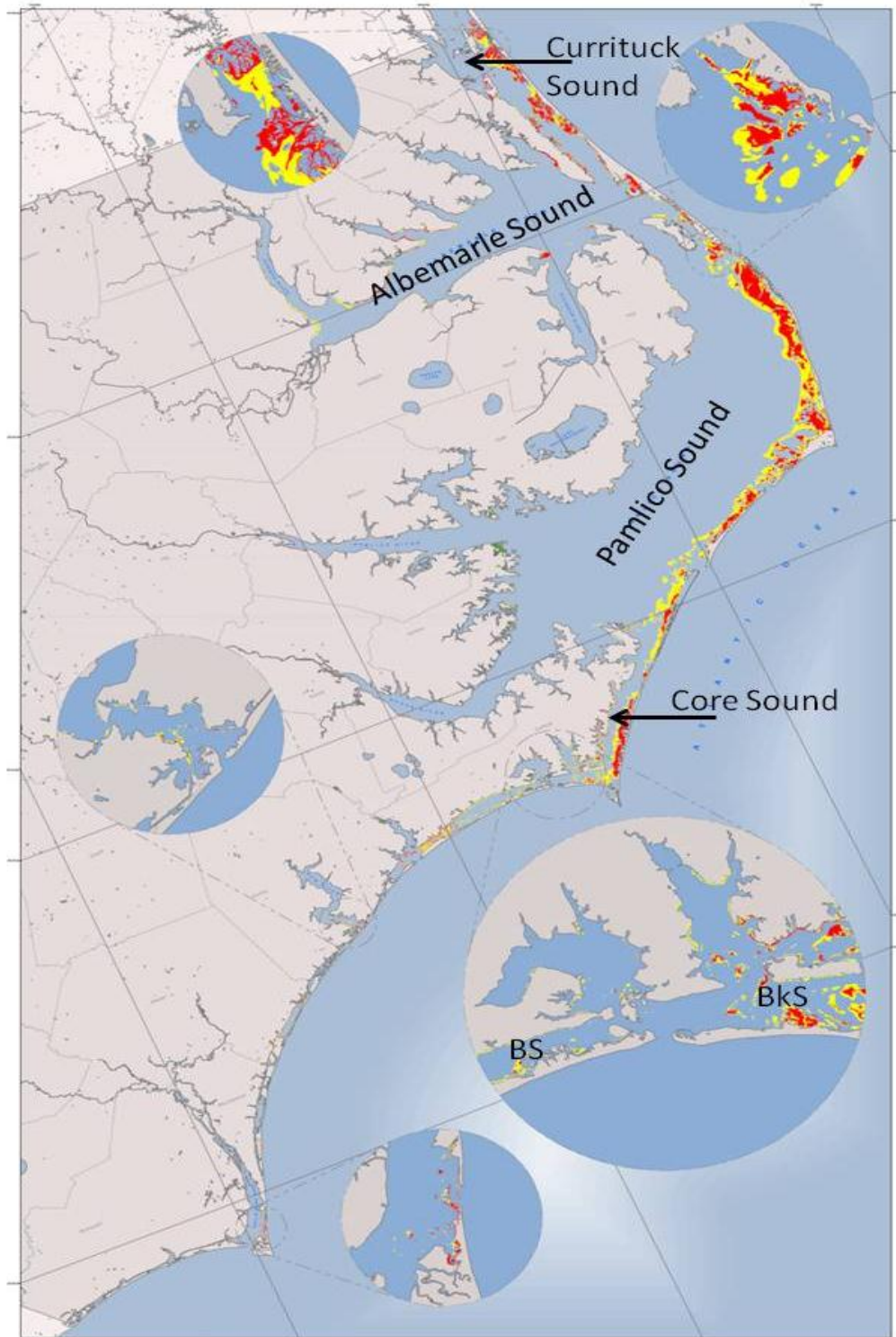


Figure 2. Map of submerged aquatic vegetation (SAV) in North Carolina. Dense SAV (>70% cover) is noted in red, patchy SAV is identified in yellow. This map was published in 2011 by the Albemarle-Pamlico National Estuary Program (APNEP). Water body abbreviations: Bogue Sound = BS, Bogue Sound; BkS = Back Sound.

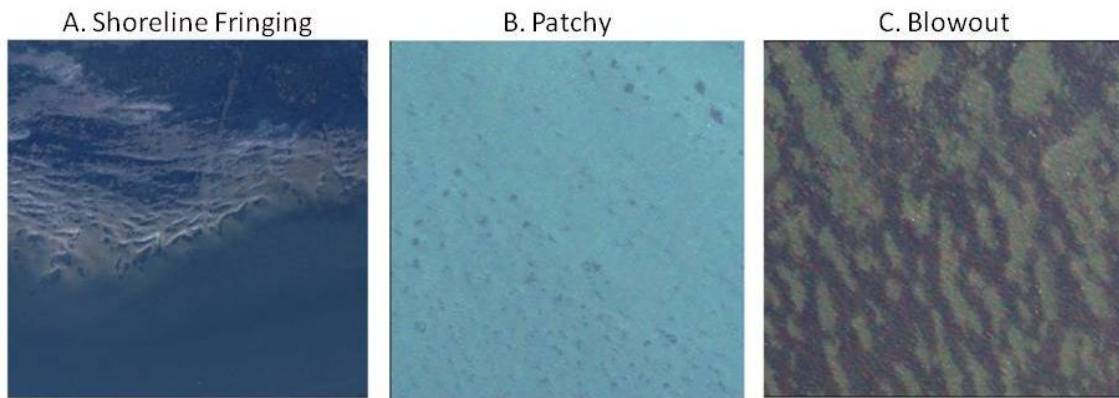


Figure 3. Three seagrass distribution archetypes common to high-salinity environments of NC. These are images taken from: A. Shoreline fringing bed with continuous and patchy SAV cover in Bogue Sound, B. Patchy bed in Core Sound, C. Continuous bed in Core Sound interspersed with unvegetated blowouts

seagrasses, *Zostera marina* and *Halodule wrightii*, with a third species (*Ruppia maritima*) intermixed with the other two. This third species is more tolerant of a wider salinity range than the other two marine seagrasses (Figure 4).

High-salinity species	Photos
<p><i>Halodule wrightii</i> (Shoal grass)</p> <p>Photo by: P. Prado</p>	
<p><i>Ruppia maritima</i> (Widgeon grass)</p> <p>Photo by: P. Prado</p>	
<p><i>Zostera marina</i> (Saltwater Eelgrass)</p> <p>Photo by: P. Prado</p>	

Figure 4. SAV species found in the high salinity environments of coastal North Carolina. Photos by P. Prado.

The marine SAV in the high salinity areas of NC is a unique community of species (Figure 4). *Zostera marina* is distributed throughout temperate regions globally and living at its southern range limit in NC. *H. wrightii* has a predominantly tropical distribution in the western hemisphere and is at its' northern range limit in NC. *Ruppia maritima* is a cosmopolitan species found in both temperate and tropical environments and frequently occurs with the other two species (Thayer et al. 1984, Street et al. 2005, Short et al. 2007, Deaton et al. 2010). Depending on species composition, intra- and inter-annual coverage in the meadows can vary substantially. Cooler water temperatures in the fall, winter and spring favor *Z. marina*, while the warmer summer and early fall temperatures favor *H. wrightii*. Mixed communities of these species display bi-modal peaks in seasonal abundances so that the optimal times for detecting and monitoring these species (index periods) are different (Figure 5).

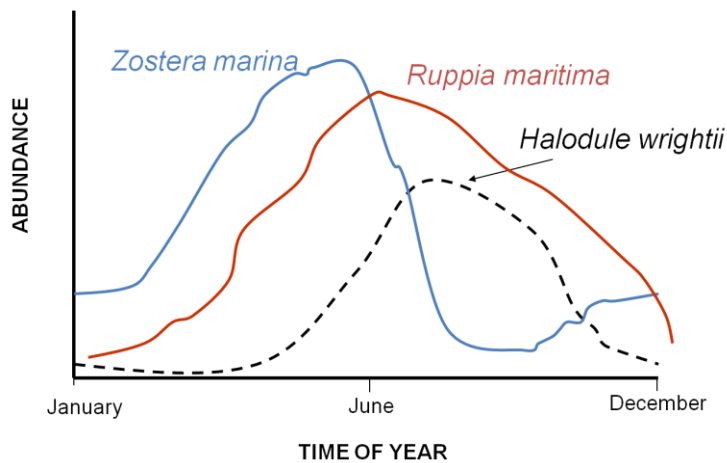


Figure 5. Abundance throughout the year of three seagrass species commonly found in high- salinity environments of North Carolina.

The distribution of these species is made even more complicated by the sexual reproductive strategy of *Z. marina*. Although each of the three species have perennial life history strategies, *Z. marina* reproduces prolifically by sexual reproduction and seed dispersal (Thayer et al. 1984, Jarvis et al., 2012), which leads to widespread distribution of annual meadows formed exclusively by seed. During summer periods of high temperature stress in shallow water, these annual meadows of *Z. marina* senesce and can completely disappear, so there is either minimal or no evidence of their distribution in mid- to late summer (Figure 5). In the following fall and early winter, *Z. marina* beds recover by seed, grow and expand rapidly by vegetative reproduction in spring, forming either patchily distributed or continuous meadows depending on reproductive success and the dispersal of seeds (Jarvis et al. 2012). *H. wrightii* is primarily a tropical seagrass, but does not reproduce sexually in NC and depends exclusively on asexual reproduction for growth, meadow maintenance and dispersal. This species thrives in the warmer season between late May and October and senesces in fall and winter when there is a significantly diminished abundance (Figure 5). *Ruppia maritima* reproduces both sexually and asexually, but is more ephemeral than either of the other two marine species and usually is found

as a sub-dominant component of the SAV bed in marine communities. *Ruppia maritima* abundance increases at locations more distant from the inlets, in the lower salinity environments of northern Pamlico Sound, and in Albemarle and Currituck Sounds (Ferguson and Wood 1994).

Environmental conditions and SAV communities in the rest of the NC coastal system are distinctly different from those which occur on the barrier shelves of Pamlico Sound and in Core, Back and Bogue Sounds (Street et al. 2005, Deaton et al. 2010, Figure 6). The western boundary of the estuarine system is bordered by a gradually sloping coastal plain with many large watersheds and numerous rivers that regularly deliver freshwater, colored dissolved organic matter and sediments to the coastal water bodies (Stanley 1992, 1993, Cooper 2000, Mallin et al. 2000) resulting in salinity decreases and increased turbidity proximal to the rivers (Figure 1).

Low-salinity species	Photos	Low-salinity species	Photos
<i>Ceratophyllum demersum</i> (Coontail) <small>Photo by: W. Wellner</small>		<i>Potamogeton perfoliatus</i> (Redhead grass) <small>Photo by: C.S. Krahforst</small>	
<i>Hydrilla verticillata</i> (Hydrilla) <small>Photo by: Wisconsin Dept. of Natural Resources</small>		<i>Ruppia maritima</i> (Wideon grass) <small>Photo by: C.S. Krahforst</small>	
<i>Myriophyllum spicatum</i> (Eurasian watermilfoil) <small>Photo by: C.S. Krahforst</small>		<i>Stuckenia pectinata</i> (Sago pondweed) <small>Photo by: K. Peters</small>	
<i>Najas quadalupensis</i> (Busy pondweed) <small>Photo by: wesserpest.com</small>		<i>Vallisneria americana</i> (Wild celery) <small>Photo by: C.S. Krahforst</small>	
<i>Potamogeton crispus</i> (Curly-leaf pondweed) <small>Photo by: P. Ferrari</small>		<i>Zannichellia palustris</i> (Horned pondweed) <small>Photo by: C.S. Krahforst</small>	

Figure 6. SAV species found in the low salinity environments of coastal North Carolina.

Longer term fluctuations in climate, precipitation and river discharges leads to significant water quality gradients and both intra-and inter-annual fluctuations in environmental conditions, especially salinity and turbidity (Burkholder et al. 2004).

The limited amount of observation and monitoring data in these lower salinity SAV communities suggests that the abundance of SAV is poorly documented, the species are more ephemeral, and there is much greater spatial and temporal variation than the persistent seagrass meadows in the higher salinity barrier shelves and sounds. Here, there are no marine seagrasses, and SAV communities consist of at least ten different species with a diversity of complex morphologies and life history strategies adapted to lower salinities and more ephemeral and widely fluctuating environmental conditions (Figure 6). These SAV communities include *Najas guadalupensis* (bushy pondweed), *Vallisneria americana* (wild celery), *Potamogeton crispus* (curly-leaf pondweed), *Potamogeton perfoliatus* (redhead grass), *Stuckenia pectinata* (sago pondweed), *Zanichellia palustris* (horned pondweed), *Ceratophyllum demersum* (coontail), and non-native species *Myriophyllum spicatum* (Eurasian watermilfoil) and *Hydrilla verticillata* (hydrilla). *Ruppia maritima* is also commonly found in the low salinity zone.

The lack of quantitative and sustained monitoring data for the low salinity regions of NC has made it difficult to describe and understand their distribution and seasonal growth cycles. This deficiency has also limited our ability to compile a comprehensive state-wide estimate of SAV status and trends. However, based on historical information from a wide variety of sources, there is evidence suggesting a widespread distribution of SAV in the western regions of the sounds and in the lower salinity environments of the river systems in NC (Brinson and Davis 1976, Davis and Brinson 1983, Street et al. 2005, Deaton et al. 2010, Quible and Associates 2011).

The first state-wide aerial survey of SAV coverage during 2006-2008 indicated NC has 136,000 acres of SAV (Figure 2, <http://portal.ncdenr.org/web/apnep>), placing it third in aerial abundance behind Florida and Texas. As in past efforts to map SAV in NC with remote sensing and interpretation of digital imagery (e.g. Carraway and Priddy 1983, Ferguson and Wood 1994), this more recent estimate included interpretation of higher quality imagery from the barrier shelves and sounds and much lower quality imagery in the river systems and western sound regions. Interpretation of this imagery re-affirmed that the largest proportion of SAV detectable using aerial imagery occurs on the barrier shelf of Pamlico Sound, and in Core, Back and Bogue Sounds. In the rest of the state, aerial coverage of SAV was underestimated because a portion of the imagery was either not interpretable or water quality made it difficult to reliably detect benthic signatures, especially those occurring in deeper water. Thus, NC likely has substantially more than 136,000 acres of SAV; however, the total amount of SAV and where it occurs will remain unknown, as well as its status and trends, until mapping and monitoring of the undetected (invisible) portion of the resource can be accomplished.

The extensive size of the NC coastal ecosystem, along with its multi-dimensional bio-physical complexity and the uncertainties of remote sensing, have made it very difficult to implement a comprehensive state-wide SAV monitoring program. Despite this, the NC Division of Marine Fisheries (NCDMF), along with other state and federal agencies, academic institutions, and non-government organizations continue to recognize the economic and aesthetic value of SAV communities (see summary in CHPP and APNEP Comprehensive Conservation Management Plan). This recognition is consistent with the regional, national and global consensus among scientists and managers that acknowledges the need to monitor the status and trends of SAV resources (McKenzie et al. 2000, Orth et al. 2006a, Waycott et al. 2009, <http://www.seagrasswatch.org/publications.html>, <http://www.seagrassnet.org/>). A recent global analysis of site and basin specific SAV monitoring surveys indicated the prevalence of seagrass declines worldwide and the acceleration of declines during the three most recent decades (Waycott et al. 2009). These analyses included recognition of losses proximal to NC in the mid-Atlantic region of Virginia (Orth and Moore 1983, Orth et al. 2010, Williams et al. 2010) and New Jersey (Lathrup et al. 2001), and further north in Massachusetts (Costello and Kenworthy 2011). Evidence of declines in these other western Atlantic populations, which include seagrasses and lower salinity SAV species that also occur in NC, signaled an urgent need for NC to consider developing and implementing an SAV monitoring program. Hence, funding made available by the Coastal Recreational Fishing License Program (CRFL) provided an opportunity to initiate consideration for developing a state-wide monitoring program. This report summarizes the results of a two-year project funded by CRFL investigating the development of SAV monitoring protocols and recommendations for implementation of a state-wide SAV monitoring program.

Review of SAV Monitoring Programs

Environmental monitoring is the repeated observation or measurement of some quantitative metric to assess the status and trends of biological (e.g., density) and/or physical (e.g., salinity) parameters, a specific organism (SAV species), or the habitat (area covered) of a system (Lathrup et al. 2001). With recent advances in geospatial technology (e.g., GPS) and Geographic Information Systems (GIS), we are now able to spatially articulate monitoring data to create status and trends maps of these environmental metrics and habitats. Often, monitoring programs are designed with the intent to detect change in space and time using one or several metrics and a distribution map of SAV habitat as indicators of change. Ideally, the most useful monitoring programs are capable of identifying the causes of change so that responsible parties and their agencies can make more confident decisions resulting in effective management and protection of natural resources.

Despite a wide consensus recognizing the need for SAV monitoring (Waycott et al. 2009), science has not yet provided resource managers with a standardized approach or a strict

set of protocols for SAV change detection, especially in areas that are prone to turbid waters. Considering the wide range of environments where SAV occur and the different goals and strategies of resource management agencies, standardization of protocols may not be the best approach. Nonetheless, there are fundamental principles which can be considered and used as a guide for management agencies to select the most appropriate and cost effective approaches that fit their particular system. Lessons learned from an evaluation of existing monitoring programs worldwide and here in the U.S. illustrate the range of options available. Assessment of some of these examples below provides the context within which resource managers can evaluate the options best suited for the conditions in North Carolina.

Global Programs

The first principle that should be considered in designing a monitoring program is establishing the goals and associated objectives. The specific objectives of a monitoring program should guide the selection of metrics and sampling protocols. If the data and outcomes derived from the protocols do not match the objectives, then the monitoring program will fail to achieve its intent. Globally, monitoring programs have been driven by a wide range of objectives. For example, in one of the first attempts at global-scale monitoring, the Seagrass Net Program (<http://www.seagrassnet.org/>) was originally designed to foster more widespread awareness and scientific knowledge of seagrasses by public and government organizations, specifically including those located in remote, underdeveloped nations. Program and data management is centrally located in the U.S. while program staff conducts training workshops and supervises local community and agency involvement in monitoring. Monitoring plans are simple and site-specific, but involve a standard transect sampling design that allows analyses of long-term trends and comparisons between sites (Short et al. 2006).

Likewise, the Seagrass Watch Program was originated in northeastern Australia and designed with objectives comparable to Seagrass Net, but the sampling methods were modified and adapted to the bio-geographic conditions of the Indo-Pacific region (<http://www.seagrasswatch.org>). Both the Seagrass Net and Seagrass Watch programs continue to grow and expand into more regions of the globe, educating the wider international communities, raising awareness of coastal management issues, and building local and global capacities through long-term monitoring programs that support conservation of SAV resources. In addition to the information and reports available through their websites, these two monitoring programs have contributed to publishing a world seagrass atlas (Green and Short, 2003), a seagrass research methods textbook (Short and Coles 2001) and a seagrass monitoring manual (Short et al. 2006). Three important lessons learned from these global SAV monitoring programs were:

- 1) larger scale monitoring programs can be achieved by incremental steps with consideration of local needs,

- 2) protocols must be flexible so they can be modified to fit environmental conditions, and
- 3) building capacity through partnerships is very important for sustaining funding and implementing larger scale long-term monitoring programs.

Site-Specific Programs

There are several site-specific and basin-focused SAV monitoring programs in Florida and three state-wide programs centered in Virginia, Massachusetts, and Washington that are large enough to provide meaningful information for evaluation on the scale comparable to the NC coastal system (Table 1). Collectively, these programs have comparable goals, focusing on the management and conservation of SAV resources. They have sufficient longevity, exceeding at least 10 years, and demonstrate the use of several different approaches and sampling methods. Only the Washington state program incorporates performance based probabilistic sampling which evaluates a specific level of change in SAV using sampling and statistical protocols that quantify the accuracy, uncertainty and power of their change detection method.

The first two example programs rely primarily on polygon-based interpretation of aerial imagery to map and monitor the status and trends of SAV. These programs are: 1) a Massachusetts state-funded program (http://maps.massgis.state.ma.us/images/dep/eelgrass/eelgrass_map.htm), and 2) a multi-state program located in the Chesapeake Bay, and the coastal bays of Virginia and Maryland (<http://web.vims.edu/bio/sav/index.html>). In Massachusetts, aerial imagery for detecting SAV is collected and interpreted in portions of the state on a staggered schedule so that that entire SAV resource is assessed over a period of approximately five to ten years (Costello and Kenworthy 2011). The Chesapeake Bay program has a higher sampling frequency for acquiring imagery than in Massachusetts; aerial monitoring is conducted and reported annually. This program is run primarily through one state academic institution, the Virginia Institute of Marine Science (VIMS), but the imagery data is supplemented by extensive coordination between regional partners at local, state and federal institutions in Virginia, Maryland and Delaware. These other institutions provide additional capacity to examine the effects of stressors (e.g., temperature, water quality) on the long-term status and trends of SAV by providing information obtained from extensive in-water¹ sampling of physical and biological parameters at separately funded research monitoring sites and from other bay-wide survey programs (Orth et al. 2006b, Williams et al 2010, Orth et al. 2010).

There is no official comprehensive state-wide SAV monitoring program in Florida, but there is an effort by the Florida Fish and Wildlife Conservation Commission (FWCC) to acquire and compile aerial imagery from all available sources to map SAV resources and to develop statistical tools for a statewide integrated monitoring network (SIMM)

¹ For this report, in-water sampling refers to snorkeling, SCUBA diving or wading.

Table 1. General characteristics of representative large scale SAV monitoring programs. Shown are three international programs and six from the United States. Characteristics include the approximate area of the water body where the monitoring occurs (km²), longevity of the monitoring program, and sampling frequency. Also shown are the different sampling designs and approaches used in each program indicated by either yes or no. NA = not applicable. ND = not determined. * In the Indian River Lagoon fixed transects are sampled every six months and aerial remote sensing is planned for every two years. # Performance-based monitoring program.

Location	Relative Size (km ²)	Longevity (yr)	Sampling Frequency	Sampling Design and Approaches Used					
				<i>Probabilistic</i>	<i>Synoptic</i>	<i>Remote Sensing</i>	<i>In-Water</i>	<i>Fixed Transects</i>	
International									
Seagrass Watch	NA	15	Annual	No	No	No	Yes	Yes	
Seagrass Net	NA	15	Quarterly	No	No	No	Yes	Yes	
Bermuda Platform	370	6	Annual	Yes	Yes	No	Yes	Yes	
United States									
Chesapeake Bay	11,000	25	Annual	No	No	Yes	No	No	
Massachusetts	ND	14	5 yr – 10 yr	No	No	Yes	No	No	
Indian River Lagoon, FL*	400	17 / 24	6 m / 2 yr*	No	No	Yes	Yes	Yes	
Florida Bay, FL	2,000	16	Annual	Yes	Yes	No	Yes	Yes	
Florida Keys (FKNMS)	8,000	15	Annual	Yes	Yes	No	Yes	Yes	
Puget Sound, WA#	2,600	11	Annual	Yes	No	No	No	No	

<http://myfwc.com/research/habitat/seagrasses/publications/simm-report-1/>). Three large scale long-term monitoring programs established in Florida's coastal waters make significant contributions to this integrated monitoring network, but state-wide coverage is incomplete.

In the Indian River Lagoon, Florida SAV monitoring is conducted primarily by one state agency, the St. John's River Water Management District (SJRWMD). This program uses a combination of aerial photography obtained approximately every two years and in-water sampling of fixed transects (sentinel sites) sampled twice annually (Morris et al. 2001, Steward et al. 2006). A second Florida program, located further south in the Florida Keys National Marine Sanctuary (FKNMS), monitors seagrass annually using a probabilistic-based synoptic approach with in-water point sampling and fixed transects located at a subset of sentinel sites (Fourqurean et al. 2001). This program is managed and run through Florida International University (FIU) and funded primarily by the U.S. Environmental Protection Agency (USEPA). A third program in Florida Bay also samples annually using a probabilistic-based synoptic design with in-water point sampling (Hall et al. 1999, Durako et al. 2002). This program also recently added fixed transects at pre-determined sentinel sites. Monitoring in Florida Bay is primarily funded by two state agencies, the South Florida Water Management District and the FWCC. Implementation of the program is shared by matching support from the Florida Fish and Wildlife Research Institute and the University of North Carolina, Wilmington, NC.

Data on SAV distribution and abundance acquired in both the Florida Bay and FKNMS sampling programs rely almost exclusively on information collected in the water, using either SCUBA divers or snorkelers (Durako et al. 2002, Fourqurean et al. 2002). Data are acquired by accepted peer-reviewed scientific methods and include non-destructive standardized visual assessments of species composition, cover and abundance in quadrats, as well as supplemental destructive sampling of shoot density and biomass using standard sized cores. The sentinel sites also incorporate measurements of seagrass primary productivity measured by leaf marking techniques in situ. This in-water field-based sampling of plant condition metrics and environmental variables involves processing a large volume of samples collected over broadly-distributed sampling sites and secures a large amount of quantitative data which is used to evaluate the status and trends of the resource (Fourqurean et al. 2001). Both of these programs are closely associated with other environmental monitoring and water quality sampling programs so that the seagrass monitoring data can be interpreted within the context of factors affecting their status and trends (Fourqurean et al. 2003). The in-water methods, however, are labor-intensive and require highly trained personnel and specialized technical equipment (e.g., diving gear and safety equipment). The inclusion of quantitative, non-destructive visual assessments minimizes the cost of data acquisition, but this can be offset by the additional costs of processing the highly informative destructive sampling with biomass cores and measurements of primary productivity.

The Indian River Lagoon monitoring program utilizes long-term sentinel sites with in-water sampling at fixed in combination with aerial remote sensing to monitor SAV. In this program, landscape scale patterns of change derived from polygon analyses of imagery are supplemented by point sampling on transects. For in-water transect monitoring this program relies on non-destructive quadrat sampling for characterizing species composition, measuring abundance, and estimating SAV cover. Seagrasses in the Indian River Lagoon are distributed in water depths generally < 2.0 m, so most of the sampling can be done by snorkelers and post-processing of field data does not require labor-intensive processing of sediment cores. This program is also closely aligned with water quality monitoring programs conducted by SJRWMD, making it a powerful tool for conducting SAV change analysis at multiple scales, early detection of impending stressor effects, and the development of water management programs for SAV protection and conservation (Virnstein 1990, Virnstein 2000, Steward et al. 2005, Steward and Green 2007).

Washington is the only state in the US which has a statewide performance-based SAV sampling and monitoring program. Nearly the entire Puget Sound seagrass resource is sampled annually by the Department of Natural Resources Submerged Vegetation Monitoring Program (SVMP) using an underwater video camera deployed from a large vessel (http://www.dnr.wa.gov/ResearchScience/Topics/AquaticHabitats/Pages/aqr_nrsh_eelgrass_monitoring.aspx). Underwater videography was selected as the preferred monitoring method because the primary indicator species, *Z. marina* (eelgrass), grows to depths that exceed the capability of detection by aerial remote sensing. The deeper depths, strong tides and cold temperatures also make in-water sampling on a sound-wide scale impractical and prohibitive. Given the generally good visibility and the deep depths in Puget Sound, the underwater video camera can be towed at a relatively high speed (3 kts) and still discriminate the presence or absence of seagrass and thus is capable of acquiring data over large spatial scales in relatively short periods of time.

Briefly, the overall objective of the SVMP sampling design is to provide statistically-valid inferences of Puget Sound-wide eelgrass abundance annually (status) and over time (trends), as well as changes in eelgrass depth distribution (Berry et al. 2003). The primary programmatic performance measure of SVMP is designed to produce results annually and long-term (5- and 10-year) with the ability to detect a 20% decline in *Z. marina* abundance with suitable statistical power over 10 years at the sound-wide scale (Gaeckle et al. 2009). Annually, individual polygons in Puget Sound (1000 m long and out to a depth of 10 m) are randomly drawn from pre-determined strata (smaller fringing beds, larger flats beds, and focus areas). In each subsequent year, 20% of the polygons are replaced by new polygons in a rotational design (Skalski 2003). The video data is post-processed and classified by laboratory technicians to develop estimates of SAV cover and maximum depth distribution within the randomly selected polygons. Replicate video transects (n ≈ 11) randomly selected within each polygon utilize a modification of the point intercept method to acquire presence/absence data for SAV in 1 m²

areas continuously along each individual transect. The fractional coverage of SAV within a transect is computed and a mean and variance for each polygon are calculated. Multiple polygons randomly selected throughout the Sound are used to make final estimates total amount of SAV and the variance of SAV aerial coverage for all of Puget Sound each year, as well as changes in maximum depth distribution of *Z. marina*. A weighted linear regression analysis is used to test for significant slopes to evaluate long-term trends (5 or 10 yr) in SAV abundance for the entire Sound (Gaeckle et al. 2009).

Development of the SVMP began in the early- to middle-1990's as part of the larger Puget Sound Ambient Monitoring Program (PSAMP). The PSAMP recognized the value of SAV and its potential role as an indicator of Puget Sound health. The larger goal of the PSAMP is to correlate environmental trends with stressors and more specifically, to differentiate the effects of natural and anthropogenic stressors on SAV. In the nearly two decades since the monitoring program began, the SVMP matured through incremental stages that included: evaluating videography methods (Norris et al. 1997), identifying Sound-wide sampling replication, stratification requirements, statistical validation of replication and sampling power (Berry et al. 2003, Dowty et al. 2005), identification of sentinel sites (core/focus sites) (Berry et al. 2003), and implementation of monitoring. Sound-wide sampling actually began in the summer of 2000, and the program staff and associates continue to adjust and modify sampling protocols and parameter analyses suggested by past experience and evaluation of each year's results (Gaeckle et al. 2009). These modifications have incorporated more multi-parameter assessments of SAV change at different scales and illustrate how the monitoring program is evolving to more quantitative and sophisticated analyses as more data are collected.

As demonstrated by the Washington state SVMP, boat-based² videography offers a practical and demonstrably successful option for monitoring SAV. This program's strengths include non-destructive methods, with almost no impact on the resource, and rapid underwater video acquisition. The program also benefits from focus on one main indicator organism, *Z. marina*. In Puget Sound, *Z. marina* is a perennial species, and there is very little natural variability in distribution and abundance during an annual monitoring schedule. Thus, there are no unique requirements for selecting an index monitoring period similar to the problem faced in NC.

Another method widely used for monitoring SAV in low-salinity habitats and lakes is hydroacoustics or SONAR. Aquatic plants are known to be acoustically reflective due to the gas bubbles they contain and could be detected on SONAR or analog echosounders (Maceina and Shireman 1980, Maceina et al. 1984, and Duarte 1987, Miner 1993). More recently, the echoes of *Z. marina* could be easily discriminated on an echogram from a digital echosounder (Sabol et al. 1997, Sabol and Burczynski 1998). A U.S. patent for the method and apparatus for

² For this report, boat-based refers to any monitoring done from a vessel.

hydroacoustic detection of SAV was granted soon after these reports (Sabol et al., 1998). This patented method used single-beam SONAR with a 420-kHz transducer.

The SONAR method has been most well examined in freshwater ecosystems beginning with the work to monitor aquatic plant growth in inland waterways by the Army Corp of Engineers (Sabol and Johnston 2001). Since then, several studies have been conducted that show the usefulness of SONAR for mapping SAV in high-salinity and low-salinity regions of lakes, rivers and estuaries. Entire lakes have been mapped for SAV and change analysis in Lake Biwa, Japan, (Hamabata and Kobayashi, 2002), in Minnesota (Valley et al. 2005, Valley and Drake 2007), and in Wisconsin (Sabol et al. 2009). In estuaries, SONAR has been used to document the presence and map the distribution of SAV (Sabol et al. 2002). The US Naval Undersea Warfare center used single-beam 420 kHz SONAR and several brands of side-scan sonar to detect seagrass *Z. marina* in Narragansett Bay, Rhode Island where underwater mines were the primary target (McCarthy and Sabol, 2000). Studies were done by these authors in tanks to discover the target strength of *Z. marina*, and it was measured at -21 dB re 1 μ Pa with no change in acoustic response between 20-700 kHz³. In their conclusions, these authors wrote, “The use of hydroacoustic techniques for mapping submerged aquatic vegetation has been demonstrated.” After reviewing these studies, we felt that single-beam SONAR approaches could be used in relatively turbid NC rivers and estuaries to detect change in SAV.

These examples from U.S. programs illustrate five general categories of SAV monitoring approaches being used: 1) remote sensing, 2) in-water sampling by snorkel and SCUBA, 3) boat-based videography, 4) boat-based SONAR, and 5) a combination of these approaches. We already know from past experience in NC that remote sensing can be used to quantify a large portion of the coastal SAV resource if data acquisition and interpretation are carefully planned and supervised by experienced staff. Remote sensing alone, however, is not capable of detecting the entire scope of SAV coverage in NC, particularly in turbid or deeper water environments. Therefore, it will be necessary to develop land-or boat-based monitoring protocols to achieve comprehensive coverage in a NC monitoring program. However, shoreline access to submerged resources like SAV is not a practical approach over much of the state’s geographic range. Access to a large portion of the resource requires a boat-based operation whether you are conducting ground-truthing for remote sensing programs or in-water sampling. It may be possible to minimize in-water sampling efforts using alternative boat-based approaches, such as underwater videography or remote sensing with hydroacoustics (SONAR).

³ Target strength is a measure of acoustic reflectivity of an object, with all values being negative, because echoes have less acoustic energy than the original ping when detected at the transducer. Target strength is measured in decibels (dB) and typically varies between -130 dB and 0 dB in strength relative to a reference level, 1 μ Pa).

Objectives

The overall goals of this project were to; 1) evaluate the development of performance-based SAV monitoring protocols for NC, and 2) draft recommendations for a long-term statewide SAV monitoring plan. To achieve these goals we evaluated prior experience monitoring SAV in the NC estuarine system and reviewed existing national and international SAV monitoring programs. We also considered the logistical challenges posed by the large size and multi-dimensional bio-physical complexity of the NC estuarine system and recognized proposed evaluate approaches to monitoring that incorporate multiple methods and scales. Based on a review of the methods used in other programs, we examined the potential application of two non-destructive boat-based methods in combination with aerial remote sensing and in water sampling. Hence, the specific project objectives were to:

- 1) determine the feasibility of developing monitoring protocols with a performance measure capable of detecting at least a 10% inter-annual change in SAV abundance,
- 2) evaluate a point-intercept visual census technique using a low-light underwater video camera deployed from a small vessel,
- 3) evaluate a boat-based hydroacoustic technique using the BioSonics 420 kHz single beam SONAR system with EcoSAV2 software deployed from a small vessel,
- 4) evaluate the capabilities of remote sensing SAV using aerial imagery in NC, and
- 5) develop recommendations for implementing a state-wide monitoring program incorporating the best available methods for a given region.

METHODS

Study Sites

We established two sets of study sites to evaluate underwater video and SONAR methods: 1) Intensive-assessment, and 2) Rapid-assessment sites. Intensive assessment sites involved more intensive data collection at a site and comprehensive testing of underwater video and SONAR techniques than rapid assessment sites. More intensive data collection was necessary to test the feasibility of developing a monitoring program capable of detecting small (~10%) inter-annual change in SAV abundance. The primary objective of the rapid assessment sites was to explore a new monitoring techniques technique to rapidly survey and map areas in low salinity environments by identifying SAV presence/absence. This method targeted only

low-salinity areas because SAV classification based on aerial imagery in this environment had been unreliable and thus SAV distribution and abundance largely undefined.

Intensive Assessment Sites

Four intensive study sites were selected for the evaluation of our boat-based methods and protocols. Two of these were in high-salinity environments (Newport River and Jarrett Bay) and two were in low-salinity environments (Blounts Bay and Sandy Point; Figure 7; Table 2).

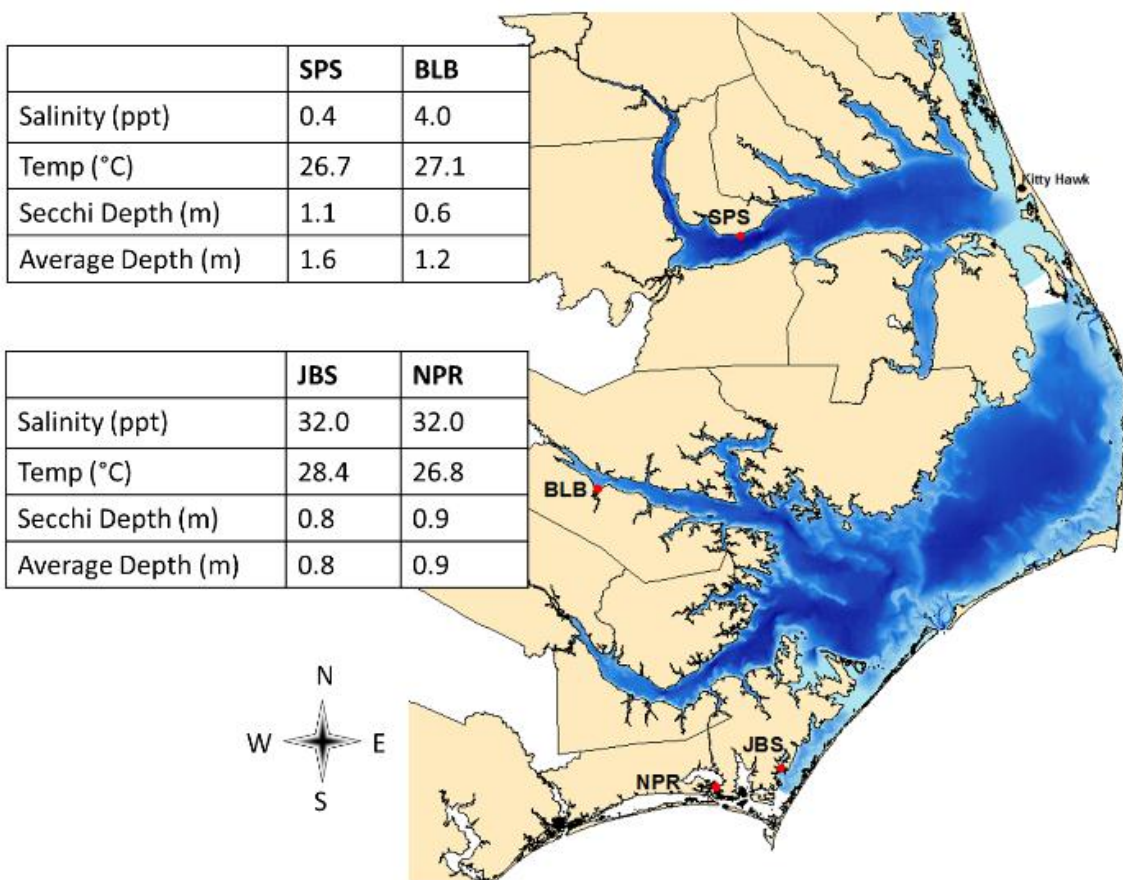


Figure 7. Intensively studied sites in 2009 and 2010 at Sandy Point (SPS), Blounts Bay (BLB), Jarrett Bay (JBS), and Newport River (NPR), and their average environmental conditions.

Table 2. Summary of study site types, site names and abbreviations, and salinity levels.

Site Type	Site Name	Site Abbrev.	Salinity Level
Intensive	Newport River	NPR	High-salinity
Intensive	Jarrett Bay	JBS	High salinity
Intensive	Sandy Point	SPS	Low salinity
Intensive	Blounts Bay	BLB	Low salinity
Rapid	Blounts Bay	BY	Low salinity
Rapid	Batchelor Bay	BB	Low salinity
Rapid	Fishermans Bay	FB	Low salinity
Rapid	James Creek	JC	Low salinity
Rapid	Neuse River	NR	Low salinity
Rapid	Perquimans River	PR	Low salinity
Rapid	Ross Creek	RC	Low salinity
Rapid	Sandy Point	SP	Low salinity
Rapid	Trent River	TR	Low salinity

Newport River

This is a high-salinity SAV site located near the mouth of the Newport River (hereafter NPR). Our survey area was defined using historic SAV distribution based on 2006 imagery as a guide to ensure that our survey captured both the shallow and deep edges of the SAV distribution. The final NPR sample polygon encompassed 103,600 m². At NPR, SAV is primarily maintained by seed recruitment; however, some perennial clones exist. During periods of peak biomass, NPR is generally characterized as having a shoreline fringing distribution, with regions of dense, continuous cover near shore transitioning to patchy SAV with increasing depth and distance from shore. Dominant species located here were: *Z. marina* and *H. wrightii*; isolated patches of *R. maritima* were also found.

Jarrett Bay

Jarrett Bay (hereafter JBS), another high salinity study site, was selected because it contains a long history of SAV classification from aerial photography. This site is dominated by *Z. marina* and *H. wrightii*, with some *R. maritima* mixed in the shallow regions. It is primarily a shoreline fringing seagrass bed with nearly all seagrass located in < 1 m of water. Dense, near shore portions of the JBS seagrass bed are largely perennial while further offshore (between 10 – 50 m) seagrass is very seasonal and exists via seed recruitment and germination.

Sandy Point

Sandy Point (hereafter SPS) is representative of low salinity SAV communities in NC. During periods of peak growth in late summer SAV can become very dense and may extend into 3 m of water or more. During winter months, most of the species at SPS senesce, losing all or most above ground biomass, but remain present (Luczkovich 2005). The following spring, germination of seeds and regrowth from belowground tissues happen rapidly, transitioning this site from nearly bare sand to dense, lush SAV. This site is dominated by *P. pectinatus* and *P. perfoliatus* throughout the summer. From May through July, *N. guadalupensis* and *S. pectinata* are prevalent in the system but their presence declines through the summer. In August, *V. americana* becomes dominant and stays dominant through the month of September. *M. spicatum*, *Z. palustris*, and *R. maritima* are periodically intermixed with the other species at this site.

Blounts Bay

Blounts Bay (hereafter BLB) was selected because it is a good representation of the lower salinity SAV communities of NC and for its proximity to areas with historic SAV data. Patchy SAV occurs here in < 1 m of water. This site is dominated by *P. pectinatus*, *P. perfoliatus*, and *N. guadalupensis* in May and June, but changes to *S. pectinata*, *R. maritima*, *Z. palustris*, and *V. americana* in late summer.

Rapid Assessment Sites

Nine rapid assessment study sites were selected that represent SAV beds in low-salinity environments in NC (Figure 8, Table 2). These sites were chosen based on historical information obtained from the NC Division of Water Quality (Jill Paxton, NCDWQ personal communication), NC Division of Marine Fisheries (NCDMF), and the 2011 SAV map produced by the Albemarle-Pamlico National Estuary Program (APNEP; Figure 2). Three of the sites (BB, PR, SP) were located in Albemarle Sound, three in the Pamlico River (BY, JC, RC), two in the Neuse River (NR, TR), and one in Bay River (FB). All of these sites are in areas of low salinity; the sites in Albemarle Sound have the lowest salinity, and FB has the highest salinity of all of rapid assessment sites studied.

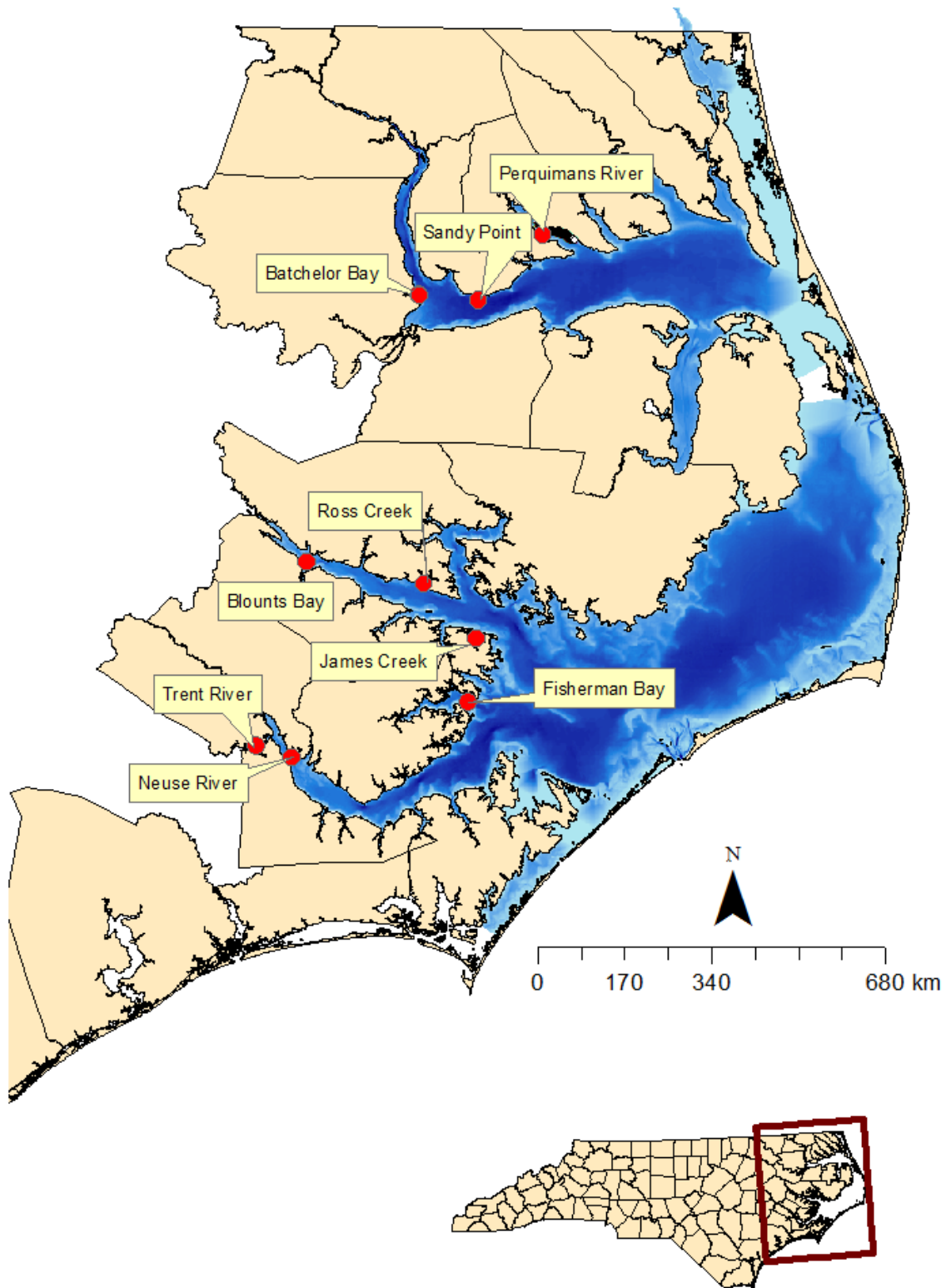


Figure 8. Study areas for rapid assessment study sites (low-salinity areas) using shore-parallel SONAR surveys paired with systematic drop camera points.

Boat-Based Monitoring Techniques

Underwater Videography

To evaluate the feasibility of using underwater video to collect quantitative information on SAV distribution and abundance, specific equipment was selected given the unique conditions of NC SAV environments. Equipment and configuration used in this project facilitated portability on a small vessel while ensuring acquisition of high quality video images and limiting sources of variation in acquiring and classifying SAV habitat. To overcome expected limitations due to underwater visibility, we tested a lightweight compact black and white high resolution (600 lines) underwater video camera (Sartek, model #SDC-MSS). With a light sensitivity of 0.0003 Lux, this camera provided clear underwater video images during periods of extreme turbidity and low light conditions (Secchi depths < 10 cm), which are frequently encountered in NC coastal waters. For field deployment, the video camera housing was mounted ahead of a small wheel secured to the base of a PVC pole approximately 13 cm above the substrate with the lens pointing down (Figure 9). This distance and orientation was governed by the focal length of the lens and standardized the video image frame size at approximately 20 cm x 20 cm. The wheel enabled the entire apparatus to roll along the bottom as the vessel navigated forward along each transect. The pole was secured to the gunnel of the vessel by an aluminum frame which permitted a pole operator to raise and lower the camera during deployment and secure the entire device out of the water during movement between transects and sampling sites. The maximum depth the pole could be deployed was 2.5 - 3.0 m. The aluminum gunnel clamp was designed so that it secured to the gunnel but could be moved and adjusted to fit a variety of different vessels.

During data acquisition, the operator positioned the vessel at a predetermined waypoint using a differential global positioning system (DGPS)-based navigation system and advanced along a transect line toward a terminal waypoint, attempting to maintain a forward speed between 0.5 kt. and 1.0 kt. Preliminary tests revealed that speeds in excess of 1.0 kt. resulted in blurred images that were difficult to classify. The vessel operator was accompanied by a second individual that adjusted the vertical elevation of the pole in the gunnel mount, ensuring that the camera was stabilized at the proper height above the bottom. A third individual aboard the vessel managed the electronics, spot-checking the video signal and DGPS to ensure that data were being properly acquired. Data along the vessel track was collected as a GIS ready shape file using the high precision Trimble DGPS, with the antenna mounted at the top of the camera pole. Winds and tides frequently prevented acquiring a perfectly straight transect line.

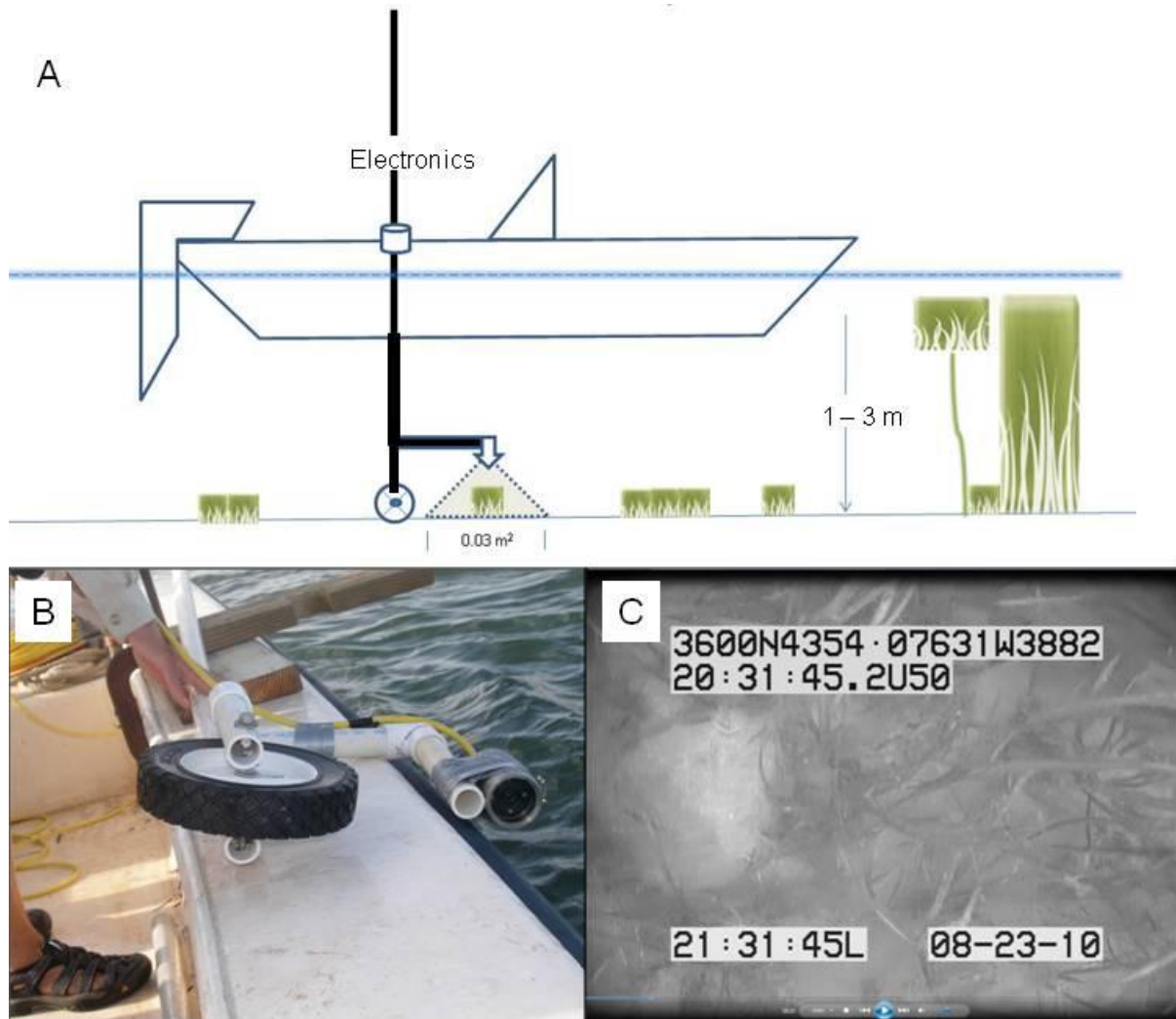


Figure 9. Underwater SAV video collection methods. (A) Schematic of vessel-mounted underwater video camera; (B) photograph of the underwater camera (Sartek®) and wheel mount; (C) screen capture of underwater video with position, date, and time stamp from the vessel-mounted GPS and electronics. Camera is in down-facing orientation at a fixed height above the bottom (13 cm) and frame size of 0.04 m².

The electronics on board the vessel were configured to simultaneously send both the video and DGPS information through an on board device (Horita) to a digital video tape which stamped the time, date and geographical coordinates on each individual video frame (Figure 9C). The DGPS position was updated every second and stored as a point shape file, ensuring an exact match of the video frame with the vessel track line during video classification. A backup copy of the stamped video data was then stored on DVD tape for post-processing (Figure 10).

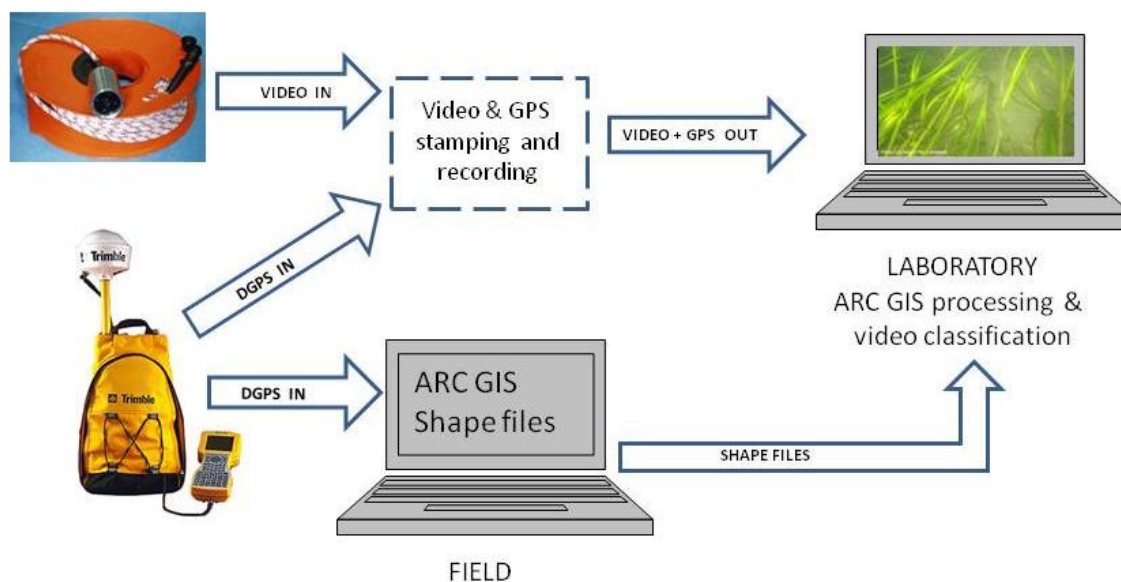


Figure 10. Diagram of underwater video and geographic data collection methods. Merging video from a high resolution underwater camera (Sartek®) with high precision differential global positioning system (DGPS, Trimble®) while in the field produced geo-rectified underwater video that was classified in the laboratory.

The underwater video was post-processed and classified in the laboratory. Step by step directions for file preparation and classification are located in Appendices 1 and 2. Video data were analyzed for the presence of SAV at 3 s intervals (~1 m distance interval along a transect) by a trained observer. Preliminary surveys identified that at a vessel speed of ~1 kt and a video capture rate of 30 frames per second, classifying one frame every 3 sec minimized the risk of classifying the same frame more than once and is nearly equivalent to classifying one frame (400 cm²) every meter. SAV presence-absence was scored using a binomial code (1 = present, 0 = absent) and entered into the shape file at the matching position and time stamp. Seagrass was defined as present if any portion of a rooted SAV (leaf, flower, basal area, or entire plant) was visible in the analyzed frame. Any frame that was obstructed (i.e. the bottom could not be distinguished in the frame) was given a designation of unclassifiable. Unclassifiable points were removed prior to analyses.

Video Classification Training

To ensure that all SAV video classifications were uniform among observers, all personnel were trained using a standardized approach that allowed us to measure inter- and intra-observer classification variation (following methods derived in Reeves et al. 2006). Here, observers with little practical experience but knowledge of the project were defined as novice (hereafter NOV).

Persons with prior experience classifying SAV transect video were categorized as experienced observers (hereafter EXP).

A total of six SAV training transects were provided to all observers (three NOV and three EXP; Table 3). Three of the six transects were repeated three times for intra-observer comparison, for a total of 12 training transects. The training video was approximately 2 hr. in length, and observers were asked to complete the video classification in less than 8 hr. but this could extend over a period of days to weeks. Video classifiers were not asked to conduct this analysis in a single 8-hr period because accuracy was assumed to decrease throughout the day as the observer became tired of classifying video. Video classification was completed using methods defined in the previous section; briefly, one frame every 3 s. was classified using a binary code (1 = present, 0 = absent). For each transect, the fraction of SAV was calculated as ratio of total SAV presence points by total number of classified points. To test the null hypothesis, that there was no difference in fraction of SAV (F_{sav}) classified by observer type (NOV and EXP), a model II ANOVA was used. We assumed observers were representative of the potential variation of all possible observers; they were therefore treated as replicates of observer type.

Table 3. Description of SAV habitat attributes for selected video tracks used in the observer calibration exercise, including total number of image classifications (total classifications). Segments denoted by asterisk were classified three times by each observer. Fraction of SAV (F_{sav}) was calculated as mean of all observers and all replicates for each track.

Track Number	Total Classifications	F_{SAV}	Habitat description
1*	197	70	Relatively dense and continuous SAV cover.
2*	183	19	Patchy to sparse SAV.
3	190	74	Shallow water SAV, nearly continuous cover. Good ambient light and water clarity.
4*	180	63	SAV are small patchy clones and seedlings. Plants are generally clear of epiphytes. Good water clarity and ambient light.
5	194	14	Patchy SAV transitioning to sand.
6	194	50	Generally patchy throughout track.

SONAR Monitoring Method

The hydroacoustic data (hereafter called SONAR) were obtained using a BioSonics DT-X echosounder with a 420-kHz single-beam transducer deployed from a small vessel (Figure 11). A Garmin 17X HVS WAAS-enabled or JVC 212W DGPS unit was integrated with the SONAR for highly precise, highly accurate geo-referenced data. The GPS antenna was positioned on a pole mounted to the console of the vessel, which was ~1 m away from the transducer. The transducer was positioned ~0.3 m under the surface of the water using a gunnel mount. The vessel followed transect lines at a speed between 2.5 and 5 kt., with an average speed of 3.3 kt. (1.7 m/s). Because the transducer was fixed on the vessel and the sonar beam is conical in shape, spreading at a 1:10 ratio of diameter to depth, this created a variable sized “footprint” on the bottom. Shallow pings cover a smaller area and deeper pings cover a greater area, thus in a single acoustic report of 10 pings, an area of 0.07 m² of the bottom at 1 m depth and 0.14 m² at 2 m was surveyed. With increased boat speed, the linear distance covered by an acoustic report increased. The linear distance sampled in a single acoustic report averaged 3.4 m with 5 pings per second. Pulse duration was set at 0.1 ms.

SONAR signals were received and recorded to the memory of a Panasonic Toughbook laptop computer model CF-29 using BioSonics Visual Acquisition software (Figure 12). The data were imported into BioSonics EcoSAV2, which interprets the echo-envelope of a signal and classifies a point as SAV present (1) or absent (0) and the parameters in EcoSAV2 were adjusted in the software to address false-positive detections in areas with soft sediments (see Appendix 3). All data collected in < 0.4 m from the transducer are in the near-field, and excluded by the EcoSAV2 algorithm. Thus, for this study, only depths > 0.7 m (near-field plus transducer depth) were considered. The EcoSAV2 algorithm groups all the pings in a file (typically one transect) into acoustic reports of ten pings each, computes the % SAV cover for each acoustic report using the EcoSAV2 algorithm (see below), exports an output (*.CSV) comma separated text file with the latitude and longitude for each acoustic report, along with the date, time, acoustic report mid-ping number, depth in m (adjusted for transducer depth), SAV cover (%), and plant height (m) for that ping report. The SAV cover (%) for each acoustic report was determined by the total number of SAV positive points divided by the total number of pings within the given report. Because an acoustic report occurred at a distance interval of ~3 m along each transect, a 300-m transect would have approximately 100 acoustic reports obtained from ~1,000 pings. The output of EcoSAV2 was exported into a Microsoft Excel spreadsheet, and imported into statistical software such as SYSTAT 13 or R 2.12.1., or into ArcMap 9.3 GIS software.

Acoustic (Single-beam SONAR) Method

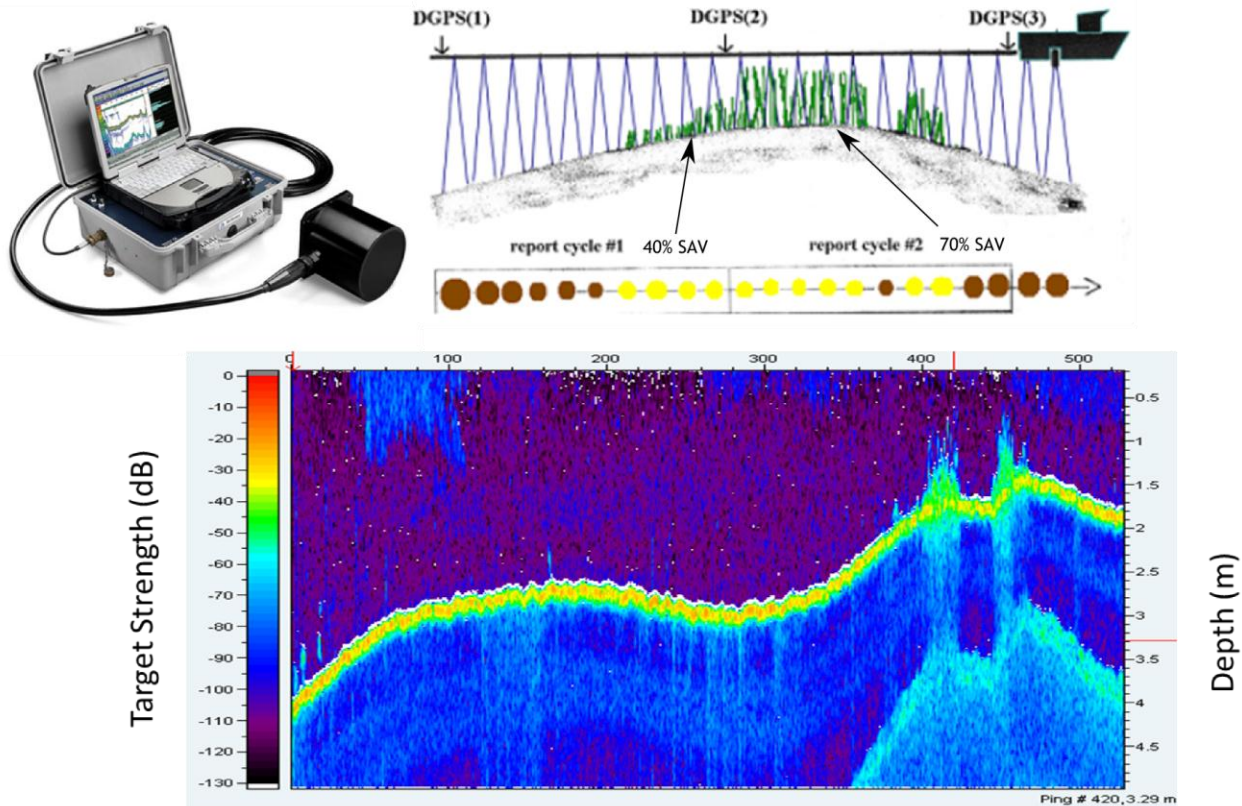


Figure 11. SONAR system (BioSonic DTX echosounder with single-beam 420-kHz transducer, and Panasonic Toughbook laptop computer for data acquisition). BioSonic ECOSAV2 software was used to post-process each data file acquired by the DTX. All pings are classified by the ECOSAV2 algorithm as positive or negative for SAV and each acoustic report of 10 pings is summarized by latitude and longitude as % SAV cover (number of SAV-positive pings/10 possible pings x 100) in the ECOSAV2 output. The upper diagram (from BioSonic, Inc.) shows how the SONAR system is used from a moving vessel with two hypothetical acoustic reports shown (yellow pings are SAV positive, brown pings are SAV negative). Each ping in the diagram is shown as a circle, with 10 acoustic pings per report cycle, and all reports are geo-referenced at the mid-ping location using differential GPS. In this example, 40% SAV and 70% SAV was measured for the two acoustic reports. The bottom panel is an echogram showing what appears to the operator on screen of the laptop as the vessel has passed over a SAV bed (green acoustic targets above the bottom between pings 400 and 500). Depth (m) was collected at each ping as well, so a continuous display of bottom depth and SAV coverage was obtained along transects, and these variables (date, time, latitude, longitude, % SAV cover depth, and plant height in cm above bottom) are reported by ECOSAV2 in an output file

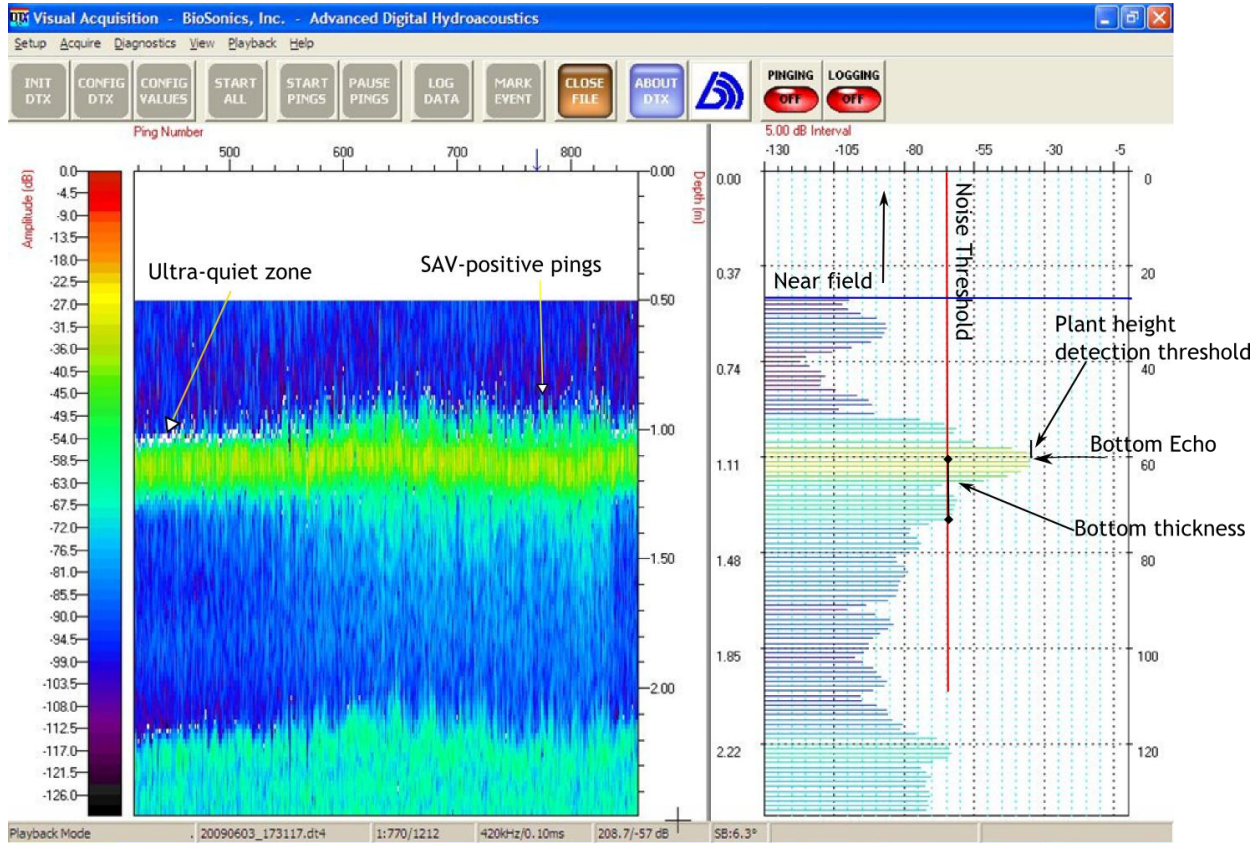


Figure 12. Left: The echogram from Visual Acquisition software of the SAV at NPR acquired by the BioSonics DTX system in June 2009. The SAV plants are visible as a green region extending above the bottom beginning at approximately ping 400. The ultra-quiet zone (white zone) just above the bottom is an indication that the bottom is not covered with SAV at pings prior to that. Right: The single-ping echo envelope of the same site at ping number 770 (SAV-positive arrow shown in echogram). The echo envelope shows a bottom echo at 1.1 m depth and a plant echo extending from the bottom to echo to the depth of 0.9 m (canopy height). From this difference (canopy depth to bottom depth), a SAV plant height can be computed. EcoSAV2 algorithm parameters are indicated on this overlay.

EcoSAV1 (and EcoSAV2, which has an improved user interface, but is otherwise similar in the algorithm used to EcoSAV1) is a post-processing algorithm, so files collected by Visual Acquisition software (which has a real-time echogram display) are analyzed for SAV presence after data collection is completed. The EcoSAV2 algorithm is described in Appendix 3 (summarized from the EcoSAV2 guide to users, BioSonics, Inc.). Note that some algorithm parameters in Appendix 3 are user-defined, and data files collected in the field can be re-analyzed with alternative user-determined settings.

Diver Surveys

Following methods of other monitoring programs (e.g. Durako et al. 2002, Fourqurean et al. 2002), we completed an assessment of SAV using an in-water diver survey method. Diver surveys were done while dropping quadrats while wading in very shallow water, or while using snorkeling gear working at depths less than 2 m. At SPS, we used SCUBA because SAV was detected at depths > 2 m. Two persons worked to get the quadrat data at these sites using a handheld Garmin 76Cx map GPS receiver to locate sampling points. Diver surveys were completed in 2009 and 2010 at all intensive assessment sites.

In 2009, diver surveys were completed using 1 m² quadrats sectioned into 25 cm x 25 cm squares, divers recorded the number of squares occupied by SAV. The diver surveys were done only at NPR in this year. Quadrat locations were randomly distributed across the site with a minimum separation distance of 2 m (n quadrats = 29). This approach may slightly over-estimate SAV cover over methods using basal area, but it eliminates between-diver error associated with estimating percent cover based on visual assessments of basal or canopy cover. For more information on quadrat site selection, see Appendix 6.

Diver surveys were completed in 2010 at all intensive sites at each visit in order to compare the quadrat data with SONAR and to assess the general trend of SAV cover in the main area of the bed (< 2 m depth) over time. For these diver surveys, we used slightly modified methods to improve compatibility with the SONAR detection method. At each intensive sampling site (BLB, NPR, JBS, and SPS), diver surveys of SAV percent cover, species composition, and canopy height (cm) were collected using 1 m² quadrats sectioned into one hundred 10 cm x 10 cm (0.01 m²) cells. After SONAR sampling was completed, 100 random points at depths < 2 m were selected using Microsoft Excel's random number generator from all the acoustic reports in the EcoSAV2 output file along the transects obtained from the SONAR. The mid-ping positions of each randomly selected acoustic report were loaded as waypoints onto a handheld Garmin GPSmap 76Cx. Divers navigated to each GPS waypoint and collected percent cover (number of cells with SAV present divided by 100 cells) and SAV species composition from up to 65 (mean = 41) of the randomly selected points within a given SAV bed. For each randomly selected waypoint, three quadrat sub-samples were haphazardly collected, where the quadrat sampling began at the waypoint and moved toward shore. This allowed us to incorporate the variability of SAV at a single waypoint. From the three quadrats, we estimated the median percent SAV cover at each waypoint.

Remote Sensing Monitoring Method

Aerial imagery for coastal NC was collected over a two year period from Spring 2006 to Spring 2008. Efforts were made to meet all the environmental parameters outlined in Ferguson

et al. (1993), Dobson et al. (1995), or Finkbeiner et al. (2001) when obtaining remotely-sensed aerial imagery to map SAV during all NC mapping efforts. These environmental parameters are described in detail in Appendix 4 of this report. All imagery was collected with the same airplane-mounted sensor, Intergraph's Z/I Digital Mapping Camera (DMC). The DMC is a four band camera that collects data in the blue, green, red and near-infrared spectrum. The statewide mission was conducted in fall 2007 and spring 2008 and flown at 24,000 ft. (7315 m) with a pixel size of 1 m. Separate imagery for Bogue and Back Sounds and the mainland side of Core Sound collected in May and June 2006 was flown at 10,000 ft. (3048 m) for a pixel size of 0.3 m. The 2006 imagery was flown under separate contract for NOAA and used because of the superior water quality during the 2006 acquisition.

The digital photos were loaded into ArcGIS for manual on-screen digitizing using the procedures as described in Rohmann and Monaco (2005). Digitizing scale was typically set to 1:3,000, except when larger homogenous areas required zooming out to a broader scale, typically 1:6,000. Habitat boundaries were delineated around benthic habitat features (e.g., areas with specific color and texture patterns). The image mosaic was occasionally manipulated in terms of brightness, contrast and color balance to enhance interpretability of subtle features and boundaries. This can be extremely helpful, especially in deeper water where subtle boundaries or problems caused by turbidity can make features difficult to detect. Minimum Mapping Unit (MMU), the smallest feature that is delineated, was approximately 0.03 ha. Deciding on a MMU is a balance between providing maps with sufficient detail to meet the requirements of parties using the maps and the time and cost to produce the maps.

Sampling Design

Intensive Assessment Sites

SONAR, video, and quadrat surveys were collected along these transects and throughout each site in 2009 and 2010 (Table 4). Each intensive site had a survey region that was defined by a rectangular area approximately 300 m x 300 m (0.09 km²). If the SAV distribution extended beyond the boundaries of the original survey area it was expanded to encompass the deepest depths to which SAV was distributed (SAV deep edge). The survey regions were extended at two sites, SPS and NPR. At each site, 48 transect lines were determined *a priori* using a systematic approach. In this approach, the starting point for the first transect was randomly sampled from the discrete set {1, 2, ..., M }, where $M = (L/n)$, L gives the length (in meters) of the baseline in each site (300 m x 300 m box), and n is the number of transects. Thus there were 300 hundred separated potential starting sites to choose from. Following random selection of the first transect location, remaining transects were evenly spaced M meters apart (Figure 13). For all study sites except NPR, this transect layout was followed. In the early phase of this study, it was not known whether the directionality of transect lines had any influence on our ability to

detect changes in SAV cover. To examine this question, in 2009 the NPR transects were completed in two directions across the study area, with 15 transects in approximately the N-S direction (perpendicular to shore) and 10 transects in approximately the E-W direction (parallel to shore). To examine the effect of transect orientation, we graphically examined the mean value and standard error (SE) for the fraction of SAV on each transect.

Table 4. Months in 2009 and 2010 where SONAR (S), video (V), and quadrat (Q) surveys were conducted at each intensively surveyed site.

Site	Jun. (2009)	May (2010)	Jun. (2010)	Jul. (2010)	Aug. (2010)	Sep. (2010)
BLB		S/Q	S/V/Q		S/Q	S/Q
JBS			S/Q	S/V/Q		S/Q
NPR	S/V/Q	S/Q	S/Q		S/Q	S/Q
SPS			S/Q		S/V/Q	S/Q

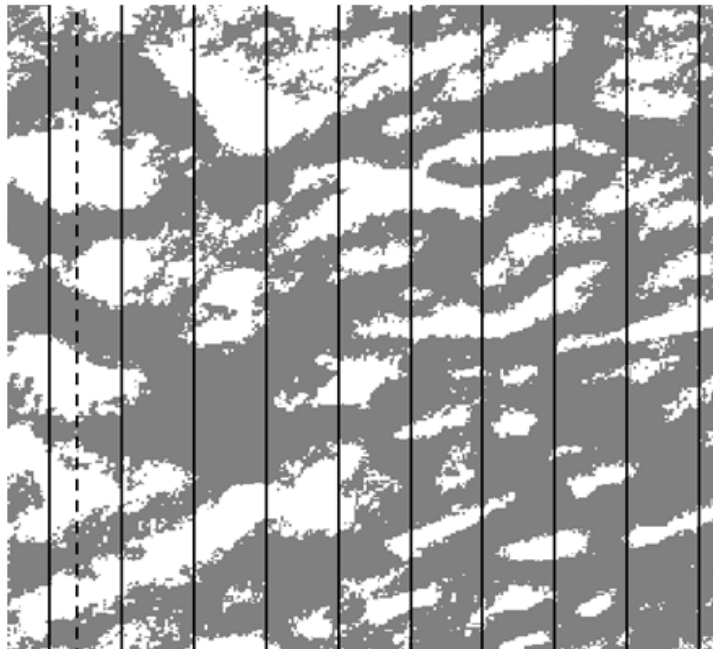


Figure 13. A visual depiction of a systematic sampling of a potential SAV study site, using a grayscale image of seagrass distribution in NC. The placement of the first transect is selected randomly anywhere to the left of the dashed line; thereafter, transects (solid lines) are equally spaced across the baseline of the survey area.

Rapid Assessment Sites

Following two years of surveys and investigations at the intensive sites, it became evident that monitoring the entire state's SAV resources by underwater video would result in an unrealistic effort and extremely high cost. We also recognized that a large portion of the turbid low salinity SAV areas had never been monitored by any method and could not be detected by aerial remote sensing, thus leaving a potentially large area of unmapped and unmonitored resource in NC. Without prior knowledge of the SAV resource distribution it will be difficult to define a sampling universe for probabilistic based sampling in any future regional or statewide monitoring program. To address these issues, we began evaluating the potential for developing a more rapid SAV survey and mapping protocol in low salinity areas using a combination of SONAR and the underwater video configured as a drop camera for point-source video validation of the acoustic data.

To select sites and transects within sites, we used county shoreline maps obtained from NC One Map (<http://www.cgia.state.nc.us/DataResources.aspx>) and a bathymetry map from NOAA (http://coastalgeospatial.noaa.gov/back_gis.html). Using the measuring tool in ArcMap we determined the distance from shore to the 1 m isobath to create a buffer layer around the county map. The polygon was “erased” by the shoreline using the data management toolbox and converted into a straight line using the polygon to line tool. A new polygon was created that encompassed ~10 km of shoreline. This buffered shoreline was clipped to the new polygon, creating a line following the shoreline that was ~10-km long. Next, the shoreline was merged into one continuous line using the “merge” function in the data management tool box and the “explode” function in the editor menu. Points were placed at 100-m intervals along this line using the “divide” tool in the editor menu. This generated a transect line that was recorded as an ArcGIS 9.3 shape file along the meandering shoreline at an approximate depth of 1 m (Figure 8). These points were then exported into a handheld Garmin GPSmap 76Cx. This line was used as an approximation for locating video drop camera points in the field. Once the starting point was selected within a given site (see below), a single 10-km long shore-parallel transect was sampled using the combined sonar and video drop camera method. When collecting the video and SONAR data, we followed the 1-m isobaths, even if it meant straying from the previously created line.

To facilitate surveying these long transects at the rapid assessment sites, we modified the SONAR deployment. For each site, we used the same SONAR system except we placed the transducer on a BioSonics BioFin towing body hooked to a boom mount on a vessel and towed through the water (Figure 14). The transducer was positioned at a depth ~0.6 m below the surface of the water. We towed the BioFin through the water, similar to the intensive site sampling, except that we sampled along the 1-m isobath, moving shore-parallel. The SONAR data were analyzed in exactly the same manner as stated in the SONAR methods section.



Figure 14. Photos of the SONAR (Biosonics DTX transducers on tow body, BioFin) and tow body being deployed at NR.

For point-source video validation of the SONAR data, we attached the SARTEK low-light video camera to a fully-extended 4-m pole using zip ties at a distance of ~20 cm from the bottom of the pole. This camera position created a different distance above the bottom than was used at the intensive sites for videography. Because the camera was lowered to the bottom, rather than rolled along the bottom at a fixed focal distance, the area sampled was potentially larger than at the intensive sites. Instead of driving the camera along a transect (as was completed at intensive sampling sites), we deployed the pole-mounted camera at 100-m intervals along the transect at a distance above the bottom or the SAV canopy in order to visualize the presence or absence of SAV. We began to collect video data at the end of a transect, creating a starting waypoint on the handheld GPS unit. From this point, we followed our transect line ~100 m away from the point (as measured on the GPS) and collected another video sample for SAV. This process continued down the entire length of a transect.

At each sample point, a waypoint was created with an average GPS position because the drop camera was lowered three times in rapid succession from the boat at each point. One person recorded the underwater video frames on a mini-DV tape at each point along a transect, while a second individual drove the vessel, collected the waypoints, and handled the drop camera. In the lab we reviewed the video and documented SAV presence or absence at each recorded point. At all sites except BY and NR, a waypoint was taken at the point of the camera

drop using a Garmin GPSmap 76Cx. At BY and NR, we simply went directly to pre-defined 100-m interval points on the transect line and did not take a GPS reading. Data from these latter two sites were removed from further accuracy analyses because we were unable to determine how close or how far the points at these sites were actually taken from the SONAR transect line. The video data were analyzed so that every point was assessed for SAV and if any of the three drops contained SAV the point was classified as SAV present (1) which may result in an overestimate of SAV presence. If SAV was absent in all three camera drops, the point was classified as SAV absent (0).

Time and Costs Estimates of Monitoring Methods

Throughout this study, all equipment used, the number of personnel needed to complete all tasks, and the time spent while in the field and lab to prepare, demobilize, and analyze data were recorded to make preliminary cost estimates for each method. We did not include travel costs as these were variable depending distance of the site from each laboratory. One-time cost estimates were also calculated for equipment acquisition.

Data Analysis

This section describes methods of analysis for data collected by the underwater video and SONAR techniques. Where analysis methods are consistent between the two techniques, a single method is described with any differences between techniques noted, this includes fraction of SAV calculation and power analysis. Also included here are detailed analyses specific to SONAR data, including accuracy assessment and cokriging.

Fraction of SAV

Calculating the fraction of SAV (F_{sav}) for each transect and study site facilitated a comparison between the video and SONAR survey methods. The F_{sav} represents the number of SAV-positive observations (i.e., any non-zero observations) divided by the total number of observations taken along a transect for each method. This effectively provides paired measures of F_{sav} between video and SONAR along each transect within a given site.

To match the binary data collected using the video method, the SONAR SAV cover (%) data were converted to a binary data set where 1 = SAV present and 0 = SAV absent. Next, these data were used to calculate F_{sav} along each transect, which was determined using the following equation:

$$F_{SAV} = N_{SAV} / N_{Total}$$

where N_{SAV} is the number of SONAR reports or classified video images with SAV present within a transect and N_{Total} is the total number of SONAR reports or classified video images within a single transect. The F_{sav} for each study site was calculated as the mean (\pm standard error or SE) of the F_{sav} for all transects at the site.

Accuracy Assessment

The SONAR method is a remote sensing technique for which accuracy assessments are needed to gain confidence in the estimates of SAV detection and classification. The purpose of this analysis was to determine the accuracy of SONAR at detecting SAV. For all of these analyses, we assumed that the underwater video reflected the true distribution of SAV.

To obtain accuracy assessments of SONAR by transects and across sites, the nearest SONAR report to each video point (nearest neighbor) was determined at a range of distances independent of depth, using the “near” and “join” functions in the ArcToolbox for ArcGIS 9.3. For intensively surveyed sites, nearest neighbor distances of 1 m through 3 m were used for SONAR classified at depths ≥ 0.7 m. For rapid assessment sites, a nearest neighbor distance of 3 m was used. Only video points scored as present (1) or absent (0) were used; all unclassified or unclassifiable video points were removed. The SONAR percent cover data were converted into binary data (0 = SAV absent, 1 = SAV present) to match the video classification. These data were exported from ArcGIS 9.3 for use in Systat 13.0 to obtain accuracy values. A simple matching correlation coefficient was calculated, which produces a correlation coefficient output between 0 and 1 which was multiplied by 100 and used as to estimate a percent accuracy. Each site (intensive and rapid assessment sites) had an accuracy assessment computed this way. Accuracy was estimated only once per site when video and SONAR were collected simultaneously (4 intensive sites and 9 rapid assessment sites).

Surface Interpolation Analyses

Kriging and cokriging are geostatistical interpolation tools used to estimate values at locations between sample points which have not been sampled. The output from a kriging analysis is a surface with estimated values of the kriged parameter. Kriging is a data smoothing technique that minimizes the effects of outliers and as a result decreases variation within the interpolated surface. Kriging modeling involves three steps: 1) the calculation of a variogram, 2) modeling of the variogram, and 3) interpolating a surface using the modeled variogram (Holdaway and Brand 2000). The goal of a kriging model is to reduce mean error (error is defined here as the difference between a predicted value and the observed value for the kriged

parameter), median absolute error, and root-mean-square error (Isaaks and Srivastava 1989). Cokriging is very similar, except there are two predictor parameters, such as SAV cover and water depth.

Our bathymetric kriging models in this report used only one variable (depth in m), while the SAV kriging surface used cokriging models with two variables to estimate the interpolated surface (SAV cover and depth). We used ordinary kriging (and cokriging) in the Geostatistical Wizard of ArcGIS 9.3 to obtain visualizations of the SAV bed distribution and depth variations at each intensive study site. The kriging approaches used the point data from the ECOSAV2 algorithm (geo-referenced acoustic reports from the SONAR) to produce an interpolated surface for each a study area. A cokriging approach was used to predict SAV cover from depth because light is a known limiting factor for SAV growth and is a function of depth (e.g. Dennison 1987). The cokriging model assumed that depth and SAV presence are highly correlated.

A kriging or cokriging model's effectiveness is determined through cross-validation and sensitivity analysis (Holdaway and Brand 2000). In a cross-validation analysis, each observed data point is deleted and the remaining points are used to predict the observation point. The predicted value is then subtracted from the actual value, leading to a standard error calculation (Cressie 1991). For the standardized error plots shown in this report, we used the Geostatistical Wizard in ArcMap 9.3 to subtract the predicted values one at a time from the measured values and divide these by the estimated kriging standard errors.

We also conducted sensitivity analyses of three types of cokriging models to predict SAV presence at each intensive site. To conduct a sensitivity analysis, three kriging models (“Ideal Cover”, “Ideal Binary”, and “Local Binary”) were created for the NPR intensive site in 2009. “Ideal” models were ones in which the cross-validation parameters (mean error and root-mean-square error) were minimized by adjusting the lag distance and nearest neighbor distances used in computing the semi-variogram, which were initially set at a lag distance of 12 m and 5 nearest neighbors (ArcMap default values). These were adjusted to include more or fewer points by changing the lag distance (from 7 to 30 m) and the number of nearest neighbors (from 2 through 30 points, see details in Appendix 7). We called these models “ideal”, because they represent the best cross-validation result. In the “Ideal Cover” model, we used the SAV cover (%) from the acoustic reports directly as outputted from EcoSAV2. In the “Ideal Binary” model, we used a dichotomized SAV data set, where acoustic reports with SAV cover (%) $\geq 10\%$ were converted into SAV present (1), otherwise were scored absent (0). For the third model, “Local Binary,” very small lag distances and number of nearest neighbors were used for the interpolation. In this model, we used dichotomized SAV data as input, the lag distance was set at 10 m and the number of nearest neighbors was set at 6. While this model did not produce the best cross-validation results for the site, it reduced smoothing of the interpolated surface, allowing “local” SAV and depth values to be more influential in fitting the modeled SAV surface. For all three

models, cokriging produced an SAV prediction surface that varied from 0.0 (SAV absent) to 1.0 (SAV present with high probability), in steps of 0.1. This surface was then clipped to the study region and converted into an SAV presence polygon, where SAV > 0 was predicted (values 0.1 or greater up to 1.0). Next, the polygon was converted into a raster model, with a pixel-size of 1.0 m, using the conversion tools in ArcToolbox.

The kriging surfaces from these models in the sensitivity analysis were compared with known observed data points to find the best-fitting SAV surface. One way to do this validation was to compare the surface from each of the models to the known SONAR observations. The ECOSAV2 output percent cover is the known SONAR observation to which the cokriging surface is compared in this kind of validation. These comparisons are not reported in the Results, but can be observed in the cokriging surfaces and sonar data presented in Appendix 8. Another way to determine the best-fit kriging model was to compute accuracy relative to video of the cokriging surfaces at NPR, in which video points obtained at that site were placed on top of the SAV cokriging raster surface. The video points that were entirely contained within a specified surface were selected, using the 'select by location' option in ArcGIS. These points were then "punched through" the rasterized cokriging model, using the 'extract values to points' in the spatial analyst toolbox. This created a new column in the video data set that contained the SAV value (1 or 0) from the cokriging surface for each point overlaid. This data set was exported from ArcGIS 9.3 and used in Systat 13 to determine the variation in the accuracy for each of the models. To do this, a two-way table was used with the presence-absence of SAV determined by video as row variable and the cokriging SAV presence-absence results as the column variable. A bootstrapping re-sampling approach was then used to determine the accuracy of each cokriging model. For the bootstrap, we selected a sample size of 100 video comparison points at random from the 7515 available at NPR, and this video sampling effort was replicated 100 times with replacement. The overall accuracy was then computed for each replication and used to determine the variability in the accuracy relative to video points for each cokriging surface. All of the three cokriging models (“Ideal Cover”, “Ideal Binary”, and or “Local Binary”) were compared and the model with the highest accuracy relative to the video classification was chosen. The selected model's input variables were used to set the cokriging parameters for the other intensive sites at all survey dates.

For each of the intensive sites, the measure of the area covered by SAV was determined by computing the area predicted to have SAV within each cokriging surface by survey date. This SAV-positive area estimate was divided by the total area interpolated with cokriging at each study site to obtain the proportion of area covered by any SAV (hereafter called Relative Abundance of SAV, RA_{sav}):

$$RA_{sav} = \frac{\text{Area of SAV}}{\text{Total kriging Area}}$$

If the entire area was covered with SAV at a site, then $RA_{sav} = 1.0$; if no SAV was present at a site, then $RA_{sav} = 0.0$. This provides us with a parameter (RA_{sav}) to estimate the change in a SAV bed over time.

Power Analyses for Detecting Change in SAV Abundance

We conducted two types of power analyses: 1) simulated video transect data derived from three binary SAV distribution archetypes mapped using ISODATA clustering of aerial multi-spectral digital imagery, and 2) simulated SONAR transect data, derived from a cokriging surface of a binary map of SAV from each intensively studied site.

Simulated Video Transects

To conduct a quantitative power analysis from underwater video transect data it would be necessary to “oversample” the range of SAV distribution types that occur in NC. Due to the slow rate of data acquisition using underwater video transects (>100 hrs / site), this would require a prohibitive amount of time and expense to conduct the necessary amount of sampling. To overcome this handicap, we utilized a “virtual sampling” approach that utilized binary coded aerial imagery to simulate video transect data from a representative range of SAV distributions typical to high salinity environments in NC. Virtual sampling had the advantage of exploring the sampling intensity required to detect change for a variety of different SAV bed distributions without investing months of field and laboratory time to acquire data.

Three SAV distributions, encompassing nearly the full range of potential spatial variation, were selected from high resolution digital imagery of seagrass beds in Bogue Sound, Carteret County: 1) shoreline fringing meadows with narrow, medium and wide widths, 2) patchy beds typical of open water, and 3) larger beds interspersed with unvegetated blowouts (Figure 15; see remote sensing survey for detail description of acquisition specifications).

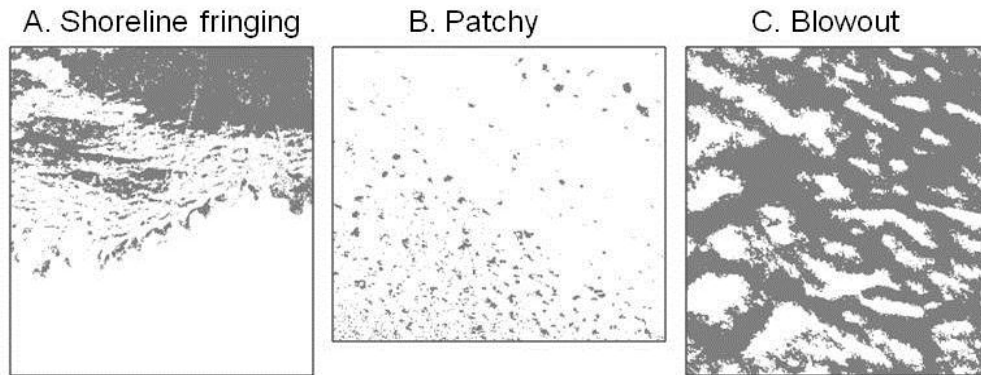


Figure 15. Three seagrass distribution archetypes, common to high-salinity areas of NC, used in power analyses. In each case, an aerial photograph was taken from Bogue or Back Sound, NC, digitized such that individual pixels represented approximately 0.333 m x 0.333 m, the area typically in each video frame along boat-based transects. Gray represents cells occupied by SAV (presence), while white represents absence of SAV.

We derived the SAV information for presence/absence by extracting and classifying spatially articulated seagrass distribution data from the three digital images using the Iterative Self-Organizing Data Analysis Technique (ISODATA) unsupervised clustering algorithm (Jensen 2005). In remote sensing clustering algorithms, pixels with similar spectral properties are assigned to subsets (called clusters). ISODATA is iterative because it makes a large number of passes through the dataset until specified results are obtained. The ISODATA algorithm was used to form 100 initial clusters. These clusters were then labeled by personnel (Don Field) experienced in interpreting imagery to derive seagrass coverage. Even though the classification was to be binary (either seagrass or bare substrate), it was important in the initial cluster labeling to identify a much larger number of classes due to the range of seagrass reflectance. For example, several different classes of seagrass were identified based on natural brightness variation caused by variation in depth. Then iterative ISODATA classifications were performed on the two categories individually by masking out the other categories. Referred to as “cluster busting,” the computer is allowed to query the multispectral properties of the masked scene with user-specified criteria to identify mutually exclusive clusters in n-dimensional feature space. By masking out all data but a single category, the spectral variance is greatly reduced, thus decreasing classification errors. After several classification iterations of the masked data, final classification labels were assigned to the spectral clusters to obtain seagrass presence or absence (Figure 15).

Next, each of the three digital representations of the landscape archetypes were imported into the R programming environment, where the resolution of the image approximately represented a 0.33 by 0.33 meter square (the level of resolution that is actually obtained in field-based video transects). The contiguous image was 902 x 902 pixels, while the blowout and

patchy images were 1006 x 1024 pixels and 1005 x 1015 pixels, respectively. Each pixel's color was used to classify it as either containing (presence) or not containing (absence) SAV. We examined the power to detect 10%, 20%, and 40% declines in SAV coverage using two consecutive occupancy surveys on the three realistic landscapes from Bogue and Core Sounds, NC (Figure 15).

Two types of surveys were simulated: systematic sampling (SYS; identical method to video and acoustic transect identification) and simple random sampling (SRS). Simple random sampling involved generating random numbers on the base line (the southern terminus of the sampled area) without replacement. For SYS, the starting point for the first transect was randomly sampled from the discrete set $\{1, 2, \dots, M\}$, where $M = \text{floor}(L/n)$, L gives the length (in pixels) of the baseline in each photograph, and n is the number of transects. Following random selection of the first transect location, remaining transects were evenly spaced M pixels apart. Simulated transects all ran north-south, along the depth gradient, as this direction minimized variance among transects.

Declines in SAV coverage were simulated by drawing SAV presence for pixel i in the second survey, Z_i^* , from a Bernoulli (Z_i, p) distribution (Fewster 2011). Here, p was 0.9 for a 10% decline and 0.8 for a 20% decline, and Z_i represents occupancy of pixel i in the original landscape. Power and type I error was calculated for each procedure by simulating 100 datasets for 10, 15, ..., 50 transects and calculating the number of times that statistical tests rejected the null hypothesis of no decline. For SRS, we employed two-sided t-tests. For SYS, we used two approaches to calculate variance. First, we considered using the variance formula for SRS; this approach is known to be conservative, but is often used because there is no theoretical, unbiased variance estimator available for systematic sampling (Thompson 2002). To implement this approach, we started by calculating a pooled variance estimate of

$$\text{Var}(\hat{D}_2 - \hat{D}_1) = S_{pool}^2(2/n),$$

where \hat{D}_1 and \hat{D}_2 are the landscape wide estimates of SAV coverage over all n transects (Cochran 1977) for the first and second surveys. The null hypothesis was considered to be rejected in this case if $|\hat{D}_2 - \hat{D}_1| > t_{0.975, df=n-1} * \sqrt{\text{Var}(\hat{D}_2 - \hat{D}_1)}$ when calculating type I error rates and $(\hat{D}_1 - \hat{D}_2) > t_{0.975, df=n-1} * \sqrt{\text{Var}(\hat{D}_2 - \hat{D}_1)}$ when calculating power.

As a second approach for calculating variance under SYS, we used a method recently developed by Fewster (2011) for distance sampling surveys. This approach involved fitting a nonparametric smooth function to transect totals to approximate survey to survey variance in density (or “encounter rate” when detectability of objects in transects is <1.0). For our purposes, this involved the following steps:

- 1) Fit a generalized additive model (GAM) to observed transect counts. Differences in transect lengths can be easily accommodated by including an offset within the GAM.
- 2) Use the GAM to predict transect counts (total number of occupied cells) for all possible transect lines. Call these predictions $\hat{\mu}_i$ for transect i .
- 3) For each possible systematic survey (i.e., for each possible starting position $j \in \{1, 2, \dots, M\}$), calculate $\hat{A}_j = \sum_{k \in S_j} \hat{\mu}_k$ and $L_j = \sum_{k \in S_j} L_k$, where L_k gives the length of transect line k and S_j identifies the set of transects included in systematic survey j .
- 4) Following Equation 5 in Fewster (2011), calculate variance as

$$\text{Var}(\hat{D}) = \frac{1}{M} \sum_{j=1}^M \frac{\hat{A}_j + \hat{A}_j^2(1-1/\hat{N})}{L_j^2} - \left\{ \frac{1}{M} \sum_{j=1}^M \frac{\hat{A}_j}{L_j} \right\}^2.$$

Here, \hat{N} gives the estimated number of occupied pixels in the image and is computed as $\hat{N} = \hat{D} \times \# \text{pixels}$.

We then used the simple relation $\text{Var}(\hat{D}_2 - \hat{D}_1) = \text{Var}(\hat{D}_2) + \text{Var}(\hat{D}_1)$ for power and type I error computations, assuming $\hat{D}_2 - \hat{D}_1$ was approximately t -distributed.

Simulations proceeded by laying down virtual transects over landscapes and calculating requisite quantities (e.g. Figure 13).

Simulated SONAR Transects

The statistical power at various levels of sampling effort (SONAR transects) was computed for 10%, 20%, and 40% change in SAV using the simulation approach described above for the underwater video. The methods paralleled the approach just described, but with SAV distributions determined from SONAR data collected as part of this study. To obtain a landscape of SAV presence and absence needed for input to the R code, we converted the SONAR transect data to a cokriging prediction surface using geostatistical methods in ARCMAP 9.3 (see cokriging section above). The prediction surface of SAV presence or absence was generated by cokriging SONAR data (depth and % SAV) used to predict presence or absence of SAV at each of the Intensive Sites on four dates (NPR, June 2009; JBS, July 2010; BLB, July 2010; SPS, August 2010). To do this analysis, we rotated the sampling frame for three of the survey sites to have a horizontal baseline with transects running along the depth gradient from shallow water to deep water. NPR was rotated -27 degrees, BLB was rotated 39 degrees, and JBS was rotated 94.5 degrees SPS was not rotated. These rotated presence-absence cokriging surfaces were converted to a matrix of cells 1m on each side, with ~ 300 cells along the columns and rows. Each 1 x 1 m cell represented the presence or absence of SAV distribution derived from the cokriging of SONAR at each site. The matrix was entered into R statistical software and transects were simulated using the same R code as described in the section above for the

simulated video transects, but here the sample was taken along each transect at the same distance (3 m or every 3 cells) as an acoustic report. As above, we used three approaches: (i) simulated the simple random sampling (SRS) with shore-normal transects laid down along the baseline at random, (ii) naïve systematic sampling transects SYS_1 , and (iii) systematic sampling with the method of Fewster (2011) (SYS_2), which lowers the transect-to-transect variance by applying a general additive model (GAM model) to the transect F_{sav} data.

RESULTS

Boat-Based Monitoring Techniques

Underwater Videography

Intensive Assessment Sites

Underwater videography collection for SAV presence/absence detection was completed at four intensive assessment sites. Classifiable video was collected under conditions with a wide range of underwater visibility. The video camera was sensitive enough to visualize SAV in extremely turbid waters. For example, at SPS, snorkelers had to be within 5 cm of the substrate to visualize SAV presence/absence while the video was clear and classifiable at the fixed height of 13 cm above the substrate. Data analysis and findings specific to each intensive assessment site are described in detail below.

Newport River (2009)

NPR had the most comprehensive survey by both video and SONAR techniques. *Z. marina* was the primary seagrass observed at NPR while occasional small patches of *R. maritima* and/or *H. wrightii* were encountered. Fraction of SAV cover for all transects combined was 50% using video classification methods and 28% based on diver quadrat surveys (Table 5). Fraction of SAV quantified by underwater video was significantly different between the two survey directions (N-S and E-W oriented transects; Table 5). SAV cover using underwater video was significantly greater in the E-W than in the N-S direction ($\chi^2 = 25.983$, $p < 0.001$). Diver-quantified SAV cover in quadrats ranged from 0 to 98% among sampled quadrats and was less than that measured using underwater video (Table 5). Extreme values of fraction of SAV cover between the two sample directions quantified by video transects, were similar (Figure 16); SAV cover ranged from 0.16 – 0.80 in the east-west direction and 0.15 – 0.68 in the north-south direction. There was a clear gradient in SAV cover across the NPR site. East-west oriented transects had lowest cover at extreme north and south edges of the site (E-W01 and E-W10), while SAV occurred in greater densities within the middle of the meadow. Also, N-S oriented

transects generally exhibited decreasing cover when moving from east (N- S01) to west (N-S15). This gradient in SAV cover is shown in a geo-rectified color-coded plot of all data points (Figure 17). SAV distribution classified by 2006-08 statewide aerial surveys captured the densest areas of SAV; however in our 2009 survey, SAV extended well beyond this area, both along-shore and offshore (Figure 17).

Table 5. Sampling effort and Fraction of SAV from NPR using classified underwater video transects and quadrats (1 m²).

Method	Direction	N _{points}	N _{transects}	Fraction of SAV	SE
Video	East-West	3757	10/10	0.530	0.008
Video	North-South	3948	15/15	0.472	0.008
Video	All combined	7705	25/25	0.500	0.006
Quadrats	All combined	29		0.288	0.054

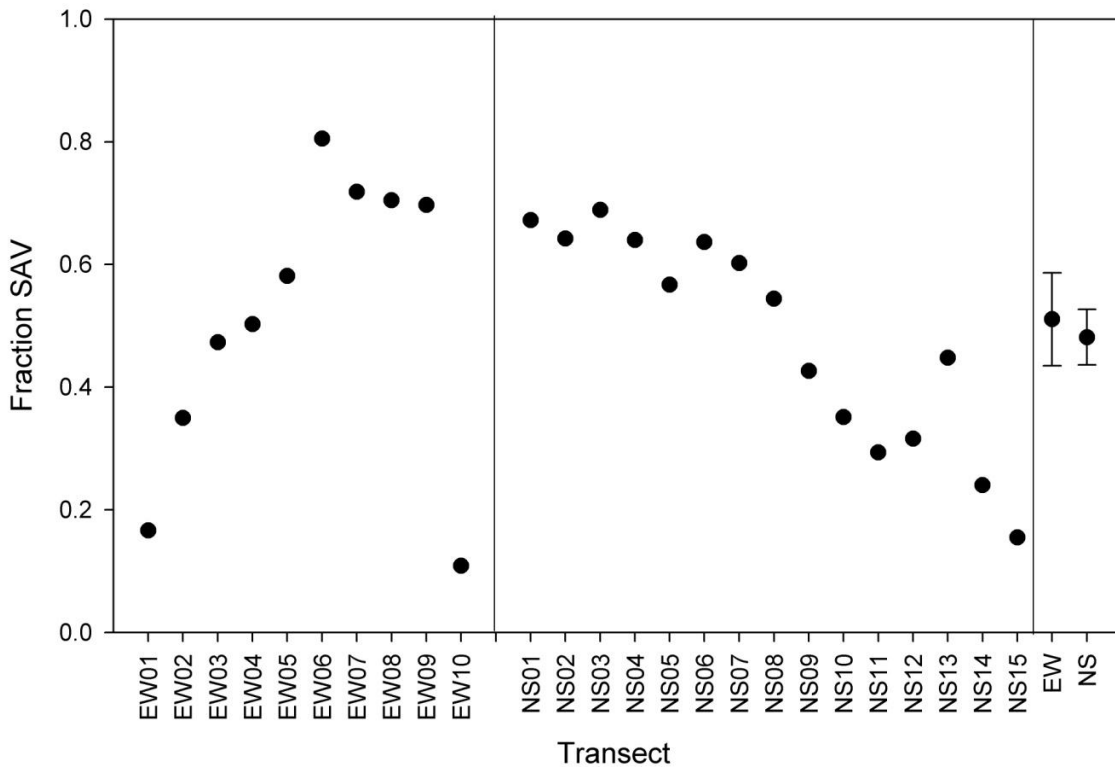


Figure 16. Fraction of SAV cover by transect at NPR in 2009, as classified by underwater video methods. Grand mean fraction SAV cover (\pm SE) by transect direction (E-W and N-S) are also provided.



Figure 17. Classified underwater video transects at NPR overlain on an aerial photograph of the site. Each point represents a classified video frame; SAV presence is colored green and absence is beige. SAV extent, based on aerial imagery from the 2006-2008 statewide SAV mapping, is delineated by yellow polygons. Dark areas in lower portion of the image are emergent marsh.

At NPR, we addressed how transect orientation might affect our ability to detect changes in SAV cover. By completing 15 transects in the N-S direction (perpendicular to shore) and 10 transects in the E-W direction (parallel to shore), we evaluated the best direction to place transects across a site, yielding the highest power to detect changes in SAV cover (Figure 17). Extremely low SAV cover at E-W1 and E-W10 are likely driven by depth limitations with insufficient light at E-W1 and desiccation stress at E-W10 contributing to the low cover estimates. Knowing we have captured both the shallow and deep edges of a seagrass bed is

important to change detection, as it has been previously identified that change generally occurs first along the margins of a seagrass meadow, especially the deeper edges. However, variance of SAV cover among E-W transects is slightly higher than of N-S transects (Figure 16) resulting in reduced power to detect change in SAV cover. Based on the video classification data from this survey and those of power analysis (data not shown), it was determined that the best orientation of transects is along the depth gradient.

Jarrett Bay (2010)

Nine of 48 pre-selected random transects were surveyed using underwater video in July 2010 at JBS. SAV was found in shallowest portions of the survey site and was virtually absent beyond a depth of approximately 1 m. The densest SAV was in extremely shallow water and inaccessible by boat. SAV transects were started at the closest point to shore, 0.3m depth, and were generally within 0.6 m of the edge of the SAV meadow at the site. SAV cover was fairly consistent across transects, with a mean fraction of SAV occurrence across the site at 8.6% (Figure 18). Nearly all SAV was located in the 10 m closest to shore (Figure 19). In water deeper than 1 m, there appeared to be SAV in small clumps, but after closer examination it was evident these clumps were simply SAV leaf detritus attached to worm tubes that looked like intact shoots. To avoid misclassifying worm tubes as SAV presence, detailed video was recorded and time was spent in the field with video classifiers to gain familiarity with the worm tubes. Nearly all SAV was defined by aerial classification in the 2006-08 state-wide mapping effort. SAV points were rarely detected beyond the aerial mapping polygon (Figure 19).

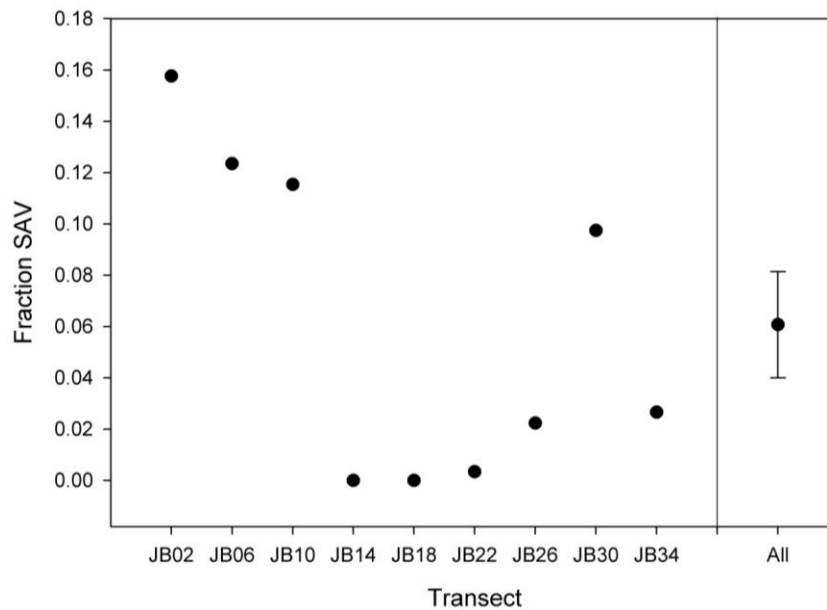


Figure 18. Fraction of SAV cover by transect at JBS and mean (\pm SE) for all transects in 2010 classified by underwater video.

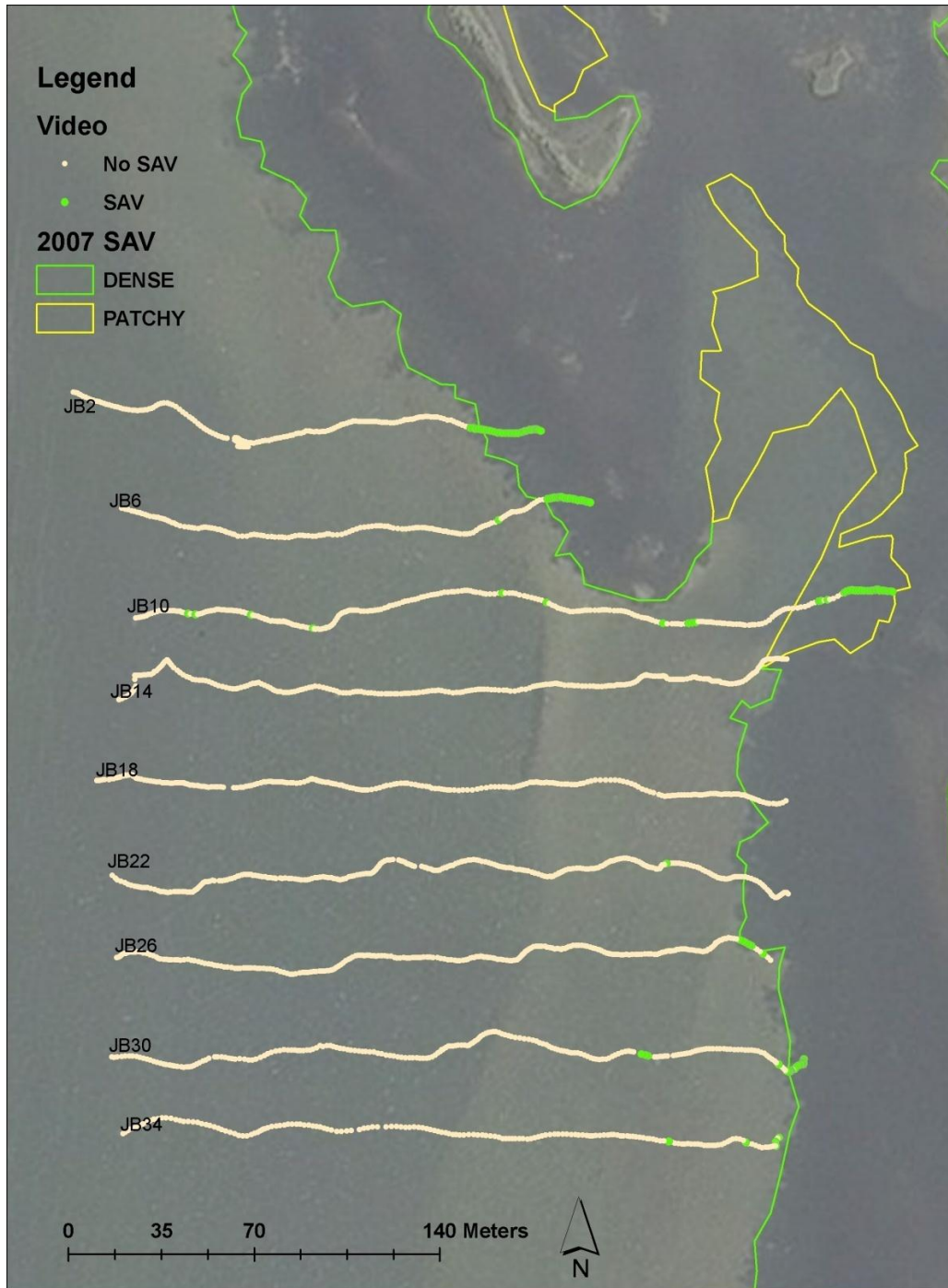


Figure 19. Classified underwater video from JBS in 2010. Each point represents a classified video frame; SAV presence is colored green and absence is beige. SAV extent, based on aerial imagery from the 2006-08 state-wide SAV mapping, is delineated by green (dense SAV) and yellow (patchy SAV) polygons.

Sandy Point (2010)

Four of 48 pre-selected transects were surveyed using underwater video at SPS in August 2010. SAV occurred across a broad depth range, with small sparse patches found as deep as 3 m. SAV coverage ranged from nearly continuous and dense to sparse, isolated patches. The species present at the site are listed below in the SONAR results section. The plants were tall, posing an entanglement problem with the video camera and pole mount. A slight modification to the camera mount was made by removing the wheel and manually adjusting the height of the camera above the SAV canopy. This modification reduced entanglement, but also made it difficult to maintain a fixed height above the bottom. The video display screen was checked frequently to ensure the video was focused and SAV could be differentiated from other marine plants. A second challenge at this site was leaf detritus. While snorkeling at the site, the dredged channel was inspected for rooted plant material. A considerable amount of leaf detritus was found at the bottom the channel, but no rooted plants were observed. Differentiating between detritus and rooted material on the underwater video was difficult. Thus the cover estimates for transects SP32 and SP36, located in and on the edge of the channel, may be an over-estimate [mean (\pm SE): 0.17 (\pm 0.02) and 0.18 (\pm 0.02), respectively].

Along the four preselected transects, SAV cover ranged from 0.17 (\pm 0.02) to 0.82 (\pm 0.02) (Figure 20). Mean fraction SAV among pre-selected transects was 0.44 (\pm 0.01). SAV was observed outside the survey area so three additional camera drifts were completed in water offshore of the 300 x 300 m survey area. Due to water depth ($>$ 1.8 m), a standard transect could not be completed due to additional drag on the camera pole mount. Thus, a simplified drift transect was completed with the camera held at a fixed height above the bottom. Three depth profiles were followed to examine SAV across various depth ranges: consistently held at 2.75 m (drop 1), drift from 0.5 - 1 m (drop 2), and a drift from 1.2 – 2.8 m (drop 3). SAV transitioned from dense to sparse in between 1.2 - 1.6 m; sparse, isolated patches were found in 2.8 m of water (Figure 21). Inspection of SAV distribution classified by aerial imagery indicated that the imagery underestimated SAV distribution during the period of peak biomass recorded by underwater video (Figure 21).

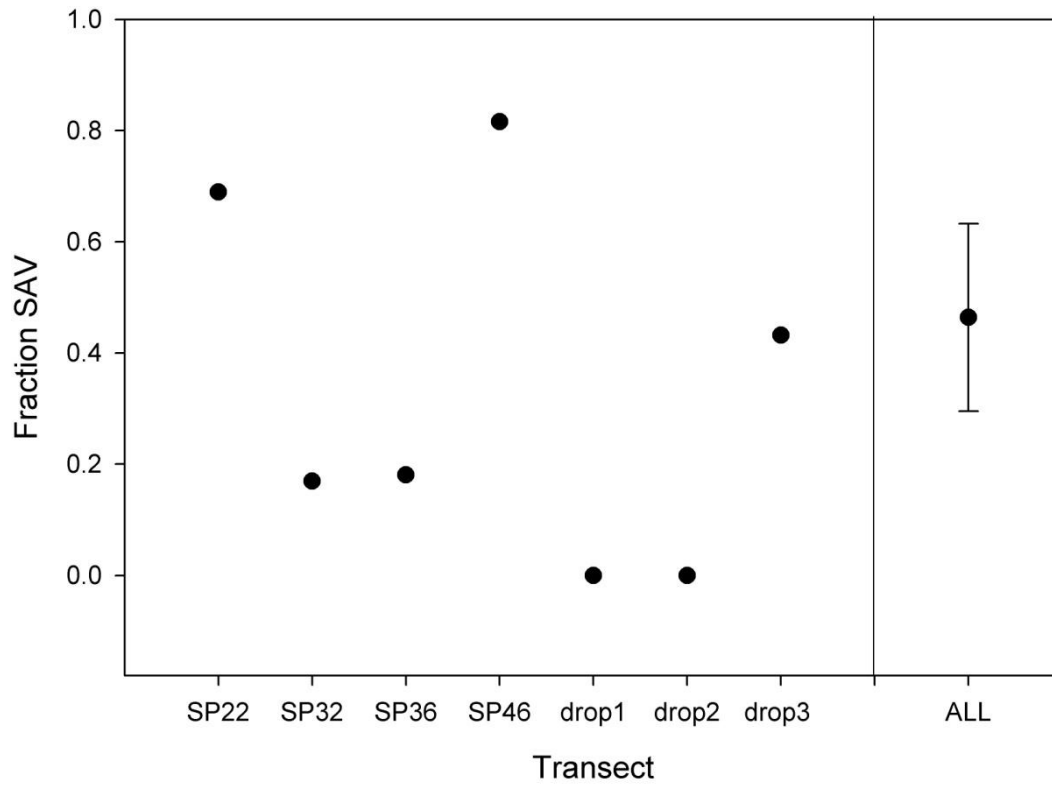


Figure 20. Fraction of SAV cover by transect and mean (\pm SE) for all random transects, excluding drops, at SPS in 2010, as classified by underwater video.

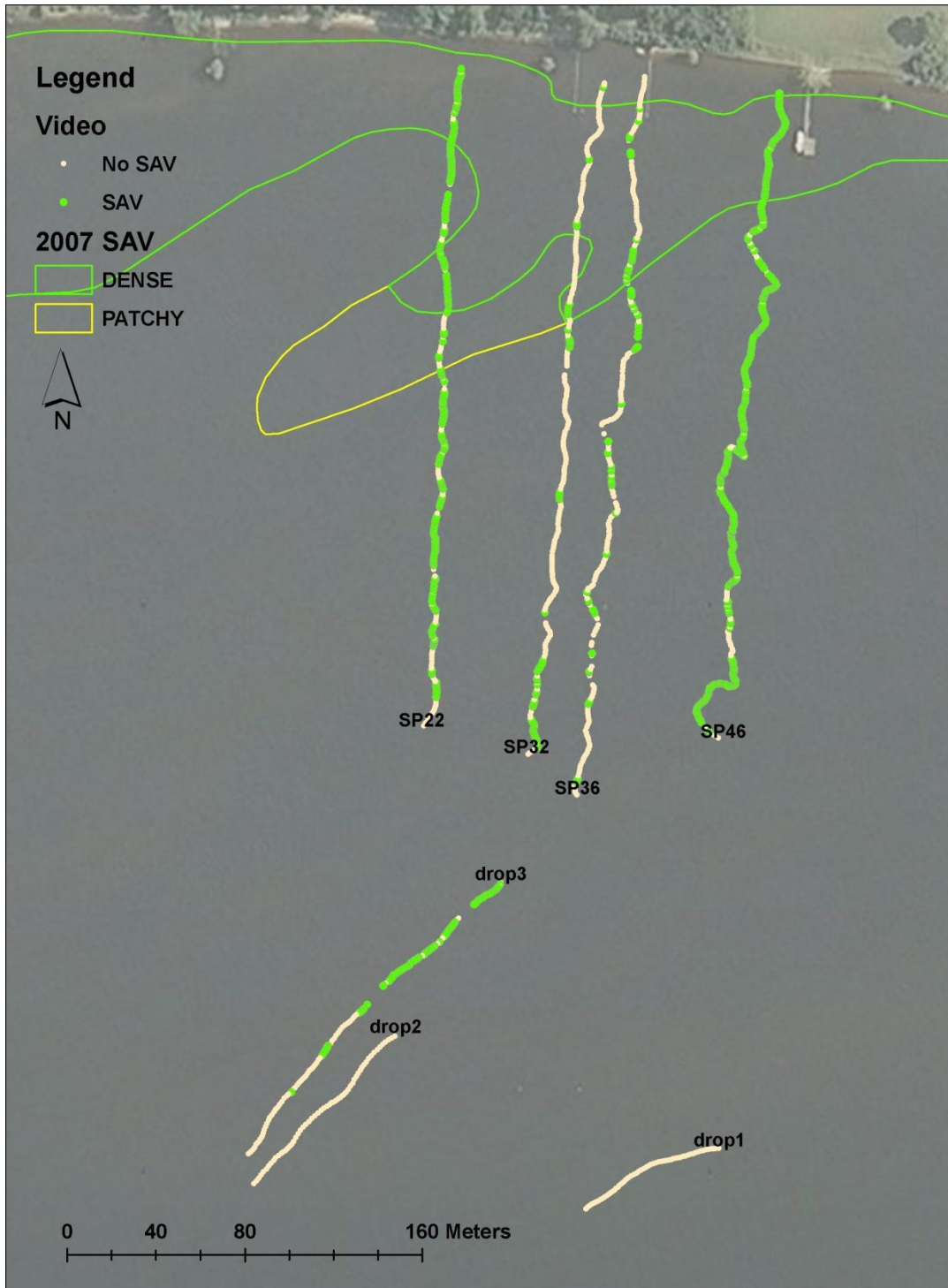


Figure 21. Classified underwater video from SPS in 2010. Each point represents a classified video frame; SAV presence is colored green and absence is beige. SAV extent, based on aerial imagery from the 2006-2008 state-wide SAV mapping, is delineated by green (dense) and yellow (patchy) polygons.

Blounts Bay (2010)

Seven of the 48 pre-selected transects were surveyed in June 2010 at BLB. SAV was found in the shallowest portions of the survey site and was virtually absent beyond a depth of approximately 1.5 m. SAV was comprised primarily of *S. pectinata* and *R. maritima*, with *Z. palustris* and *V. americana* intermixed. Although we anticipated complications from entanglement of long leaf blades to the camera system, this was not an issue at BLB. SAV was entangled on the camera mount only once, but it did not obstruct the image; entangled SAV was obvious and analyzed frames were scored accordingly. SAV cover was fairly consistent across transects (Figure 22; ranging from 0.19 – 0.34 fraction SAV), with a mean fraction of SAV occurrence across the site at 0.25 (± 0.01). SAV was consistently detected about 50 m beyond the deepest edge of SAV as delineated by aerial imagery in 2006-08 state-wide mapping (Figure 23).

Two additional transects were completed perpendicular to the pre-selected, shore-normal transects (Figure 22, Figure 23). These two transects, cross deep and cross shallow, bisected the areas of low and high SAV cover (respectively) to evaluate the uniformity of SAV distribution across the entire surveyed area (300 m x 300 m). Cross shallow covered an area of nearly continuous cover (mean = 0.66 ± 0.03), much higher than any shore perpendicular transect (max cover at BB28 = 0.34 ± 0.03). Beyond 120 m from the shoreward ends of the transects there was very little SAV (mean = 0.02 ± 0.01), occurring only in sparse isolated patches (Figure 23). Beyond a depth of 1.5 m, the sediment transitioned from sandy-mud to very soft mud, conditions that are not favorable for SAV colonization.

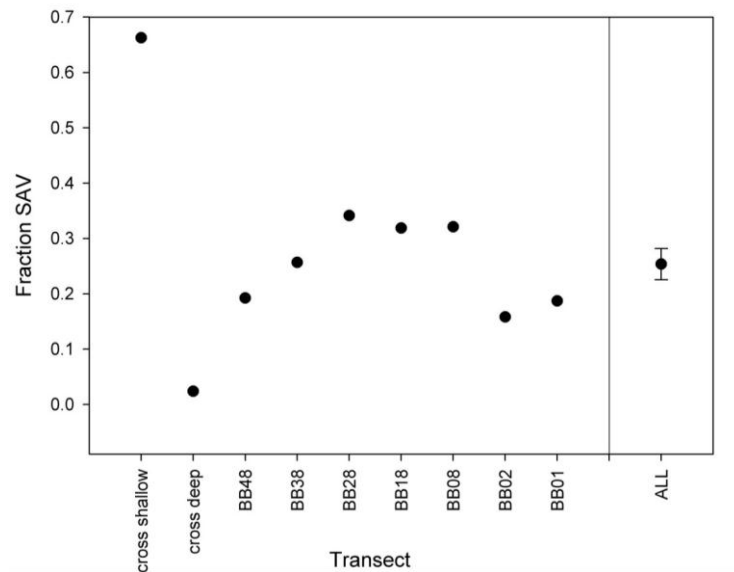


Figure 22. Fraction of SAV cover by transect and mean (\pm SE) for all random transects, excluding cross, at BLB in 2010 classified by underwater video.

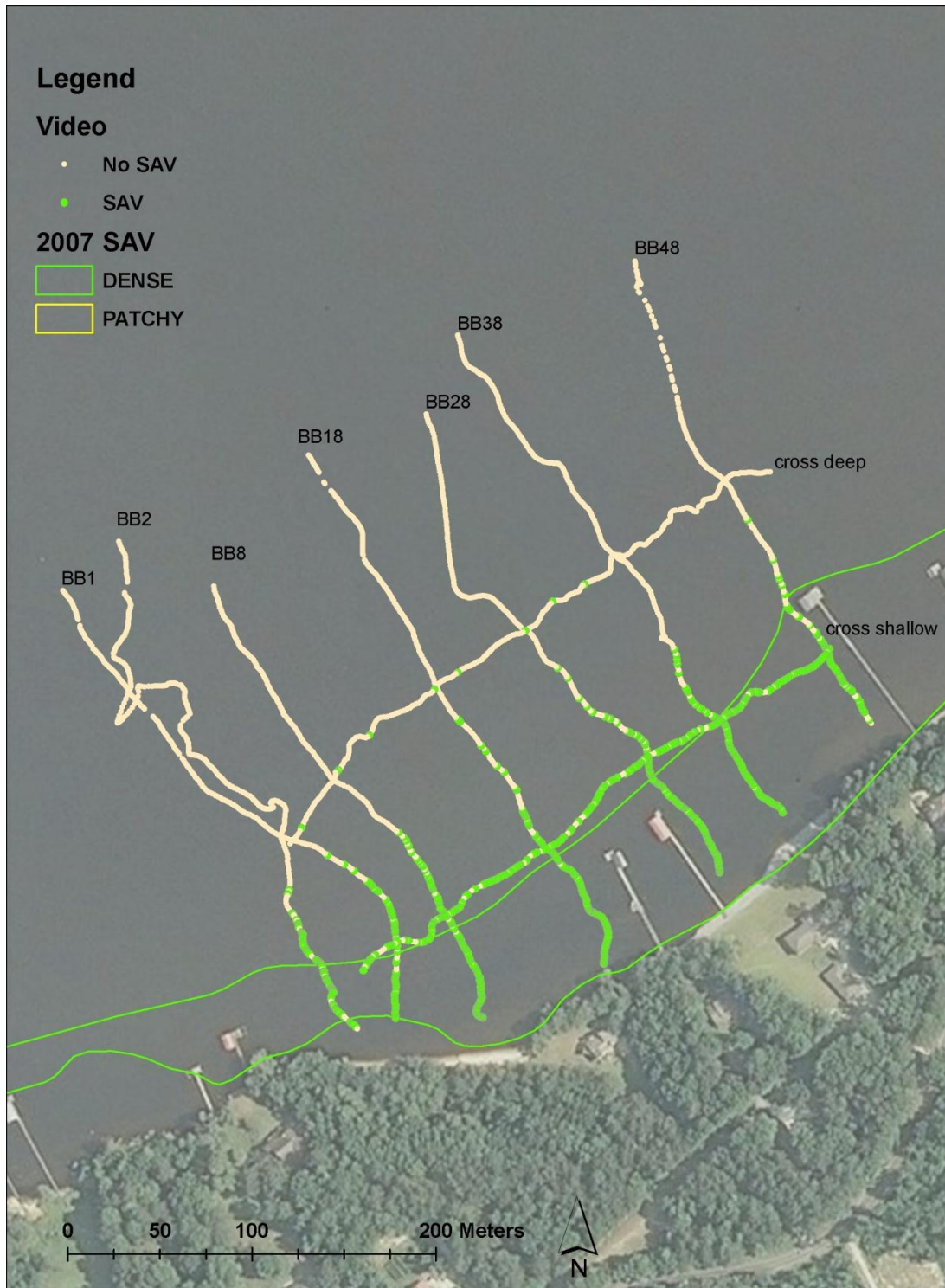


Figure 23. Classified underwater video from BLB in 2010. Each point represents a classified video frame; SAV presence is colored green and absence is beige. SAV extent, based on aerial imagery from the 2006-2008 state-wide SAV mapping, is delineated by polygons.

Video Classification Training and Observer Calibration

Inter-Observer

Our video classification training exercise was successful. The F_{sav} quantified by NOV was not significantly different from EXP observers (Table 6). Because the tracks selected *a priori* represented a range of F_{sav} , the significant difference in the F_{sav} quantified across various transects was not unexpected (Table 6). There was also no significant difference in the interaction between track and observer type which identifies that the pattern of no difference between the type of observer (NOV or EXP) holds true across all F_{sav} cover classes (e.g. all tracks).

Table 6. Model II ANOVA effects table.

Variable	SS	Df	MS	F	Significance
Track	2.5316416	5	0.506328	715.1194	<0.0001*
Type (EXP, NOV)	0.0008520	1	0.000852	1.2034	0.2799
Track × Type	0.0031913	5	0.000638	0.9015	0.4908

Generally, variance among all observers was small with NOV variance being within that of EXP (Figure 24, Figure 25). The largest among-observer variance occurred on tracks 4 and 6; however, NOV variance was within EXP variance. These tracks contained intermediate levels of SAV cover. Track 4 was collected during a period of seedling germination, when SAV clones (patches) were very small. Variable plant densities and differences in plant morphology likely contributed to the larger inter-observer variance. Where plant densities, both low and high, were more uniform (Track 1, 2, 3, 5), classification of SAV was more consistent among observers (Table 7, Figure 24). The lowest amount of inter-observer variance was on the tracks with the lowest plant densities (< 20%, Tracks 2 and 5).

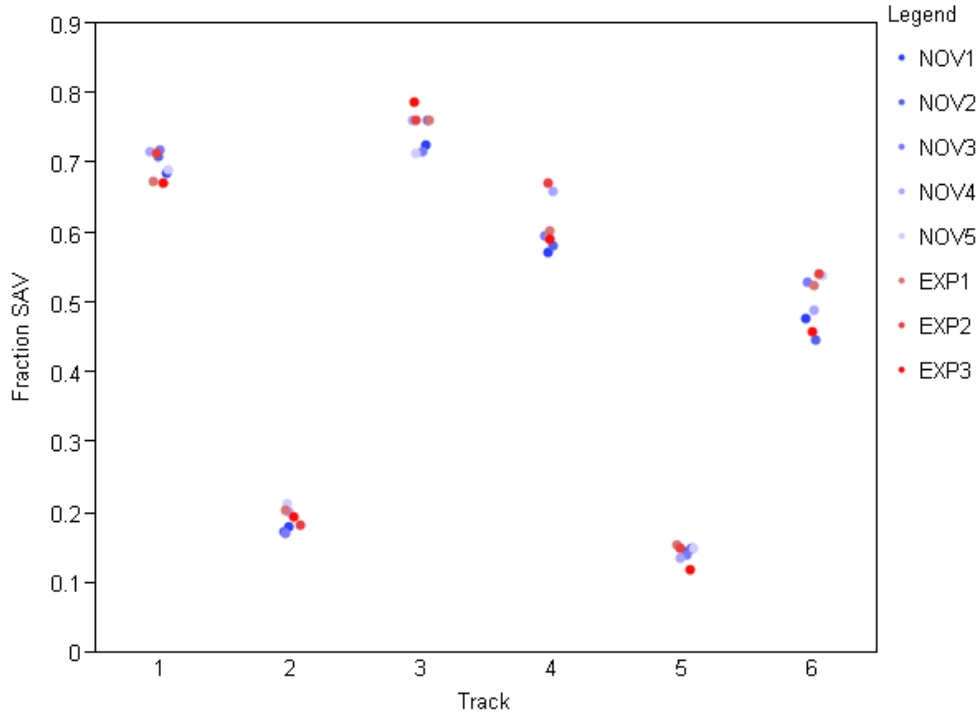


Figure 24. Fraction of SAV for all observers (five novice [NOV] and three expert [EXP]) and all tracks. For repeated tracks, initial classifications are plotted (n per track ranged from 180 – 197).

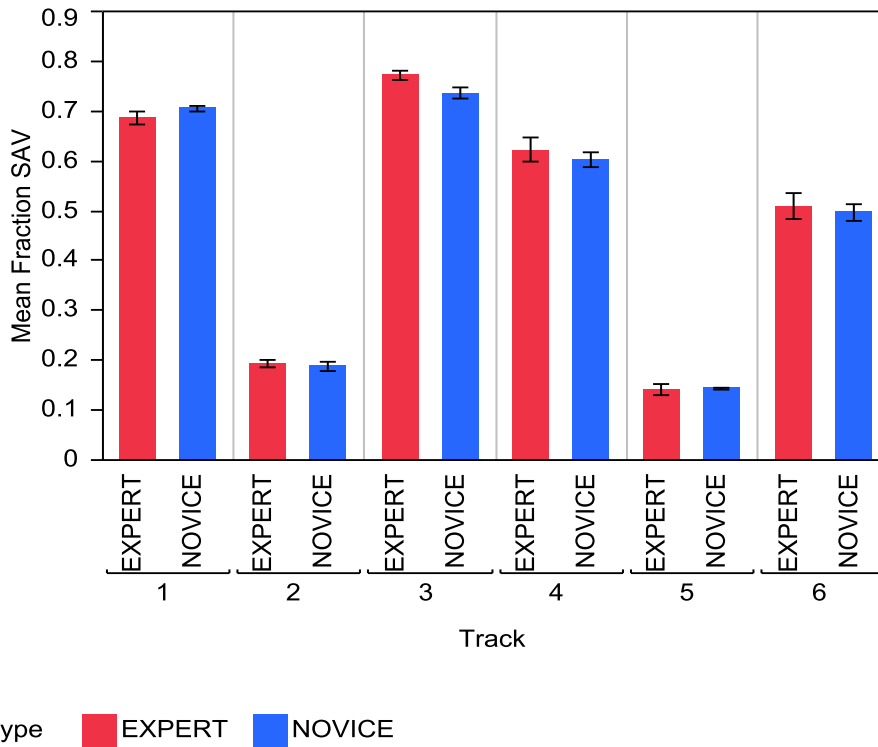


Figure 25. Mean fraction SAV as classified by expert (n = 3) and novice (n = 5) classifiers from underwater video.

Table 7. Fraction of SAV by observer for all test tracks. Only the initial classifications of repeated tracks (denoted by *), were used in this comparison.

Observer	1*	2*	3	4*	5	6
NOV1	0.687	0.18	0.726	0.572	0.149	0.479
NOV2	0.711	0.172	0.763	0.583	0.145	0.448
NOV3	0.719	0.171	0.717	0.598	0.139	0.531
NOV4	0.716	0.202	0.762	0.661	0.135	0.49
NOV5	0.691	0.214	0.714	0.595	0.149	0.539
EXP1	0.675	0.204	0.763	0.603	0.155	0.526
EXP2	0.714	0.182	0.763	0.672	0.149	0.541
EXP3	0.672	0.193	0.789	0.592	0.119	0.459

Intra-observer

Intra-observer variance for all transects and all observers was low with the highest intra-observer variance for a single track of 0.04 and mean difference for a single track per observer of 0.03 (Table 8). Track 2, comprised of SAV that was generally low in cover and very patchy throughout the track, had the least variance among all three replicates (Table 8). Intra-observer variance for Track 1 was intermediate; replicates 1 and 3 had little intra-observer variance, while variance in replicate 2 was noticeably larger. Similar to inter-observer results, track 4 had the largest variance within and among observers (Figure 25, Figure 26). Variance within and between novice observers (Figure 27) was greatest on track 4, but within the expert variance.

Table 8. Fraction of SAV by observer for all replicate video tracks including the absolute maximum difference of the fraction of SAV for an individual track replicate (max diff) and mean of absolute differences of the fraction of SAV.

Observer	Track	Rep 1	Rep 2	Rep 3	Mean SAV	Max diff.	Mean diff.
1-NOV	1	0.687	0.713	0.703	0.701	0.014	0.009
	2	0.18	0.186	0.191	0.186	0.006	0.004
	4	0.572	0.628	0.639	0.613	0.041	0.027
2-NOV	1	0.711	0.646	0.691	0.683	0.037	0.024
	2	0.172	0.169	0.158	0.167	0.009	0.005
	4	0.583	0.594	0.589	0.589	0.006	0.004
3-NOV	1	0.719	0.709	0.717	0.715	0.006	0.004
	2	0.171	0.206	0.199	0.192	0.021	0.014
	4	0.598	0.656	0.654	0.636	0.038	0.025
4-NOV	1	0.716	0.704	0.708	0.71	0.006	0.005
	2	0.202	0.196	0.21	0.203	0.007	0.005
	4	0.661	0.656	0.676	0.664	0.012	0.008
5-NOV	1	0.691	0.734	0.705	0.71	0.024	0.016
	2	0.214	0.215	0.204	0.211	0.007	0.005
	4	0.596	0.663	0.631	0.63	0.034	0.023
EXP1	1	0.675	0.705	0.696	0.692	0.017	0.011
	2	0.204	0.193	0.21	0.203	0.010	0.006
	4	0.603	0.572	0.628	0.601	0.029	0.019
EXP2	1	0.714	0.743	0.716	0.725	0.018	0.013
	2	0.182	0.188	0.198	0.19	0.008	0.006
	4	0.672	0.676	0.703	0.684	0.019	0.013
EXP3	1	0.672	0.689	0.721	0.694	0.027	0.018
	2	0.193	0.21	0.243	0.215	0.028	0.018
	4	0.592	0.638	0.55	0.594	0.044	0.030

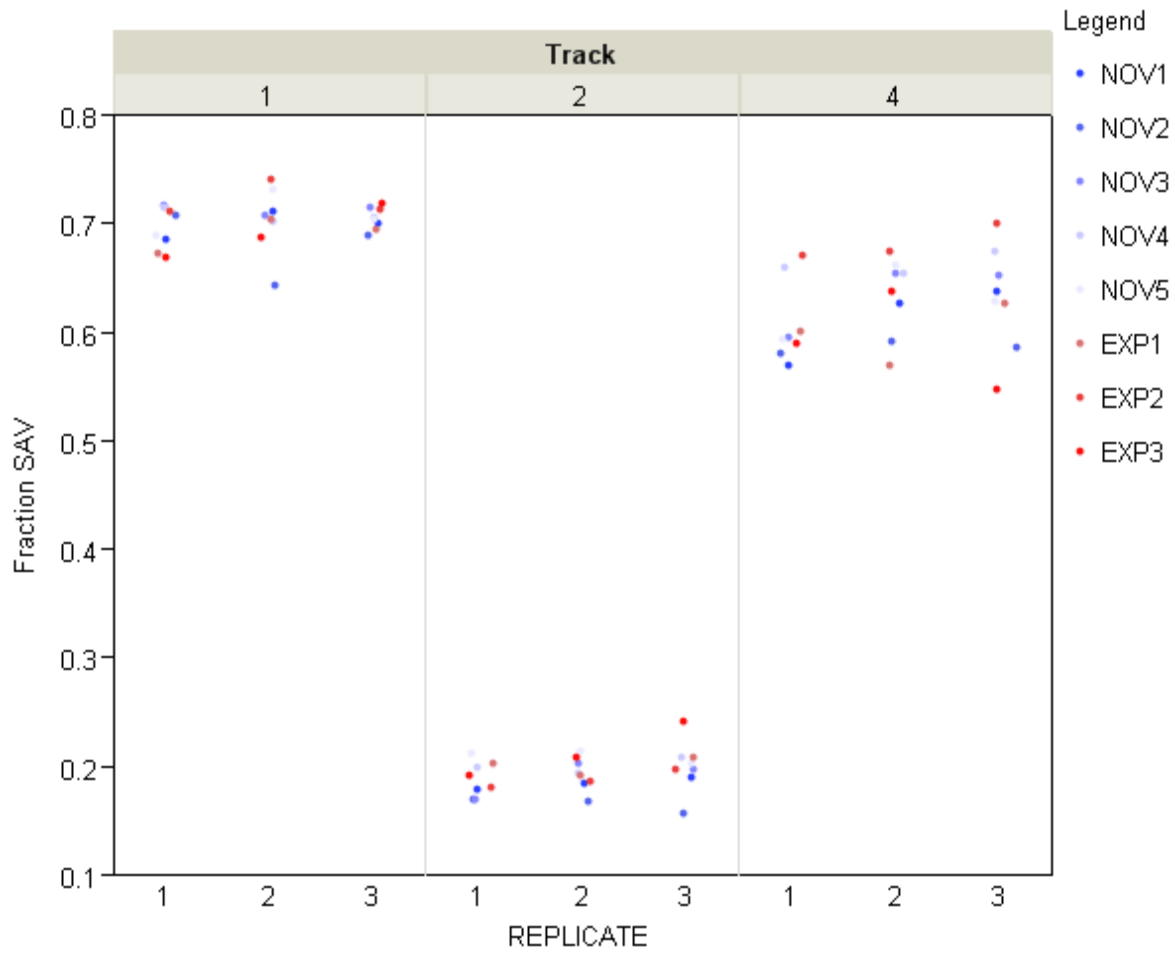


Figure 26. Fraction SAV for replicate tracks by observer, five novice (NOV) and three experts (EXP).

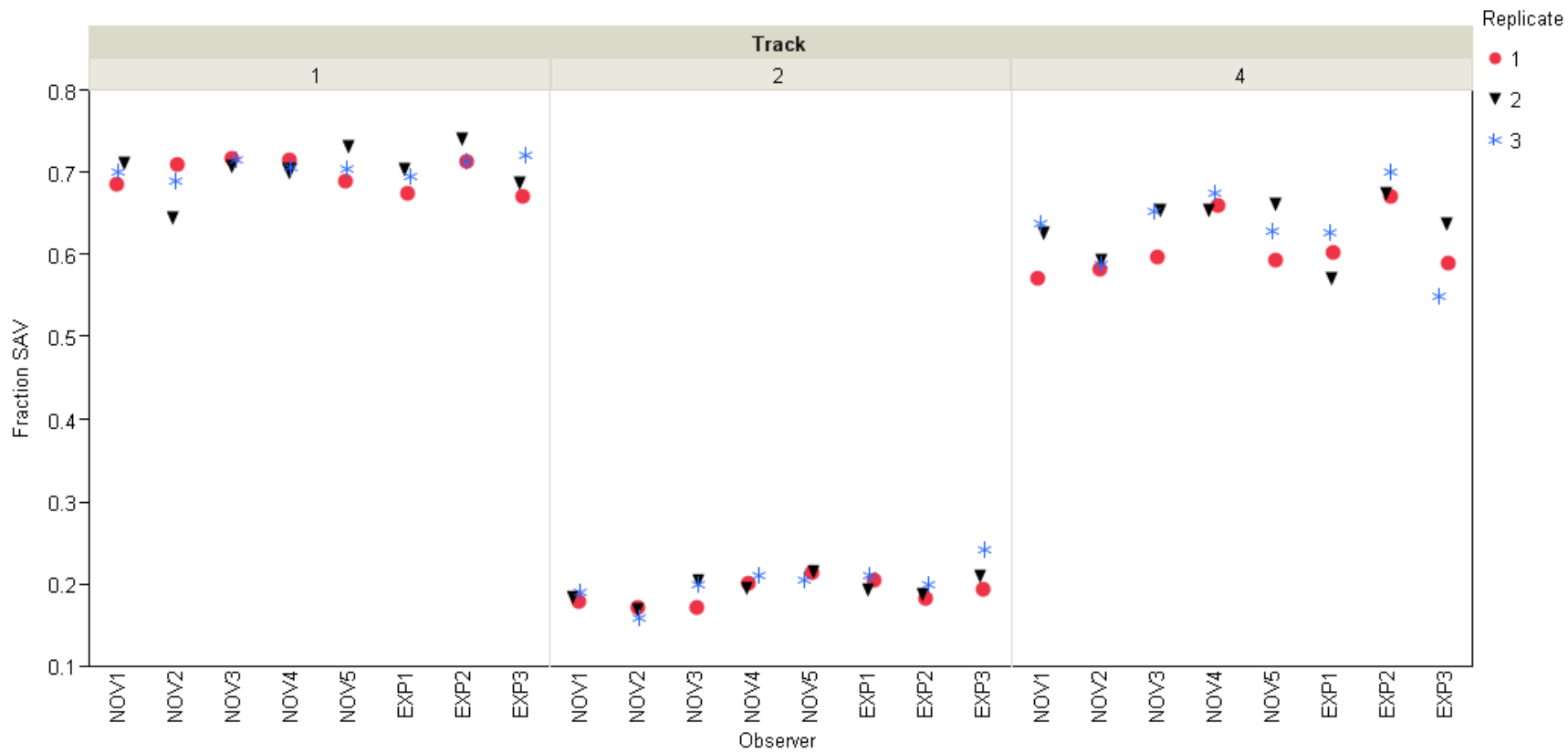


Figure 27. Fraction SAV as quantified by observers (five NOV and three EXP) by replicates for three repeated tracks.

SONAR

Intensive Assessment Sites

Fraction of SAV

The SONAR method allowed us to assess the changes in F_{sav} over time at the four intensive study sites. There was a significant decline in F_{sav} during summer 2010 at both of the high-salinity study sites (Figure 28, Table 9; $p < 0.000001$). The repeated SONAR surveys were analyzed at each of the intensive sites using transects as sampling units. A comparison of the mean F_{sav} , using a repeated measures ANOVA with Site as a between factor and Season (May and June samples were combined into an early SAV growing season group and August and September as a late growing season) as a within-site factor, showed there was significant between-site and within-site variation in mean F_{sav} (Table 10). In addition, there was a significant interaction between Site and Season, with the high-salinity sites showing declines and the low-salinity sites showing slight increases in mean F_{sav} .

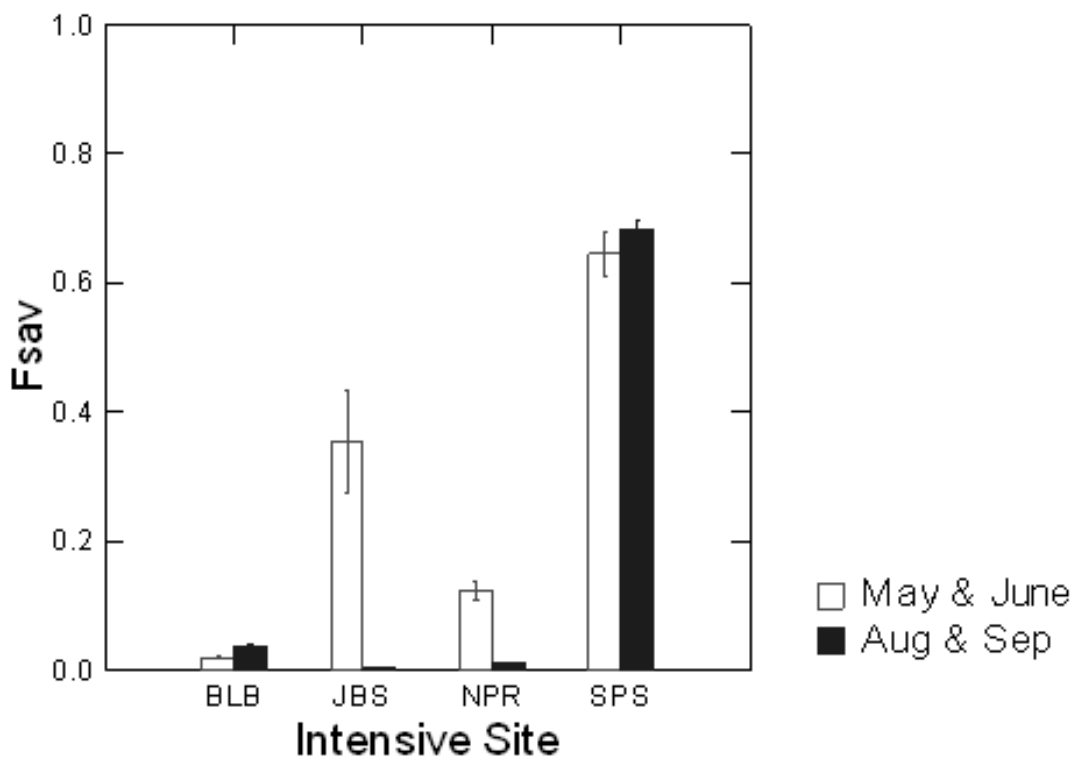


Figure 28. The fraction of SAV ($F_{sav} \pm 1$ S.E.) derived from SONAR at the four intensive sites in the SAV growing season in 2010. The growing season was defined as May through September and divided into samples taken early (May-June) and late (Aug – Sep) in the growing season.

Table 9. Repeated measures ANOVA of the F_{sav} data derived from SONAR method by factors Site and within-Site by Season in 2010.

Source	df	Sum Sq	Mean Sq	F-Value	Pr(>F)
Site	3	39.152	13.050	693.49	<0.000001
Error	244	4.592	0.019		
Within Site					
Season	1	1.106	1.106	64.28	<0.000001
Season*Site	3	2.675	0.892	52.07	<0.000001
Residuals	244	4.178	0.017		

Table 10. Hypothesis tests (repeated measures ANOVA F_{df} , and P-values) of no change in fraction of SAV (F_{sav}) between the early and late growing season in 2010 within each of the intensive sites.

Within-Site Hypothesis Contrast	BLB	JBS	NPR	SPS
Early Season vs. Late Season	$F_{1,244} = 64.28$	$F_{1,244} = 40.87$	$F_{1,244} = 139.74$	$F_{1,244} = 3.71$
P-value	< 0.000001	< 0.000001	< 0.000001	< 0.055

NPR and JBS declined in mean F_{sav} from early growing season (May and June) to late growing season (Aug and Sep), while BLB and SPS remained constant over this same period. BLB had a low mean F_{sav} (0.025) and SPS had a high F_{sav} (0.67) over this 5-month period (Table 11). On average over the 5-month period, the F_{sav} measure obtained from SONAR was highest at SPS (Jun. – Sep. mean $F_{sav} = 0.674$), followed by JBS (mean $F_{sav} = 0.125$ Jun., Jul., Sep. 2010), NPR ($F_{sav} = 0.028$ from Jun. 2009, Jun. 2010, Aug. 2010, Sep. 2010), and the lowest was at BLB ($F_{sav} = 0.025$ May, Jun., Sep. 2010; Table 11).

Table 11. The mean fraction of SAV ($F_{sav} \pm$ S.E) at the four intensive sites for each month sampled (May – September) derived from SONAR data in 2010.

Site	Early Growing Season			Late Growing Season		
	May	June	July	August	September	All Dates
NPR	0.172 (±0.023)	0.067 (±0.009)		0.038 (±0.007)	0.009 (±0.001)	0.028 (±0.004)
JBS		0.353 (±0.077)	0.025 (±0.004)		0.003 (±0.001)	0.125 (±0.029)
BLB	0.011 (±0.001)	0.045 (±0.005)		0.030 (±0.005)	0.041 (±0.005)	0.025 (±0.002)
SPS		0.645 (±0.033)	0.76 (±0.192)	0.689 (±0.014)	0.672 (±0.022)	0.674 (±0.014)

Accuracy Assessment

A combination of data acquired by SONAR and underwater video was used to assess the accuracy of the SONAR data at each intensively studied site. Both data sets were collected from different vessels on the same pre-determined transects and were expected to overlap. However, the currents, wind, and GPS error made it difficult to drive the two vessels precisely over the same transects, thus introducing a level of error in the accuracy assessment (Figure 29). When all four sites were combined, the accuracy of the SONAR decreased with distance to the nearest neighbor, leading to the most accurate results at distances < 3 m. Video and SONAR points that were within 3 m of each other and at a minimum depth of 0.7 m (see Methods for a detailed explanation) were used in all further analyses.



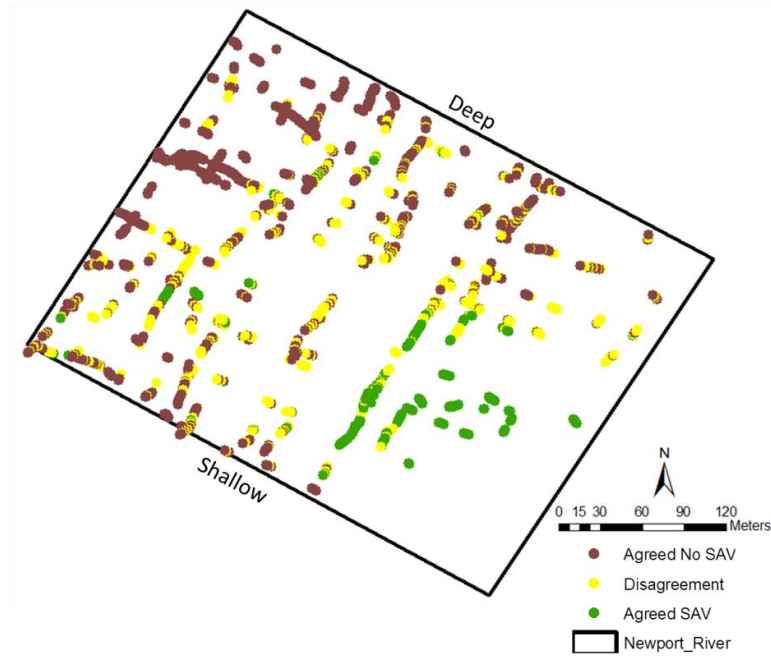
Figure 29. Transects driven at NPR in June 2009 by the SONAR (yellow dots) and underwater video (black dots) methods.

Accuracy by site ranged from 69.4 to 98.2%, with an overall average accuracy of 77.4% (Table 12). The results from these accuracy analyses show that disagreements tend to be highest in regions on the edges of the main SAV bed at a site. For example, at NPR in June 2009, the region of poorest accuracy was just outside of the main bed located in the SW corner of the study site (Figure 30A). Of the ~1700 comparison points, 520 (30.6%) were disagreements, and most of them (85.2%) were when SAV was identified by the underwater video but not with SONAR. At SPS in August 2010, disagreements between the two methods occurred both on the edge of the main channel (see Appendix 8) and at several points throughout the region of the study site. Of the ~1230 comparison points, 287 (23.0%) were points of disagreement (Figure 30B). Most of these disagreements (64%) occurred when SONAR detected SAV but SAV was not detected by underwater video.

Table 12. Accuracy of the SONAR at the four intensive sites and over all sites (2009/2010) at a nearest neighbor distance of 3 m and a depth ≥ 0.7 m.

Site	N	Accuracy (%)
BLB	273	82.1
JBS	620	98.2
NPR	1702	69.4
SPS	1246	77.0
Overall	3827	77.4

A



B

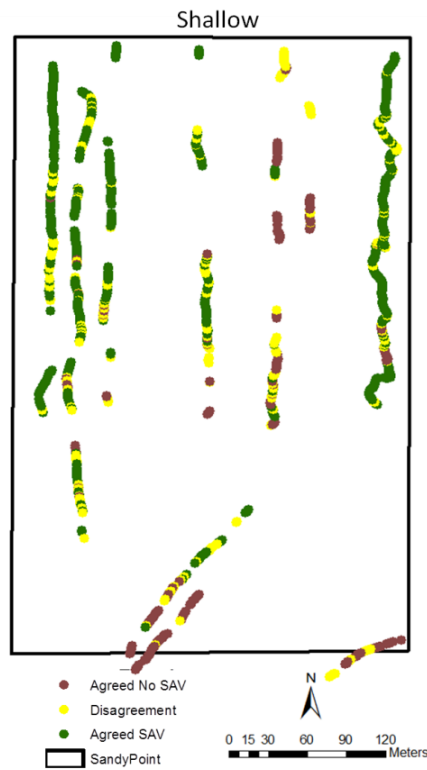


Figure 30. Two examples of the nearest neighbor accuracy analysis at the SONAR comparison points: A) NPR June 2009 and B) SPS August 2010. The circles represent points of agreement that no SAV is present (brown), SAV is present (green), or points of disagreement about the presence of SAV (yellow) between the underwater video and SONAR.

Surface Interpolation Analyses

The SONAR acoustic reports were used to create a kriging surface of bathymetry and cokriging surface of the relative area of the SAV bed (RA_{sav}) for each intensively studied site in 2009/2010. For the June 2009 survey at NPR, a *post-hoc* accuracy analysis was conducted on three cokriging models to determine the best-possible model to use for surface interpolation of the RA_{sav} surface. Once the most accurate model was selected, the RA_{sav} was obtained from the cokriging prediction surface at each site and analyzed for the total area of SAV present by month. A bathymetry kriging prediction surface was produced for each site and each month to determine the locations where SONAR accuracy is expected to decline. The maps are plotted with the kriging results for one time period at each site. See Appendix 8 for additional images of SAV bed kriging surface areas, bathymetry kriging surface areas, SONAR transect lines, and quadrat surveys of SAV cover (%).

Model Validation

The three cokriging models (Ideal Cover, Ideal Binary, and Local Binary) produced from SONAR data collected at NPR in June (2009) showed slightly different results. Both binary cokriging models predicted similar SAV surfaces (Figure 31), producing the largest areas of RA_{SAV} . However, the Local Binary model generally predicted a few more patches of SAV and a slightly larger SAV bed than did the Ideal Binary model. The Ideal Cover model had the smallest area of SAV but it still predicted the main area of the bed. The accuracy results, using re-sampling of 100 points, repeated 100 times indicated that the overall accuracy between the three models were similar, with each model predicting a median accuracy of ~65% (Figure 32). Because the Ideal Binary model had the highest accuracy (66%), the remainder of the sites were analyzed using this cokriging method (i.e. binary SAV cover with cross-validation parameters minimized) for all sites and dates. The model results are shown in Appendix 8. The results of these models were used to calculate RA_{sav} for each site and date, which is presented below.

**Predicted SAV Surfaces from Three Cokriging Models
Newport River, Jun. (2009)**

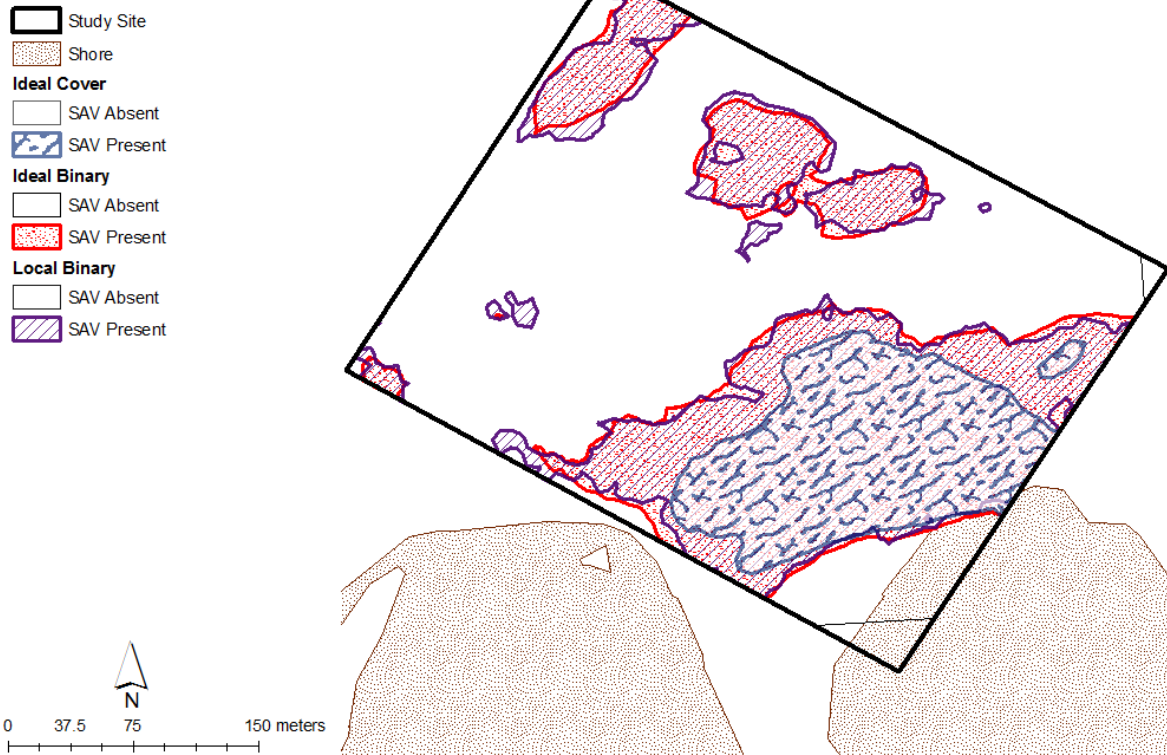


Figure 31. The SAV surface, rated as either SAV present or absent, using three cokriging models at NPR in June 2009: 1) the Ideal Cover model, which uses SAV cover (%) estimated from the acoustic reports produced in EcoSAV2; 2) the Ideal Binary model that uses a lag distance of 12 m and the 25 nearest neighbors; and 3) the Local Binary model, which uses a lag distance of 10 m and 6 nearest neighbors. The Ideal Binary and Local Binary cokriging models are very similar to one another, providing the greatest estimated area of SAV coverage. The Ideal Cover has the lowest area of SAV cover. All three models agree that a large bed of SAV is located in the lower right (SE corner) of the site. Ideal cover model does not show a bed in the upper right (NW corner) of NPR.

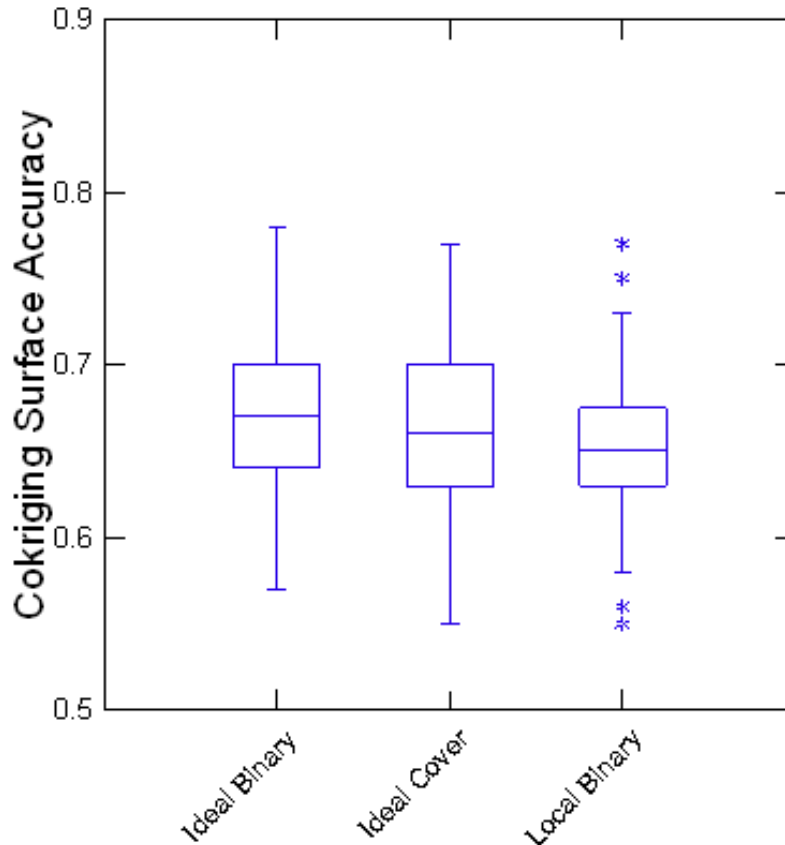


Figure 32. The bootstrapping accuracy values (relative to video classification) for 100 randomly selected comparison points, replicated 100 times for the three cokriging models used to estimate the presence of SAV at NPR in June 2009. The Ideal Binary model used depth (m) and presence-absence data on SAV determined from SONAR and ECOSAV2, with a lag distance of 12 m and 25 nearest neighbors to predict the surface. The Ideal Cover model used depth (m) and SAV cover (%) from ECOSAV2 acoustic reports to predict the surface, with a lag distance of 13 m and 35 nearest neighbors. The Local Binary SAV model used a “local” smoothing of the depth and SAV presence-absence data, with lag distance of 10 m and 6 nearest neighbors to predict the surface. The cross-validation results of the first and third models were optimized. The line within the box indicates the median, the upper and lower hinges includes the 25th and 75th percentiles, and * represent outlier values 1.5 times the inter-quartile range from the upper and lower quartiles

Newport River (2009 -2010)

In June 2009, the SAV bed at NPR was a relatively shallow site, with the majority of the area in a depth ≤ 1 m (Figure 33A). The ideal binary SAV cokriging surface from the SONAR data showed overall low SAV cover at this site ($RA_{sav}=0.392$, Table 13), with the majority of the SAV located in the southern region of the study site (Figure 34A). This indicated that the SAV at this site was commonly found in depths <0.7 m and very little was found in the deeper areas of

the study site. In the SONAR surveys conducted in 2010, the SAV bed was not as extensive as that observed in 2009. The RA_{sav} values ranged between 0.006 and 0.382 (Table 13) in 2010. The bed seemed to die out throughout the summer, with the lowest observed SAV bed areas in August and September 2010 (Figure 35). There was an overall absolute intra-annual change of up to 39%. For additional cokriging and kriging results, see Appendix 8.

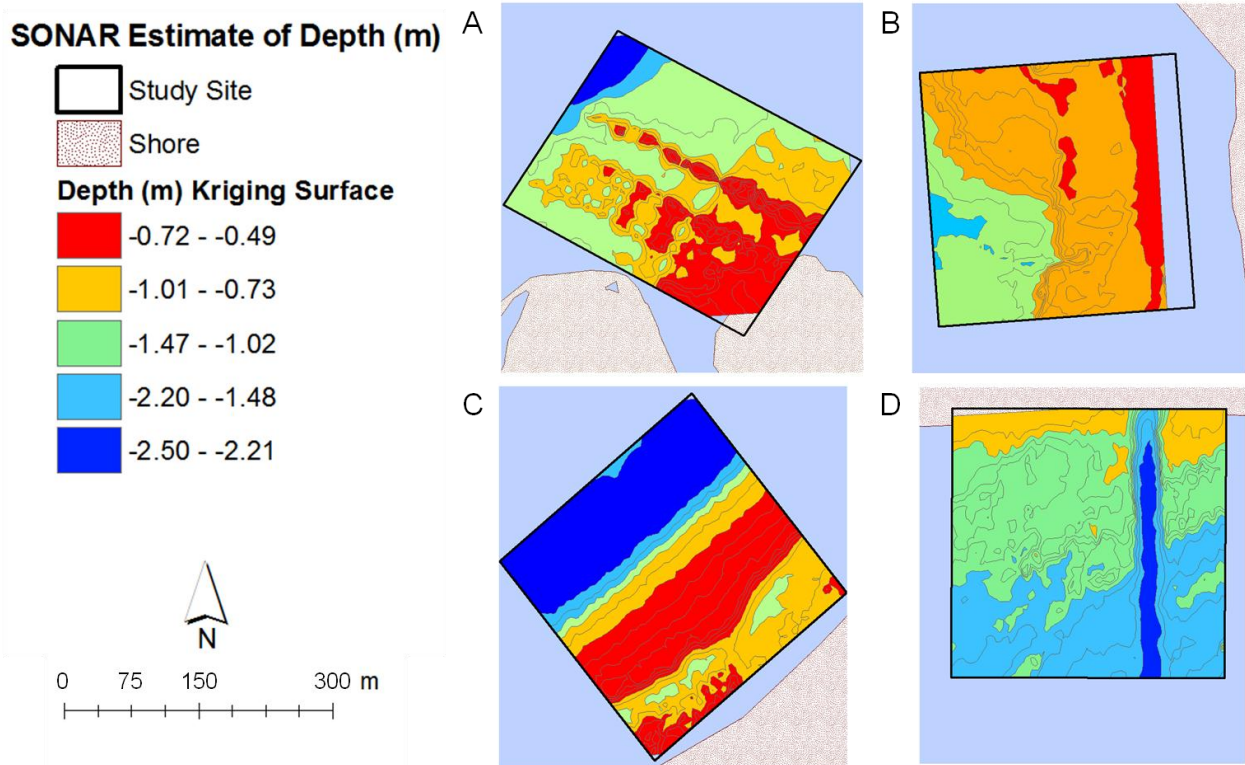


Figure 33. The prediction surface of depth using a kriging analysis obtained from classified SONAR reports at the four intensively-studied sites. Each image is from the 2009-2010 study period at: A) NPR (June 2009), B) JBS (June 2010), C) BLB (August 2010), and D) SPS (June 2010).

Table 13. The total area and SAV-present area determined from a cokriging analysis of SAV presence/absence and depth (m) obtained at each site and date by SONAR surveys. The relative area of SAV (RA_{sav}) represents the proportion of the area covered by SAV by year, month, and site. The Ave. SE is the average standard error of the cokriging model, which is a combination of both measurement error and the variation around an interpolated point (see Appendix 8). In August and September 2010, the SPS site was extended offshore by 150 m (SPS Extend) to capture the deep edge of the bed. *Individual cokriging models were not produced for the extended regions. Instead, the extended models were clipped to the 90,000 m² study region.

Site	Month/Year	Total Area (m²)	SAV Area (m²)	RA_{sav}	Ave. SE
NPR	Jun. 2009	107,059	41,920	0.392	0.3164
NPR	May 2010	102,710	39,185	0.382	0.3922
NPR	Jun. 2010	107,419	16,618	0.155	0.1752
NPR	Aug. 2010	107,985	669	0.006	0.0904
NPR	Sep. 2010	108,073	795	0.007	0.0990
JBS	Jun. 2010	81,041	61,235	0.756	0.3677
JBS	Jul. 2010	90,031	14,230	0.158	0.1240
JBS	Sep. 2010	80,904	0	0.000	0.0619
BLB	May 2010	91,761	2,248	0.024	0.1290
BLB	Jun. 2010	68,868	9,103	0.132	0.1405
BLB	Aug. 2010	91,703	28,986	0.316	0.1401
BLB	Sep. 2010	91,681	16,826	0.184	0.1671
SPS	Jun. 2010	89,474	89,464	0.999	0.4250
SPS	Aug. 2010	90,027	90,026	0.999	*
SPS Extend	Aug. 2010	147,433	146,589	0.994	0.3936
SPS	Sep. 2010	90,030	89,661	0.996	*
SPS Extend	Sep. 2010	147,417	143,352	0.972	0.3882

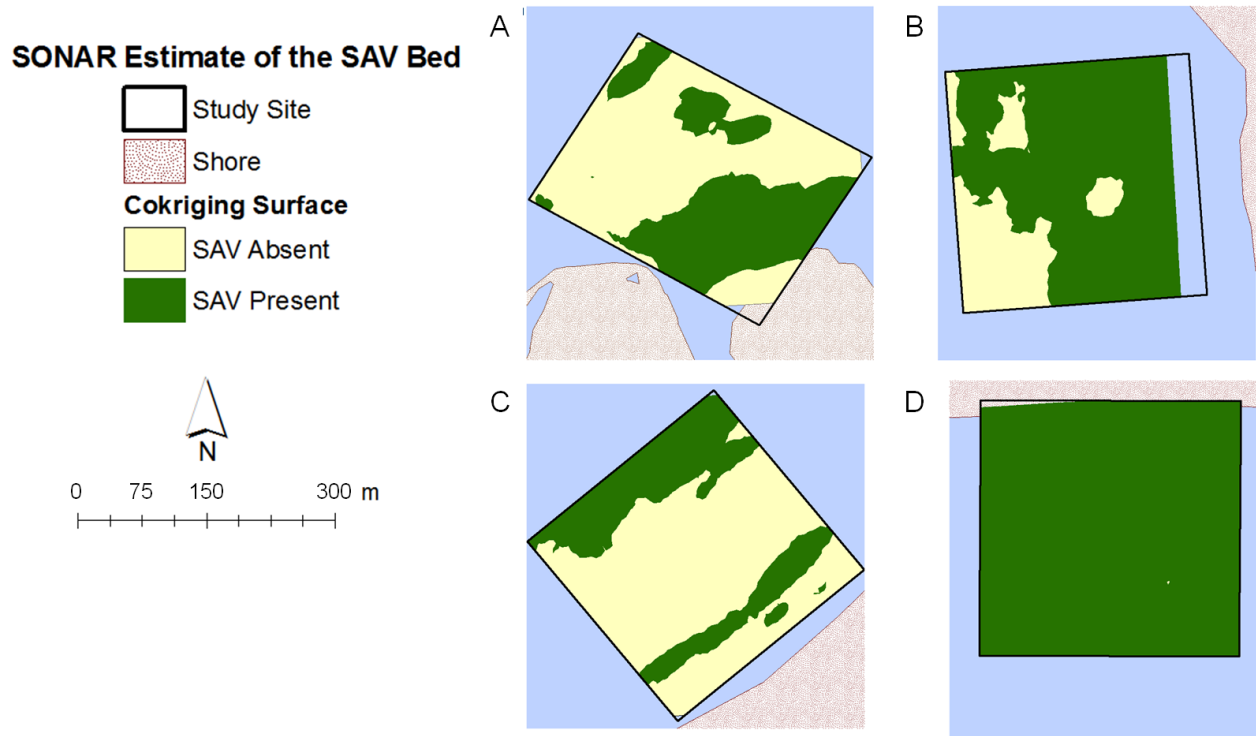


Figure 34. The prediction surface showing the presence or absence of SAV using a cokriging analysis of depth and SAV (0, 1) obtained from classified SONAR reports at the four intensively-studied sites. Each image shows the peak prediction during the 2009-2010 study period at: A) NPR (June 2009), B) JBS (June 2010), C) BLB (August 2010), and D) SPS (June 2010).

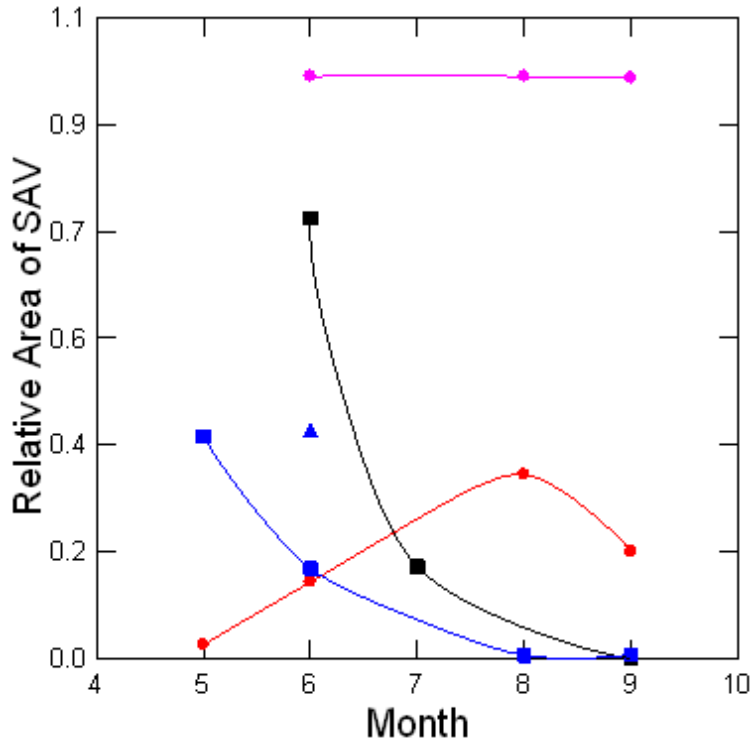


Figure 35. Relative area of SAV (R_{sav}) at JBS 2010 (black square), NPR 2009 (blue triangle), NPR 2010 (blue square), BLB 2010 (red circle), and SPS 2010 (pink circle) using the cokriging surface created from the SAV presence/absence data from SONAR reports.

Jarrett Bay (2010)

JBS is also a very shallow location. In June 2010, the majority of the site was in depths ≤ 1 m (Figure 33). At this time, the bed at JBS was extensive ($RA_{sav}=0.756$, Table 13) and present at depths up to 1.3 m (Figure 34, Figure 35). By July 2010, the bed had begun to die back ($RA_{sav}=0.158$, Table 13), with extensive SAV loss in areas at water depths ≥ 1 m (see Appendix 8. Depth Kriging and SAV Cokriging Models from the SONAR Acoustic Reports). By September 2010, the results from the SONAR acoustic reports indicate that SAV had completely disappeared (Table 13). This high-salinity seagrass bed slowly died out throughout the summer (Figure 34). There was an overall absolute intra-annual change of up to 76%.

Blounts Bay (2010)

At BLB in August 2010, the water depth varied between 0.5 and 2.4 m (Figure 33). The shallowest portion of the bed was a shoal ~ 80 m from shore. At its peak when $RA_{sav} = 0.316$ (Table 13), the kriging surface area suggested that the bed was located in a very shallow region (≤ 0.7 m, Figure 34) and in the deepest region of the site (between 2.2 and 2.4 m). In May 2010,

the bed was nearly non-existent (Table 13), peaked in August and then proceeded to die-back by September 2010 (Figure 35). According to the cokriging surface created by the SONAR report data, over the entire summer, there was $\approx 30\%$ intra-annual change in the bed area.

Sandy Point (2010)

At SPS the SAV depth distribution was deeper than observed at the other three intensive study sites. In Jun. 2009, the water depth varied from 0.8 to 2.5 m, with the majority of the site in depths ≥ 1.3 m (Figure 33). Initially, the specified 300 x 300 m box was surveyed, but in June 2010, a $RA_{sav} = 0.999$ (Table 13) was observed, indicating that the edge was not identified in the survey (Figure 34). In Aug. 2010, the site was extended offshore by 150 m in an attempt to locate the edge of the SAV bed. Within the initial site, the bed cover did not change throughout the entire sampling period (Figure 35, Table 13), even when the extended region was included in the analysis, an extensive bed ($RA_{sav} = 0.972$) was clearly evident in September 2010.

In summary, SPS had high proportion of SAV present at each survey date in the summer of 2010 ($RA_{sav} = 0.97 - 1.0$), while other sites varied throughout the summer (Figure 35). The two high salinity sites (NPR and JBS) showed dramatic declines in SAV from May through Sep. (from RA_{sav} of 0.4 or 0.7 in early summer, 0.0 in late summer). The low salinity sites reached a peak in RA_{sav} in Aug. 2010. This magnitude of intra-annual changes will need to be considered when selecting index periods for monitoring SAV.

Diver Surveys

The F_{SAV} percent cover data collected from quadrats at depths ≤ 2 m showed intra-annual variability of SAV at all sites in 2010, except BLB (slope = 0.452, Figure 35). While the general trend was an increase in SAV median percent cover at BLB from May through September 2010; the linear trend line shows no significant difference for the sampling period ($p = 0.797$, Table 14). The other low salinity site (SPS) showed a significantly positive trend (slope = 8.579, $p < 0.001$), as the SAV median percent cover increased by month. The two high salinity sites indicated the opposite trends, with a decline in SAV. At JBS, this trend was marginally significant (slope = - 4.955, $p = 0.044$) but at NPR, the trend is highly significant (slope = -6.126, $p < 0.001$).

Table 14. The best fit line for F_{sav} by month (2010) for the four intensively surveyed sites with divers.

Site	Number surveyed waypoints	Slope	Constant	F-ratio	p-value
BLB	164	0.452	22.186	0.006	0.797
JBS	101	-4.955	49.714	4.174	0.044
NPR	219	-6.126	51.000	87.241	<0.001
SPS	163	8.579	6.328	13.655	<0.001

Rapid Assessment Sites

Fraction of SAV

In September 2011, F_{sav} , as measured by the SONAR, varied among the low-salinity areas surveyed on the 10-km shore-parallel transects (Table 15). SP had the largest F_{sav} value (0.966), followed by BB, TR, NR, RC. At the other four rapid assessment sites there was relatively little F_{sav} , with less than 4% of the acoustic reports indicating SAV presence. When the SONAR identified the presence of SAV along the transect, the SAV patch-length typically extended less than 4 m (Table 15) but a single patch of SAV could extend up to 1729.8 m. The type of variation observed in this data set is important to consider when choosing sites for monitoring SAV change detection.

Table 15. Survey date (2011), number of acoustic reports obtained along each transect, mean depth sampled, F_{sav} , maximum and median SAV patch lengths, and maximum and median unvegetated patch lengths at rapid assessment sites.

Site	Survey Date	SONAR Reports	Mean Depth (m)	F_{sav}	Max. SAV Patch Length (m)	Median SAV Patch Length (m)	Max Unvegetated Patch Length (m)	Median Unvegetated Patch Length (m)
BB	9/29/11	4412	1.12	0.703	1442.0	5.8	5.8	5.8
BY	9/01/11	8133	1.55	0.009	17.6	3.2	10.1	3.6
FB	9/19/11	4581	0.87	0.011	35.2	3.4	171.4	6.8
JC	9/30/11	5586	0.94	0.014	14.0	3.7	131.1	7.6
NR	9/14/11	6470	1.70	0.226	111.8	2.0	4.0	4.0
PR	9/20/11	3860	1.18	0.033	17.9	3.1	55.6	6.7
RC	9/08/11	4903	1.24	0.217	49.8	2.4	7.4	3.5
SP	9/02/11	3927	1.32	0.966	1729.8	16.5	3.1	5.5
TR	9/27/11	4725	1.41	0.388	397.5	3.8	7.2	6.3
Mean		5177.4	1.23	0.285	424.0	4.9	44.0	5.5
Median		4725	1.24	0.217	49.8	3.4	7.4	5.8
S.E.		457.9	0.09	0.115	224.5	1.5	21.3	0.5

Accuracy Assessment

To determine the accuracy of the SONAR on the 10-km shore-parallel transects, the same procedure was used as in the 2009/2010 data set for the intensive study sites, but these data were not limited by depth (Table 15). The accuracy of the sites ranged from 53% (TR) to 100% (FB), at a nearest neighbor distance ≤ 3 m. The overall accuracy was 82% for all seven sites (Figure 36). Two sites with the lowest accuracy values were TR (53%) and RC (75%, Figure 36).

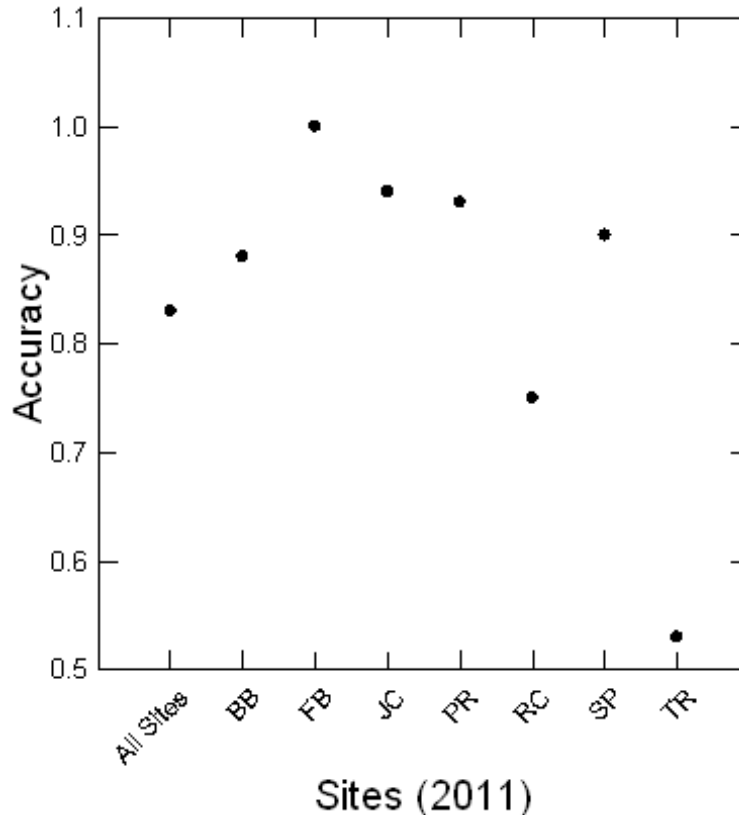


Figure 36. Accuracy of SONAR at the Rapid Assessment Sites and over all seven sites in the 2011 sample event.

Power Analyses for Detecting Change in SAV Abundance

Simulated Video Transects

Overall, this analysis revealed that the systematic SYS_2 approach of Fewster (2011) resulted in more precise variance estimates and a greater ability to detect change with less effort than did simple random sampling (SRS) or naïve systematic sampling (SYS_1) (Figure 37). For contiguous and blowout images, application of SYS_2 resulted in $> 80\%$ power of detecting a

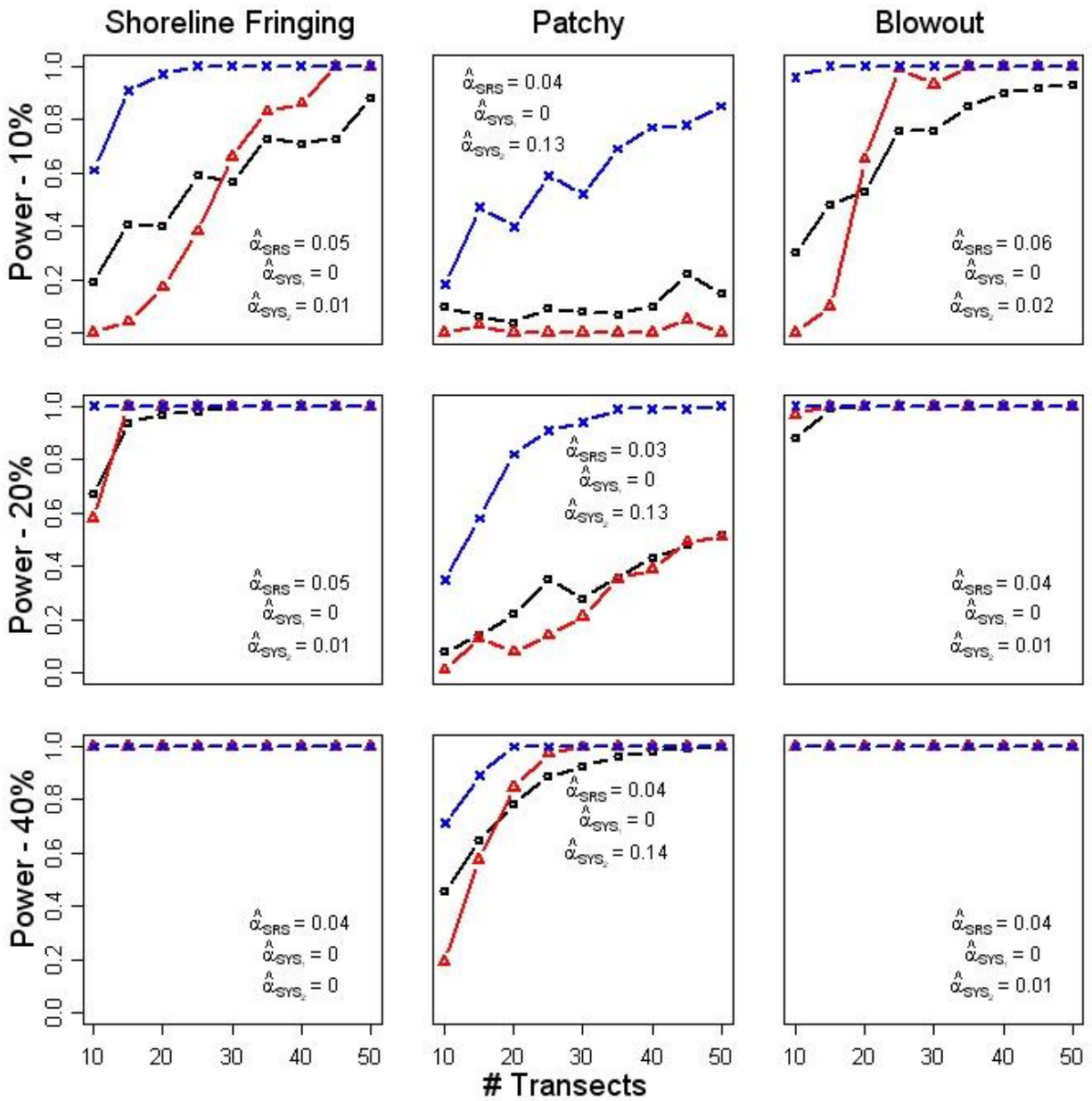


Figure 37. Predicted power to detect 10% declines (top panels), 20% declines (middle panels), and 40% declines (bottom panels) in SAV as a function of number of transects. Left panels give results for contiguous habitat, center panels give results for patchy habitat, and right panels give results for the blowout study area. Black circles represent results from simple random sampling (SRS), red triangles give results for systematic sampling where the naïve SRS variance estimator is employed (SYS₁), and blue x's give results for systematic sampling using the approach of Fewster (2011) to get variance estimates (SYS₂). Also shown are the realized proportion of simulations that resulted in type I errors (α).

10% population decline with just 10-15 transects, while still controlling for type I error rates. In contrast, the SRS and SYS_1 estimators often needed double the number of transects to achieve comparable power. However, the SYS_2 estimator did not work as well for the patchy landscape, with a type I error rate of 0.13-0.14. This value is substantially over the nominal value of 0.05, suggesting that this procedure will falsely reject the null hypothesis more than anticipated. Also, it appears necessary to employ at least ten transects with the SYS_2 method in order to have enough degrees of freedom to fit the GAM model.

There is a clear advantage of employing a systematic sampling design in SAV surveys, with the SYS_2 approach for estimating variance producing more realistic estimates of variance, at least for contiguous and blow out landscapes, however, sparse and patchy landscapes present change detection problems for all designs. On one hand, the SYS_2 approach likely underestimates total variance because the GAM does not do a very good job of characterizing the variance between neighboring transect lines for highly variable landscapes, and therefore produces type I error rates that are high. On the other hand, SRS variance formulae likely overestimate variance for systematic sampling (Thompson 2002), resulting in low power to detect differences.

Simulated SONAR Transects

The simulation of the power available to detect a change in SAV using SONAR showed that a single day's sampling effort (up to 50 transects per day) could detect 10% change between two surveys if the systematic sampling was used and variance was computed using the appropriate method. The number of transects required to have a 0.8 power of detecting a 10% or 20% change in SAV using the SONAR method between years was very high with SRS and SYS_1 , no matter which of the four sites we simulated (Figure 38). At most sites, using SRS and SYS_1 sampling methods, 50 transects was insufficient to detect a change of 10% or 20% with 0.8 power. We could, however, detect a 40% change in SAV with 30-40 transects at most sites using the SRS and SYS_1 methods. However, if the method of Fewster (2011) was used to establish transect-to-transect variance, with systematic transect sampling and a GAM model used to compute the variance, a reasonable number of SONAR transects (see below) is required to detect 10% change in SAV with high statistical power (Figure 38). We would need about 25-30 SONAR transects at all intensive sites to detect a 10% change in SAV between surveys made at two points in time with a power of 0.8. The number of transects required at SPS to detect a 10% change with 0.8 power was very low (10 transects), intermediate at JBS and NPR (25 transects) and highest BLB (30 transects).

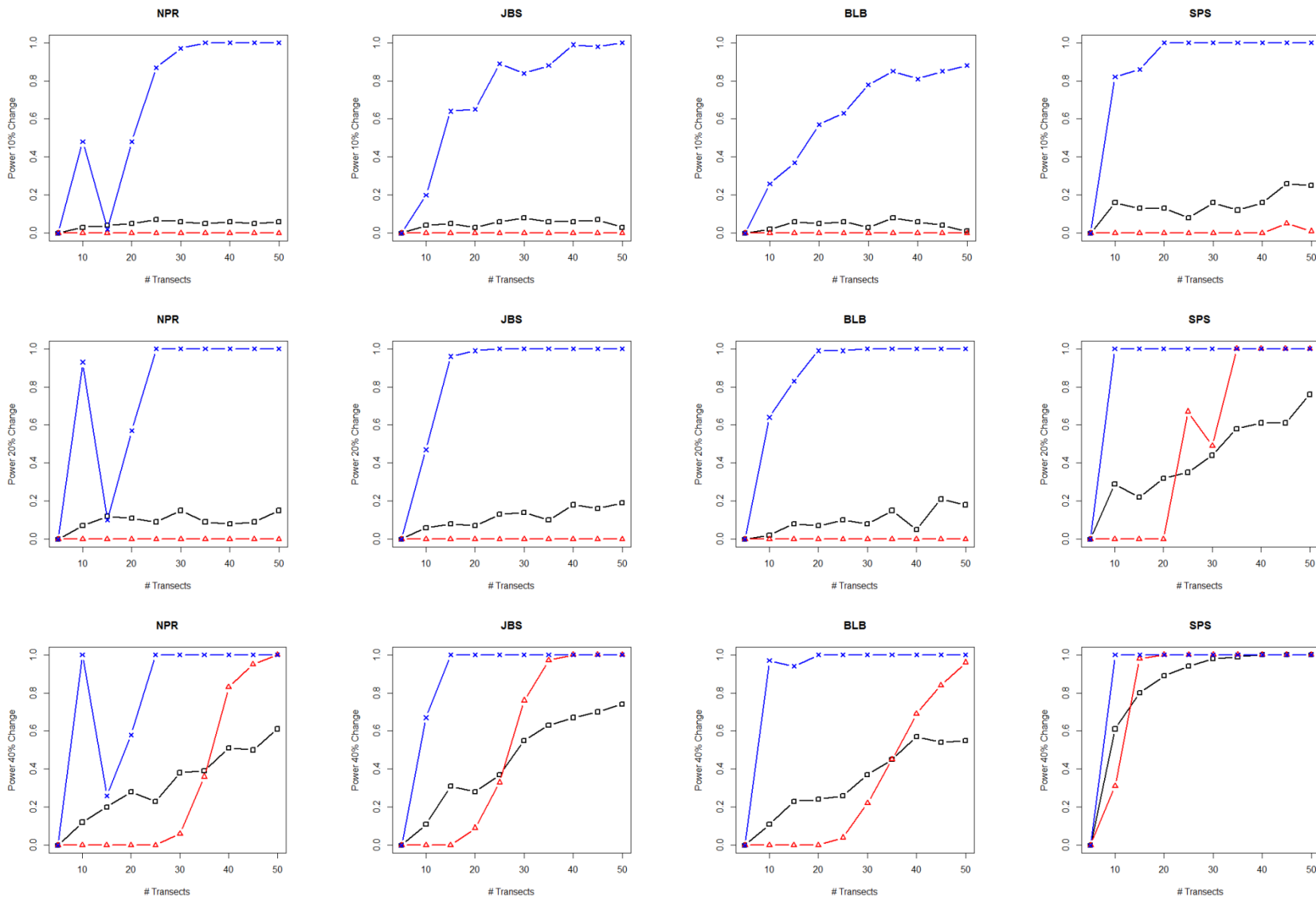


Figure 38. Power to detect 10%, 20%, and 40% change in SAV simulated over a surface obtained from the Ideal Binary cokriging model at each of the intensive sites using three power simulation models: 1) SRS (black circles), 2) SYS₁ (red triangles) and 3) SYS₂ (blue x's). In each case, the SYS₂ (Fewster 2011) model has the greatest power to detect changes with a small number of transects. With all simulations, fewer transects are required to detect a 40% change in SAV than 20% or 10% change.

Remote Sensing Results

The coast-wide mapping for SAV in NC classified 138,378 acres of total SAV. Of that total, 112,417 acres, (81.2%) was primarily high-salinity seagrass located on the barrier island shelves in Albemarle, Pamlico, Core, Back and Bogue Sounds. Of the total, 25,961 acres (18.8%) was low salinity SAV. As shown in Figure 39, the majority of the SAV in the state (103,782 acres), all of it seagrass, was located in the shallow waters on the sound-side of the Outer Banks between Cape Lookout, and the Route 64 bridge between Manteo and the Outer Banks. Of the currently known SAV resource in NC, the seagrass in the barrier island shelf region accounted for 92.3% of the state's seagrass and 75.0% of the state's total SAV.



Figure 39. Dense (dark green) and patchy (light green) SAV distribution in NC mapped as part of the 2007-2008 coast-wide effort.

The challenge for monitoring the SAV resources in NC will continue to be the low salinity SAV of the Albemarle, Pamlico and Currituck Sounds, the river systems that feed into the Sounds and the inner banks regions of western Pamlico Sound. Despite drought conditions in October of 2007, when the imagery for those areas was acquired, a large percentage of the photos for the low salinity regions showed water column turbidity that made SAV interpretation difficult. Therefore, estimates for low salinity SAV in those areas are almost certainly underestimates. In addition to this uncertainty, is the cost of acquiring imagery for an area prone to turbidity. Of the 1347 images that were required to cover all areas of interest for the 2006-2008 mapping effort, 930 (69%, Figure 40) were needed to cover the areas of low-salinity SAV. Therefore 69% of the imagery (and costs associated with the imagery acquisition) was needed to cover an area that is difficult, if not impossible, to interpret via aerial surveys and contains only 18.8% of the total known SAV mapped in the state to date.

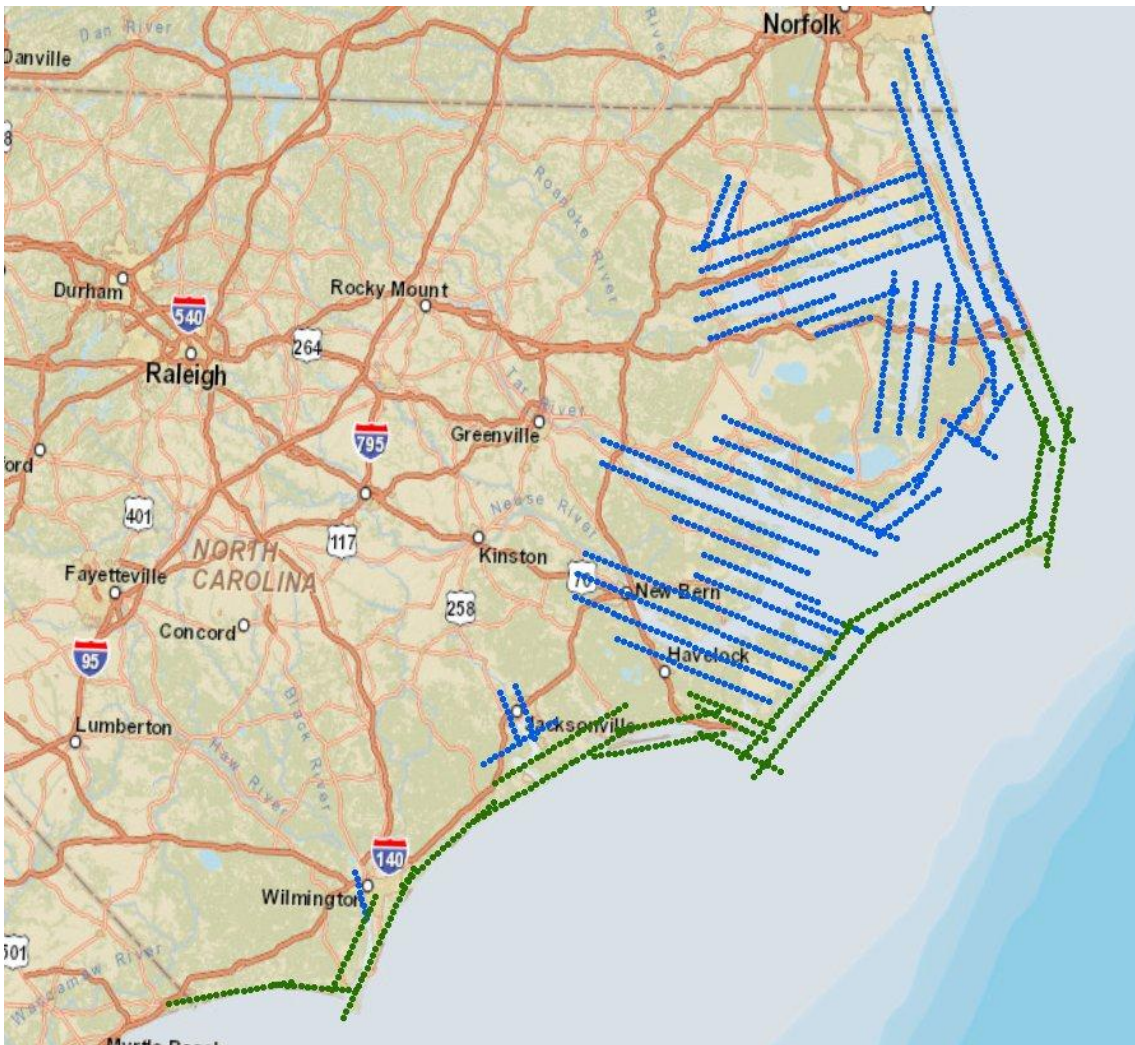


Figure 40. Aerial images (represented as dots) collected during the 2007/08 coast-wide SAV mapping effort. Photos in regions of high (green) and low (blue) salinity are indicated.

Accuracy Assessment of Remote Sensing

Prior to the start of the field missions (for both the 2007-08 coast-wide mapping and the 2006 mapping in Bogue, Back and Core Sounds), a stratified random sample of points was generated. Points were generated for two strata: 1) a seagrass strata, with points generated from a GIS file with all previous mapping efforts within the study area (unpublished data), and 2) all areas of < 2 m depth not within the seagrass GIS layer. The maximum depth of seagrass in the study area was approximately 2 m. Step 2 was an attempt to cover areas < 2 m that may have had seagrass during the earlier mappings but were incorrectly mapped as unvegetated, or to survey areas that may have been colonized by seagrass since the previous mappings. The bathymetry data used to determine areas < 2 m was publicly available data downloaded from the NOAA National Geophysical Data Center (http://www.ngdc.noaa.gov/mgg/gdas/gd_designagrid.html?dbase=grdcrm).

While over 1,000 randomly selected points were visited in the field for the 2007/2008 coast-wide acquisition, it was deemed necessary that all points would be used to train interpreters in the classification process. Therefore, no random points were withheld for an accuracy assessment. Seagrass distribution data at these sites was gathered by visual inspection from small boats, wading when possible, and with rakes when the water was too deep for wading and too turbid to visualize the bottom from the boat.

An accuracy assessment was performed using 107 randomly generated field points on the 2006 classification for Bogue and Back Sounds and the mainland side of Core Sound. Seagrass distribution data at these sites was gathered with underwater video and direct inspection of the bottom by snorkeling. The overall accuracy of the three class map (dense seagrass, patchy seagrass, and unvegetated) was 75.7%. Two misclassifications were the major source of error: classifying areas as dense seagrass that were actually patchy seagrass (six points), and classifying areas as unvegetated that were actually patchy seagrass (16 points). Application of a minimum mapping unit (approximately 0.2 ha) was the cause of the misclassified dense seagrass points – in all cases the field point landed in a patchy area that was in a larger dense polygon but was too small to be mapped as an individual patchy seagrass polygon.

To show the effects of misclassification within the two seagrass classes, another accuracy assessment was performed based on one seagrass class, i.e. the map and field points were re-coded to one seagrass class (combining dense and patchy into one class). The overall accuracy of this map was 82.2%. For areas that were classified as unvegetated but where there was actually seagrass present, one of the main causes of error appeared to be that the amount of seagrass was below the level of detection of the sensor. At 10 sites classified on the map as unvegetated, the percent cover of seagrass from the field data was estimated at < 5%. Most of these sites were near 2 m deep, at or near the deep water limit of seagrass, usually with one to

several sparse patches between 20 and 40 cm in diameter. Close visual inspection of the imagery around these points showed no indication of the presence of seagrass. To show the effects of misclassification associated with areas below the level of detection of the sensor, another two class error matrix was generated (seagrass, unvegetated), where the 10 field points mentioned above were recoded from patchy seagrass to unvegetated. The overall accuracy of this map was 91%.

Time Requirements for Monitoring Techniques

SONAR and Underwater Videography

Total time required per site using an example with 25 underwater video transects for collection and classification was nearly 119 person hours and 19 person hours for acoustic surveys (Table 16). These time estimates do not include transit to/from the survey site, as this can be highly variable. Acoustic data acquisition required three people for 5 hours each to conduct a complete survey at the site. Due to slower vessel speeds, acquisition of video data required three people for 18.75 hours each to complete a surveyed site ($n = 25$ transects). It is important to note that the time estimates in Table 16 are for trained persons familiar with GPS and GIS protocols, video classification, and acoustic sampling. Training personnel is not included in these estimates, but may add a significant amount of time and cost. Training persons on video classification is explained in more detail in the section entitled “Video Classification Training and Observer Calibration.” Equipment costs are largely a one-time initial investment (Table 17) with additional costs for maintenance. These expenses and those of a more perpetual nature such as video tapes, data backup equipment, truck/vessel fuel, and travel costs will need to be considered in an overall cost estimate. The perpetual costs were not itemized here as they may not be relevant and can vary widely by organization.

Diver Surveys

The time required per quadrat (Table 16), including preparation, data entry, and data analysis is approximately 19 min. In one day’s effort, three people could complete 100 quadrats at a site. This means that for about 16 hours of work, data on 100 quadrats at a site could be collected, entered, and analyzed. These estimates do not include mobilization, truck/vessel fuel and travel costs. It is important to be cautious about this cost-estimate because we did not conduct a power analysis on these data and do not actually know how many quadrats it would take to successfully detect a low level of change in SAV bed aerial coverage. The data collected in this study clearly show that, even with 65 quadrats (Appendix 8), the bed extent is not comprehensively delineated. The time presented in Table 16 is meant for tool validation rather than an extensive assessment of the SAV beds at a site.

Remote Sensing

The cost to map SAV habitat of NC would be approximately \$575,000. For the imagery, assuming an inflationary increase from the last mission, based on increased fuel cost, etc., would be approximately \$350,000. Interpretation would cost approximately \$150,000. This estimate is based on estimates from several projects conducted by the NOAA Coastal Services Center, estimating an average cost for interpretation at \$260 per square mile. Finally, the cost of field exercises for ground-truthing is approximately \$75,000. That is based on four field trips at seven days for each field trip, with five days in a boat and two days for mobilization/demobilization. This estimate also includes two personnel at \$75/hr, travel for two personnel, daily boat rental at \$1000, and additional funds to cover costs of drop cameras and other equipment.

Table 16. Time requirements (hours) per transect and site for underwater video, SONAR, and quadrat data collection and analysis. This quadrat data cost-calculation is to check the accuracy of the cokriging surface predicted by the SONAR.

Activity	Underwater video (hr)		SONAR (hr)		Quadrat (hr)	
	Per transect	Per site	Per transect	Per site	Per quadrat	Per site ^ψ
Site plan/ waypoint designation	0.25	6.25	0.08	2	0.2	2
Data Acquisition[§]	2.25	56.25	0.2	15	0.3	30
Datafile Preparation	0.25	6.25	0	0	0.02	2
Classification/ Interpretation	1.75	43.75	0.08	2.0	0.02	2
QA/QC & analysis	0.25	6.25	0.08	0.42	-	-
TOTAL:	4.75	118.75	0.44	19	0.9	36

*NOTE: Transect length was defined at 300 m and a site is comprised of 25 transects;

[§]Video data acquisition was estimated as 0.75 hr./transect per person and requires three people to collect data; acoustic data collection also required three people at 5 hours each to complete a site. Quadrat data can be collected by a single person, which is the basis used here. All estimates exclude transit time to/from site.

^ψA sample-size of 100 quadrats was assumed per site for comparison with SONAR data. No power analysis was done to estimate the number of quadrats needed to detect change in SAV. These time-estimates assumed one person is collecting and analyzing the quadrat data.

Table 17. One-time costs associated with evaluated SAV monitoring tools.

Activity	Cost
<i>Underwater videography</i>	
Underwater camera	\$ 1,525
Video recording unit and Horita	\$ 1,400
GPS (basic - differential)	\$300 – 10,000
<i>SONAR</i>	
Equipment (echosounder, GPS, transducer, computer, cables)	\$27,717
ECOSAV2 software	\$ 3,000
<i>Quadrats</i>	
Equipment (PVS pipe, glue, PVC elbows, string) for ten 1 x 1 m quadrats with 100 cells	\$130
GPS (basic)	\$300
Snorkeling gear (snorkel, fins, mask, wetsuit) per person	\$500
<i>Remote Sensing</i>	
Imagery	\$350,000
Interpretation	\$150,000
“Ground-Truthing”	\$75,000

DISCUSSION

Among the SAV monitoring programs currently being globally (reviewed in the introduction), it is clear there is no consensus regarding the approach or metrics to assess change in SAV distribution and abundance. Our surveys of the high- and low-salinity environments of NC suggest that a multi-tool approach would result in the most comprehensive and cost-effective method for monitoring SAV. By combining multiple tools (underwater video, SONAR, diver quadrats, and aerial remote sensing), the strengths of each tool can be maximized while minimizing their limitations.

Strengths & Limitations of Underwater Videography

A thorough field test of our underwater video equipment has revealed its strengths and limitations as they relate to the development of a performance-based SAV monitoring protocol for NC (Project objective 2). Underwater videography paired with the sub-meter accuracy of differential GPS (DGPS) has many advantages including: high spatial and visual resolution

without destructive sampling, the capability for species identification, ease of use, effectiveness across the depth range of SAV distribution, and moderately low equipment costs. Additionally, this method can be applied to sampling designs that meet the assumptions of standard parametric statistical tests, making rigorous comparisons and change detection possible.

The special low-light optics of the camera used in this project were ideal for the high turbidity, low light conditions in many subaquatic environments encountered in NC. High image resolution, combined with the small frame size enabled video classifiers to differentiate some SAV species, identify small organisms, and qualitatively characterize the substrates associated with SAV communities. While these were not objectives of this project they may be of interest as added value to components of future monitoring projects. Being able to survey across a range of depths and differentiate species can minimize the need for diver observations, which may involve costly personnel training, equipment, and safety risks. Where aerial imagery cannot reliably detect SAV change in NC, including low salinity environments and areas of deeper water (>2 m), underwater videography is a demonstrated alternative method for SAV classification and change detection. Archives of underwater video can also provide a historical visual record; should substrate or species community change such that the visual record may prove valuable to explore other community trends.

While the advantages of underwater videography are numerous, there is one important limitation to consider – time requirement. Underwater videography collection can involve lengthy field time (~60 hrs to complete a site [300 x 300 m area]). Further, video interpretation requires additional time and personnel (~45 hrs per site). There are some automated video classification programs and software packages that may reduce the time required to classify video. These were not tested as part of this project, but may be worth exploring. Automated techniques are likely to work best in more uniform habitats (continuous SAV or continuous sand with sparse SAV). We have not tested such methods and thus cannot comment further on specific recommendations.

Another way to reduce video classification time requirements would be to optimize transect length based on SAV distribution. Specifically, transects may not have to be 300m long, especially where the majority of the SAV resource is adequately mapped with another approach such as aerial imagery or exists within a narrow-band near shore. Such an example is BLB (Figure 23), where nearly all SAV was detected within 200 m of shore. Shortening transects to 200 m would reduce field data acquisition and video classification times.

Alternatively, the underwater video camera can be modified for use as a drop camera to rapidly acquire point data at multiple locations for estimating SAV distribution and abundance. Another important application of underwater video is to use it to precisely locate the deep edge of an SAV meadow. The deep edge of an SAV meadow is an important metric, as it has been

shown that this is the location where changes (expansion and retraction) are most likely to first occur in an SAV bed. Underwater video can also be used as a point-source validation tool for remotely sensed data collected by aerial imagery or SONAR, as was illustrated for the accuracy assessment analyses for the intensive and rapid assessment sites. By reducing video collection time to rapid drop camera deployments (instead of long transects) and laboratory video classification to points or small defined areas, the personnel overhead required for ground-truthing a site (i.e. an accuracy assessment of the SONAR data) is significantly reduced while the data coverage of a site is still comprehensive.

Strengths & Limitations of SONAR

The strengths of the SONAR system (BioSonics DTX echosounder and transducer, ruggedized laptop, Visual Acquisition and EcoSAV2 post-processing software) are its portability in a rugged case and field computer. It is a system which can be calibrated to international standards (Urlick 1983, Foote 1991, Foote 1995, McLennan and Simmons 2005, Foote et al. 2005, Foote 2006, Foote 2008), using a high-frequency (420-kHz) transducer that has the ability to be mounted on different types of small and maneuverable vessels. This SONAR system has the ability to rapidly, cost-effectively and simultaneously acquire geo-referenced data on SAV cover (%), plant height (m), and bathymetry. In this report, SAV cover (%) was converted into a simple presence/absence protocol to allow comparison with the underwater video method; the plant height (m) output was not extensively explored. The number of SONAR transects needed to detect a 10% relative change with a high power (0.8) and low type I (0.05) and II (0.2) errors, in a 300 m x 300 m site, is approximately 30 transects, according to the GAM model (Figure 38). Acquisition of these data can be accomplished in one day or less of fieldwork with only two personnel. In this study, we routinely obtained 48 transects in a single day.

The BioSonics DT-X has a simple set-up and can be operated with as few as two persons in a field situation. EcoSAV2 software can easily be used and the algorithm parameters specified by a trained analyst. This allows a repeatable survey to be completed with known parameters, and GIS-ready output files can be produced within hours of returning to the base station, or even in the field if so desired. It also can acquire additional data on bathymetry, bottom sediment composition, and fish abundance with a 200-kHz transducer and additional processing software from the same output data files.

The ability to detect change in SAV is a strength of the SONAR method, provided that the plants are “tall”, with plant heights well above the bottom and relatively abundant in one of the surveys. This situation often occurs in lakes and low-salinity regions of estuaries. Several studies have been conducted that show the usefulness of SONAR for mapping SAV in lakes, rivers and estuaries. Entire lakes have been mapped for SAV and change analysis done over

time. Japanese investigators (Hamabata and Kobayashi, 2002) studied three species of macrophytes (*Hydrilla*, *Myriophyllum*, and *Egeria*) in Lake Biwa, Japan, and documented a large increase in coverage over a six year period between 1994 and 2000. These authors did not state the type of SONAR they used, but ran shore-normal transects at intervals around the entire lake to obtain these estimates.

Perhaps the best example of a SONAR method used to assess the SAV distribution in a series of lakes was done by Ray Valley and colleagues in Minnesota (Valley et al. 2005, Valley and Drake 2007). In this study, they used the BioSonics single-beam SONAR with a 420-kHz transducer and classified the bio-volume (computed as plant height/water depth * % cover of SAV in each acoustic report) of SAV calculated from the SONAR files using the EcoSAV algorithm. The data for this study were acquired on shore-normal transects spaced at 10m apart along the entire shoreline of each lake. The data were analyzed with a series of geostatistical methods (IDW, Spline and universal kriging) to develop a SONAR-based map of the SAV in each of the three lakes they studied. The resulting kriging layers (after depth trends were removed) were found to be the best predictors of SAV cover when verified by examining the SONAR echograms for over 2500 verification points within each lake. Although they did not report an overall accuracy value for the method, they did show plots of error (calculated by subtracting predicted SAV from observed SAV) taken across a range of depths and found good agreement between the kriged surface and the observed SAV at depths up to 8 m. The kriging prediction surface explained 70-80% of the variability in observed SAV in two lakes, and ~ 50% variability in another lake. At the shallow depths (1 m) the error was greatest, with kriged prediction being lower than observed. They also performed a sensitivity analysis, changing the spacing of the transects from 10 m through 40 m, but this analysis showed little effect of the prediction surface error, since they simultaneously changed the minimum grid cell resolution to account for the increased interpolation distances.

Another experimental demonstration of the effectiveness of SONAR to detect changes in a lake SAV was done by Sabol et al. (2009). They used herbicide applications to reduce the percent cover and plant heights of invasive *Myriophyllum spicatum* and other freshwater and low-salinity SAV species in Eagle Lake, Wisconsin. Eight weeks after herbicide 2-4-D was applied to this lake, a dramatic reduction in SAV cover (40% reduction) and plant height (3.5 feet to 0.3 ft.) was detected using the BioSonics single-beam SONAR system, which is very similar to the unit we have been testing in this NC study. Ground-truthing showed that this SONAR system was a good predictor of plant biomass. Change image maps of the lake pre-and post-herbicide treatment were rapidly produced, and such approaches could be used in NC rivers and estuaries to detect change in SAV.

In estuaries, SONAR has been used to document the presence and map the distribution of SAV (Sabol et al. 2002). The same BioSonics single-beam SONAR system with differential

GPS system used in the current study has been evaluated for use in estuarine SAV beds, using 0.3 x 0.3 m quadrats taken under the transducer and underwater video as a ground truth (Sabot et al. 2002). In that study, both low-salinity SAV (*V. americana*) and high-salinity seagrasses (*Thalassia testudinum*, *H. wrightii*, and *Syringodium filiforme*) were detected and ground-truthed. Bottom depth, plant height and plant biomass were all highly correlated with the echosounder signal ($R^2 = 0.98$ for depth), and a good agreement (80%) was obtained compared to most of the video verification points, but some points had low agreement (25%); overall the video to SONAR correlation had an $R^2 = 0.54$. These points of low agreement between video and SONAR were places where the vegetation was short and sparse *H. wrightii*, not exceeding 3.7 cm in height and with a biomass 60 g/m². There was an overall R^2 of 0.73 between the biomass of SAV from the quadrat data and the SONAR echoes. These results are similar to our findings that SONAR method was accurate 70-80% of the time when compared to videography, but the differences could be attributed to areas where the SAV did not exceed a threshold of plant height or density. Thus, a limitation of the SONAR technique is that the SAV being mapped must be tall (> 5 cm) and relatively dense.

Classification accuracy of bottom habitats and vegetation has also been investigated for single-beam SONAR. In one case, Preston et al. (2006) reported a high degree of accuracy (95%) when comparing the SONAR classifications to SCUBA diver survey lines. In this study, SONAR was compared with video, and we obtained relatively high accuracy in our testing (77%). In spite of these demonstrations of SAV change detection, the accuracy of the SONAR can vary widely by site and this needs to be further investigated in the NC Albemarle-Pamlico estuarine system before it can be recommended for change detection at all sites. It is likely to be a very useful reconnaissance tool for conducting preliminary sampling to map the as yet undetected SAV locations throughout the low salinity regions of NC. It may also be feasible for detecting large-scale changes in SAV in the low salinity regions, and we recommend this be further investigated (see Proof of Concept Section below).

The limitations of the SONAR are its inability to discriminate species of SAV, the low sensitivity when plants are short (near the plant height detection threshold) or sparse, the depth-limitation that is both due to the depth of the transducer in the water and the near-field (40 cm) of the acoustic pulse. The phenomena of very short and sparse SAV plants is often observed in the in the high-salinity regions of NC, but can also occur in the low-salinity regions. In these situations, accuracy can decline, and thus SONAR may not be the only approach for monitoring change in SAV beds. An accuracy analysis indicated the system has an average accuracy level of 77% when compared to simultaneously-collected underwater video frames, but this declined in shallow water where much of the high-salinity SAV occurs.

The BioSonics DT-X has the greatest startup costs of the two boat-based methods for both equipment and software. New lower-cost SONAR technologies have been placed on the

market (see below); these systems have not been tested for their SAV-detection thresholds but may be worth further exploration. The SONAR system in this study offers a lower cost per-transect when compared to the video method, due to the greater area that can be surveyed analyzed per unit of time. The downside is that the accuracy of detecting SAV and the ability to detect small changes in the SAV bed are sacrificed for surveying a larger area.

Start-up costs for the SONAR method are high, but new technologies are being developed which could reduce cost. The BioSonics MX system released in 2011 (<http://www.biosonicsinc.com/>) also has a rugged field case, a 205-kHz transducer instead of 420 kHz, and includes Visual Habitat software (which is based on the algorithm tested here, ECOSAV2). It is packaged as an all-inclusive system for aquatic vegetation surveys (outputs include SAV % cover, canopy height, biomass, bathymetry, and substrate classification). This BioSonics MX scientific echosounder system is considerably less expensive than the DTX system used in the study reported here, and the cost includes the software, but is not as user-configurable. In addition, another new SONAR technology for mapping SAV was developed and released in 2011. That system relies on consumer echosounders (Lowrance HDS5) and a proprietary cloud-based data analysis method (ciBioBase) is being marketed now by Contour Innovations, LLC (<http://www.cibiobase.com/>). This system has the least cost for the equipment, because it relies on a consumer model of echosounder developed for the boating and fishing industry. However, analysis is completed by submitting the data files acquired with the echosounder to Contour Innovations, LLC, and there is an annual subscription fee for this vegetation analysis service (e.g., \$4300/year for unlimited uploads). Total cost of operation will be significant due to the need to continued site licensing costs, but this cost is not incurred at the start of the survey operations. Both systems have possible trade-offs in terms of data accuracy that can be obtained and neither were available for testing in this project. If they are adopted, they should be verified for accuracy using underwater video and the protocol described in this study.

Other hydroacoustic technologies have been used to map and detect SAV. Side-scan SONAR has been employed to map SAV (Lee Long et al. 1998, Moreno et al 1998, Forte and Martz 2007). The RoxAnn system, a sediment hardness and bottom-type detection algorithm which is used in conjunction with a single-beam echosounder, can be trained to detect SAV (Edsall et al. 1997), but has not been routinely used, because it must be calibrated for detection of SAV at each site-specific survey. A new Geoswath Interferometric Multibeam Sonar technology has also been used to study the bathymetry along with side-scan SONAR was used to map SAV in Currituck Sound, NC (Forte and Martz 2007). This system seems to be well-suited to bathymetric and SAV surveys, but is very costly (~\$240,000 depending on options selected) and was not tested here. These alternative hydroacoustic technologies hold great promise, because of their wider footprint on the bottom and their photographic image-like quality of side-scan SONAR. However, the side-scan SONARs incur greater processing costs because they

require subjective image interpretation and do not provide a method of estimating plant height and density.

The cost of the SONAR technology for boat-based mapping and monitoring SAV may continue to drop if accuracy is deemed reliable and the approach is adopted by more users at universities and state and federal agencies.

Strengths & Limitations of Diver Surveys

Diver and snorkel surveys with quadrats are often used to assess changes in SAV cover and distribution. Aside from the SCUBA gear, the sampling equipment is inexpensive and easy to assemble. The methods we used in this study were generally non-destructive, and training requirements were minimal. Our goal in this project was to utilize diver surveys to supplement information obtained by other sampling methods (e.g., remote sensing, underwater video surveys, and SONAR surveys), rather than to use quadrat estimates as a sole indicator of change in SAV abundance or area.

One problem with using quadrats to estimate change in SAV is that they can be time-consuming, depending on the density and cover characteristics. Quadrat surveys require trained individuals to estimate SAV cover based on a visual assessment. When a bed is very patchy, or the water is turbid or deep, significantly more effort is needed to determine distribution and abundance and how a bed changes over time. To facilitate a more efficient sampling technique, a rapid visual assessment method has been adopted in many surveys (Braun-Blanquet 1972, Kenworthy et al. 1993, Rose et al. 1999). For example, in Florida, 50 m transects are established at randomly selected sites to characterize seagrass beds (Fourqurean et al. 2001). Along each 50-m transect, ten quadrats (0.25 m²) are visually surveyed for seagrass and the data are used in a kriging model to display species distributions and assess changes in the bed over time. However, the quadrat method can have high sampling error, which leads to a decrease in power and thus an increase in the number of quadrat samples (range: 36 to >99, median = 99) needed to detect change (Mumby et al. 1997). Thus, the more heterogeneous a bed, the more effort is needed to survey and successfully detect change.

In beds that are fairly homogenous, many researchers have exclusively used diver surveys with quadrats to assess changes within the bed structure. Heidelbaugh and Nelson (1996) conducted a power analysis of 1 m² quadrat surveys in Sebastian Inlet, Florida. They observed that a low number of quadrats (<12) were needed to detect a 10% change within a seagrass bed with a power of 0.9. However, the coefficient of variation (CV) for the mean cover at the studied seagrass beds ranged from 3-7%. In NC, the simulation modeling conducted using aerial photos, suggests that the coefficient of variation (CVs) of SAV bed cover ranges from 3 to

16% (Figure 41). Shoreline fringing and blowout bed forms have the lowest CVs, with a maximum CV of 6%, while patchy SAV beds have CV values that can be greater than 16%. Since three of the four intensively studied sites represented patchy SAV beds, the heterogeneity of the sites will hinder our ability to detect changes in SAV coverage within the structure of the bed.

In this study, we did not intend to utilize the quadrat surveys as a sole source of SAV bed change information. We sampled particular areas of the study regions, which helped us to focus on the accuracy of the SONAR and at no time was the entire region sampled with the quadrat method. Therefore, we were unable to estimate how many transects were needed to successfully detect change in areal coverage using a quadrat method. Instead, we suggest using quadrats as a method to assess how the density of a bed is changing throughout time, and to utilize SONAR, underwater video, and aerial photographs collected from over flights to survey changes in the area of SAV. These techniques allow for higher resolution of the bed at multiple scales, when compared to quadrat surveys with equal (time) effort. We assume that less effort is needed to detect the same level of change in the SAV bed if one or more of the other methods is used.

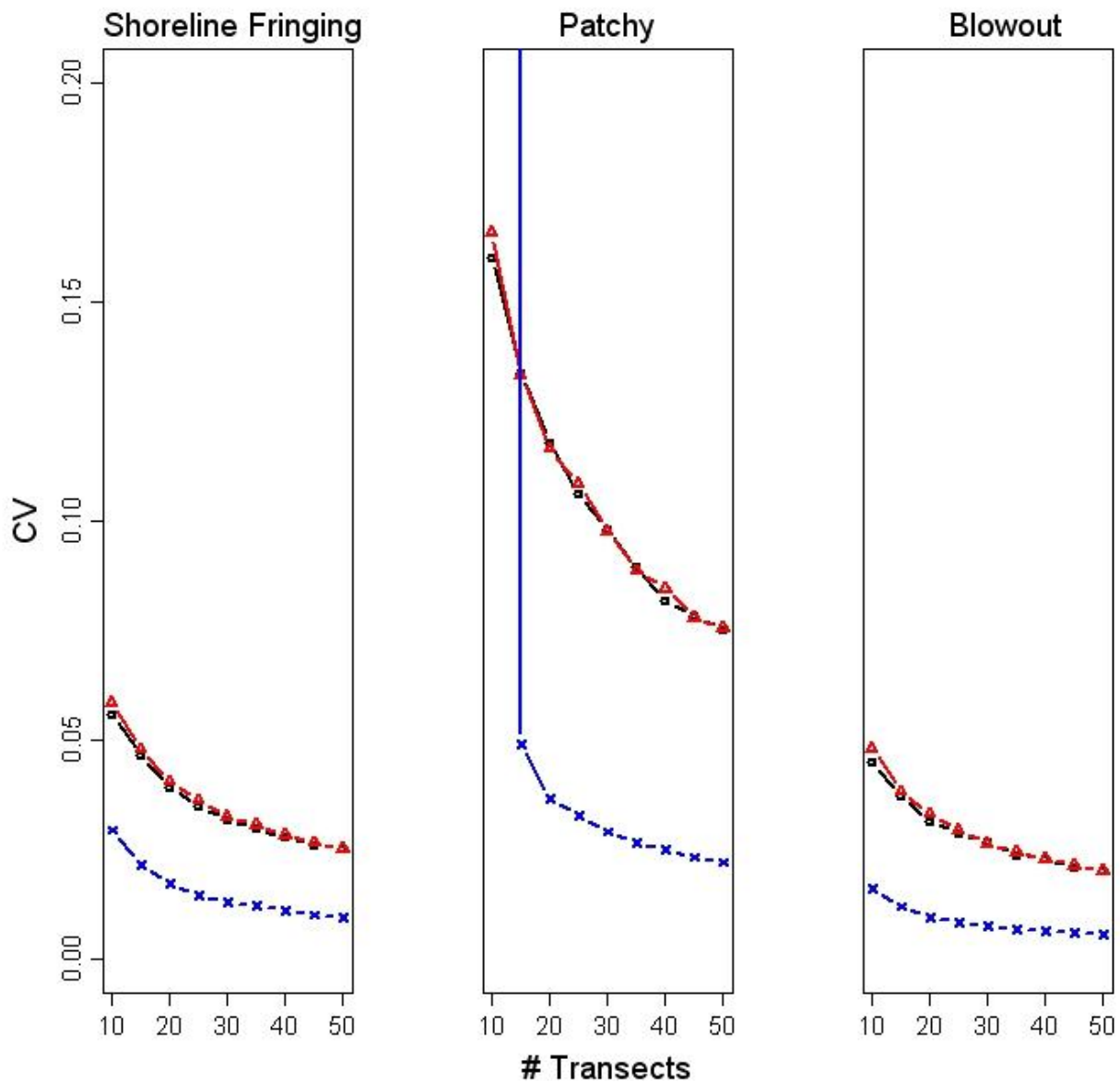


Figure 41. Coefficient of variation (CV) in estimates of predicted SAV density as a function of the number of transects and sampling design/analysis type. Left panels give results for contiguous habitat, center panels give results for patchy habitat, and right panels give results for the blowout study area. Black circles represent results from simple random sampling (SRS), red triangles give results for systematic sampling where the naïve SRS variance estimator is employed (SYS₁), and blue x's give results for systematic sampling using the approach of Fewster (2011) to get variance estimates (SYS₂).

Strengths & Limitations of Kriging and Cokriging SONAR Data

An advantage to interpolating a surface from point data is that it allows for a description of general trends within an area, especially when the collection of exact point data is not plausible (Isaaks and Srivastava 1989). In this study, we collected SAV presence/absence with the SONAR at the intensive study sites at a relatively fine-scale (~6.3 m between transects, ~3 m between acoustic reports). The accuracy of the SONAR, assuming the video was 100% accurate, was between 69 - 98% (Table 12), with an average accuracy of 77%. At NPR in June (2009), the accuracy of the SONAR data was 69.4%, while the cokriging model median accuracy was 66% (Figure 32). The cokriging model accuracies will be highly influenced by the errors associated with the tool used to obtain the data points. Kriging models do not take into account the variance in the model itself, nor the inaccuracies of the tool (Todini and Ferraresi 1996). This is a serious limitation of surface interpolated maps. Ultimately, this can be partially minimized if kriging is used for intensive sampling efforts on a local scale (Walter et al. 2001, Valley et al. 2005). Keeping transects spaced evenly throughout time and space will help reduce the inherent error of the kriging method. Because classification errors from cokriging are often correlated between two surveys (Burnicki 2011); cokriging should be able to detect changes in the SAV beds that are visible to the SONAR sensor.

Geo-statisticians are aware of the error associated with surface interpolation and are working to rectify this issue (e.g. Saito and Goovaerts 2002), but there is currently no accepted practice to entirely remove this error. At this time, the best we can do is to be aware of the error and understand where in the kriging model these errors are the highest, such as when the standard error of the prediction surface is highest. We can then use a stratified post-hoc sampling approach, based on simulated underwater water video point comparisons in different strata of predicted sampling error, to determine if accuracy changes with the predicted standard error from an interpolated map. In our study, accuracy declined with increases in standard error of the prediction surface (see section on the sentinel site approach below).

In this study, we selected ordinary cokriging models that were "Ideal", minimized the errors in the cross-validation analysis (see Appendix 8). A *post-hoc* analysis of three different cokriging models produced for the NPR site suggested that the median accuracy relative to video did not change appreciably with the models (Figure 32). However, they did indicate different regions where the SAV bed was located (Figure 31). The dominant part of the bed was identified in all three cases, and this result was confirmed by high agreement with underwater video in that region (Figure 17). In this study we suggest using one model, the "Ideal Binary" model with depth (m) and SAV converted to presence-absence data as the best for all cokriging models because: 1) it minimized the errors associated with cokriging, 2) maximized the area of the SAV bed, when compared to the cover (%) method, providing a larger region for the state agencies to

both protect and monitor for change, and 3) it maximized the accuracy of the cokriging surface, as it compares to the underwater video method.

When exploring change over time, it is advisable to select the best-fit model for each site and each time period. Modeling attempts to simplify the complex ecology of a system. Thus, using the same model over time leads to the introduction of additional model errors because the ecology of the region you are trying to detect change in will also vary (Lehmann 1998). Using the best-fit cokriging model, which optimizes the interpolation of the surface from the data points, gives the best-possible representation of the SAV bed. This interpolated surface can then be used to calculate the relative area of the SAV bed and detect changes in the bed over time, provided both the modeling and tool errors are taken into account and the accuracy is checked by either underwater video or water quadrat sampling in the water.

Strengths & Limitations of Remote Sensing Surveys

One of the most significant advantages of any survey based on imagery from orbital or sub-orbital platforms is that large areas can be covered at relatively low costs. However, the biggest limitations of remotely sensed imagery for mapping any submerged habitat are the strict environmental requirements for successful application (Appendix 1). These limitations greatly reduce the number of days when imagery can be obtained. In particular for NC, persistent turbidity in low salinity areas, caused by non-point source run off and dissolved organic matter from coastal forested wetlands, greatly inhibits our ability to obtain useable remotely sensed products for these areas (Figure 42). In NC, as in all areas in the Southeastern and Gulf Coasts of the US, the atmospheric haze is prevalent from late May through the summer and is a major problem for surveys that are usually flown at 10,000 or 20,000 ft. (3048 or 6096 m).

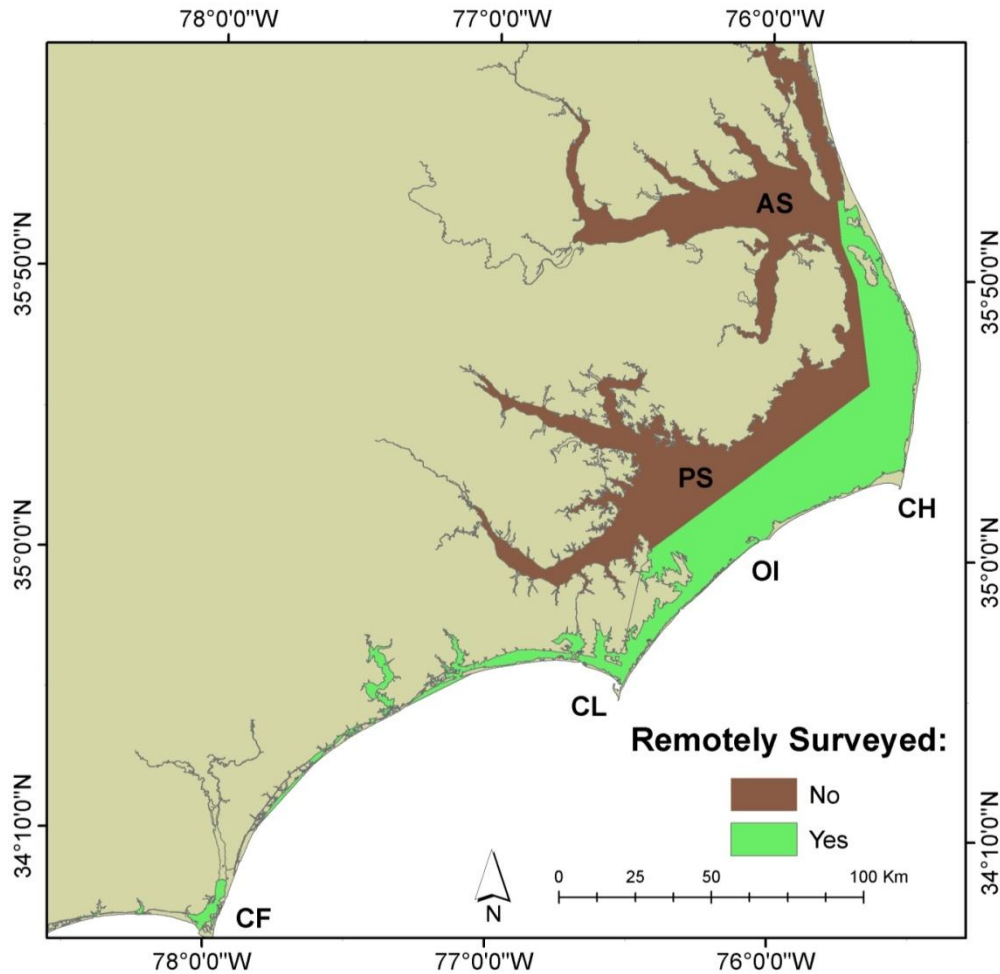


Figure 42. North Carolina estuary and river systems highlighting areas that can (green) and cannot (brown) reliably detect SAV using aerial surveys. Water body abbreviations: AS, Albemarle Sound; PS, Pamlico Sound; CH, Cape Hatteras; OI, Ocracoke Inlet; CL, Cape Lookout; CF, Cape Fear.

Monitoring Tool Comparisons

Although our SONAR surveys coincided with underwater video in space and time, the two methods were not collected simultaneously (i.e. on the same boat) and methodological differences, such as vessel speed, also contributed sources of variation. Although we targeted the same vessel transects using the two methods, the completed transects differed slightly in spatial overlap due to wind and tidal offsets between the two vessels (Figure 29). This small spatial offset may be responsible for some of the differences in the F_{sav} quantified at the study sites.

There were differences in estimates of F_{sav} between the SONAR and underwater video methods. The SONAR provided lower estimates of F_{sav} , when compared with the underwater

video method at BLB, and NPR, and JBS while at SPS, the F_{sav} estimate was higher with SONAR (Table 17). The reasons for these differences have to do with the limitations of the SONAR method and possible differences in exact positioning along a transect during the surveys. The video method is more sensitive to short (< 5 cm) and sparsely distributed SAV plants, which are often missed by the SONAR; this was observed at NPR, JBS, and BLB (see Appendix 8). In contrast, at SPS, where the plants are very tall (0.3 m in height above the substrate), the SONAR method obtained a higher F_{sav} value, in part because the underwater video method only looks at SAV in a fixed region ~13 cm above the bottom. The SONAR distinguishes any plants (vertical canopy or root basal stems) within the water column, whereas the underwater video method most distinguishes the rooted portions and plant stems within ~13 cm of the bottom. This methodology can miss very tall plants, rooted beyond the video frame, but with a canopy occurring vertically along a transect. However, the underwater video method can be modified to incorporate sites with tall plants by adjusting the camera’s height above the bottom, as was done in the video method at SPS.

Table 18. Mean and standard deviation (SD) of F_{sav} by transect and method at each intensive site and over all four sites. Relative change detection levels between 10 and 40% were calculated for each method and used in the power analysis.

Site	Method	Mean F_{sav}	SD
NPR	Video	48.2	17.5
	SONAR	19.8	16.9
JBS	Video	6.3	6.6
	SONAR	3.4	3.9
BLB	Video	22.9	3.9
	SONAR	3.2	2.2
SPS	Video	64.6	33.1
	SONAR	81.1	11.8
All Sites	Video	35.5	15.3
	SONAR	26.9	8.7

The power to detect a change with both methods also declined where an SAV bed was patchy (Figure 38). Patchiness of a SAV bed will increase the variation among transects, resulting in larger standard deviations relative to the mean F_{sav} . JBS was a patchy bed, as can be observed from the high standard deviation relative to the mean in both the methods (Table 18). NPR and BLB appeared to be less patchy using the underwater video method, with higher means than standard deviations, but were patchy as measured with the SONAR method likely due to inherent differences in the two methods to detect short plants. The lowest power to detect a 10% change was in the patchy sites (NPS, JBS, BLB), and the greatest power to detect a 10% change with both methods was in the SAV bed at SPS, which could be considered a continuous bed. The low variation of F_{sav} relative to the mean at SPS required the least number of transects to

detect a 10% relative change in both methods. The quadrats taken at SPS in August indicate that there was an average of 80.2% cover (Table 18) at depths ≤ 2 m. Additionally, the SONAR showed that the relative abundance of this bed did not change over time (Table 18), with the entire 300 m x 300 m area covered by SAV from June through September (2010).

It is important to note that three of the four intensively studied SAV beds varied in F_{sav} throughout the year (NPR, JBS, and BLB). These sites experienced large declines or increases, as much as 60% in F_{sav} as measured by SONAR (see Appendix 8). When the SAV at a given site has high intra-annual variation, relative levels of change detection that exceed the typical within-bed variability will have to be used to determine any significant inter-annual changes in F_{sav} . Thus, to detect long-term changes in SAV over years, the time of year that the survey is taken (index period) will be critical, and this should be standardized in a monitoring protocol. By using the appropriate index periods to conduct the surveys, high-salinity and low-salinity strata can be surveyed when the variation in F_{sav} is most-likely to be due to only inter-annual changes, not seasonal changes. This allocation of boat-based survey effort is desirable from a personnel management stand point as well, with effort of field crews focused on different areas at different times of the year due to SAV species-specific changes within a season.

Depending on the environment, SAV classified using aerial imagery, relatively shallow and clear waters can capture nearly all the SAV within a site. For example, at JBS very isolated points of SAV were detected beyond the boundaries of the SAV delineated by aerial imagery classification. The alongshore, dense fringing bed configuration in high salinity environments may be an area that can be entirely mapped using aerial imagery. However, SAV resources at other sites, such as NPR, BLB, and SPS, occur in areas of reduced visibility (e.g., low salinity, deep water or higher current) and are underestimated by aerial imagery classification (e.g. SPS, Figure 21). Under such conditions, targeted sampling with a combination of methods, SONAR and underwater video, may be needed to locate the deep edge of SAV distribution and aid in change detection. Suggestions for quantitatively targeting sampling in high salinity environments would include reduced transect length, yet ensuring that the deepest edge of the distribution is exceeded. Extending transects a full 300 m is likely unnecessary. However, for low salinity environments, transects may need to be extended beyond 300 m, as was the case for SPS. Since we are considering recommending the cokriging SONAR method to estimate the RA_{sav} of a bed and how it changes over time, having only shore-normal transects are not advisable. Both shore-normal and shore-parallel transects that saturate the environment with observations points, will lead to the more-accurate surface interpolation and thus a more-reliable change-detection level.

Underwater video has proven to be invaluable as a calibration and validation tool for the SONAR technique. Conditions such as soft sediment, shallow water, short plants, or very sparse plants caused the SONAR to misclassify SAV presence/absence. Underwater video data

provided essential information to definitively identify whether SAV was present or absent. However, the underwater video method alone, as demonstrated in the intensive site assessments, is cost-prohibitive. Thus, utilizing the underwater video data to validate the cokriging model produced by the SONAR acoustic reports may represent the most cost-effective and reliable method to employ for detecting change in SAV over time and space. Because these data are georectified and stamped with the time and date, it will also provide a photographic record of the site.

Diver quadrats at our study sites also provided data that would have been missed by the underwater video and SONAR. For example, at JBS, what appeared to be small, isolated seagrass clones were identified by snorkelers as worm tubes with SAV leaf detritus; these are potentially classified as false positives with the SONAR. It is important to note that even with the high resolution camera, differentiating worm tubes with leaf detritus from live seagrass clones may not have been possible. Further, some SAV species are indistinguishable in the underwater video. Deploying divers or snorkelers to conduct a quick reconnaissance of a site to obtain voucher plant specimens should be considered by monitoring programs. In shallow locations (< 0.5 – 0.7 m) where neither boat-based method can be deployed (i.e. in the shallow regions of BLB and JBS), quadrat surveys with divers or snorkelers can be used as an alternative monitoring protocol if the bed extends all of the way to shore. In addition, diver and snorkel surveys can provide information on how bed architecture with regard to canopy height and species composition' is changing over space and time. The trends observed with these in water surveys were slightly different from the trends reported by the SONAR. At SPS, the area of the bed did not change over time (Table 11, Table 13), but the diver survey method indicated that there was a significant increase in the density of SAV.

Monitoring Protocol Recommendations

General Monitoring Strategy

As a general strategy for developing a state-wide performance-based monitoring program in NC, we are recommending the use of a combination of methods in a phased approach organized by geographical stratification and implemented in a rotational sampling scheme (Figure 43). The goals and action plan of this strategy should strive to achieve a sustainable and long-term statewide monitoring program through a series of steps that identifies priorities for locating and initiating sample sites, maximizes existing capabilities, and utilizes the most appropriate and best available methods to quantify the status and trends of SAV resources. This recommendation is based on the need for a solution to a very challenging sampling problem with limited financial and infrastructure resources.

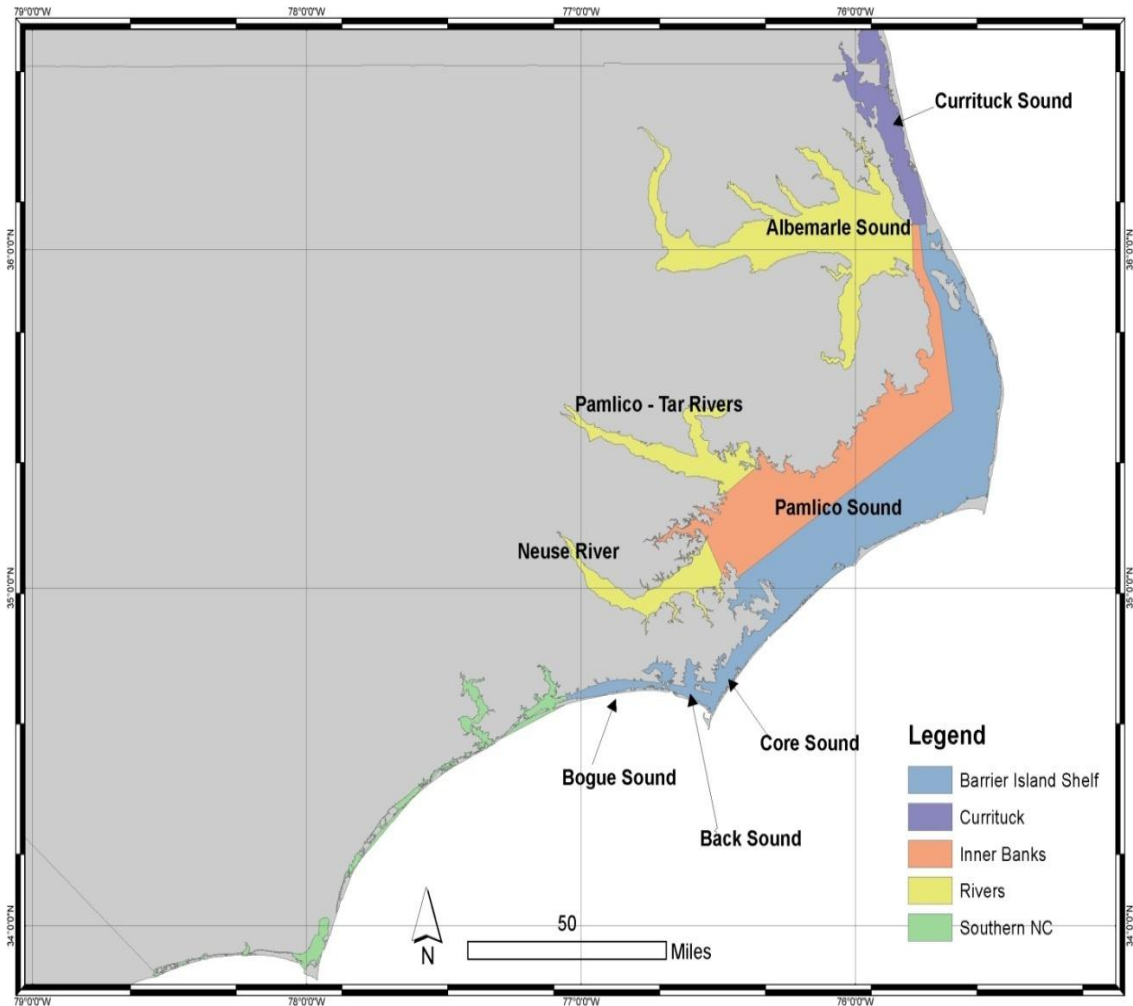


Figure 43. Proposed geographical stratification of North Carolina estuaries and river systems. SAV monitoring would be phased in across five zones and implemented in a rotational sampling scheme over time.

The general problem is that the overall size and bio-physical complexity of NC’s coastal system make it impractical to monitor with one method. In addition to this problem, there is still a significant deficit in our knowledge about the distribution and abundance of SAV in approximately 40% of the potential resource area – the areas with low-salinity SAV. A partial solution to this problem is to stratify the coast into smaller, more manageable geographic units with clearly distinguishable biological and physical features that facilitates immediate implementation and longer-term program development. A second element of the solution is to implement monitoring in discrete phases using: 1) multiple approaches based on knowledge of SAV distribution in each stratum, 2) approaches best suited for a stratum, and 3) informed prioritization of management needs. As a critical component of the second element, we recommend establishment of a network of permanent sentinel sites to facilitate the most rapid implementation of a monitoring program. Using this geographic stratification as the basis for a

statewide plan, we recommend that the sampling effort be conducted in phases where, each year, only one stratum is intensively monitored. With this plan, the entire coast would be assessed in recurring 5-10 year cycles. In the following narrative, we describe and discuss the justification and specific details of this general approach.

Geographical Stratification

Based on SAV community composition and distinctive physical attributes, the NC coastal ecosystem can be stratified into two large regions based on primarily on salinity and SAV species composition, similar to the zonation scheme used in the Chesapeake Bay monitoring program. In the Chesapeake Bay, they distinguish three regions by salinity and SAV species composition; upper bay, middle bay, and lower bay (http://web.vims.edu/bio/sav/sav11/exec_summary.html). As suggested in the NC CHPP, SAV characteristics can be recognized as two major regions based on salinity (high and low). The high salinity zone is hydrologically dominated by ocean tides and marine conditions and consists mainly of three seagrasses, *Z. marina*, *H. wrightii* and *R. maritima* (Figure 1). The low salinity zone is hydrologically dominated by wind energy and freshwater discharge in the associated rivers and tributaries and occupied by one or more of seven possible SAV species with a wider diversity of growth forms and life history strategies than the marine seagrasses (Table 1). In each of the two zones, we recommend a further level of stratification.

The high salinity zone should be subdivided into two strata. The first is a barrier island shelf and lagoon stratum that extends from approximately Oregon Inlet (or the Route 64 bridge between Manteo and the Outer Banks) to Bogue Inlet, and the second is a southern stratum that extends from Bogue Inlet to just north of Cape Fear. Knowledge of SAV in this southern stratum is limited, which is the primary reason for the separate delineation. The barrier island shelf and lagoon stratum constitutes the largest proportion of SAV resource documented in NC (Figure 2). Based on past experience, the barrier island and lagoon stratum has the longest record and the most reliable demonstration of repeated monitoring with aerial remote sensing. This is the largest documented area of SAV in NC, and we recommend that this stratum continue to be monitored primarily by aerial remote sensing on a 5-year repeating cycle. This will ensure that this stratum is adequately monitored while allowing more program resources to be directed at resolving critical deficiencies in the low salinity zone where the inventories of SAV are inadequate and almost no monitoring is occurring.

To facilitate implementation of more efficient sampling in the low salinity zone, we recommend that this zone be divided into five strata; 1) Currituck Sound, 2) Albemarle Sound, 3) Inner Banks of Western Pamlico Sound, 4) Pamlico River and 5) Neuse River. Differences in watershed and estuarine characteristics among the strata, as well as potential differences in SAV communities and stressors, warrant consideration of these further subdivisions. Stratification

based on measureable and meaningful characteristics has another important benefit by reducing the size of the monitoring area. Reducing the size of the monitoring areas to smaller and more discrete manageable units will facilitate prioritization of actions, program development, and implementation of monitoring plans.

Phased Sampling Program

We recommend that sampling be conducted in phases beginning with the immediate planning and implementation of a remote sensing acquisition of SAV coverage in the barrier island shelf and lagoon stratum. Immediate initiation of this phase will enable the monitoring program to conduct an SAV change analysis based on the 2006-2008 remote sensing data acquisition. Any effort to gather remote sensing data should also pay special attention to selection of the appropriate index period. Until the index periods are determined and fixed, analysis of remote sensing data may be limited.

Concurrent with the remote sensing effort in the barrier island shelf and lagoon stratum, we recommend initiating a second phase of the program. This phase should establish sentinel sites in a designated high-priority stratum in the low-salinity zone. Once the sentinel sites are selected (see the section below on selection criteria) in the high priority stratum, a boat-based pilot monitoring project should be initiated using the best available monitoring methods. Here, we recommended further development of the combined SONAR and underwater video camera method and, where necessary, snorkel and diver quadrat surveys.

Mechanism for Establishing Priorities

Designation of strata, site selection priorities, and number of sentinel sites should be established by a forum consisting of responsible parties managing SAV resources and experienced personnel from interested and informed backgrounds. These individuals may include, but are not limited to: staff from state resource management agencies (e.g., DMF, NCDENR), interested partners (e.g., SAV Partnership, APNEP), stakeholders (e.g., fishing industry, agriculture), expert scientists from state and federal institutions in NC (e.g., NOAA, USGS, EPA, USFWS, NPS, UNC, NCSU, ECU, ECSU, Community Colleges), and NGOs (e.g., Nature Conservancy). Ideally, the forum could be established and operated within the broader framework and overlapping objectives identified in the NC Coastal Habitat Protection Plan (CHPP) and APNEP's Comprehensive Conservation and Management Plan (CCMP). The CHPP clearly articulates the critical habitat value of SAV and the need for monitoring the status and trends of SAV in NC as a priority, while an action within the APNEP CCMP is "facilitating the development and implementation of an integrated ecosystem monitoring network".

Identifying and monitoring ecosystem stressors and the response of indicator organisms are key elements of APNEP's CCMP and consistent with SAV protection and conservation in the CHPP.

An established SAV Partnership has identified SAV baseline mapping and monitoring as an objective. This Partnership can provide the framework for the forum. The partnership was established in 2006 with an Memorandum of Understanding (MOU) entered into by the NC Department of Environment and Natural Resources (NCDENR) [Albemarle – Pamlico National Estuary Program (APNEP), Division of Coastal Management (DCM), NC National Estuarine Research Reserve (NCNERR), NCDMF, Division of Water Quality (DWQ), Division of Water Resources (DWR), Ecosystem Enhancement Program (EEP)]; North Carolina Department of Transportation (NCDOT); North Carolina Wildlife Resources Commission (NCWRC), Elizabeth City State University (ECSU); University of North Carolina - Coastal Studies Institute (UNC-CSI); The University of North Carolina at Chapel Hill - Institute of Marine Sciences (UNC-IMS); The University of North Carolina Wilmington (UNCW); North Carolina State University (NCSU); North Carolina Sea Grant (NCSG); East Carolina University (ECU); North Carolina Coastal Federation (NCCF); The Nature Conservancy (TNC); United States Department of Agriculture [Natural Resources Conservation Service]; and the United States Department of the Interior (DOI) [U.S. Fish and Wildlife Service (FWS) and National Park Service (NPS)].

In the statement of purpose and in the Action Plan, this MOU identifies SAV monitoring as an explicit component of the agreement and recognizes the mutual benefits and interests by all of the cooperating parties to utilize monitoring as a means to address management needs. To implement the goals of the MOU, the Action Plan designates that the signees establish a committee of technical experts to plan and coordinate a comprehensive and cooperative long-term monitoring program. To date, one of the many demonstrated accomplishments of this partnership has been the acquisition of the most comprehensive map documenting SAV distribution ever produced in NC (Figure 2). The resources of this partnership should be leveraged to facilitate the development and implementation of a long-term SAV monitoring program beginning with the establishment of sentinel sites.

Sentinel Sites

As discussed above in our recommendation for establishing the five monitoring zones in NC, it is impractical to expect to have a comprehensive coast-wide program without geographically stratifying the state. Even after establishing these geographic strata, the individual monitoring zones are still large and bio-physically complex. Additionally, several zones still lack complete resource inventories, so it will be difficult to design a synoptic and probabilistic-based random sampling program in those zones until the inventories are completed. As a solution to this problem, we recommend that NC consider the immediate development of a

sentinel site monitoring plan that draws upon historical knowledge of SAV distribution and vulnerability of existing SAV.

Definition of Sentinel Sites

In a sentinel site approach, relatively small numbers of fixed locations are selected for intensive study. More specifically, sentinel sites are specific locations in the environment that have the capacity for intensive study and sustained long-term observations to detect and understand changes in the ecosystems they represent (Jassby, 1998, Christian and Mazelli 2007). Three critical factors govern the scientific rationale behind the selection of representative sentinel sites: 1) the sites should have key physical and biological attributes that represent the larger ecosystem; 2) the sites should have significant ecological value associated with the presence of key species that are significantly important to ecosystem function (e.g., SAV); and 3) there is a high likelihood of detecting change.

In addition to the scientific rationale behind site selection, there is also a “management rationale.” In the case of SAV change detection, the selection of sentinel sites should also consider the potential stressors that may be responsible for change. The stressors should align with the selection of sites according to *a priori* knowledge so that resource agencies can use the monitoring data to consider appropriate management policies and actions. This is generally regarded as prospective monitoring and can be used to detect and measure anticipated ecological problems.

The likelihood of detecting change is nearly always the most difficult factor to address. This difficulty is two-fold. First, monitoring must be capable of distinguishing the response of an indicator (SAV), from its background variability, often referred to as the “signal to noise” ratio. In NC, our results suggest that this ratio is low, with lots of background noise and seasonal variation in SAV, which can obscure long-term changes in SAV. Second, the monitoring program must be capable of distinguishing the “signal to noise” ratio of the stressor and be able to identify the spatial and temporal correspondence between the indicator and the stressor. In cases where there is the possibility of multiple stressors (see APNEP Comprehensive Conservation Management Plan), multivariate correspondence analyses are even more challenging. In many instances the spatial scale of the system is quite large so there needs to be multiple sites that form a network sufficiently comprehensive to obtain the appropriate spatial coverage of the indicator and the stressors. With regard to the stressor, three conditions must be fulfilled: 1) the sentinel site, or some subset of a network of sites, must encounter the stressor; (2) at least some sites in the subset must be responsive to that stressor; and (3) the background variability at those sites must not disguise the response to the stressor of interest. Since the possible stressors of SAV and criteria for site selection are almost never known in advance and may be a random probability-based process, selecting sentinel sites presents challenging statistical problems. One such problem with sentinel sites is the inability to extrapolate measures

of SAV abundance to the broader estuarine strata. The extrapolation to broad areas of the sounds may be accomplished by using a stratified random sampling approach to select sites. The power to detect change within sentinel sites is enhanced relative to a stratified random survey, but the changes, if detected, cannot be generalized to the entire region. We recommend that ultimately the monitoring program should incorporate both stratified random and sentinel site approaches, but that the sentinel sites should be a priority.

The scientific and management rationale behind site selection must be balanced by several practical considerations. Capacity refers directly to the accessibility of a site; sentinel sites must be logistically reachable to sustain repeated observations on meaningful temporal scales. One of the major challenges in establishing and maintaining a network of sentinel sites are limited financial, staffing and infrastructural resources. Some of these limitations can be overcome by strategic selection of sites, sampling during optimum index periods to minimize effort, and consideration for locations that have existing monitoring and observing infrastructure and/or local support for continuity of monitoring activities.

Sentinel Site Selection in North Carolina

As per the discussion above and considering our recommendation for geographical stratification of monitoring zones in NC, the process for sentinel site selection should initially address each zone separately. Thus, we recommend that each geographic zone have its own network of sentinel sites. We also recommend pursuing a larger goal that develops a coast-wide network. This larger network would consist of subsets of each zone that would be incorporated into a more extensive coast-wide program.

Despite a sense of urgency in recognizing the need for monitoring SAV, it will be important to establish a consensus of priorities that facilitates program development without further delays. The size and complexity of the SAV resource restricts our ability to immediately comprehend and implement a coast-wide selection of sentinel sites and necessitates a measured step by step process that incorporates spatial elements of prioritization. This first step can begin with the selection of priority geographic strata from our recommended list (Figure 43). Since we are recommending that the high-salinity barrier shelf and lagoon strata be monitored primarily by aerial remote sensing with an accuracy assessment, we have already recommended one priority. Consequently, this reduces the areas for consideration to the other four strata. This recommendation is not intended to ignore the establishment of sentinel sites in the high-salinity zone. However, since we are recommending the continuation of remote sensing in this zone, we do not want to suggest delaying selection and prioritization in the other zones where there is little or no monitoring at all. We recognize the benefits of sentinel sites in the large barrier shelf and lagoon zone and the committee can return to this stratum in the future to evaluate recommendations for individual sites.

The next step in the site selection process should consider the intersection of four criteria: 1) current knowledge of the spatial distribution and composition of SAV resources in the zones, 2) knowledge and understanding of the location and magnitude of stressors and their effects on SAV, 3) accessibility of sites within a zone, and 4) the spatial distribution and capacity of existing or planned environmental monitoring programs. All of the steps in this process, as well as implementing the actual monitoring program, can be facilitated by the spatial articulation of information and data using a dedicated Geographic Information System (GIS) project. This can be an expansion of the SAV project that has already been started at NOAA's Center for Coastal Fisheries and Habitat Research. The CCFHR project contains a great deal of imagery and all available SAV data layers. We recommend that the monitoring program be staffed with expertise to manage the data and the GIS. The use of GIS in this site selection process also facilitates more sophisticated analyses of spatial data and provides opportunities for landscape-level assessments of the potential effects of ecosystem stressors on SAV (Li et al. 2007). The narrative that follows generally describes our recommendations for each of the steps and development of the GIS.

As per our definition of sentinel sites, the process of prioritizing zones and site selection should consider representativeness of the SAV habitat. Current knowledge of the spatial distribution and composition of SAV resources in the four zones under consideration is fragmented and incomplete, so our ability to delineate a comprehensive sampling universe is limited. However, there is sufficient knowledge to begin a quantitative evaluation of locations which might be considered representative of the SAV ecosystem. As a first step in the process, for each of the four zones we recommend developing a geo-spatially articulated map of "potential SAV habitat." Formally defining and describing potential habitat based on physical, biological and ecological attributes of a system and the living requirements of a specific resource is a tool that scientists and managers are using to establish the scientifically-based spatial context for mapping, monitoring, and assessing natural resources (Lathrup et al. 2001, Steward et al. 2005, Li et al. 2007). SAV in a large portion of the estuarine area of NC is similar to other examples of natural resources where their precise distribution and dynamics are not well documented in space and time. Thus, to define the spatial context for a sampling or assessment universe, we utilize what we know about the resource to predict an expected distribution. This is what is referred to as "potential habitat" (see for example, Li et al. 2007, Latimer and Rego 2010). The map of potential SAV habitat should be derived from a compilation of all available data on SAV presence and distribution confirmed by direct observations from, for example; remote sensing, field surveys, research monitoring, and other historical information. The compilation of potential SAV habitat has already been initiated by NCDMF and can be updated using data from this CRFL project, new reconnaissance sampling using accuracy checked SONAR transects, an inventory of more recent surveys by institutional based research programs, and other current and historical field observations.

Where possible, the second most important element of this potential habitat map should include a bathymetry data layer which clearly identifies depths to the 4-m depth contour. In NC, the 2-m depth contour is a scientifically defensible conservative estimate for the expected lower depth limit of SAV distribution. During the course of this study, SAV was identified in waters up to 4 m deep. This suggests that depth contours beyond 2 m should be considered, especially in the low-salinity region. Initially, the upper boundary of SAV distribution can be characterized by a shoreline data layer. These two boundaries define the upper and lower limits of where we expect SAV to occur, thus, the potential habitat. In time and with additional empirical data, each of these boundaries and the extent of their long-shore dimensions can be refined to develop a more precise map of potential habitat by incorporating criteria for “no-grow” features where SAV is not expected (*sensu* Li et al. 2007). These no-grow areas might include locations such as navigation channels, hard bottom reefs, high wave exposure sites, and physically modified shorelines. A GIS-based spatial analysis of the overlap between the confirmed SAV habitat and potential habitat can also be used to spatially quantify and identify the gaps in our knowledge of SAV distribution. Where SAV is not recorded but is expected, field based reconnaissance sampling can be used to validate the overlap of confirmed and potential habitat. This GIS exercise will build confidence in our expectation that potential habitat is a reliable predictor of actual SAV habitat. This spatial exercise will also serve as a guide to direct and prioritize the selection locations where reconnaissance surveys can be used to close the gaps in our knowledge of SAV distribution in each of the strata. Once these gaps are closed, the monitoring program will have a more comprehensive baseline map of actual and potential habitat. The final baseline map of SAV habitat will provide the best possible estimate of a sampling universe where sentinel sites might be located.

Further evaluation of the baseline habitat map should consider one of the main criteria for sentinel site selection: are the locations of known SAV habitat spatially and ecologically representative of the zone? Factors that should be considered in this assessment include the SAV species composition and presence in the historical record. In the case of riverine systems, the upstream boundaries for possible site selection should be established by committee consensus. Where possible, sentinel sites should be distributed so they represent the long axis of the system as well as the opposing shorelines. This distribution will gain the best-possible representation of environmental gradients and SAV community structure within a zone.

The capacity to sustain monitoring to detect the effect of stressors on SAV depends on several factors which must also be considered in the selection of representative sentinel sites. The first consideration should be a thorough assessment of SAV stressors in each zone (what they are and where they occur). Many of the possible stressors effecting SAV in NC are already identified and described in the CHPP, but need to be prioritized with regard to confirming where they are, their relative magnitude of effect, and their overall relative importance. Ideally, if the monitoring program intends to develop a broader network of sentinel sites throughout NC, this

assessment should consider whether a stressor is unique to a zone, or if it is expected to occur in multiple zones. The forum can utilize information in the APNEP CCMP to help in identifying local and regionally distributed stressors. Simultaneous consideration of a stressor's effect on SAV and its distribution in the zones can be used to create data layers in the GIS that serve as the primary sources of information for developing a stressor map. Spatial analysis tools should then be used to quantify overlap between the SAV habitat and stressor layers and identify locations where sentinel sites should be prioritized.

The next factor to consider in site selection is the accessibility of candidate sites. Since most, if not all, of these sites will be accessed and sampled from a small vessel, the locations of public and private boat ramps and digitized navigation charts should be incorporated in the GIS. Distance to boat ramps and navigation routes can be used to evaluate accessibility of individual sites within and between zones.

Another important factor in assessing the capacity of candidate sites is a consideration of the proximity of existing and/or planned environmental monitoring stations, as well as proximity to Strategic Habitat Areas (SHAs), such as primary and secondary nursery areas (A. Deaton, NC DMF, pers. comm.). A thorough inventory of existing monitoring stations including their location, parameters sampled, and the type and frequency of sampling can provide information and data on possible SAV stressors. This compilation can be facilitated through the APNEP CCMP which has closely related monitoring goals. When available, relevant environmental monitoring data should be incorporated into ArcGIS as separate data layers. Similarly, SHAs have been prioritized for most of the estuarine regions considered in this SAV study, and should be considered when prioritizing SAV sentinel sites. Spatial analysis can be used to assess the correspondence between candidate sites with SAV and available monitoring data. Locations having closely corresponding monitoring stations and SAV presence should be considered as high priority.

The evaluation of capacity and establishment of priorities should also consider the geographic locations, expertise and infrastructural capabilities of institutions which could be solicited to conduct monitoring. The State of NC has a number of agencies and academic institutions either already involved in coastal monitoring programs or strategically located such that they could readily access specific strata to conduct monitoring.

Use of the GIS platform and spatial analytical tools provides the opportunity for more sophisticated landscape analyses in the prioritization of zones and the selection of sentinel sites. Landscape level analyses can facilitate improvements in the site selection process by identifying stressors and their potential effects on SAV at larger scales of the estuary and watershed. This is based on the premise that watershed- and estuary-scale stressors affect estuarine environmental quality (i.e., water quality), and in turn, these are critical to the health and condition of SAV (Li

et al. 2007). Factors that have been included in a landscape approach were land cover, point and non-point source nutrient discharge, septic tank density, precipitation, fresh water discharge, salinity, and wind fetch (Li et al. 2007). A landscape approach can also incorporate important spatial features in an estuary such as depth, width and shoreline dimensions. As suggested from a statistical assessment of sub-estuaries in the Chesapeake Bay (Li et al. 2007), this landscape approach may be a very useful in NC for distinguishing differences in stressors within and between strata, identifying the most important stressors in each strata, and setting priorities for locating monitoring sites.

The landscape approach will not resolve the “missing environmental data” problem in the individual strata. Unfortunately, coastal monitoring infrastructure in NC is sparse and not yet well coordinated and the lack of point data will make it difficult to accurately interpolate stressor maps and locate sentinel sites with corresponding environmental data. This is a recognized problem in the Chesapeake Bay and Indian River Lagoon monitoring programs where water quality stations are sited offshore in deep water and are not commensurate with the shallower SAV sampling stations. APNEP’s monitoring component should consider this dilemma as they develop a comprehensive integrated network of sampling stations and parameters. This exercise of SAV sentinel site selection will have added value in that it can be used by APNEP to help prioritize the future selection of sites that benefit their integrated monitoring program. In the meantime, a landscape approach that includes estuarine and watershed characteristics can partly compensate for this limitation while providing important data for predicting variation in SAV distribution and abundance and linking changes in SAV to watershed and estuarine level management initiatives (Li et al. 2007).

Sampling Strategy and Design

As per our recommendation for using a rotational strategy in a coast-wide monitoring program, initially the sentinel sites in just one stratum should be monitored each year. As the monitoring program’s capacity is increased, it will be possible to sample and monitor multiple strata in future years. Once selected, sentinel sites should be sampled during an “index period” when SAV cover and abundance is expected to be at or near a seasonal peak. Index periods for the low-salinity strata in NC occur between May and September (Quible and Associates 2011). The high-salinity strata have a similar window for the index period, but peaks within the period are better understood with respect to the seasonal abundance of the three species (Thayer et al. 1984, Street et al. 2005, Deaton et al. 2010). The peaks in the high-salinity zone depend on whether the tropical species or the temperate species is dominant. If *Z. marina* is dominant, the peak index period will be in May-June, but if *H. wrightii* is present, then the peak will be in August-September. Likewise, in the low-salinity zone, for any individual location, peak abundances can shift within this five month window, depending on the SAV species composition

and recent environmental conditions (e.g., climate, precipitation, storms) (Quible and Associates 2011).

As it is unlikely that all sites will be sampled at the same time, it will be important to complete all sites in a zone within the five-month window. During the next repetition of the monitoring cycle, each site should again be sampled as near as possible to the calendar date of the previous sample. Periodic visits to each of the sentinel sites during the index period can provide additional qualitative observations on shifts in peaks or changes in species composition (see for example, Quible and Associates 2011). These observations over the long-term can be used to develop a better understanding of species phenology and adjust the timing of sampling events as the monitoring program matures into other geographical zones. Using this relatively simple design, the change in SAV monitoring metrics can be statistically analyzed using either logistic regression or repeated measures ANOVA, depending on the metrics selected for monitoring. All sentinel sites should have a design that incorporates depth stratification and includes sample replication so that a standard deviation and variance of the metric can be computed.

Sampling Metrics

We recommend adopting “non-destructive” sampling methods when measuring SAV species composition and abundance. Non-destructive methods are rapid, inexpensive, and minimally disturb the resource. Abundance can be estimated by the two boat-based techniques we evaluated in this CRFL project: 1) direct measurements of SAV presence/absence using an underwater video camera, and 2) indirect measurements by remote sensing percent cover with SONAR. The limitations of each of these techniques can be minimized by further development and testing of a method combining the use of rapidly acquired SONAR data that is assessed for accuracy by underwater video (see “Proof of Concept” discussion below).

Species composition and abundance metrics can also be acquired in-water using snorkel or SCUBA divers. With proper inter-calibration between observers, visual methods are accurate and repeatable (www.seagrasswatch.org, Fourqurean et al. 2001). A commonly practiced in-water non-destructive measure of abundance used in low-salinity regions of NC is a visual assessment of percent SAV cover recorded as a proportion of the area within a quadrat placed on the bottom (Quible and Associates 2011, www.seagrasswatch.org). Recently, Quible and Associates (2011) successively applied this method using snorkelers to identify the species composition and to quantify the abundance of SAV at 17 sites in Albemarle Sound over a period of five years. Since SONAR alone cannot identify species composition, it would be necessary to do additional sampling in the water and/or with a video camera to determine species composition. As both of the boat-based methods have reduced capabilities to acquire data in relatively shallow water < 0.5 m deep, it may be necessary to acquire data by a combination of

all three of these methods. Likewise, the underwater video camera and SONAR methods provide alternatives to SCUBA diving for sampling deeper water where snorkeling is inefficient.

In addition to the biological metrics, we recommend a specific set of physical parameters be incorporated into routine SAV site monitoring. The following list explains each of the recommended parameters.

1. The maximum depth distribution of SAV should be determined at multiple locations in each site. Changes in the maximum depth distribution of SAV can be used as an indicator of water quality stress, especially stressors associated with water clarity (Dennison et al 1993). To facilitate an assessment of this metric, the depths of each site should be characterized by constructing a geospatially articulated bathymetry map of each site that extends from the shoreline to at least 50 m offshore of the existing deep edge of SAV distribution. The locations of SAV can be superimposed on this map at each sampling time to assess changes in SAV depth distribution. It is important to note that the SONAR survey will produce bathymetric maps, but tidal and wind-tide effects should be considered while data collection with SONAR is underway.
2. The sediment grain size and organic matter content of each site should be characterized at the start of monitoring using standard methods. Sonar can be helpful here and with proper ground-truthing (with sediment cores) SONAR method can be successfully used to map bottom-type.
3. At a minimum during each sampling event, water temperature, dissolved oxygen, wind speed and direction, water/tide level, Secchi disc depth, water turbidity, and the attenuation of Photosynthetically Active Radiation (PAR) should be acquired. Ideally, all sampling teams should be outfitted with water quality datasondes to facilitate the collection and management of a wide array of standard water quality parameters. Ideally, the SAV sentinel sites can become part of the APNEP CCMP's integrated monitoring network with comprehensive coverage of SAV as the indicator organism and water quality data as measurements of the stressors.
4. A comprehensive bio-physical description of the adjacent shoreline within 1 km of either side of the sentinel should be completed. We recommend including factors such as land use category, riparian shoreline features, and shoreline modifications identified by the recently released NCDCM estuarine shoreline map (http://dcm2.enr.state.nc.us/Maps/shoreline_mapintro.htm).

As a better understanding of SAV distribution is achieved in the low-salinity strata and deficiencies in the resource inventory map are eliminated, the long-term monitoring program can then proceed to develop a synoptic and probabilistic based sampling approach within each stratum. To facilitate reaching this goal, the prioritization process should continually evaluate whether the baseline maps for any of the individual strata are deemed representative and adequate for synoptic sampling. In the meantime, the program should continue to monitor

established sentinel sites, add sentinel sites in each stratum as deemed appropriate, and design a sentinel site program for the two strata in the high-salinity zone. Sentinel sites can also be used as an interim spatial-gap measure until we get comprehensive and accurate estimates of the spatial extent of the undetected (hidden or invisible) SAV. We also envision using sentinel sites to fill temporal gaps between strata visits (e.g., 5 year cycle) through annual visits to obtain a record of inter-annual or natural variation in SAV distribution and abundance.

Proof-of-Concept for Developing a Combined SONAR and Underwater Video Survey Method for SAV in the Albemarle - Pamlico Estuarine System

Sentinel Site Approach Using Intensive Site NPR (June 2009) as an Example

The following is a recommendation for sentinel site sampling. Ideally this would be initiated at areas where remote sensing is not applicable (e.g. low-salinity areas), but this approach can be applied to all areas of NC. This proposed effort builds upon the information learned throughout this project and maximizes the strengths of each boat based method (SONAR and underwater video) while minimizing the methods' limitations. For example, sentinel site surveys using only underwater video would be very accurate; however, it would require extensive investment in personnel time, and is therefore neither practical nor desirable. Relying solely on SONAR surveys to classify SAV presence at sentinel sites also has its drawbacks. While SONAR is a rapid approach, its accuracy is variable (ranging from 60 – 94%), substantially affecting the power to detect change in SAV area coverage. For this reason, using the SONAR technique alone is not desirable. Therefore, we are recommending a multi-tool approach to sample sentinel sites, using SONAR and underwater video. A site-by-site analysis is necessary to determine the magnitude of change that is detectable with SONAR. Here we provide an example of how to determine this change level and supplement the SONAR method using underwater video. Briefly, SONAR data are converted to a predicted SAV surface which is verified and assessed for accuracy using video camera drops at randomly selected points. In this way, the predicted surface is validated for accuracy which can be used to define the detectable magnitude of change for each site and sampling interval.

Presented below is a detailed description of the recommended method and an illustration of results using data collected in June 2009 at intensive site NPR. Data collection at this site followed methods that were slightly different from those being recommended and thus, this synopsis is for demonstration purposes only. The conclusions, while informative, should not be used for any quantitative analysis. Instead, we suggest that a separate survey be conducted that aims at answering the questions posed here.

Using the methods described for transect selection and SONAR data collection earlier in this report, we recommend the SONAR data be converted into a surface layer (ArcGIS Raster format) of predicted SAV using cokriging (Figure 44). Details of the cokriging steps to be

followed are described in Appendix 8. An additional step to the cokriging approach is to export the standard error (SE) surface that is associated with the SAV predication surface (Figure 45). This can be obtained by right-clicking on the cokriging surface in ArcGIS 9.3 and selecting the 'Create Prediction Map' option. It is important to consider the SE of the predicted surface because this is a measure of uncertainty for the cokriging of the SAV presence/absence prediction map. Regions with high SE values are likely to have lower accuracy because the SONAR points used to interpret the surface are further apart and hence less reliable. To quantify the accuracy of the cokriging model, video validation points should be distributed across the site, but also across the predicted surface's error range. In this example, the cokriging standard errors (SE) were grouped into three categories: low, medium, and high. These categories were selected because this analysis is being done *ex-post-facto* and the distribution of the video validation points is limited to what was collected for the power analysis exercise. It was important to have sufficient video points within each SE category. For this example, only three SE categories had sufficient observations (> 800) to conduct an effective exploratory analysis at NPR for data collected in 2009. Ideally, SE would be thoroughly evaluated at a site, where the number of categories and grouping of categories would be determined by how the accuracy of the method varies with increased SE levels and video validation points distributed accordingly.

Underwater video validation points should be stratified across the site based on the area encompassed by each SE category and then randomly placed within each SE category area. In the example, SE areas were as follows: low 38%, medium 55%, and high 7% of the total site area. The 100 underwater video validation points, which is estimated to be a day's effort of data collection, were then randomly distributed across the site based on these SE category ratios (Figure 46). This means that for the 100 underwater video points, 38 were randomly selected from the low SE category, 55 from the middle, and 7 from the high SE category. Using a remote sensing technique called 'punching through', the underwater video validation points (scored as SAV present/absent) were compared to the SAV prediction surface derived from the cokriging. Punching through describes the method of extracting the SAV surface values (SE and SAV presence or absence) at the exact location of each underwater video validation point, or in essence, punching an underwater video point through the SAV and SE predication surfaces and retaining the SAV predicted value (present/absent) and SE category for each collected underwater video observation.

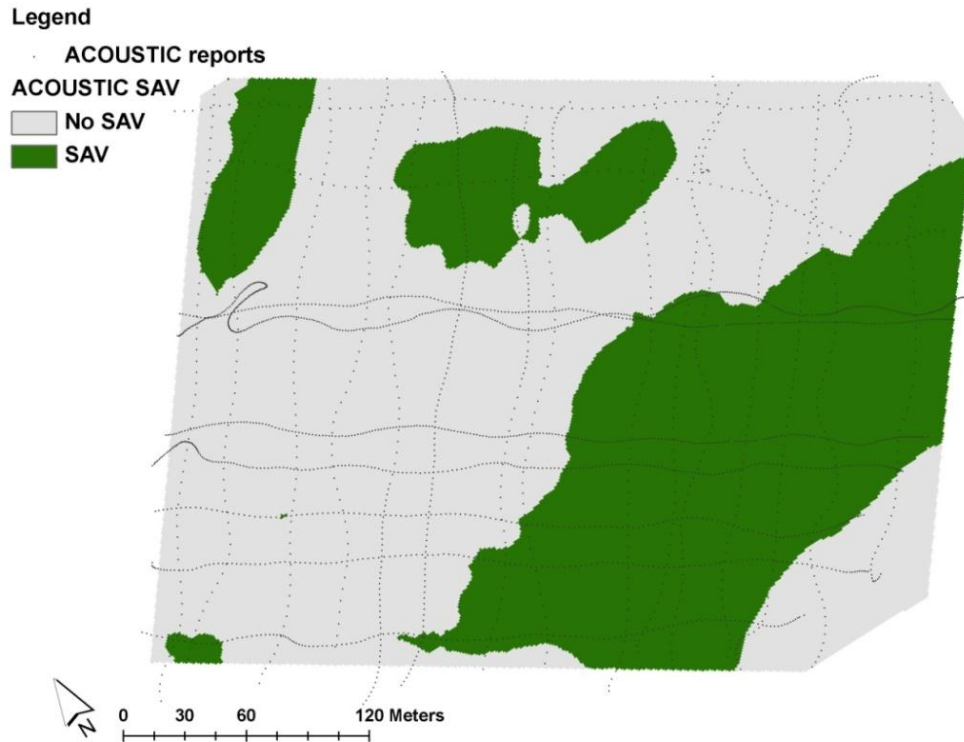


Figure 44. SAV prediction surface from cokriging at NPR.

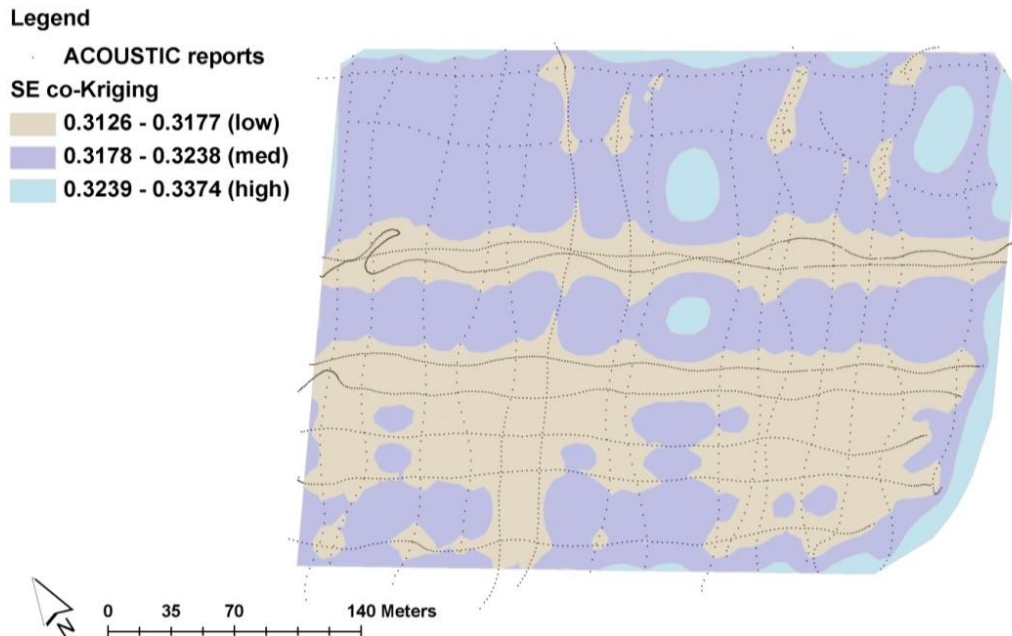


Figure 45. Standard error (SE) associated with the SAV prediction surface at intensive site NPR using geospatial cokriging of SONAR data.

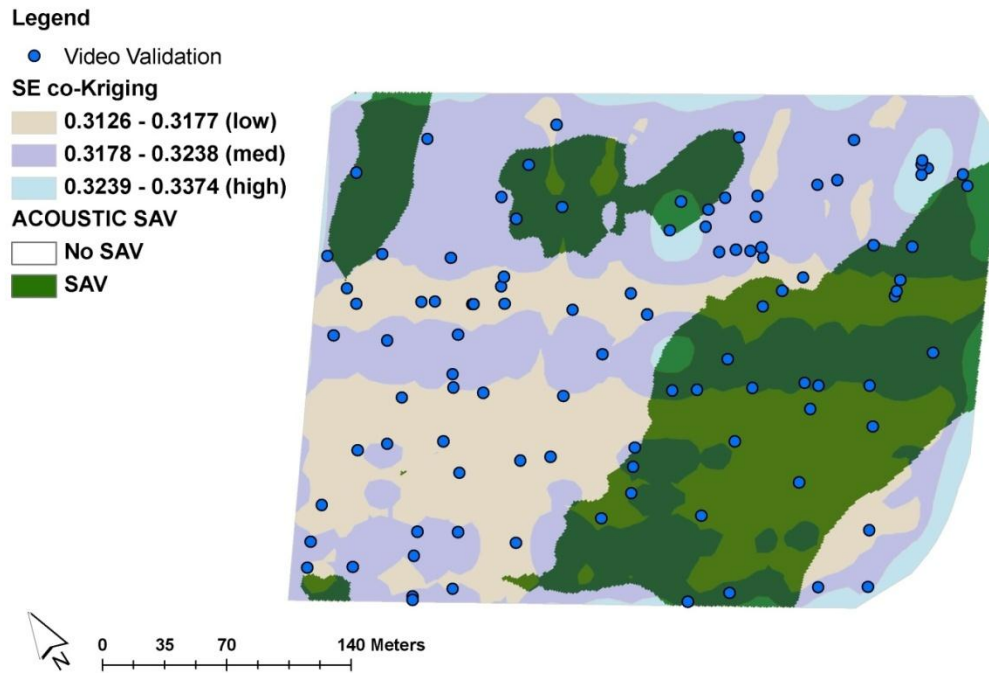


Figure 46. One hundred random underwater video validation points were used to assess the accuracy of the SAV prediction surface at intensive site NPR using cokriging. Underwater video points were stratified by total area of each standard error (SE) classification: low ($n = 38$), medium ($n = 55$), and high ($n = 7$).

Once a video classification and SAV prediction from SONAR is obtained for each point, an accuracy assessment can be conducted for the site. Following methods described in the accuracy assessment section above, each point can be identified as a classification of disagreement or agreement between the two methods. Classification agreement can be further evaluated for SAV (Figure 46). The total number of agreements to the total number of classifications quantifies the SONAR method's ability to detect SAV, which leads to the determination of a change detection level. In the example, 70% of the SONAR points agreed with the underwater video validation points. This can be further broken down by SE. In this example, the SAV predicted surface with low SE, had 68.4% agreement between points (26/38 points), at the medium SE level, the methods agreed 69.1% of the time (38/55 points), while in the region of highest SE, also had the highest accuracy at 85.7% (6/7 points). Thus, with an overall accuracy of 70%, the smallest amount of SAV abundance change that could be reliably detected is operationally constrained to 30%. This value is going to be highly influenced by the form of the SAV bed and the limitations of the SONAR (see the section above). In this example, it is evident that disagreements often occurred (30%, 9/30 points) at the edges of the SAV bed (Figure 46), where SAV most-likely has a more patchy distribution. In addition, two of the disagreement points were in very shallow water where the SONAR method struggles to

successfully identify SAV. The remainder of the disagreement points (63%) occurred outside of the main bed, where there are clear regions of no SAV interspersed with smaller areas where SAV is present. This region is similar to a patchy SAV bed and it is expected to take more effort to accurately classify.

The pattern observed in this example of increasing accuracy with increasing standard error is counter to our expectation. As mentioned at the beginning of this section, the example used here should only serve as an example of the capabilities of the method and the trends and conclusions of the example should not be considered as truth. As a result, we performed a bootstrap resampling analysis from the NPR site with all underwater video and SONAR cokriging points available for comparison. This bootstrap analysis is described below and will serve as an introduction to the combined methods we are recommending for further testing at sentinel sites.

Accuracy of the SONAR Cokriging Surfaces

The accuracy of cokriging surfaces needs to be investigated if the approach is to be used in a sentinel site protocol. Here, we simulate accuracy of the cokriging SAV prediction surface at different levels of video drop camera effort using a Monte-Carlo resampling approach. We used the SONAR cokriging surface and video drop camera comparison method from SONAR and video data set already collected at NPR site, following the methods just described above.

This data set was analyzed in Systat 13 using the “Tabulate” command, using the three SE strata from the cokriging map with bootstrap re-sampling used to compute accuracy in each case from the distribution of underwater video drop points. Different numbers of video drops were randomly selected (n with video drop sample size intervals of 10 through 100, 500, 1000 video drops) and each level of video sampling effort was randomly sampled with replacement 100 times. Accuracy was computed each time by summing the number of correct classifications (the counts of video drop points at which SAV was present in both the SONAR and video, or both absent in the SONAR and video), then dividing by the total number of video drops. Mean accuracy was computed for each of the cokriging SE strata zones. All these strata showed a convergence in accuracy after 30 video drops, but strata 1 (low SE) and 2 (mid SE) had noticeably smaller variability and higher mean accuracy, with an asymptotic accuracy of 70 % for stratum 1 and 65 % for stratum 2 after 100 video drop camera points (Figure 47). Stratum 3 (high SE) had the most variable accuracy of the three strata and mean accuracy was lowest in this stratum (54%). The cokriging surface of SAV presence or absence at this site was 65-70% accurate over most of the study area, but when the cokriging SE was large, accuracy fell to 54%.

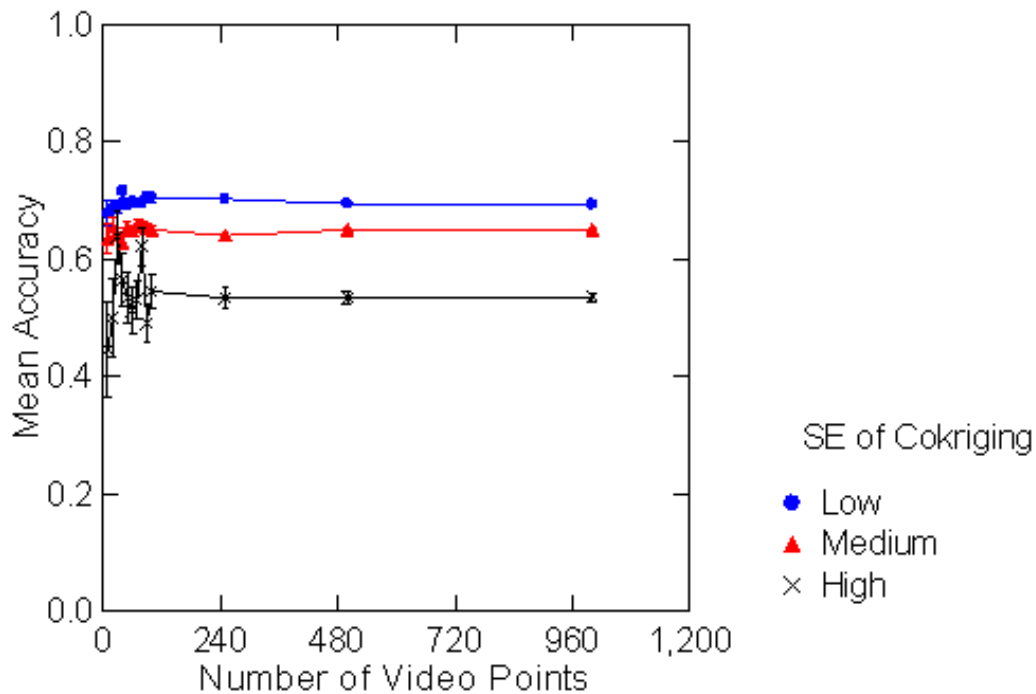


Figure 47. The accuracy within each standard error (SE) stratum from cokriging surfaces of SONAR obtained at intensive site NPR in 2009 when compared against different number of video drop camera points. For each level of video camera sampling effort, a re-sampling estimate of 100 bootstrapped samples was used to derive the mean accuracy.

We have shown the accuracy in quantifying % SAV cover with the BioSonics DTX SONAR with ECOSAV2 averages 77% when compared to underwater video camera imagery, but it varied between 69% and 98% at the four Intensive and nine Rapid Assessment sites in our CRFL-funded study conducted in 2009-2011. This wide range of accuracy is due to several factors: 1) the SONAR does not detect short plants (< 6.8 cm) because of a limitation in the ECOSAV2 algorithm, which intentionally omits such plants to avoid false positives caused by detritus and other targets associated with the bottom; 2) algae that exceeds this plant threshold will be detected, but algae can be discriminated by a human reviewing the videography, and has not been included in the definition of SAV that was counted on video; and 3) in sparse and patchy beds, the two methods differ because of navigation and GPS positioning error. All of this leads to the two methods “seeing” different parts of any survey.

We feel that this SONAR method is a promising tool for surveying SAV in the low-salinity region of the APES and at sentinel sites. But, since SONAR technology is developing rapidly and these new technologies are untested, they cannot be used on a routine basis by NCDMF. It is our opinion that the SONAR method is still in need of further accuracy assessments and methods development for use in NC estuarine areas.

Suggested Project Design for SAV Acoustic Reconnaissance Surveys for Low-Salinity Areas in the Albemarle – Pamlico Estuarine System

Described below is the project design for further development of a SONAR monitoring protocol suggested by this initial study. APNEP and ECU should partner to do the following:

- 1) Purchase a Lowrance HDS-5 Sonar System with Structure Scan (this is cheaper than BioSonics DTX or MX, requires no training on easier to use for surveys and field personnel). Cost: ~ \$1,300 for equipment. This does not include a software analysis suite, so SONAR data collected by the Lowrance echosounder cannot be analyzed without a contract with Contour Innovations (see 3 below).
- 2) ECU would provide the existing BioSonics DTX or purchase a new MX system (\$10,000 including software) with the SONAR equipment to run as a side-by-side comparison alongside the new Lowrance/ciBioBase system.
- 3) Contract with Contour Innovations (ciBioBase) to do the kriging of the data collected with the Lowrance HDS echosounder and analyze the data using uploads to ciBioBase (1-day turnaround of data processing), using depth and biovolume as predictors (\$4300/year for unlimited uploads).
- 4) Use 60 shore-normal transects from 0.7 m to 4 m depth (~500 m) spaced 25 m apart. Collect data along the transects at 3 knots (1.5 m/s). This will take approximately 2 days of SONAR surveys to complete each site. Our rapid assessment survey indicated that maximum linear size of SAV patches are approximately 1500 m long at the most heavily inhabited sites (~1400 m at Batchelor Bay and ~1700 m at Sandy Point). This will result in survey polygons that are about five times as large as the 300 m x 300 m polygons we have done in our preliminary work. The spacing of transects are what is recommended by Valley et al. (2005). Because they will be spaced in a systematic manner, the reduced variance method of Fewster (2011) can be used to analyze the data.
- 5) Repeat this SONAR survey at 25 locations in Albemarle Sound, Pamlico River, and Neuse Rivers (over a five-month period, May through September, e.g., 10 days per month allowing for weather and other interfering water conditions, waves, storms, etc.) . Sites will be selected (at random within our low-salinity strata or as directed by agency needs in consultation with the SAV Partnership).
- 6) Use at least 100 video camera drops taken at random within each 1500 m x 500 m polygon to determine accuracy of the sonar cokriging surface of SAV. This will take another day per site (five days per month). The sample size of 100 video comparison

points is based on the bootstrapping analysis done in this report; above this sample size, little gain in accuracy estimate was observed. This can be done by a separate boat and video team dedicated to this task, but working an area as soon as possible after a SONAR survey is completed and krigs produced.

- 7) Investigate the accuracy of the cokriging surface at each site by computing the agreement between video points and SONAR kriging surface, determining SAV presence at each comparison point

$$Accuracy = \frac{(Agree\ sav + Agree\ no\ sav)}{Total\ comparison\ points} \times 100$$

ciBioBase will provide kriging surfaces for all polygons and raw data to ECU for computation of the accuracy values within one day of the SONAR data collection for use in determining the SONAR accuracy. ECU will produce cokrigings (depth and SAV cover) from the BioSonics DTX SONAR data. ECU will collect the SONAR and video data, and compute the accuracy estimates for both the Lowrance and BioSonics DTX SONAR data.

Conclusions

This project documents the recommended protocols we have developed for The State of North Carolina to conduct boat-based surveys of SAV in both low-salinity and high-salinity regions of the Albemarle Pamlico Estuarine System (APES). We have developed a combined underwater videographic and SONAR protocol that can be used to monitor changes (as small as 10% and up to 40% change) in SAV between two surveys at the same site separated in time by a maximum of 5 years. We investigated in-water techniques (diver quadrats) only for comparison with SONAR data, not for estimating change in SAV, but report costs for both boat-based and in-water methods. Both SONAR and video methods were developed for their power to detect changes used along a series of shore-normal transects in a small survey area (a 300 x 300 m polygon, 90,000 m²), called an intensive site in this study, and we computed the necessary sample sizes in terms of the number of transects to detect 10%, 20%, and 40% changes in SAV. We recommend that at least 30 SONAR or video transects, systematically selected at 10-m intervals from a random starting position along one of the baselines following the method of Fewster (2011), are needed at the patchiest sites investigated here to detect a 10% change with high probability (statistical power). The SONAR method has distinct advantages that include lower data acquisition and analysis costs (0.44 h per transect, 19 h per site) than video, the use a computer algorithm called ECOSAV to rapidly process the echosounder data, generation of output to GIS-ready files along with geo-referenced bathymetry, plant height and plant cover data, survey repeatability over short time periods (e.g., seasonal surveys) and calibration of the equipment to international standards.

Drawbacks of the SONAR method include the high equipment acquisition costs, an average of 77% accuracy when compared with video (there are both false-positives and false-negatives), and the need for some operator training. Video imagery was used to determine the accuracy of the SONAR method, which can underestimate the SAV area when it is sparse in distribution and plants are short (< 6 cm or 2.4 inches). The advantages of videography method includes its high precision, ability to detect plants in sparse areas that are short, and the ability to identify SAV species, but it requires much higher costs to acquire underwater video imagery along a transect and process the data (4.8 h per transect, 119 h per site) than SONAR. The videography method taken along transects is not practical for surveying the large number of sentinel sites that we recommend should be done each 5 years in the APES. Both boat-based methods do not provide adequate coverage in very shallow water > 0.7 m (2.3 ft), so that aircraft-based photographic remote sensing should be used in broad areas of shallow water, like behind the NC barrier islands (Outer Banks). The boat-based SONAR method works very well for reconnaissance in the low-salinity areas, where the SAV distribution is poorly known, and along the deep edge of the high-salinity regions. We conducted a Rapid Assessment reconnaissance survey to estimate SAV patch sizes at nine additional sites in the low-salinity regions of Albemarle Sound, Pamlico and Neuse Rivers. These regions have what has been termed “invisible grass”, because the SAV is present but not visible on the remotely sensed photographs, due to the high light attenuation in the turbid waters found there.

Based on the data in this report, we present a SAV sentinel site survey protocol that combines SONAR and video approach. We simulated a sentinel site protocol survey along transects taken with both methods at the Newport River in 2009, analyzed the SONAR data with cokriging of depth and SAV cover, then made a comparison of the cokriging surface with video camera drops at randomly selected points to determine accuracy. We tested this protocol with different numbers of video points at the Newport River using our already collected data and Monte-Carlo simulations. We achieved 70% accuracy detecting SAV with sampling efforts greater than 100 video camera drops, but this protocol needs further testing with new field data. We have begun such a protocol validation study, surveying within a 1500 m x 900 m sentinel site using our recommended protocol, as part of a remote sensing survey of SAV in Currituck Sound (funded by APNEP). These combined SONAR and video boat-based methods are recommended to be used at multiple sentinel sites distributed throughout the APES region, on a 5-year rotation within strata, with the number of and specific location of these sites to be determined by the NC SAV partners group. New SONAR technologies (single beam, side-scan, multi-beam) are being developed marketed; their cost-effectiveness and accuracy should be investigated in future CRFL-funded studies.

Annual Budget Expenditures

Summary of Expenditures for ECU Tasks (9/15/2009 – 8/31/2012)

Fund	Account Pool	Budget	Expenditures	Budget Balance
	Salaries total	86,541.00	82,470.36	4,070.64
	Benefits Budget Pool	10,167.00	5,641.74	4,525.26
	Supplies Budget Pool	4,345.00	14,576.97	-10,231.97
	Equipment Budget Pool	10,530.00	5,851.42	4,678.58
	Contractual Services Pool	15,931.00	1,630.87	14,300.13
	Travel Budget Pool	7,140.00	5,154.67	1,985.33
	Current Services Pool	1,020.00	571.94	448.06
	Other Fixed Charges Pool	0.00	442.50	- 442.50
	Indirect Overhead Cost	14,216.00	12,952.43	1,263.57
		149,890.00	129,302.90	20,597.10

Budget Deviations

Salaries were not fully expended because funding arrived too late for the doctoral student Cecilia Krahforst to be paid in Fall semester 2011. She was paid from other ECU accounts, and performed the APNEP/CRFL project work.

The supplies line was over spent because our boat costs were applied there, whereas the money for boat rentals was requested under contractual services. This overage in supplies was offset by money in the contractual services line.

The equipment budget has an excess because the requested heading, pitch, and roll sensor for the 420 kHz transducer and DTX echosounder system was not installed by BioSonics, Inc., at the recommendation of the technicians at BioSonics, who stated that it would not aid in getting more accurate data.

We had planned for simultaneous SONAR, video and remote sensing sampling to test the proposed protocols for sentinel site SAV surveys during the second year of this project. These various sampling methods were to be done at the same time in the Spring (high salinity) or Fall (low salinity) at a sentinel site. Due to weather-related delays (Hurricane Irene in Fall 2011, and Tropical Storm Alberto in Spring 2012), the lack of water clarity at the survey sites, and thus the ability of remote sensing aircraft to acquire acceptable imagery, this exercise had to be postponed. We are attempting to cooperate with APNEP to accomplish this task now (Fall 2012). This postponement resulted in excess money in the contractual services and travel budget lines.

The DTX system was sent to BioSonics to be calibrated prior to the start of the surveys, and this resulted in a fixed services charge (FedEx ground shipping).

REFERENCES

- Berry, H.D.; A.T. Sewell; S. Wyllie-Echeverria; B.R. Reeves; T.F. Mumford Jr.; J. Skalski; R.C. Zimmerman; and J. Archer. 2003. Puget Sound Submerged Vegetation Monitoring Project: 2000-2002 Monitoring Report. Nearshore Habitat Program, Washington State Department of Natural Resources. Olympia, WA. 60 pp. plus appendices.
- Biber, P.D.; H.W. Paerl; C.L. Gallegos; and W.J. Kenworthy. 2004. Evaluating Indicators of Seagrass Stress to Light. Pages 193-209 in SA Bortone (ed.), *Estuarine Indicators*. CRC Press, Boca Raton.
- BioSonics, Inc. 2004. User Guide for EcoSAV 1. BioSonics Inc., 4027 Leary Way, NW, Seattle, WA 98107, USA. Available for download at www.biosonicsinc.com
- Braun-Branquet, J. 1972. *Plant Sociology: the study of plant communities*. Hafner, NY.
- Brinson, M.M.; and G.J. Davis. 1976. Primary productivity and mineral cycling in aquatic macrophyte communities of the Chowan River, North Carolina. UNC-WRRI, Raleigh, NC, Report No. 120, 137p.
- Burnicki, A.C. 2011. Spatio-temporal errors in land-cover change analysis: implications for accuracy assessment. *Inter. J. of Remote Sensing* 32(22):7487-7512.
- Burkholder, J. D. Eggleston, H. Glasgow, C. Brownie, R. Reed, G. Melia, C. Kinder, G. Janowitz, R. Corbett, M. Posey, T. Alphin, D. Toms, N. Deamer. 2004. Comparative impacts of major hurricanes on the Neuse River and Western Pamlico Sound ecosystems. *Proceedings of the National Academy of Science* 101: 9291-9296.
- Carraway, R.J.; and L.J. Priddy. 1983. Mapping of submerged grass beds in Core and Bogue Sounds, Carteret County, North Carolina, by conventional aerial photography. CEIP Report No. 20, 88p.
- Christian R.R.; and S. Mazzilli. 2007. Defining the coast and sentinel ecosystems for coastal observations of global change. *Hydrobiologia* 577:55–70.
- Cochran, W.G. 1977. *Sampling Techniques* (3rd Edition). New York: John Wiley & Sons.
- Cooper, S.R. 2000. The history of water quality in North Carolina estuarine waters as documented in the stratigraphic record. UNC-WRRI 2000-327.
- Costello, C.; and W.J. Kenworthy. 2011. Twelve-year mapping and change analysis of eelgrass (*Zostera marina*) areal abundance in Massachusetts (USA) identifies statewide declines. *Estuaries and Coasts*. 34:232-242.
- Cressie, N. 1991. *Statistics for Spatial Data*. John Wiley & Sons, Inc. NY.

- Davis, G.J.; and M.M. Brinson. 1983. Trends in submerged macrophyte communities of the Currituck Sound: 1909-1979. *Journal of Aquatic Plant Management* 21: 83-87.
- Deaton, A.S.; W.S. Chappell; K. Hart; J. O'Neal; and B. Boutin. 2010. North Carolina Coastal Habitat Protection Plan. North Carolina Department of Environment and Natural Resources. Division of Marine Fisheries, NC. 639 pp.
- Dennison, W.C. 1987. Effects of light on seagrass photosynthesis, growth, and depth distribution. *Aquatic Botany*. 27:15-26.
- Dennison, W.C.; R.J. Orth; K.A. Moore; J.C. Stevenson; V. Carter; S. Kollar; P.W. Bergstrom; and R. Batiuk. 1993. Assessing water quality with submerged aquatic vegetation. *Bioscience* 43: 86-94.
- Dobson, J.E.; E.A. Bright; R.L. Ferguson; D.W. Field; L.L. Wood; K.D. Haddad; H. Iredale III; J.R. Jensen; V.V. Klemas; R.J. Orth; and J.P. Thomas. 1995. NOAA Coastal Change Analysis Program C-CAP): guidance for regional implementation. *NOAA Technical Report NMFS 123*, U.S. Department of Commerce, 92 pp.
- Dowty, P.; H. Reeves; S. Berry; S. Wyllie-Echeverria; T. Mumford; A. Sewell; P. Milos; and R. Wright. 2005. A study of sampling and analysis methods: Submerged Vegetation Monitoring Project at year 4. Nearshore Habitat Program, Washington State Department of Natural Resources. Olympia, WA. 133 pp.
- Duarte, C.M. 1987. Use of echosounder tracing to estimate the aboveground biomass of submersed plants in lakes. *Canadian Journal of Fisheries and Aquatic Science* 44: 732-735.
- Durako, M.J.; M.O. Hall; and M. Merello. 2002. Patterns of change in the seagrass dominated south Florida hydroscape. In: Porter, J.W. and K.G. Porter (eds.), *The Everglades, Florida Bay, and Coral Reefs of the Florida Keys: An Ecosystem Sourcebook*. CRC Press, Boca Raton, Florida, pp. 523-537.
- Edsall, T.A., T.E. Behrendt, G. Cholowek, J. W. Frey, G. W. Kennedy, and S. B. Smith. 1997. Use of remote-sensing techniques to survey the physical habitat of large rivers. U. S. Geological Survey, Contribution number 983 of the Great Lakes Science Center, Ann Arbor, MI.
- Ferguson, R.L.; L.L. Wood; and D.B. Graham. 1993. Monitoring spatial change in seagrass habitat with aerial photography. *Photogrammetric Engineering and Remote Sensing*, 59:1033-1038.
- Ferguson, R.L.; and L.L. Wood. 1994. Rooted vascular aquatic beds in the Albemarle-Pamlico estuarine system. NMFS, NOAA, Beaufort, NC, Project No. 94-02 , 103 p.

- Fewster, R. M. 2011. Variance estimation for systematic designs in spatial surveys. *Biometrics* 67(4):1518-31.
- Finkbeiner, M.; B. Stevenson; and R. Seaman. 2001. Guidance for benthic habitat mapping: an aerial photographic approach. NOAA, National Ocean Service, Coastal Services Center, Charleston, SC, 76 pp.
- Foote, K. G. 1991. Summary of methods for determining fish target strength at ultrasonic frequencies. *ICES Journal of Marine Science: Journal du Conseil* 48: 211-217.
- Foote, K. G. 2006. Standard-target calibration of active sonars used to quantify aquatic organisms. *The Journal of the Acoustical Society of America* 120: 3017.
- Foote, K. G. 2008. Standard-target method of calibrating active sonars: principles, applications, benefits. *The Journal of the Acoustical Society of America* 123: 3348-3348.
- Foote, K. G., Chu, D., Hammar, T. R., Baldwin, K. C., Mayer, L. A., Hufnagle Jr, L. C., and Jech, J. M. 2005. Protocols for calibrating multibeam sonar. *The Journal of the Acoustical Society of America* 117: 2013.
- Fonseca, M.S.; W.J. Kenworthy; and G.W. Thayer. 1998. Guidelines for the Conservation and Restoration of Seagrasses in the United States and Adjacent Waters. NOAA, Coastal Ocean Program, Decision Analysis Series No. 12. U.S. Department of Commerce, NOAA, Coastal Ocean Office, Silver Spring, MD. 222pp.
- Forte, M. and T. Martz. 2007. Currituck Sound Hydrographic and Submerged Aquatic Vegetation Survey. US Army Corps of Engineers, Field Research Facility, Duck, NC, ERDC/CHL/FRF Report 07-1.
- Fourqurean, J.W.; A. Willsie; C.D. Rose; and L.M. Rutten. 2001. Spatial and temporal patterns in seagrass community composition and productivity in south Florida. *Marine Biology* 138:341–354.
- Fourqurean, J.W.; M.J. Durako; M.O. Hall; and L.N. Hefty. 2002. Seagrass distribution in south Florida: a multi-agency coordinated monitoring system. Pp. 497-522 in Porter, J.W. and K.G. Porter (eds.), *The Everglades, Florida Bay, and Coral Reefs of the Florida Keys: An Ecosystem Sourcebook*. CRC Press, Boca Raton, Florida.
- Fourqurean, J.W.; J.N. Boyer; M.J. Durako; L.N. Hefty; and B.J. Peterson. 2003. Forecasting responses of seagrass distributions to changing water quality using monitoring data. *Ecological Applications* 13: 474–489.
- Gaeckle, J.; P. Dowty; H. Berry; and L. Ferrier. 2009. Puget Sound Submerged Vegetation Monitoring Project 2009 Report. Dated March 7, 2011. Nearshore Habitat Program, Aquatic Resources Division, Washington State Department of Natural Resources. 76pp. http://www.dnr.wa.gov/ResearchScience/Topics/AquaticHabitats/Pages/aqr_nrsh_eelgrass_monitoring.aspx

- Green, E.P.; and F.T. Short. 2003. *World Atlas of Seagrasses*. University of California Press, Berkeley.
- Hall, M.O.; M.J. Durako; J.W. Fourqurean; and J.C. Zieman. 1999. Decadal changes in seagrass distribution and abundance in Florida Bay. *Estuaries* 22: 445-459.
- Hamabata, E.; and Y. Kobayashi. 2002. Present status of submerged macrophyte growth in Lake Biwa: Recent recovery following a summer decline in the water level. *Lakes & Reservoirs: Research & Management* 7:331-338.
- Heidelbaugh, W.S.; and W.G. Nelson. 1996. A power analysis of methods for assessment of change in seagrass cover. *Aquatic Botany* 53:227-233.
- Hoffman, J.; J. Burczynski; B. Sabol; and M. Heilman. 2002. Digital acoustic system for ecosystem monitoring and mapping: assessment of fish, plankton, submersed aquatic vegetation, and bottom substrata classification. BioSonics internal report, available at www.biosonicsinc.com.
- Holdaway, M.R.; and G.J. Brand. 2000. Realistic spatial models: the accurate mapping of environmental factors based on synecological coordinates. Pp. 137-150 in H.T. Mowrer and R.G. Congalton (Eds.), *Quantifying Spatial Uncertainty in Natural Resources: Theory and Applications for GIS and Remote Sensing*. Ann Arbor Press. Chelsea, MI.
- Issaks, E.H.; and R.M. Srivastava. 1989. *An introduction to applied geostatistics*. Oxford University Press, NY.
- Jarvis, J.C.; K.A. Moore; and W.J. Kenworthy. 2012. Characterization and ecological implication of eelgrass life history strategies near the species' southern limit in the western North Atlantic. *Marine Ecology Progress Series* 44:43-56.
- Jassby, A.D. 1998. Interannual variability at three inland water sites: implications for sentinel ecosystems. *Ecological Applications* 8: 277-287.
- Jensen, J.R. 2005. *Introductory Digital Image Processing, A Remote Sensing Perspective*, 3rd ed., Saddle River, NJ, Prentice-Hall, Inc., 526 pp.
- Kenworthy, W.J.; M.J. Durako; S.M.R. Fatemy; H. Valavi; and G.W. Thayer. 1993. Ecology of seagrasses in northern Saudi Arabia one year after the Gulf War oil spill. *Marine Pollution Bulletin* 27:213-222.
- Kenworthy, W.J.; S. Wyllie-Echeverria; R.G. Coles; G. Pergent; and C. Pergent-Martini. 2006. Seagrass conservation biology: An interdisciplinary science for protection of the seagrass biome. Chapter 25 in A.W. Larkum, C.M. Duarte and R. Orth (eds.) *Seagrass Biology*, pp. 595-623. Springer, Netherlands.

- Larkum, A.W.D.; R.J. Orth; and C.M. Duarte. 2006. *Seagrasses: Biology, Ecology and Conservation*. Springer, The Netherlands. 691 pp.
- Lathrup, R.; G.R.M. Styles; S.P. Seitzinger; and J.A. Bogner. 2001. Use of GIS mapping and modeling approaches to examine the spatial distribution of seagrasses in Barnegat Bay, New Jersey. *Estuaries* 24: 904-916.
- Latimer, J.S.; and S.A. Rego. 2010. Empirical relationship between eelgrass extent and predicted watershed-derived nitrogen loading for shallow New England estuaries. *Estuarine, Coastal and Shelf Science* 90: 231-240.
- Lee Long, W. J., A. J. Hundley, C. A. Roder, and L. J. McKenzie. 1998. Preliminary evaluation of an acoustic technique for mapping tropical seagrass habitats. Research Publication No. 52. Great Barrier Reef Marine Park Authority, Townsville.
- Lehmann, A. 1998. GIS modeling of submerged macrophyte distribution using generalized additive models. *Plant Ecology* 139:113-124.
- Li, X.; D.E. Weller; C.L. Gallegos; T.E. Jordan; and H.C. Kim. 2007. Effects of watershed and estuarine characteristics on the abundance of submerged aquatic vegetation in Chesapeake Bay subestuaries. *Estuaries and Coasts* 30: 840-854.
- Luczkovich, J.J. 2005. Submerged Aquatic Vegetation Survey at Sandy Point, NC. A report to the Fund for Sandy Point, LLC and Quible and Associates, P.C. 35 pp.
- Maceina, M. J. and J. V. Shireman. 1980. The use of a recording fathometer for determination of distribution and biomass of hydrilla. *Journal Aquatic Plant Management* 18:34-39.
- Maceina, M.J., J. Shireman, K. A. Langeland, and D. E. Canfield. 1984. Prediction of plant biomass by use of a recording fathometer. *Journal of Aquatic Plant Management* 22:35-38.
- Mallin, M.A.; J.M. Burkeholder; L.H. Cahoon; and M.H. Posey. 2000. North and South Carolina Coasts. *Marine Pollution Bulletin* 41:56-75.
- McCarthy, E.M.; and B. Sabol. 2000. Acoustic characterization of submerged aquatic vegetation: military and environmental monitoring applications. Pp. 1957-1961 in *OCEANS 2000 MTS/IEEE Conference and Exhibition*, vol. 1953.
- McKenzie, L.J.; W.J. Lee Long; R.G. Coles; and C.A. Roder. 2000. Seagrass-Watch: Community based monitoring of seagrass resources. *Biol. Mar. Medit.* 7(2): 393-396.
- Miner, S.P. 1993. Application of acoustic hydrosurvey technology to the mapping of eelgrass (*Zostera marina*) distribution in Humboldt Bay, California. Coastal Zone 93. Proceedings of the 8th Symposium on Coastal and Ocean Management, July 19-23 1993, New Orleans, LA.

- Moreno A. P. Siljeström, and J. Rey. 1998. Benthic phanerogram species recognition in side-scan sonar images: Importance of sensor direction. Pp. 173-178 In A. Alippi and G. B. Cannelli (eds.), Proceedings 4th European Conference on Underwater Acoustics, Rome.
- Morris, L.J.; L.M. Hall; and R.W. Virnstein. 2001. Field guide for fixed seagrass transect monitoring in the Indian River Lagoon. St. Johns River Water Management District, Palatka, Florida.
- Mumby, P.J.; A.J. Edwards; E.P. Green; C.W. Anderson; A.C. Ellis; and C.D. Clark. 1997. A visual assessment technique for estimating seagrass standing crop. *Aquatic Conservation: Marine and Freshwater Ecosystems* 7: 239-251.
- Norris, J.G.; S. Wyllie-Echeverria; T. Mumford; A. Bailey; and T. Turner. 1997. Estimating basal area coverage of subtidal seagrass beds using underwater videography. *Aquatic Botany* 58:269-287.
- Orth, R.J.; and K.A. Moore. 1983. An unprecedented decline in submerged aquatic vegetation. *Science* 22:51-53.
- Orth, R.J.; T.J.B. Carruthers; W.C. Dennison; C.M. Duarte; J.W. Fourqurean; K.L. Heck Jr.; A.R. Hughes; G.A. Hendrick; W.J. Kenworthy; S. Olyarnik; F.T. Short; M. Waycott; and S.L. Williams. 2006a. A global crisis for seagrass ecosystems. *Bioscience* 56:987-996.
- Orth, R.J.; M.L. Luckenbach; S. Marion, K.A. Moore; and D.J. Wilcox. 2006b. Seagrass recovery in the Delmarva Coastal Bays, USA. *Aquatic Botany* 84: 26-36.
- Orth, R.J.; S.R. Marion; K.A. Moore; and D.J. Wilcox. 2010. Eelgrass (*Zostera marina* L.) in the Chesapeake Bay region of mid-Atlantic coast of the USA: challenges in conservation and restoration. *Estuaries and Coasts* 33: 139-150.
- Preston, J.; Y. Inouchi; and F. Shioya. 2006. Acoustic classification of submerged aquatic vegetation. Proceedings of the Eighth European Conference on Underwater Acoustics, ECUA 2006. S.M.J.O.C. Rodríguez (Ed.). Carvoeiro, Portugal.
- Quible and Associates. 2011. Compensatory Mitigation Plan Report Sandy Point Development. Prepared for: US Army Corps of Engineers, National Marine Fisheries Service, NC Division of Coastal Management, NC Division of Marine Fisheries, NC Wildlife Resources Commission, Quible & Associates, P.C. P.O. Drawer 870 Kitty Hawk, NC 27949.
- Reeves, B.R.; P.R. Dowty; S. Wyllie-Echeverria; and H.D. Berry. 2006. Classifying the seagrass *Zostera marina* L. from underwater video: an assessment of sampling variation. *Journal of Marine Environmental Engineering* 16:1-45.

- Rohmann, S.O.; and M.E. Monaco. 2005. Mapping southern Florida's shallow-water coral ecosystems: an implementation plan. NOAA Technical Memorandum NOS NCCOS 19, NOAA/NOS/NCCOS/CCMA, Silver Spring, MD, 39pp.
- Rose, C.D., W.C. Sharp, W.J. Kenworthy, J.H. Hunt, W.G. Lyons, E.J. Prager, J.F. Valentine, M.O. Hall, P. Whitfield, and J.W. Fourqurean. 1999. Sea urchin overgrazing of a large seagrass bed in outer Florida Bay. *Marine Ecology Progress Series*. 190:211-222
- Sabol, B. E. McCarthy, and K. Rocha. 1997. Hydroacoustic basis for detection and characterization of eelgrass. Pp I-679-I-693 In *Proceedings of Fourth Conference on Remote Sensing for Marine and Coastal Environments*, Orlando, Florida, 17-19 March 1997. Environmental Research Institute of Michigan, Ann Arbor, Michigan.
- Sabol, B. M. and J. Burczinski. 1998. Digital echosounder system for characterizing vegetation in shallow-water environments. Pp 165-171 *In* A. Alippi and G. B. Cannelli (eds.), *Proceedings 4th European Conference on Underwater Acoustics*, Rome.
- Sabol B. M., R.E. Melton, and R. L. Kasul. 1998. Method and apparatus for hydroacoustic detection of submersed aquatic vegetation. Patent No. 5,805,525 U.S. Patent Office, Washington, D.C.
- Sabol, B. M. and S. A. Johnston. 2001. Innovative techniques for improved hydroacoustic bottom tracking in dense aquatic vegetation. US Army Corps of Engineers, Aquatic Plant Control Research Program. ERDC/EL MP-01-2, Aug 2001, 20 pp.
- Sabol, B.M.; R.E. Melton; R. Chamberlain; P. Doering; and K. Haurert. 2002. Evaluation of digital echosounder system for detection of submerged aquatic vegetation. *Estuaries and Coasts* 25, 133-141
- Sabol, B.M.; J. Kannenberg; and J.G. Skogerboe. 2009. Integrating acoustic mapping into operational aquatic plant management: a case study in Wisconsin. *Journal of Aquatic Plant Management* 47:44-52.
- Saito, H.; and P. Goovaerts. 2002. Accounting for measurement error in uncertainty modeling and decision-making using indicator kriging and p-filed simulation: application to a dioxin contaminated site. *Environmetrics* 13:555-567.
- Short, F.T.; and R.G. Coles. 2001. *Global Seagrass Research Methods*. Elsevier Science B.V., Amsterdam.
- Short, F.T.; L.J. McKenzie; R.G. Coles; K.P. Vidler; and J.L Gaeckle. 2006. *Seagrass Net Manual for Scientific Monitoring of Seagrass Habitat*, Worldwide Edition. University of New Hampshire Publication. 75 pp.

- Short, F.T.; T.J.B. Carruthers; W.C. Dennison; and M. Waycott. 2007. Global seagrass distribution and diversity: a bioregional model. *Journal of Experimental Marine Biology and Ecology* 350, 3–20.
- Simmonds, J. and D. MacLennan. 2005. *Fisheries Acoustics: Theory and Practice*. Second edition. Blackwell Publishing, Oxford. 437 pp.
- Skalski, J.R. 2003. Statistical Framework for Monitoring *Zostera marina* (Eelgrass) Area in Puget Sound. In: Berry et al. *Puget Sound Submerged Vegetation Monitoring Project: 2000-2002 Monitoring Report*. Appendix L. Nearshore Habitat Program, Washington State Department of Natural Resources, Olympia, Washington. Available online: <http://www2.wadnr.gov/nearshore>.
- Stanley, D.W. 1992. Long-term trends in Pamlico River Estuary nutrients, chlorophyll, dissolved oxygen, and watershed nutrient production. *Water Resources Research* 29:2651-2662.
- Stanley, D.W. 1993. Historical Trends: Water quality and fisheries, Albemarle-Pamlico Sounds, with emphasis on the Pamlico River Estuary. Raleigh, NC: North Carolina Sea Grant Publication No. UNC-SG-92-04
- Steward, J.S.; and W.C. Green. 2007. Setting load limits for nutrients and suspended solids based upon seagrass depth-limit targets. *Estuaries and Coasts* 30: 657–670
- Steward, J.S.; R.W. Virnstein; L.J. Morris; and E.F. Lowe. 2005. Setting seagrass depth, coverage, and light targets for the Indian River Lagoon System, Florida. *Estuaries* 28: 923–935.
- Steward, J.S.; R.W. Virnstein; M.A. Lasi1; L.J. Morris; J.D. Miller; L.M. Hall; and W.A. Tweedale. 2006. The impacts of the 2004 hurricanes on hydrology, water quality, and seagrass in the central Indian River Lagoon, Florida. *Estuaries and Coasts* 29: 954–965
- Street, M.W.; A.S. Deaton; W.S. Chappell; and P.D. Mooreside. 2005. North Carolina Coastal Habitat Protection Plan, North Carolina Department of Environment and Natural Resources, Division of Marine Fisheries, Morehead City, NC. 656 pp. Online at <http://www.ncfisheries.net/habitat/chpp2k5/Complete%20CHPP.pdf>
- Thayer, G.W.; W.J. Kenworthy; and M.S. Fonseca. 1984. The ecology of eelgrass meadows of the Atlantic coast: a community profile. U.S. Fish and Wildlife Service. FWS/OBS-84/02. 147pp.
- Thompson, S.K. 2002. *Sampling*, 2nd Edition. Wiley, New York.
- Todini, E.; and M. Ferraresi. 1996. Influence of parameter estimation uncertainty in kriging. *Journal of Hydrology* 75:555-556.

- Urlick, R. J. 1983. Principles of Underwater Sound – Third Edition. McGraw-Hill Book Company, New York, 423 pp.
- Valley, R.D.; M.T. Drake; and C.S. Anderson. 2005. Evaluation of alternative interpolation techniques for the mapping of remotely-sensed submersed vegetation abundance. *Aquatic Botany* 81:13-25.
- Valley, R. D. and M.T. Drake. 2007. What does resilience of a clear-water state in lakes mean for the spatial heterogeneity of submersed macrophyte biovolume? *Aquatic Botany* 87:307-319.
- Virnstein, R.W. 1990. The large spatial and temporal biological variability of the Indian River Lagoon. *Florida Scientist* 53:249–256.
- Virnstein, R.W. 2000. Seagrass management in Indian River Lagoon, Florida: dealing with issues of scale. *Pacific Conservation Biology* 5:299–305.
- Walter, C.; A.B. McBratney; A.B. Douaoui; and B. Minasny. 2001. Spatial prediction of topsoil salinity in the Chelif Valley, Algeria, using local ordinary kriging with local variograms versus whole-area variogram. *Australian Journal of Soil Research* 39:259–272.
- Waycott, M.; C.M. Duarte; T.J.B. Carruthers; R.G. Orth; W.C. Dennison; S. Olyarnik; A. Calladine; J.W. Fourqurean; K.A. Heck Jr.; A.R. Hughes; G.A. Kendrick; W.J. Kenworthy; F.T. Short; and S.L. Williams. 2009. Accelerating loss of seagrasses across the globe threatens coastal ecosystems. *Proceedings of the National Academy of Sciences* 106:12377-12381.
- Wells, J. T. and S. Kim. 1989. Sedimentation in the Albemarle-Pamlico lagoonal system: synthesis and hypotheses. *Marine Geology* 88: 263-284.
- Williams, M.R., S.B. Filoso, B.J. Longstaff, and W.C. Dennison. 2010. Long-term trends of water quality and biotic metrics in Chesapeake Bay: 1986-2008. *Estuaries and Coasts* 33: 1279-1299.

APPENDICES

Appendix 1. Preparing video files for classification

Add the following fields to video transect shapefiles collected in the field. Make sure names and types are EXACTLY as written:

1. Field name: DMLat type: text, field properties length: 20
 this field will contain the decimal minutes values for Latitude. – see follow on section for classifying Decimal minutes

2. Field name: DMLong type: text, field properties length: 20
 this field will contain the decimal minutes values for Longitude

3. Field name: transect type: text, field properties length: 10
 This field represents the corresponding transect (as labeled in the video) that is being classified – such as ew1, ns10... to automatically fill in all fields: right click on field name, select calculate values, in box provided enter transect name surrounded by double quotes. e.g. “ew1”

4. Field name: site type: text, field properties length: 10
 the site at which this datafile was collected.
 to fill this field with all the same label: right click on the field name, go to calculate values, in the box provided write the appropriate site code in double quotes:
 newport river = “npr”

5. Field name: sav type: short integer, precision: 0
 This is the field used while classifying video the codes are as follows:
 999 = unclassified
 0 = no SAV
 1 = SAV (any the default value for this field is 0,
 2 = uninterpretable (i.e. sandstorm on video, cannot see bottom...).

When this field is created, its default is to fill all in with 0's. You need to overwrite that with a dummy code that cannot be confused w/a “no SAV” code. Right click sav column header, go to calculate values, in the bottom box write in 999, hit ok, all values in this field are now reassigned as 999.

To begin classifying video:

Cue up the video for the start point of the appropriate transect. Once the camera goes in the water and the bottom is visible, pause the video. Find the corresponding time code (minutes only – hours may differ from datafile due to UTC offset ~5hrs?) in the datafile, ensure that the GPS

position (DMLat and DMLong) are nearly identical to those displayed on the video screen. Often there is a second delay or more in stamping the video, identify what this time delay is and periodically throughout the datafile ensure you are classifying the correct position (the time is simply a guide – it is actually the place on the bottom you want to ensure you're classifying).

Classify every third second of video, using the codes provided: 0, 1, or 2

SAV is classified as present if any plant material is viewed on the screen. if it is obviously a free drifting leaf, classify as absent but otherwise – assume a leaf observed on the screen is attached to adjacent bottom – so classify as SAV present (code = 1).

Appendix 2. Converting decimal degree to degree decimal minutes

The Horita unit used to stamp GPS location and time to the collected video records position in degree minutes and seconds (DMS). To ensure that the time stamp on the video and time stamp on the shapefile are indeed an exact match, we need to also compare positions. By adding a latitude and longitude field to the shapefile that displays position as DMS position can also be compared between the two files.

To convert DD to DMS follow the steps below:

1. Add the table to ArcMap.
2. Right-click on the Table in the Table of Contents and select Open.
3. Verify 'Edit' mode is not enabled. Click the Options button and select Add Field. *this step and the following may already be done if the procedure from Appendix 4 was already completed. If so, skip to step 5.
4. Enter DMLat in the Name field and select Text from the Type drop-down list.
5. Change the length to 20.
6. Right-click on the DMLat field and select Calculate Values.
7. Click Yes, if presented with a message box.
8. Check the Advanced check box.
9. Paste the following code into the expression box:

```
Dim DDField
```

```
Dim zM1 As Double
```

```
Dim Suffix As String
```

```
Dim DMS As String
```

```
Dim zY As Double
```

```
Dim zD As Double, zM As Double, zS As Double
```

```
Dim Dchr As String, Mchr As String, Schr As String
```

```
Dim Degree As String, Minute As String, Second As String
```

```
'=====
```

```
'Adjust the variables below
```

DDField = [Latitude] 'Change to field with decimal degree values

Dchr = Chr(1) 'Character after degrees

Mchr = Chr(39) 'Character after minutes

Schr = Chr(34) 'Character after seconds

'=====

zY = DDField

If zY >= 0 Then

 Suffix = "N" 'N if Latitude, E if Longitude

Else

 Suffix = "S" 'S if Latitude, W if Longitude

End If

zY = Abs(zY)

zD = Int(zY)

Degree = CStr(zD)

zM = FormatNumber(((zY - zD) * 60),4)

zM1 = Int(zM)

Minute = CStr(zM)

'zS = FormatNumber(((zM - zM1) * 60), 2)

zS1 = Int(zS)

Second = CStr(zS)

DMS = Degree & Dchr & Minute & Mchr & Suffix

10. Change the value within the brackets next to 'DDField =' to the field in the table that contains the latitude decimal degree values. To change the characters after degrees minutes and seconds edit the value after 'Dchr =', 'Mchr =', and 'Schr =' respectively.
11. Paste the following code into the 'DMLat =' box at the bottom of the dialog box.

12. Click OK to run the Field Calculator.
13. Repeat steps 3 through 12 for the longitude values, but change the values within the code where Suffix = "N" to Suffix = "E" and where Suffix = "S" to Suffix = "W". Also, change the value next to 'DDField =' to the field in the table that contains the longitude decimal degree values.

Appendix 3. EcoSAV2 Algorithm

1. Depth increments are the lowest resolution depth units that are used by the EcoSAV2 software. This is similar conceptually to an “acoustic pixel.” The depth increment is based on the amount of time between readings taken by the echosounder and based on the speed of sound in the salinity and temperature conditions at a site (these data are obtained from a hand-held YSI water quality meter and entered by the operator in Visual Acquisition before data collection). Typically, this depth increment is 1.65 cm – 1.83 cm for speed of sound ranging between 1400 m/s to 1520 m/s.
2. The bottom echo and bottom depth is determined by finding the greatest rise in voltage squared (V^2) in the echo envelope.
3. Next, the trailing edge of the bottom echo (where V^2 falls away from the bottom peak back to the noise threshold) is examined to see if the difference in depth between the sharpest rise and trailing edge exceeds six depth increments (bottom depth threshold; six is the EcoSAV2 default). If not, the sharpest rise in V^2 is considered the bottom depth. If the trailing edge is more than six depth increments, then the sharpest rise in V^2 is considered the SAV canopy height and the bottom depth is placed at the trailing edge (six depth increments or more below the sharpest rise). This distance from sharpest rise to trailing is the “bottom thickness.”
4. The plant height detection threshold established by the user is added to the bottom echo depth (default setting for this parameter T4 is four depth increments or 6.4 cm to 7.32 cm depending on the sound speed). We altered this setting to two depth increments (3.2 to 3.7 cm) for all analyses reported here. EcoSAV2 will only detect a plant if the height of the plant above the bottom exceeds this threshold.
5. If the ping being analyzed is taken from a depth below the user-defined “Max Plant Depth,” that ping will not be used in computations; it is declared “Too Deep” in the output file. The EcoSAV2 default is for max plant depth is 6 m depth.
6. The ping must not be in the near field (acoustically, this is 0.0 – 0.4 m from the face of the transducer). These near field pings may be declared “out-of-water” or “noisy pings” and are excluded from computations. They are recorded in the output file in a separate data field.
7. A noise threshold (in V^2) must also be exceeded within the depth above the plant height detection threshold to the near field to have a SAV positive ping (-65 dB is the default noise threshold; this threshold has been established based on empirical tests done on a range of aquatic

plant species and scenarios (see BioSonics EcoSAV2 manual, Hoffman *et al.*, 2002; Sabol *et al.*, 2002).

8. The ping satisfying the criteria above (not too deep, not out of water, not too noisy, below the near field depth and above the bottom echo) is declared either “Plant” or “Bare.” The bare pings are characterized by the ultra-quiet zone (V^2 is very low, default is < -130 dB, within four depth increments of the bottom echo), which shows up as a white region just above the bottom on the echogram (Figure 12). Pings may also be declared “bare” if the plant height detection threshold is not exceeded (four depth increments), or if the bottom is not thick (bottom thickness is less than 12 depth increments).

9. “Plant” pings are those passing through the above filters: (not too deep, not out of water, not too noisy, below the near field depth and above the bottom echo, and not classified as “bare”). Thus, to be an SAV ping, the echo from the putative plants must be “tall” or exceed a height of four depth increments (default value is 6-7 cm). In addition, the ping must have a thick bottom. Very short SAV plants (less than this plant detection threshold) can cause a *false negative*, that is, the ping will be declared “bare” when, in fact, video camera evidence suggested that short SAV was present. We sometimes re-analyzed the SONAR data with EcoSAV2 plant height detection threshold parameters set to one depth increment (1.6-1.8 cm), two depth increments (3.2 – 3.6), or three depth increments (4.8 – 5.4). Setting this parameter to lower than the default plant detection threshold was an attempt to detect very short plants at some sites. Also, a ping can be declared “plant” if the distance from the top of the noise threshold (step 6 above) to the declared bottom depth (step 3 above) is greater than the plant height threshold (4 depth increments) and the bottom echo is thick (greater than 12 depth increments, the default setting) or the plant feature is “thick” (plant is greater than four depth increments). Muddy sediments can sometimes cause a positive SAV classification by having a thick bottom. We sometimes re-analyzed the data using an increased the bottom thickness parameter T2, setting it to between 13 to 15 depth increments, but only at sites in the Rapid Assessment study (14 depth increments at TR, 15 at BY, 13 at NR, 13 at RC, and 13 at PR site) when muddy bottoms occurred (based on video camera evidence) to prevent *false positives* (muddy bottoms with no SAV being declared “plant”).

Appendix 4. Specifications for remote image acquisition for SAV classification in NC

Imagery Collection Parameters

When obtaining any type of remotely sensed imagery for the purpose of mapping submerged habitats, it is recommended that all attempts are made to meet the environmental parameters outlined in Ferguson et al. (1993), Dobson et al. (1995), or Finkbeiner et al. (2001):

1) turbidity – should be as low as possible. Rain events and potential runoff should be monitored within the acquisition window.

2) tide stage – should be within 2 hours of the lowest tide as predicted by the NOAA National Ocean Service tide table.

3) wind and surface waves – 0 to 5 mph is best, 5 to 10 mph is usually acceptable if whitecaps are not prevalent.

4) sun angle – between 20 and 35 degrees; and

5) clouds and haze – obviously no clouds or haze is best, maximum amount of cloud cover recommended is 5 percent (but even small amounts of clouds and their associated shadows can obscure habitat).

6) season – with habitats such as seagrass, acquisition of imagery must be coordinated with times of maximum biomass.

Appendix 5. Selecting systematic random transects with GIS

1. Decide what direction transects will be run. Remember, transects will bisect the pattern of grass – which generally means transects will be perpendicular to shore.
2. Measure width of sample area, this is distance of box where your transects will start (or end) – for example 304 m.
3. Divide this width by the number of transects you want to run – for ex. 36
4. This value is the width of the sections, where a transect will fall. So here, transects will be 8.4m apart.
5. Pick a random number between 0 and 8.4, this is the 'random start' distance (for example 5.9, which means the first transect start point is placed 5.9m into the first 8.4m section....then every point after this is 8.4m apart (or placed 5.9 m into each random section)).
6. Create a graphic line running across the start area of your sample area that has a length of the width of the sample area minus the 'random start' distance (ex. $304\text{m} - 5.9\text{m} = 298.1\text{m}$). Create the graphic line by drawing a line using the draw tool in ArcMap, Then place the graphic line with the end of the line at the end of the start area of your box. Make a second graphic line in this file that runs across the opposite end of the box.
7. Select both graphic lines and covert them to polylines by using XTools Pro – Feature conversions – Convert graphics to feature. (By default the output will be projected in the same projection as the map document, so make sure the map document's projection is NAD 1983 UTM zone 18).For NC UTM zone is 18N. After creating the polylines, delete the graphic lines.
8. Convert both polylines to a series of points the distance you calculated that transects will be spread apart (here 8.4 m apart -- do this using XTools Pro – Feature conversions – convert features to points - specify the width of the random sections (ex.8.4m) under 'Equidistant points').
9. Double check that points at "start" and "end" of transects overlay properly on the random start and that all tran points are indeed the appropriate distance apart (here 8.4m) by using the measuring tool in ArcMap. Additionally, in the Attribute Table check to make sure there are the proper number of waypoints (In this example it would be 72).
10. Create a few new fields that will help label points:
 - a. TranNumb – short integer – precision 0
 - b. 0 – text – 10 digits
 - c. Side – text – 10 digits
 - d. Wpname – text – 10 digits
11. Start editing – file in 11 above – need to populate the 3 extra fields created
 - a. TranNumb – this is the transect number – so if you are making 36 transects, the file should have FID from 0-71. Highlight first 36 rows and rt. Click "tran numb" select Field Calculator – in box at bottom type $[FID]+1$ and select OK. This

should fill the tran numb field with 1-36. Highlight the second 36 rows and go into Field Calculator again and type [FID] – 35 and select OK. This will fill the second 36 rows in the TranNumb field with 1-36 as well.

- b. 0 – This field is used to add a “0” before transects 1 through 9 making them two digits instead of one, so for example transect 1 will become 01. Doing this allows transects 1 through 9 to follow chronologically on the GPS unit with the other 36 transects. In the Attribute Table select the first 9 rows for each side of the transects, go into Field Calculator – in the box type “0” and select OK. The first 9 rows of each side of the transects will now be two digits.
 - c. Side – select first 36 – determine if the is the start or end side of transect – go under field calculator again and equation here should read side = "end" or "start". I have been designating the start side is further from shore w/the end side nearest shore. But this is not critical to standardize.
 - d. Wptname – this is the waypoint name you would download in the GPS – in field calculator this one reads wptName = [0] &[TranNumb]&[side] – the result should be a combination of the above fields so a wpt name for start side of transect one is: 01start
 - e. Follow same methods for opposite side of transects. But equation for TranNumb is FID-36 (or whatever makes sense to make it start at 1).
 - f. Make sure 01start is directly across from 01end. You can easily check this by activating the wptname field as a label.
12. Add x, y coordinates to this file – using XTools Pro - Table operations – add X,Y,Z coordinates . add X and Y coords, specify output projection to be NAD83. This will make it easier to download to GPS. Alternatively, you can use a program called ExpertGPS to transfer the ArcMap waypoint shapefile to a handheld Garmin GPS units. Expert GPS uses the projection of the shapefile not the coordinates defined in the Attribute table to project the waypoints in the GPS.
 13. Make a polyline shapefile w/UTM coordinate system – add to project and connect the transect start & end points. This file will have 36 transects (or whatever you made), and can be used for guiding boat drivers or visualizing the site.
 14. In this line file, make a field tranNumb and using field calculator fill it in so each tran is numbered 1-36 and make sure transect 1 connects points 01start & 01end, and so on...

Appendix 6. Selecting random quadrat locations

1. Determine the separation distance between points – if you want five points and your transects are 300 m long, then $300/5 = 60$ m between points.
2. Using a random number generator – select random numbers between 0 and 60 (or your calculation in step one). You will need as many random numbers as you have transects – here we'd need 36. Make sure each number is generated from a pool of 0-60 – or selected with replacement.
3. Select all transects (from shapefile in 15 above), using Xtools Pro, extract points from lines, extract to a new file and separate points a regular interval = 60m (or distance defined in step 1). Instead of overwriting ID field, give it a new name e.g. ID2. This point file will eventually become the file that has all the random quadrat samples, so name it something accordingly.
4. Now select transect 1 from the line file. Go to Xtools Pro – extract points from line – and extract a point every 1 meter. You will use this point file to help guide you in proper placement of the quadrat points. Turn on the labels & set label field to be the FID # (or a continuous # from 0-300, where 0 is at the start of your transects)
5. Clear all selections
6. Select all points from 1m points (step 4), make sure they are overlaid on target transect (say transect 1), where point 0 is on tran1start. If they need to be moved use Editor to adjust placement.
7. Clear all selections.
8. Activate editor for file created in step 3, select the points associated with target transect (say tran1). Move the point closest to start to the random distance selected (e.g. 4) as identified by the 1m point file. Each of the remaining 4 points should be shifted along with this one and will be separated by the distance calculated in step 1 (e.g. 64 m, 128 m, 192....)
9. Clear all selections & save edits
10. Begin at step 6 and continue working this way through all transects. Remember to select all the points you want to move. Clearing selection between each step ensures that you don't shift points you didn't intend to move.
11. When you're through working down each transect. Stop editing, save edits, and add x, y coordinates to this file – using Xtools Pro - Table operations – add X,Y,Z coordinates. add X and Y cords, specify output projection to be NAD83. This will make it easier to download to GPS.

Appendix 7. Creating a Cokriging Surface Map from SONAR Reports

Creating a Cokriging Surface of the SAV Bed

1. Once the SONAR reports are imported into ArcGIS 9.3, open the attribute table and add a column called SAV.
2. In the editor toolbox, convert all of the SONAR Cover (%) data into binary data (presence/absence) by adding 1s and 0s to the SAV column. If the SONAR Cover column has SAV, the SAV column will have a 1, if not, it will have a 0.
3. Save and stop edits to the SONAR report data file.
4. In Geostatistical Analyst, open Geostatistical Wizard.
5. From the left-handed column, select cokriging.
6. For data set 1, select the SONAR report data file with “SAV” as the attribute.
7. For data set 2, select the SONAR report data file with “bottom” (i.e. depth) as the attribute.
8. When there are points in the data file with the same spatial relationship, use the maximum SAV value to create the cokriging model.
9. Do not change any of the parameters on step 1 of 4. The default model is a predicted surface without transformation.
10. On step 2 of 4, the default settings are as follows:
 - 1: Spherical model
 - 2: Lag size = 12 m
 - 3: Anisotropy is off
 - 4: Partial sill, major range, lag size, and nugget size are determined by the model and it is not advisable to adjust these individually.
11. On step 3 of 4, the default settings are as follows:
 - 1: Nearest neighbors = 5
 - 2: Neighbors to include in the model is set as at least 2
 - 3: The sector type has four choices. The default parameters are one of two, either or . Select the one that most-closely represents the transect direction.
 - 4: The ellipse model is the default model for this method. Leave this selected.
12. On step 4 of 4, the success of the model is represented. Here, the predicted errors are reported. This consists of the following parameters: mean, root-mean-square, average standard error, mean standardized, and root-mean-square standardized. An ideal kriging model has the following parameter values:

- 1: Mean = 0
- 2: Root-mean-square = 0
- 3: Average standard error = 0
- 4: Mean standardized = 0
- 5: Root-mean-square standardized = 1

13. To identify the best cokriging model, a process of switching between steps 2 and 4 is required.

- A. First, use the default model parameters and record the predicted error values on step 4 for future comparisons.
- B. Next, select an exponential model (step 2) from the model menu. Leave all other parameters as default and note the predicted error values.
- D. Compare models A and B, based on their predicted error values. Choose the one model that most-closely represents an ideal cokriging model (#12). For the data collected in this paper, the best-fit model was most-often an exponential model.
 Other model-types were initially explored but spherical and exponential models were found to produce the best cokriging surface.
- E. Next, turn-on anisotropy (step 2) with the model chosen in step D and record the predicted error values for the model.
- F. Compare the models from steps D and E and choose the one that most-represents the ideal parameters (#12). For the data collected in this paper, this was typically a model with anisotropy.
- G. Next, explore the effect of lag size of the model. Choose the lag size that produces the best model. For the data in this paper, models were explored that contained lag size values between 7 and 30 m.
- H. Last, explore how the number of nearest neighbors influences the model. Choose the number of neighbors that produces the best model. For the data in this paper, nearest neighbors between 2 and 30 were explored.

14. Once the best-possible cokriging surface is determined, produce the surface map.

15. Explore the standard error of the cokriging surface.

- A. Right-click on the prediction map produced in step 14. Select the option to "create prediction standard error map."
- B. This will create a new cokriging surface but this time of the standard errors associated with the co-kriging surface. This will allow you to determine the level of confidence in the cokriging surface.
- C. The standard error is calculated using the following equation:

$$Z(\mathbf{s}) = \mu(\mathbf{s}) + \varepsilon(\mathbf{s}) + \delta(\mathbf{s}),$$
 where $\delta(\mathbf{s})$ is measurement error and $\mu(\mathbf{s})$ and $\varepsilon(\mathbf{s})$ are the mean and random variation. For more information on measurement error, see the section on "Understanding measurement error" in the ArcGIS 9.3 desktop help manual.

16. Convert this surface into a filled contours map by right clicking on the cokriging surface, selecting data, and exporting it to a vector. Before the conversion is final, the program asks if a

“filled contour” or “contour” surface is desired. Select the filled contour option from the drop-down menu.

17. The produced surface will extend past the study site box. Since we are only interested in the region within the study site (i.e. the area that SONAR reports were collected), clip the filled contour surface to the study site box, using the “clip” tool in the analysis toolbox.

18. The produced cokriging surface will now show areas where SAV is present and absent within the specified study region but it will contain values between 0 and 1 at intervals of 0.1. Create a new column in the attribute table called SAV.

19. Repeat steps 2 and 3 with the cokriging surface.

20. Next, dissolve the layers by the “SAV” parameter in the cokriging surface using the “dissolve” tool in the data management toolbox. This will produce a cokriging surface that contains only 2 categories: 1-SAV Present and 2-SAV Absent.

21. From this point, area and other parameters can be calculated to assess how the bed changes over time.

Creating a Kriging Surface of Depth

1. In Geostatistical Analyst, open Geostatistical Wizard.

2. From the left-handed column, select kriging.

3. For the data set, select the SONAR report data file with “bottom” (i.e. depth) as the attribute.

4. When there are points in the data file with the same spatial relationship, use the mean depth value to create the kriging model

5. Follow steps 9 - 16 above.

A. Except this time try using spherical (default), circular, and exponential models. Other model-types were explored but these three model types produced the most ideal surfaces.

6. The produced kriging surface will now show the depth profile within the specified study region.

Appendix 8. Depth Kriging and SAV Cokriging Models from the SONAR Acoustic Reports

Newport River

At NPR, SAV was dominant in the SW corner of the study site (Figure 48) during both Jun. (2009) and May (2010). Quadrat surveys confirmed the existence of the bed in this region in May (2010). This area was consistently dominated by shallow waters (≤ 1.5 m deep, Figure 49). By Jun. 2010, the structure of the bed had changed. The cokriging surface suggests that there is a thin area of SAV on the southern portion of the study site and a larger region toward the north (Figure 48). While the quadrat data suggests that there is some SAV throughout the site, it is generally in low abundance ($< 10\%$), with the majority in the SW corner of the study site. One of the limitations of the SONAR system is depth. During the Jun. 2010 sampling event, over 90% of the site was in a water depth < 1.0 m. Thus, the depth may have limited the detections of SAV. Also, detections by the SONAR are not as successful when the plants were relatively sparse and spread out. The quadrats do indicate that this is the case in the SW region of the study site. By Aug. and Sep. (2010), both the quadrats and the SONAR indicate that the bed is basically gone, except for some small patches of SAV.

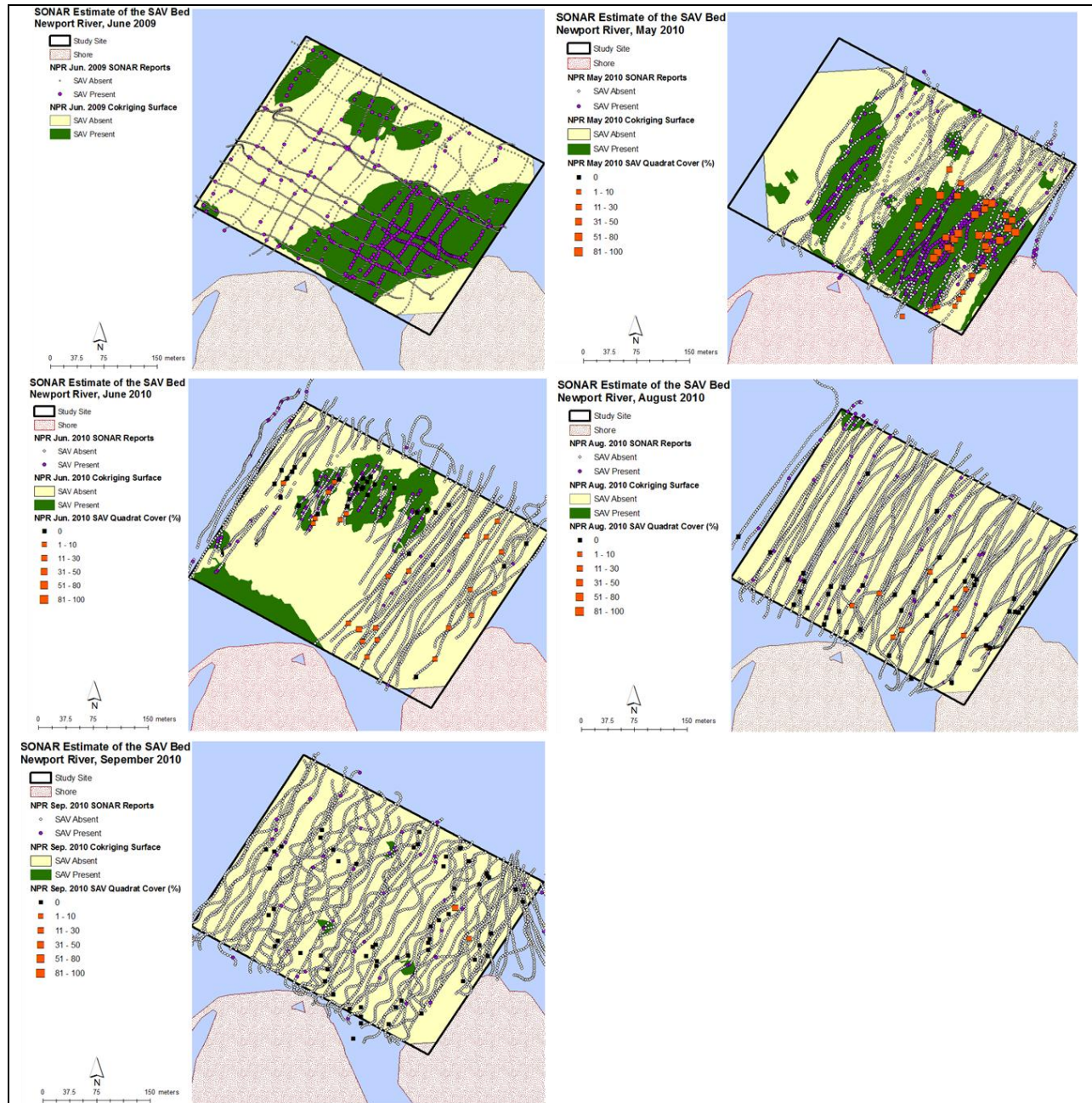


Figure 48. The data collected at the NPR SAV bed (Jun. 2009 and May - Sep. 2010). The SONAR transects are represented by circles with both SAV-positive (purple) and SAV-negative (white) acoustic reports. The cokriging surface results show the interpolation of the acoustic report data as SAV-positive (green) polygons and SAV-negative (cream) polygons. Diver survey quadrat locations are indicated in squares. Quadrats without SAV are black, quadrats with SAV have proportionally increasing orange squares.

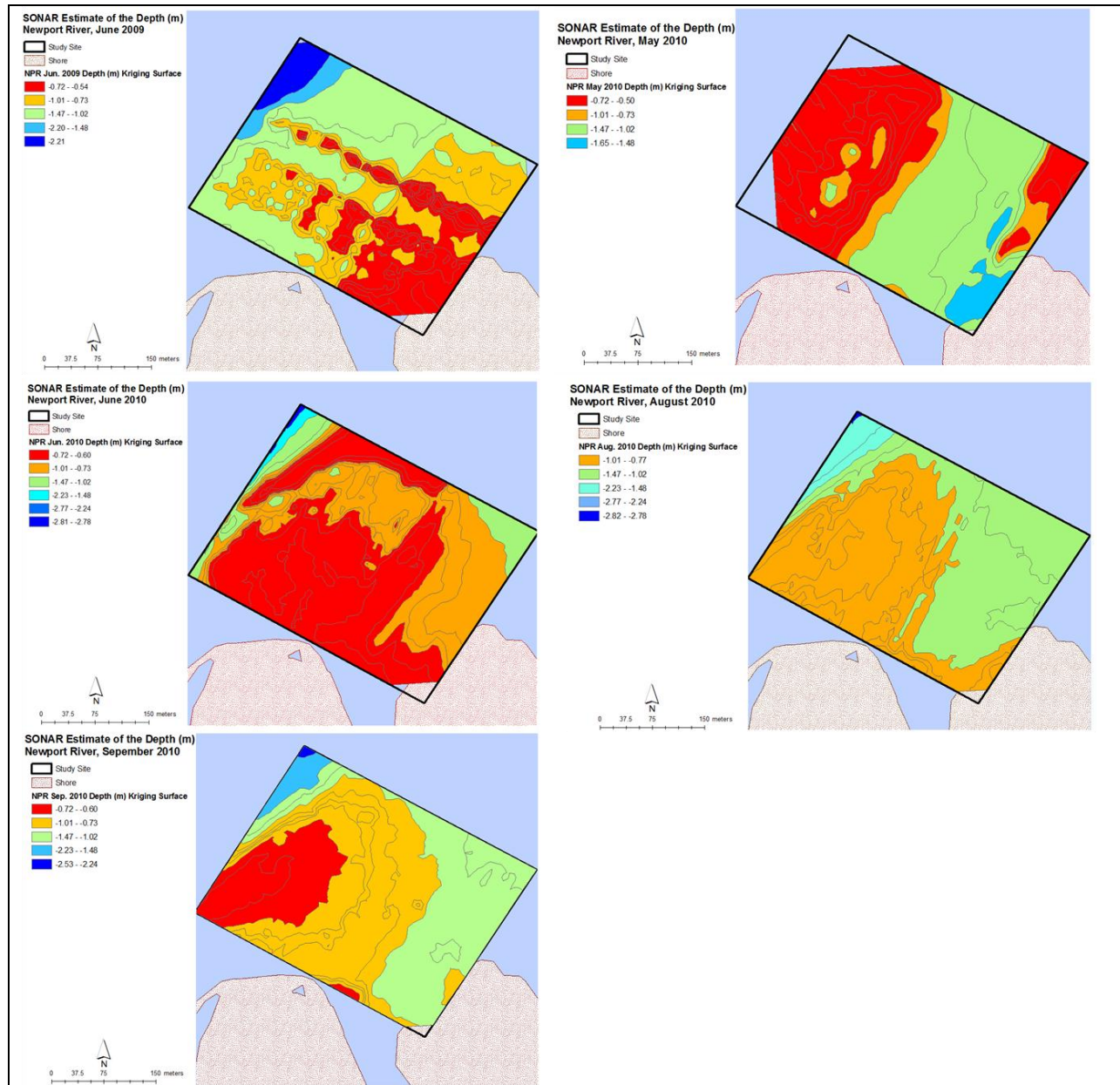


Figure 49. The depth data collected using SONAR acoustic reports at the NPR SAV bed (Jun. 2009 and May - Sep. 2010). A depth polygon is represented as a gradation of color from shallow (red) to deep (blue). The data collection in May 2010 was interrupted during the survey, thus making the bathymetry inaccurate for that month. On that day, a 2-m tidal range occurred, and the eastern side data was collected at high tide and the western side collected at low tide.

Jarrett Bay

In Jun. (2010), JBS was a fairly dense bed, extending most of the distance of our 300 m x 300 m study site (Figure 50). Quadrat surveys confirmed this observation, showing that the SAV was more dense in the shallow regions of the site (<0.8 m), when compared to the deeper locations of the study site (Figure 51). As the summer progressed, the bed in the deeper regions of the site slowly died-off, leading to a fairly dense bed close to shore (Figure 50). By Sep. (2010), the SONAR indicates a nearly unvegetated habitat, however the quadrat data suggests that there are some locations with still contain SAV. This last data set is strongly impacted by the depth at the site. Over 90% of the region in Sep. (2010) was at depths < 0.8 m.

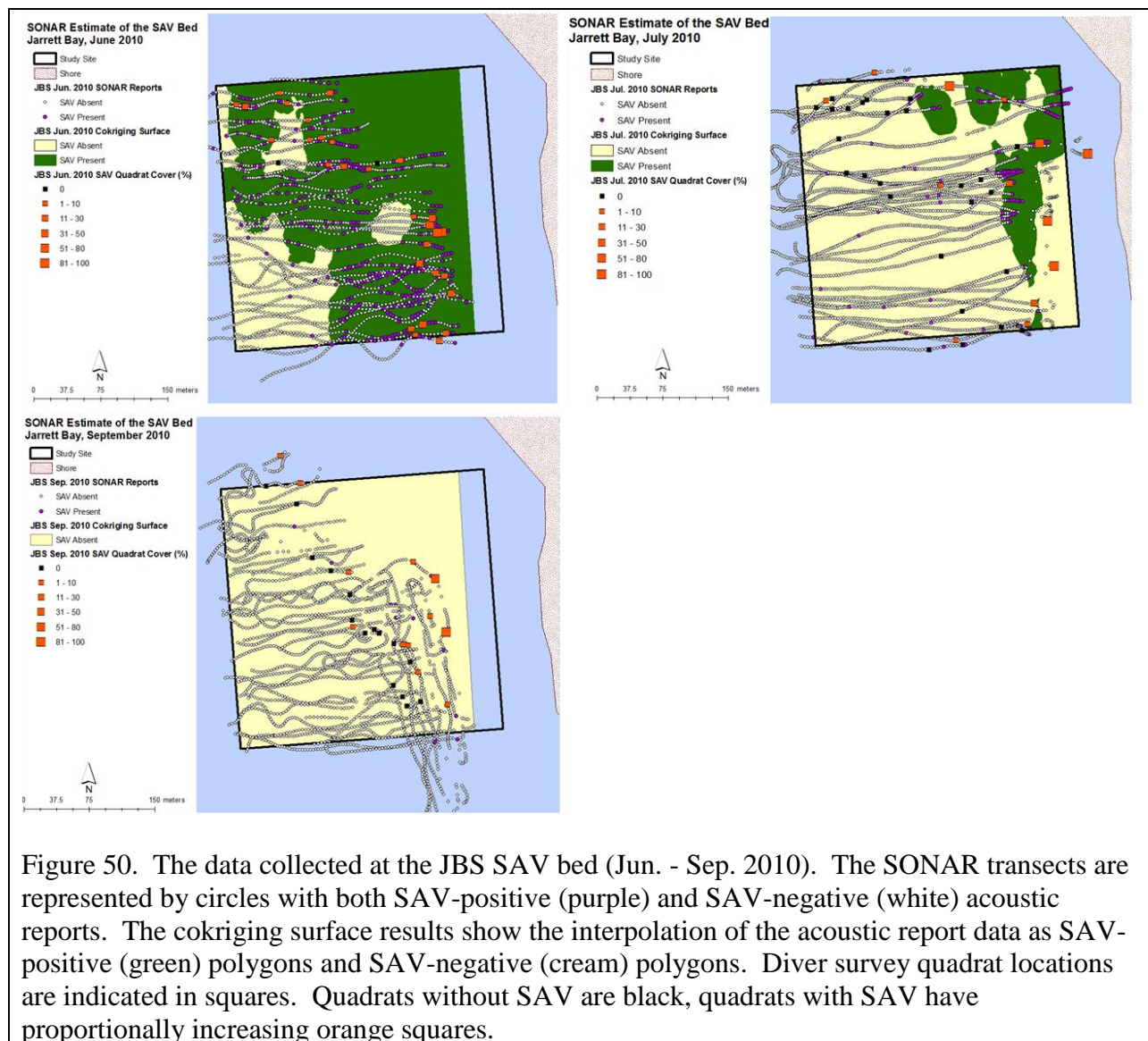


Figure 50. The data collected at the JBS SAV bed (Jun. - Sep. 2010). The SONAR transects are represented by circles with both SAV-positive (purple) and SAV-negative (white) acoustic reports. The cokriging surface results show the interpolation of the acoustic report data as SAV-positive (green) polygons and SAV-negative (cream) polygons. Diver survey quadrat locations are indicated in squares. Quadrats without SAV are black, quadrats with SAV have proportionally increasing orange squares.

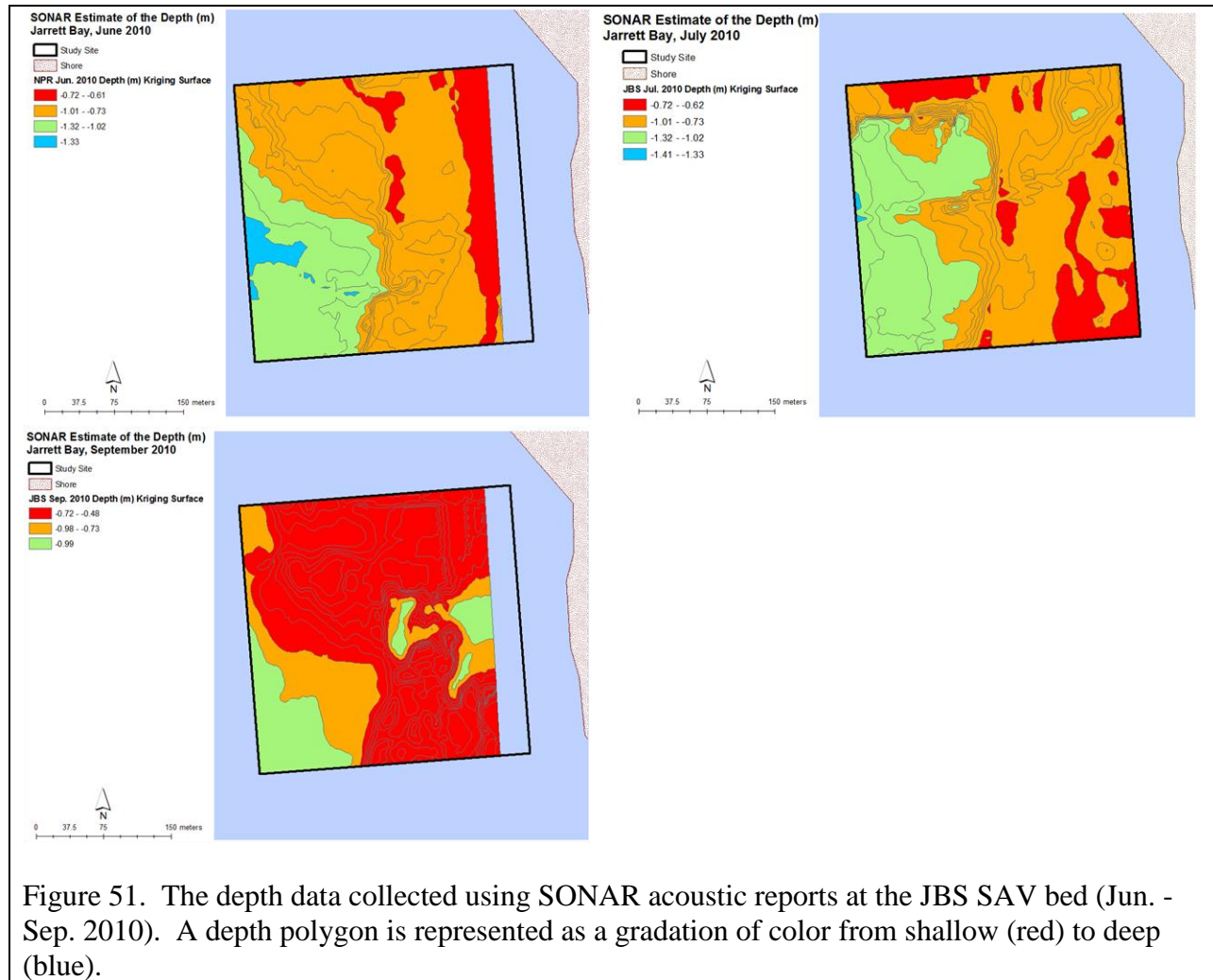


Figure 51. The depth data collected using SONAR acoustic reports at the JBS SAV bed (Jun. - Sep. 2010). A depth polygon is represented as a gradation of color from shallow (red) to deep (blue).

Blounts Bay

The low-salinity sites show a different transition when compared to the high-salinity sites. In May 2010, the cokriging model suggests that the site is nearly devoid of vegetation (Figure 52). The quadrats however, clearly show a fairly continuous bed up to 150 m offshore. One problem with this site is that the water is very shallow (< 0.8 m) in the location of the SAV bed (Figure 53). The shoal region is a concern during all months of the surveys. In June 2010, the cokriging map indicates a slightly larger bed, but because of GPS difficulties, the entire site was not surveyed with SONAR. The bed peaked in Aug. 2010 with an extensive SAV region in both the deep and shallow portions of the study site. However, we believe that the SAV bed delineated in the deep edge of the site may not be SAV, but instead is very soft-sediments, which are known to create false positives in the ECOSAV2 algorithm. If a site is known to contain these types of sediments, the algorithm can be tweaked to take this problem into account. By Sep. (2010), the SAV bed had declined a bit, with a dense region close to shore.

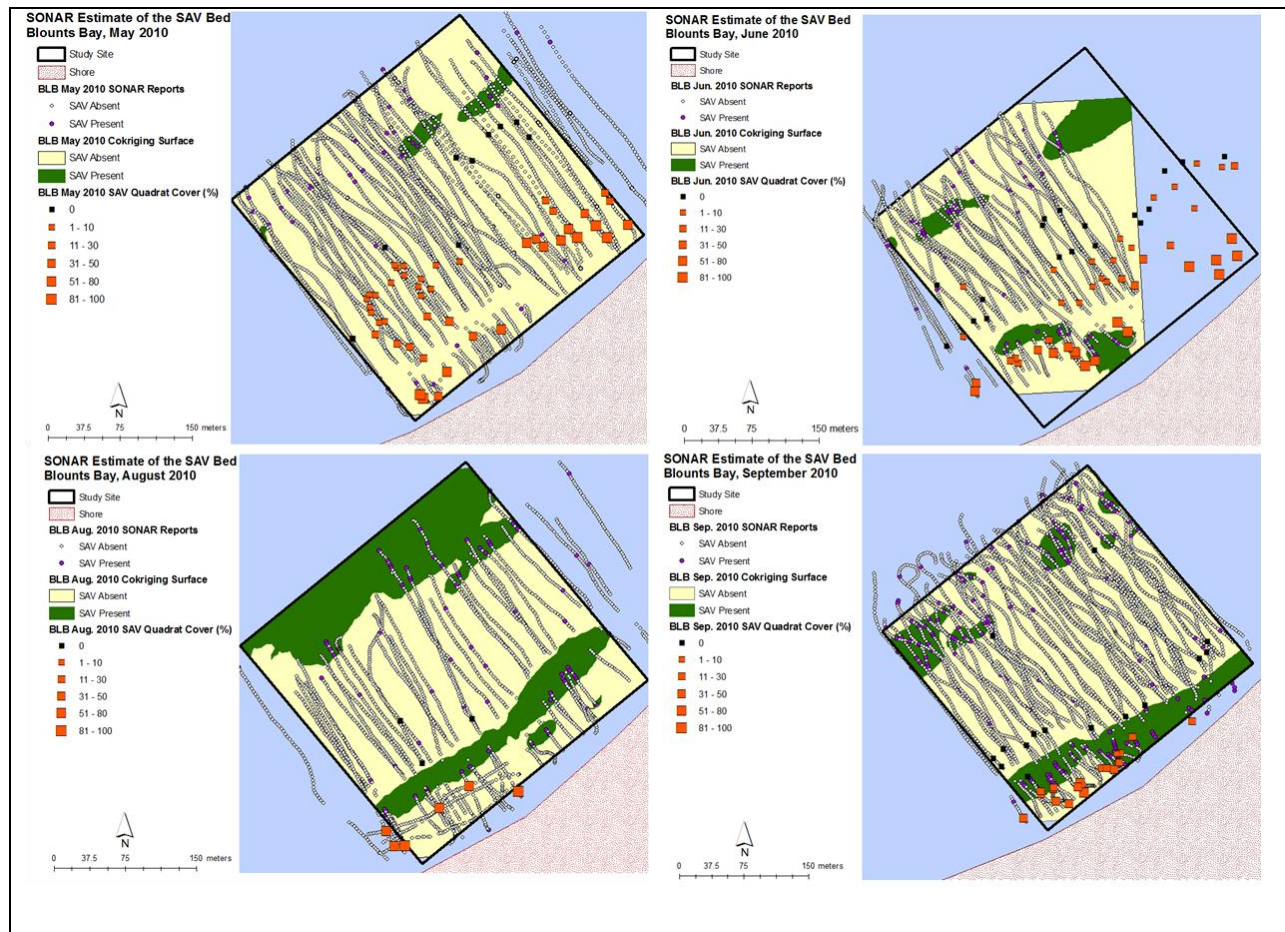
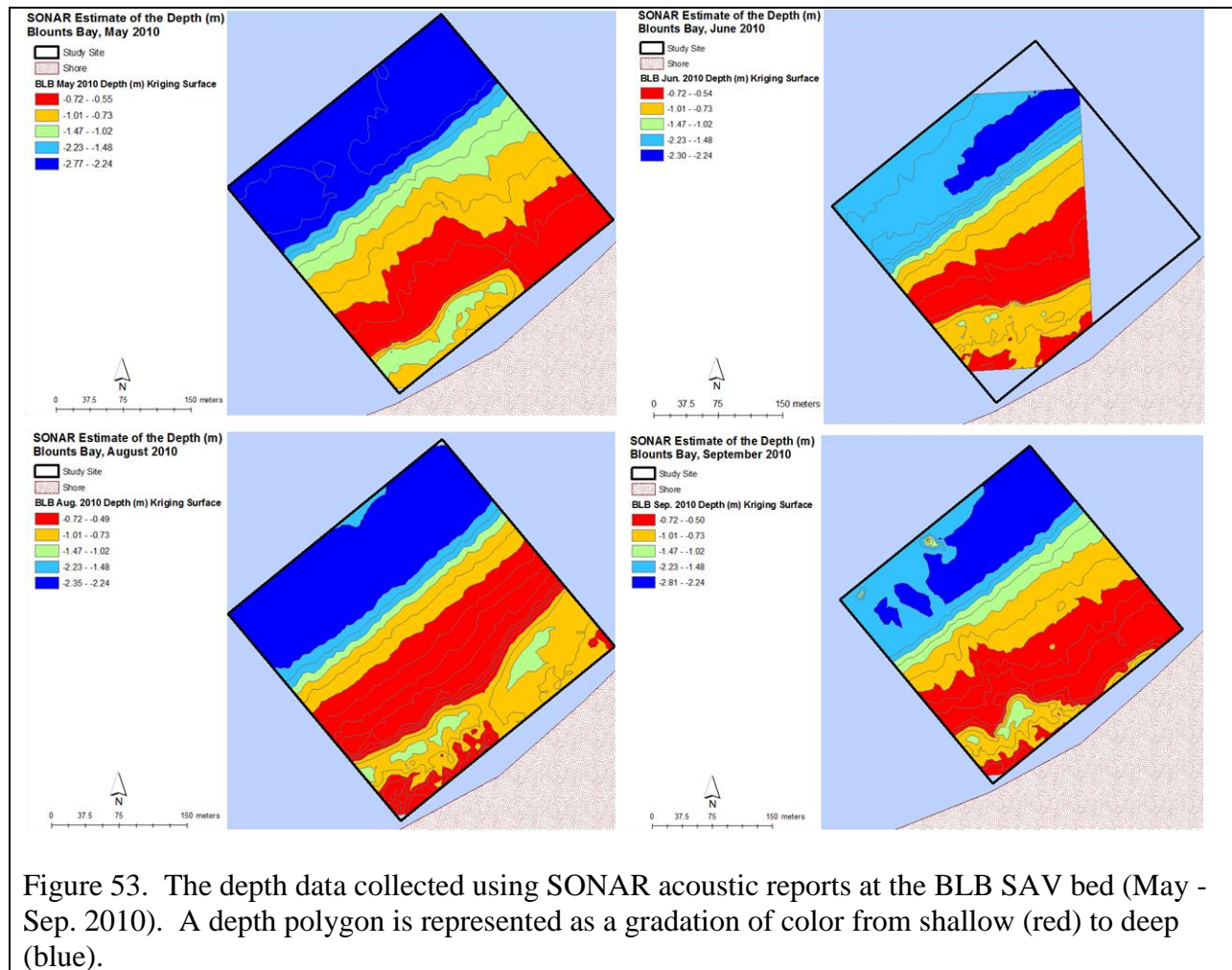


Figure 52. The data collected at the BLB SAV bed (May - Sep. 2010). The SONAR transects are represented by circles with both SAV-positive (purple) and SAV-negative (white) acoustic reports. The cokriging surface results show the interpolation of the acoustic report data as SAV-positive (green) polygons and SAV-negative (cream) polygons. Diver survey quadrat locations are indicated in squares. Quadrats without SAV are black, quadrats with SAV have proportionally increasing orange squares.



Sandy Point

Out of all of the sites surveyed in this project, SPS was the most dense, extensive bed. In Jun. 2010, the cokriging surface indicates that the entire 90,000 m² is covered by SAV (Figure 54). Quadrat sampling completed on the same day shows the same results as the SONAR. While, both methods do show that there are areas where SAV is lacking, the majority of the region is covered by SAV. In this case, it is clear that the binary cokriging model over-estimates the bed. Because SAV was still found at the edge of the site, the site was extended in Aug. and Sep. (2010). These results show that SAV is still present and continuous out to depths of 3.5 m or greater (Figure 55). It is also important to realize that of the four sites, this is also the only site where the bed did not significantly change throughout the summer months.

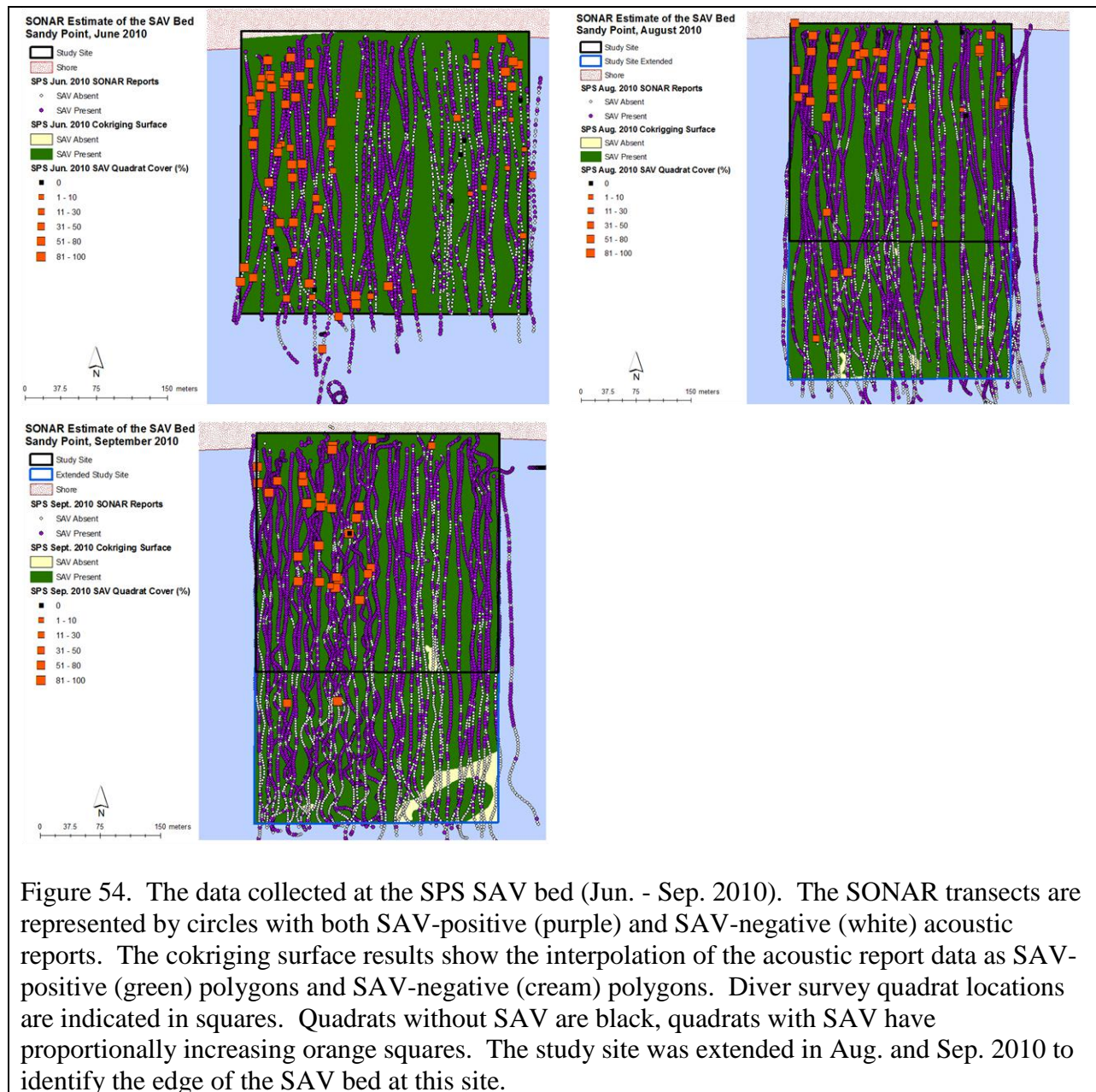


Figure 54. The data collected at the SPS SAV bed (Jun. - Sep. 2010). The SONAR transects are represented by circles with both SAV-positive (purple) and SAV-negative (white) acoustic reports. The cokrigging surface results show the interpolation of the acoustic report data as SAV-positive (green) polygons and SAV-negative (cream) polygons. Diver survey quadrat locations are indicated in squares. Quadrats without SAV are black, quadrats with SAV have proportionally increasing orange squares. The study site was extended in Aug. and Sep. 2010 to identify the edge of the SAV bed at this site.

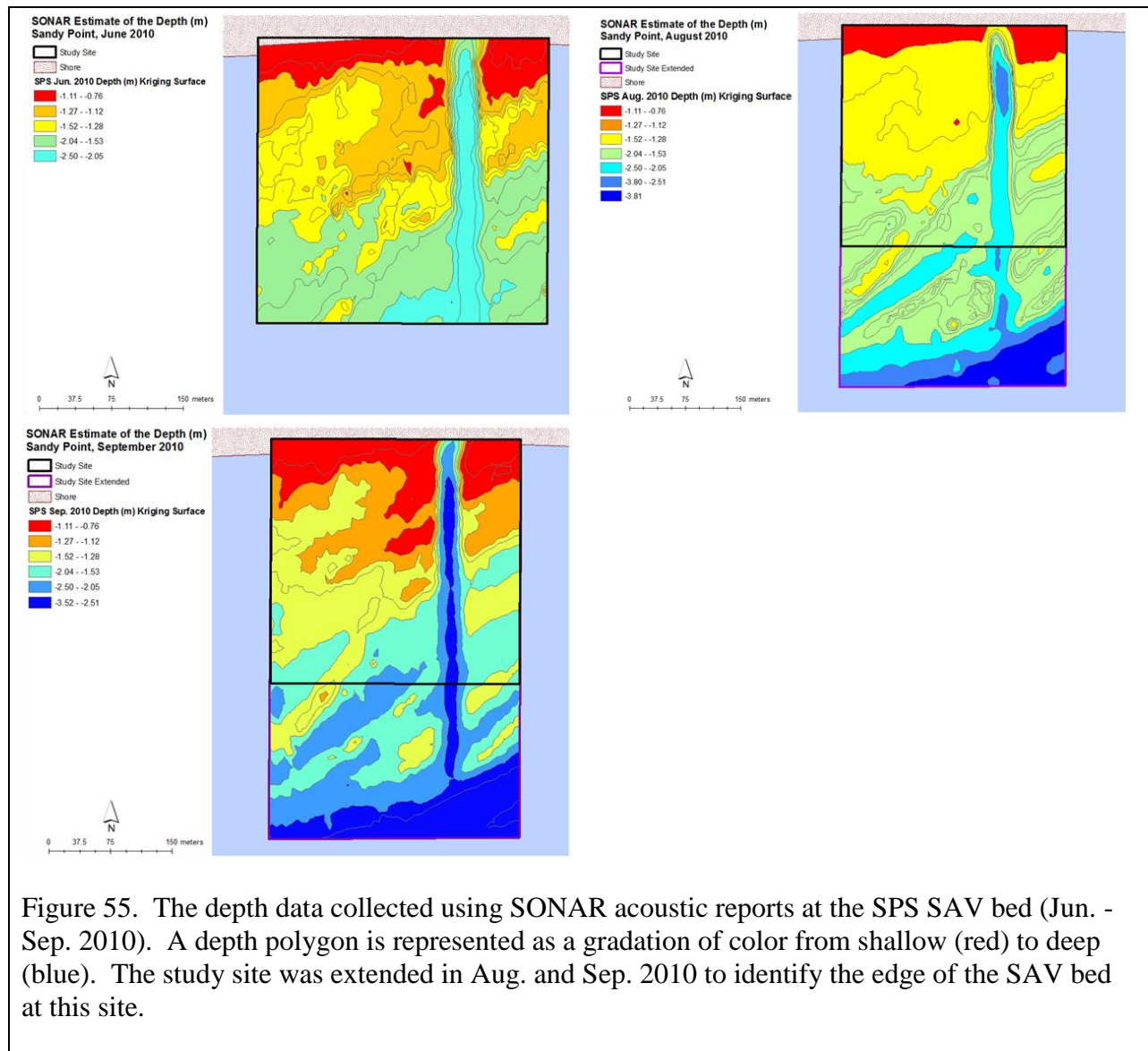


Figure 55. The depth data collected using SONAR acoustic reports at the SPS SAV bed (Jun. - Sep. 2010). A depth polygon is represented as a gradation of color from shallow (red) to deep (blue). The study site was extended in Aug. and Sep. 2010 to identify the edge of the SAV bed at this site.

Cokriging offers us the opportunity to visualize drastic changes in the SAV bed but there are limitations to the method. It is strongly influenced by the parameters placed upon it in the model. These parameters can change with each data set because the goal of kriging is to obtain the best-possible model of the site. Thus, slight changes in the model like anisotropy, number of lags, and number of nearest neighbors can produce drastically different cokriging surfaces (Table 19, Table 20). In this report, we focused on producing a model with the mean, mean standardized, average standard error, and root-mean-square near 0 and the root-mean-square standardized near 1 (Table 21, Table 22). However, if another parameter is desired (i.e. keeping the model the same at each site, regardless of the mean and error values), the user can choose to create models based on that methodology.

Table 19. The parameters used in the SAV (binary), depth (m) cokriging models produced for each site for each survey period (month, year). The parameters selected were model type, anisotropy, lag size (in m), and number of nearest neighbors. All other parameters were kept at the default levels.

Site	Month, Year	Model	Anisotropy	Lag Size	# Neighbors
BLB	May, 2010	Exponential	Yes	13	12
BLB	Jun., 2010	Exponential	Yes	12	15
BLB	Aug., 2010	Exponential	Yes	13	7
BLB	Sep., 2010	Exponential	Yes	13	24
JBS	Jun., 2010	Exponential	Yes	8	20
JBS	Jul, 2010	Exponential	Yes	14	5
JBS	Sep., 2010	Spherical	Yes	11	10
NPR	Jun., 2009	Exponential	Yes	12	25
NPR	May, 2010	Exponential	Yes	10	6
NPR	Jun., 2010	Spherical	Yes	12	5
NPR	Aug., 2010	Exponential	Yes	9	9
NPR	Sep., 2010	Exponential	Yes	12	5
SPS	Jun., 2010	Exponential	Yes	8	10
SPS	Aug., 2010	Exponential	Yes	13	5
SPS	Sep., 2010	Exponential	Yes	13	10

Table 20. The results of the SAV (binary), depth (m) cokriging models produced for each site for each survey period (month, year). The parameters were optimized to obtain a model that has a mean = 0, root-mean-square = 0, average standard error = 0, mean standardized = 0, and root-mean-square standardized = 1.

Site	Month, Year	Mean	Rt. Mean Square	Ave SE	Mean Standardized	Rt. Mean Sq. Standardized
BLB	May, 2010	<0.0001	0.1507	0.1290	0.0003	1.1650
BLB	Jun., 2010	-0.0002	0.1558	0.1405	-0.0012	1.1080
BLB	Aug., 2010	-0.0001	0.1680	0.1401	-0.0001	1.1900
BLB	Sep., 2010	<0.0001	0.1903	0.1671	0.0004	1.1360
JBS	Jun., 2010	-0.0005	0.3531	0.3677	-0.0012	0.9605
JBS	Jul, 2010	-0.0001	0.1422	0.1240	-0.0005	1.1420
JBS	Sep., 2010	>-0.0001	0.0719	0.0619	>-0.0001	1.1620
NPR	Jun., 2009	0.0016	0.2936	0.3164	0.0054	0.9278
NPR	May, 2010	0.0007	0.3258	0.3922	0.0017	0.8311
NPR	Jun., 2010	-0.0001	0.1689	0.1752	-0.0003	0.9637
NPR	Aug., 2010	>-0.0001	0.1048	0.0904	-0.0007	1.1580
NPR	Sep., 2010	>-0.0001	0.0994	0.0990	-0.0004	1.0040
SPS	Jun., 2010	-0.0001	0.4142	0.4250	-0.0003	0.9743
SPS	Aug., 2010	-0.0005	0.3906	0.3936	-0.0012	0.9923
SPS	Sep., 2010	<0.0001	0.3742	0.3882	0.0001	0.9641

Table 21. The parameters used in the depth kriging models produced for each site for each survey period (month, year). The parameters selected were model type, anisotropy, lag size (in m), and number of nearest neighbors. All other parameters were kept at the default levels.

Site	Month, Year	Model	Anisotropy	Lag Size	# Neighbors
BLB	May, 2010	Spherical	Yes	13	3
BLB	Jun., 2010	Spherical	Yes	14	5
BLB	Aug., 2010	Exponential	No	10	3
BLB	Sep., 2010	Exponential	Yes	11	7
JBS	Jun., 2010	Exponential	Yes	7	3
JBS	Jul, 2010	Exponential	Yes	7	4
JBS	Sep., 2010	Exponential	No	12	5
NPR	Jun., 2009	Exponential	No	11	3
NPR	May, 2010	Exponential	No	9	11
NPR	Jun., 2010	Spherical	Yes	7	16
NPR	Aug., 2010	Exponential	No	7	10
NPR	Sep., 2010	Spherical	No	12	5
SPS	Jun., 2010	Exponential	Yes	8	8
SPS	Aug., 2010	Circular	No	12	12
SPS	Sep., 2010	Spherical	No	11	18

Table 22. The results of the depth kriging models produced for each site for each survey period (month, year). The parameters were optimized to obtain a model that has a mean = 0, root-mean-square = 0, average standard error = 0, mean standardized = 0, and root-mean-square standardized = 1.

Site	Month, Year	Mean	Rt. Mean Square	Ave SE	Mean Standardized	Rt. Mean Sq. Standardized
BLB	May, 2010	-0.0001	0.0838	0.0978	-0.0005	0.9224
BLB	Jun., 2010	0.0008	0.0691	0.0984	0.0045	0.8521
BLB	Aug., 2010	0.0001	0.0868	0.1009	0.0008	1.0310
BLB	Sep., 2010	0.0001	0.1262	0.1350	0.0003	1.0870
JBS	Jun., 2010	0.0002	0.0441	0.0394	0.0026	1.3580
JBS	Jul, 2010	0.0004	0.0459	0.0386	0.0014	1.5650
JBS	Sep., 2010	<0.0001	0.0810	0.0755	-0.0004	1.0730
NPR	Jun., 2009	0.0019	0.0890	0.0810	0.0078	1.0680
NPR	May, 2010	-0.0001	0.2197	0.2185	-0.0003	1.0100
NPR	Jun., 2010	<0.0001	0.0834	0.0851	-0.0001	0.9963
NPR	Aug., 2010	-0.0001	0.0822	0.0367	-0.0010	1.6630
NPR	Sep., 2010	>-0.0001	0.0455	0.0424	-0.0001	1.0840
SPS	Jun., 2010	-0.0001	0.0614	0.0715	-0.0004	0.9728
SPS	Aug., 2010	>-0.0001	0.1868	0.1605	0.0001	1.1490
SPS	Sep., 2010	<0.0001	0.0950	0.1032	0.0001	0.9433